

AD-A244 902



AD \_\_\_\_\_

PATHOPHYSIOLOGY AND TOXICOKINETIC STUDIES OF BLUE-GREEN  
ALGAE INTOXICATION IN THE SWINE MODEL

(2)

FINAL REPORT

Val R. Beasley  
Wanda M. Haschek-Hock  
Wayne M. Carmichael  
William O. Cook  
Andrew M. Dahlem  
Stephen B. Hooser  
Randall A. Lovell  
Nik A. Mahmood  
Patty M. Thorn  
William M. Valentine

DTIC  
ELECTE  
JAN 17 1992  
S B D

June 26, 1991

Supported by

U.S. ARMY MEDICAL RESEARCH AND DEVELOPMENT COMMAND  
Fort Detrick, Frederick, Maryland 21702-5012

Contract No. DAMD17-85-C-5241

University of Illinois  
2001 South Lincoln Avenue  
Urbana, IL 61801

20030214015

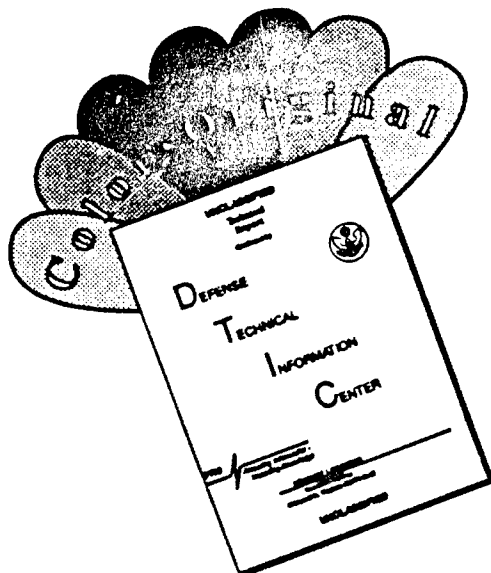
92-01491

Approved for public release; distribution unlimited.

The findings in this report are not to be construed as an official Department of the Army position unless so designated by other authorized documents.

92 1 16 073

# DISCLAIMER NOTICE



THIS DOCUMENT IS BEST QUALITY AVAILABLE. THE COPY FURNISHED TO DTIC CONTAINED A SIGNIFICANT NUMBER OF COLOR PAGES WHICH DO NOT REPRODUCE LEGIBLY ON BLACK AND WHITE MICROFICHE.

## REPORT DOCUMENTATION PAGE

Form Approved  
OMB No. 0704-0188

1a. REPORT SECURITY CLASSIFICATION UNCLASSIFIED			1b. RESTRICTIVE MARKINGS		
2a. SECURITY CLASSIFICATION AUTHORITY			3. DISTRIBUTION/AVAILABILITY OF REPORT Approval for public release; distribution unlimited		
2b. DECLASSIFICATION/DOWNGRADING SCHEDULE			5. MONITORING ORGANIZATION REPORT NUMBER(S)		
4. PERFORMING ORGANIZATION REPORT NUMBER(S)			7a. NAME OF MONITORING ORGANIZATION		
6a. NAME OF PERFORMING ORGANIZATION University of Illinois		6b. OFFICE SYMBOL (If applicable)	7b. ADDRESS (City, State, and ZIP Code)		
6c. ADDRESS (City, State, and ZIP Code) 2001 South Lincoln Avenue Urbana, Illinois 61801			9. PROCUREMENT INSTRUMENT IDENTIFICATION NUMBER DAMD17-85-C-5241		
8a. NAME OF FUNDING/SPONSORING ORGANIZATION U.S. Army Medical Research & Development Command		8b. OFFICE SYMBOL (If applicable)	10. SOURCE OF FUNDING NUMBERS		
8c. ADDRESS (City, State, and ZIP Code) Fort Detrick Frederick, Maryland 21702-5012			PROGRAM ELEMENT NO. 61102A	PROJECT NO. 3M1 61102BS12	TASK NO. AA 006
11. TITLE (Include Security Classification) (u) Pathophysiology and Toxicokinetic Studies of Blue-Green Algae Intoxication in the Swine Model					
12. PERSONAL AUTHOR(S) V.R. Beasley, W.M. Haschek-Hock, W.W. Carmichael, W.O. Cook, A.M. Dahlem, S.B. Hooser, R.A. Lovell, N.A. Mahmood, Patty M. Thorn, and W.M. Valentine.					
13a. TYPE OF REPORT Final	13b. TIME COVERED FROM 9/1/85 to 8/30/89	14. DATE OF REPORT (Year, Month, Day) June 26, 1991	15. PAGE COUNT 437		
16. SUPPLEMENTARY NOTATION					
17. COSATI CODES			18. SUBJECT TERMS (Continue on reverse if necessary and identify by block number)		
FIELD	GROUP	SUB-GROUP	Blue-green algae, phycotoxin, microcystin, cyanoginosin, anatoxin-a(s), pathophysiology, radiolabelled toxin, analysis, RA 1, anatoxin-a, cyanobacteria.		
06	16				
06	20				
19. ABSTRACT (Continue on reverse if necessary and identify by block number)					
<p>Microcystin-LR (MCLR) was stable in aqueous solution for up to several days. Stability was enhanced at low temperatures. Reversed phase high performance liquid chromatography and thin layer chromatography are effective for characterizing MCLR purity. ODS-silica gel extraction, and silica gel column chromatography with HPLC and UV detection at 238 nm are effective for toxin purification.</p> <p>Rat hepatocytes exposed <u>in vitro</u> to MCLR developed marked blebbing of the plasma membrane whereas nonparenchymal cells (Kupffer and endothelial cells) did not. Rat hepatocytes were affected by MCLR <u>in vivo</u> before sinusoidal endothelial cells; there is an early loss of hepatocyte microvilli and invagination of the plasma membrane; plasma membranes are distorted or lost before marked changes in organelles or the nucleus; hepatocytes and debris pass into small arterioles and capillaries of the lungs and peripheral circulation including renal capillaries. Rhodamine labelled phalloidin staining and fluorescence microscopy with primary cultures of rat hepatocytes and</p>					
20. DISTRIBUTION/AVAILABILITY OF ABSTRACT <input type="checkbox"/> UNCLASSIFIED/UNLIMITED <input checked="" type="checkbox"/> SAME AS RPT. <input type="checkbox"/> DTIC USERS			21. ABSTRACT SECURITY CLASSIFICATION Unclassified		
22a. NAME OF RESPONSIBLE INDIVIDUAL Mary Frances Bostian			22b. TELEPHONE (Include Area Code) 301-663-7325	22c. OFFICE SYMBOL SGRD-RMI-S	

livers of dosed rats revealed marked disorganization of the actin microfilaments of the hepatocyte cytoskeleton. In mice dosed IP, a toxic dose of MCLR induced tolerance to a subsequent "consistently lethal" dose. Livers of survivors displayed hepatocyte regeneration. Gut loop administration of MCLR *in vivo*, provided evidence for greater uptake from ileum than jejunum. Cholestyramine bound and decreased the toxicity of MCLR in rats dosed via ileal loops: activated charcoal was effective *in vitro*, but less so *in vivo*, apparently due to precipitation. Saturation of dehydro amino acids of either MCLR (N-methyl dehydroalanine) or nodularin (N-methyl- $\alpha$ -dehydrobutyrine) reduced toxicity by one-half (MCLR) to one-fourth (nodularin). Formation of hexahydro derivatives, or removal of adda revealed the essential role of adda in its correct configuration. When isolated from other components of MCLR, adda was nontoxic. Depletors of GSH or inhibitors of GSH biosynthesis did not enhance susceptibility to MCLR. GSH-MCLR was less toxic than MCLR but remained highly potent and hepatospecific.

Methods for general tritium exchange, specific tritium exchange, and biosynthesis with  $^{14}\text{C}$ - or  $^3\text{H}$ -labelled amino acids proved unsatisfactory. A method to synthesize  $^3\text{H}$ -labelled sodium borohydride was developed, and  $^3\text{H}$ -2H-MCLR was chemically and biologically stable. Over 95% of the radiolabel from a sublethal dose was in the liver of mice dosed IP within 60 min; and 58% was retained at 72 hr. When massive liver damage occurs, toxin uptake is curtailed. At a lethal dose, radiolabel accumulated in lungs and kidney, consistent with passage of hepatocytes and debris from the liver. Radiolabel in the upper small intestine suggested biliary excretion. Elimination via urine was significant for 12 hours; over 72 hours, feces accounted for 34% of the dose. Uptake of  $^3\text{H}$ -2H-MCLR by rat hepatocytes was slowed by incubation at  $0^\circ\text{C}$  or by rifampicin, suggesting energy dependency and involvement of bile acid carriers. In suspensions and in perfused liver, soluble cytosolic proteins retained the greatest fraction of radiolabel consistent with recent evidence of phosphatase inhibition.

In swine given MCLR IV, hepatic perfusion, renal perfusion, and mean arterial and central venous pressures were decreased, and portal pressure increased. Liver iron and hemoglobin indicated that 38% of the estimated blood volume was lost into the livers of lethally dosed animals. Serum bile acids, bilirubin, lactate, liver enzymes, creatinine phosphokinase, and  $\text{pO}_2$  were increased. Reductions occurred in  $\text{pCO}_2$ , hematocrits, and platelet counts. Severe hypoglycemia and hyperkalemia occurred terminally.

The naturally occurring (+) isomer of anatoxin-a (antx-a) is highly toxic, whereas the (-) isomer is neither toxic nor able to inhibit the effect of the (+) isomer. Neurophysiologic studies with anesthetized rats dosed IV with (+)antx-a indicated that the effects of the toxin are reversible within a period of hours provided that excessive doses are not given. At sufficient doses (i.e. 800  $\mu\text{g}/\text{kg}$ ), however, rats did not have return of neuromuscular function and died despite assisted ventilation, suggesting a lethal mechanism(s) in addition to respiratory paralysis. Repetitive stimulation studies suggested a presynaptic mechanism of action.

Anatoxin-a(s) [antx-a(s)] was stable for 9 months when stored at  $-20^\circ\text{C}$  under gaseous nitrogen. The toxin inhibited cholinesterases (ChE) in blood and peripheral tissues but not in whole or individual regions of the brain, or spinal cord. Antx-a(s) is a potent inhibitor of ChE in RBCs. The duration of ChE inhibition was similar to that paraoxon, but fact that inhibition occurred only peripherally was similar to pyridostigmine.

Infusion of rats with antx-a(s) revealed a rapid and marked decline in heart rate and blood pressure before a large decrease in respiratory minute volume. Atropine could counteract these effects, but rats still died after being given only 25% more antx-a(s). Antx-a(s) caused increased phrenic nerve activity with reduced tidal and minute volumes and apparent neuromuscular blockade occurred in the diaphragm. Rats provided artificial respiration survived despite a 4.7-fold lethal dose of the toxin.



# FOREWORD

In conducting research using animals, the investigator(s) adhered to the "Guide to the Care and Use of Laboratory Animals," prepared by the Committee on Care and Use of Laboratory Animals of the Institute of Laboratory Animal Resources Commission on Life Sciences, National Research Council (DHHS, PHS, NIH Publications No. 86-23, Revised 1985).

Citations of commercial organizations and trade names in this report do not constitute an official Department of the Army endorsement or approval of the products or services of these organizations.

<b>Accession For</b>	
NTIS GRA&I	<input checked="" type="checkbox"/>
DTIC TAB	<input type="checkbox"/>
Unannounced	<input type="checkbox"/>
Justification	
By	
Distribution/	
Availability Codes	
Dist	Avail and/or Special
A-1	





## TABLE OF CONTENTS

	<u>Page</u>
FOREWORD .....	1
SUMMARY .....	8
PEPTIDE HEPATOTOXINS .....	17
I. CYCLIC PEPTIDE HEPATOTOXIN PURIFICATION AND ANALYSIS AND	
TOXIN STABILITY .....	18
A. Purification and Analysis .....	18
B. Stability Evaluation of Microcystin in Aqueous Solution .....	25
II. STRUCTURE ACTIVITY RELATIONSHIPS WITH MICROCYSTIN-LR AND	
NODULARIN .....	29
A. Structure/Toxicity Relationships of Dehydro Amino Acids of Microcystin-LR	
and Nodularin .....	29
B. The Contribution of Amino Methoxy Trimethyl Phenyldecadienoic Acid	
(Adda) to the Toxicity of Microcystin-LR and Nodularin .....	49
C. Pilot Study on the Influence of Glutathione Depletion on Microcystin-LR	
Toxicity and the Toxicity of Glutathione-Bound Microcystin-LR .....	58
III. METHODS FOR PRODUCTION OF ISOTOPICALLY LABELLED MICROCYSTIN-	
LR .....	74

IV. PRODUCTION AND CHARACTERIZATION OF THE FATE OF TRITIATED DIHYDROMICROCYSTIN-LR IN MICE, ISOLATED PERFUSED RAT LIVERS, AND RAT HEPATOCYTES IN SUSPENSION .....	89
A. Production and Purification of Tritiated-Dihydromicrocystin-LR: Fate in Mice Dosed Intraperitoneally .....	89
B. Uptake and Subcellular Localization of Tritiated Dihydromicrocystin-LR in Rat Liver .....	108
V. LESIONS INDUCED IN INTACT ANIMALS EXPOSED TO PEPTIDE HEPATOTOXINS .....	128
A. Mice .....	128
Toxicity of Single and Repeated Intraperitoneal Doses of Microcystin-LR in Two Strains of Male Mice .....	128
B. Mice and Rats .....	154
Toxicity of Microcystin-LR, a Cyclic Heptapeptide Hepatotoxin from <i>Microcystus aeruginosa</i> , to Rats and Mice .....	154
C. Rats .....	179
Microcystin-LR-Induced Ultrastructural Changes in Rats .....	179
VI. LESIONS IN HEPATOCYTES INDUCED BY MICROCYSTIN-LR .....	195

VII. MICROCYSTIN-LR TOXICOSIS IN SWINE: HEPATIC AND RENAL PERFUSION, HEMODYNAMIC, HEMATOLOGIC, AND SERUM BIOCHEMICAL EFFECTS FOLLOWING INTRAVENOUS ADMINISTRATION	214
A. Arginase Activity in Swine: Tissue Distribution, Serum Half-life, and Serum Changes after Microcystin-LR Administration	214
B. The Effects of Microcystin-LR on Hemodynamic, Organ Perfusion, Clinical Pathologic, Gross Pathologic, and Blood-Gas Parameters in Swine	229
VIII. BIOAVAILABILITY OF MICROCYSTIN-LR FROM RAT INTESTINE: THE INFLUENCE OF CHOLESTYRAMINE AND SUPERACTIVATED CHARCOAL <i>IN VITRO</i> AND <i>IN VIVO</i>	264
A. An Indirect Assessment of the Bioavailability of Intestinally Administered Microcystin-LR in Rats: Influence of Cholestyramine	264
B. Comparison of the Binding Capacities of Superactivated Charcoal to Microcystin-LR <i>In Vivo</i> and <i>In Vitro</i>	277
IX. INTERPRETATION OF THE CURRENTLY REPORTED STUDIES ON CYTOSKELETAL EFFECTS AND FATE OF ALGAL PEPTIDES IN LIGHT OF OTHER RECENT RESEARCH	283
X. REFERENCES	288
ANATOXINS	309
I. CHARACTERIZATION OF THE NEUROMUSCULAR BLOCKADE PRODUCED <i>IN VIVO</i> BY ANATOXIN-A IN THE RAT; AND THE INFLUENCE OF STRUCTURAL CONFIGURATION	309

II. ANATOXIN-A(S) .....	334
Background on Algal Neurotoxins; Anatoxin-a and Anatoxin-a(s) .....	334
A. Absence of Effects of Anatoxin-A(s) on Mouse Brain Cholinesterase	
Activity .....	337
B. Reversal of Peripheral Cholinesterase Inhibition; Clinical Signs and	
Postmortem Findings in Mice Dosed Intraperitoneally with Anatoxin-a(s) ....	344
C. Inhibition of Strictly Peripheral Cholinesterase by Neurotoxins from <i>Anabaena</i>	
<i>flos-aquae</i> in Ducks, Swine, Mice, and a Steer .....	356
D. Regional Brain Cholinesterase Activity in Rats Given Anatoxin-a(s) or	
Paraoxon Intraperitoneally .....	375
E. Effect of Anatoxin-a(s) on Cardiac and Pulmonary Function and Phrenic	
Nerve Activity in Rats .....	382
F. Pathophysiologic Effects of Anatoxin-a(s) in Anesthetized Rats: The Influence	
of Atropine and Artificial Respiration .....	395
G. Stability of Anatoxin-a(s) <i>In Vitro</i> as Measured by Inhibition of Human	
Plasma Cholinesterase Over Time .....	413
III. REFERENCES .....	419
CHRONOLOGICAL BIBLIOGRAPHY OF ALL PUBLICATIONS SUPPORTED BY THE	
CONTRACT .....	429
LIST OF PERSONNEL RECEIVING CONTRACT SUPPORT, INCLUDING DEGREES	
RECEIVED .....	436



## SUMMARY

## Algal Cyclic Peptide Hepatotoxins

Stability studies with the cyanobacterial cyclic heptapeptide hepatotoxin, microcystin-LR (MCLR), indicated that the toxin would remain intact in aqueous solution for periods up to several days and stability could be enhanced by storage at subzero temperatures. Analytical methods for this algal peptide involving a combination of reversed-phase high-performance liquid chromatography and thin-layer chromatographic methods were developed and refined to ensure a high level of purity for dosing studies. In addition, purification methods involving ODS-silica gel extraction and isolation via a combination of silica gel column chromatography and high-performance liquid chromatography with UV detection at 238 nm were developed as a part of a collaborative project involving workers at the University of Illinois, Wright State University in Dayton, Ohio, and Meijo University in Nagoya, Japan.

Studies on the pathogenesis of MCLR toxicosis in mice and rats revealed early separation and rounding up of hepatocytes, severe intrahepatic hemorrhage, hepatic necrosis, pallor and death. Closer examination of tissues of rats (which survive longer following administration of MCLR than do mice) dosed IV with MCLR, with rat hepatocytes and hepatic nonparenchymal cells exposed *in vitro* using light and electron microscopy, and with rhodamine-labelled phalloidin staining and fluorescence microscopy revealed that: 1) hepatocytes were highly susceptible to MCLR in suspension whereas hepatic nonparenchymal cells were not; 2) hepatocytes were affected even before sinusoidal endothelial cells *in vivo*; 3) hepatocytes exposed to MCLR *in vitro* rapidly exhibited blebbing, whereas hepatocytes exposed *in vivo* displayed an early loss of



microvilli and invagination of the plasma membrane leading to apparent vacuolization; 4) hepatocyte plasma membranes were grossly distorted or even severely ruptured and/or lost before marked changes in organelles or the nucleus were noted; 5) hepatocytes and readily identifiable hepatocyte debris in MCLR dosed rats passes into the small arterioles and capillaries of the lungs and subsequently into the peripheral circulation including renal capillaries; and 6) lesions of the plasma membrane were correlated with marked disorganization of the actin microfilaments, an integral part of the hepatocyte cytoskeleton.

Dosing of mice with one or two intraperitoneal doses of MCLR revealed that, at a near-lethal dose, the toxin would induce a mild degree of tolerance to a subsequent, "consistently lethal" dose. In addition, livers of survivors of MCLR administration displayed marked regeneration during the study.

A method to assess the bioavailability of MCLR from the jejunum or ileum of anesthetized rats was developed using gut loops *in vivo*. Such studies provided evidence for preferential uptake of the toxin from the ileum as compared to the jejunum, which is compatible with previous data indicative of a higher content of bile acid carriers in the former. In conjunction with studies *in vitro*, it was shown that the anion exchange resin, cholestyramine, was highly effective in binding MCLR and thus decreased its toxicity in animals. Activated charcoal was effective *in vitro* but less so *in vivo*, apparently due in part to its precipitation in the ileal loop.

Studies with a crude extract from a bloom of *Nodularia spumigena* from Christchurch, New Zealand, lead to the isolation, purification, and structural characterization of the cyclic pentapeptide toxin, nodularin, in conjunction with coworkers in the laboratory of Dr. Kenneth Rinehart at the University of Illinois and at Wright State University. Toxicity testing in our

laboratory revealed similar potency and lesions as compared to MCLR. Collaboration in these structural studies with nodularin also lead to initial studies involving structure/toxicity relationships in which it was demonstrated that saturation of the dehydro amino acids of either MCLR (N-methyl dehydroalanine) or nodularin (N-methyl-Z-dehydrobutyrine) would cause only a modest reduction in toxicity by one-half (MCLR) to one-fourth (nodularin) as compared to the respective parent compounds.

Additional structure/toxicity assays revealed that hexahydro derivatives, formed by saturating not only the dehydro amino acids but also the double bonds of the hydrophobic portion of the 3-amino-9-methoxy-10-phenyl-2,6,8-trimethyl-deca-4,6-dienoic acid (Adda) residue of either MCLR or nodularin eliminated detectable toxicity in mice dosed IP. Similarly, ozonolysis-dependent removal of Adda resulted in a similar obliteration of toxicity, and yet Adda itself in the absence of other components of the cyclic peptide, whether in a free or protected amino acid form, was also without observable toxicity in similarly dosed mice.

Glutathione (GSH) conjugation is an important mechanism for detoxification of certain xenobiotics which react across double bonds; however, this process does not seem to be of extreme importance in MCLR-toxicosis. Depletors of GSH or inhibitors of GSH biosynthesis did not enhance susceptibility of animals to MCLR exposure, and moreover, administration of a GSH conjugate of the toxin revealed that the derivative was somewhat less toxic but, nevertheless, still highly potent and hepatospecific in its effects.

Various methods were investigated to permit isotopic radiolabelling of microcystin-LR (MCLR), including general tritium exchange, specific tritium exchange, and biosynthesis with  $^{14}\text{C}$ - or  $^3\text{H}$ -labelled aminoacids. None of these proved satisfactory and/or reproducible, and

consequently,  $^3\text{H}$ -labelled sodium borohydride was used to synthesize tritiated dihydro-MCLR ( $[\text{}^3\text{H}]\text{-2H-MCLR}$ ). The  $[\text{}^3\text{H}]\text{-2H-MCLR}$  was purified by loading the reaction mixture onto C18 cartridges, rinsing with water and 10% methanol, and eluting with methanol followed by reversed phase HPLC with a mobile phase of dibasic potassium phosphate and methanol. The  $[\text{}^3\text{H}]\text{-2H-MCLR}$  thus produced was over 99% chemically and over 98% radiochemically pure. Also, the label was chemically and biologically stable, as indicated by insignificant loss of radiolabel in toxin stored for 2 weeks in ethanol at  $-20^\circ\text{C}$ , and the fact biological loss of the label to form tritiated water was  $< 0.01\%$  in urine samples.

In distribution studies, male mice were dosed IP with 2H-MCLR (at  $200\text{ }\mu\text{g/kg}$ ),  $[\text{}^3\text{H}]\text{-2H-MCLR} + 2\text{H-MCLR}$  (total of  $100\text{ }\mu\text{g/kg}$ ), or  $[\text{}^3\text{H}]\text{-2H-MCLR} + 2\text{H-MCLR}$  (total of  $200\text{ }\mu\text{g/kg}$ ) or the saline vehicle, and killed at predetermined intervals. In elimination studies, euthanasia of mice given the lower dose of  $[\text{}^3\text{H}]\text{-2H-MCLR}$  occurred after a period of 72 hours to enable collection of urine and feces. Over 95% of the radiolabel from the low dose was detected in the liver within 60 minutes of dosing, and approximately 58% remained in the liver at 72 hours postdosing, indicating rapid and specific uptake into and comparatively slow elimination from this organ. At  $200\text{ }\mu\text{g/kg}$ , only approximately 50% of the dose was detected in the liver, and peak concentrations were reached at around 30 minutes after dosing; however, the total toxin uptake was still slightly higher than at the sublethal dose. These findings seem to suggest that after the liver concentration of toxin has reached a threshold at which massive damage is progressing, further toxin uptake is greatly diminished.

At the lethal dose, small amounts of radiolabel accumulated in the lungs and kidney over time, consistent with passage of hepatocytes and hepatic debris into the vasculature of these

organs where it becomes trapped after leaving the damaged liver. Radiolabel from the toxin also accumulated in the most oral portion of the small intestine in greater concentrations than in other portions of the gut suggesting probable biliary excretion. Elimination of tritium via the urine was of significance only during the first 12 hours postexposure, and approximately 3.6% of the administered radiolabel was eliminated by this route, whereas fecal elimination over 72 hours gradually increased and eventually accounted for 34% of the dose.

The [ $^3\text{H}$ ]-2H-MCLR was also taken up rapidly by isolated perfused rat livers and by rat hepatocytes in suspension at 37°C. Uptake by hepatocytes in suspension was slowed and reduced by incubation at 0°C or by pretreatment with rifampicin, suggesting that the process of hepatocyte uptake of the toxin was energy dependent and reliant upon the involvement of bile acid carriers. In hepatocyte suspensions, approximately 13 to 18% and, in isolated perfused livers, 0 to 7% of the radiolabel was present in the plasma membrane/nuclear fraction, and at least two-thirds of the radiolabel was present in the cytoplasmic fraction. In perfused liver, approximately 15% of the radioactivity was detected in the microsomal fraction. Trichloroacetic acid precipitation of cytosolic fractions from cells in suspension suggested that 50 to 60% of the tritiated compound was bound to cytoplasmic protein, and in perfused liver, 78 to 88% of the radiolabel was similarly bound. These findings suggest that, once inside the cell, the algal peptide binds preferentially to a cytoplasmic protein, which supports recent work by others indicating specific binding and inhibition of cytosolic protein phosphatases by microcystins.

Temperature pulse decay methods were used to characterize the perfusion of the livers and kidneys of swine given MCLR at either a sublethal (25  $\mu\text{g/kg}$ ) or a lethal (72  $\mu\text{g/kg}$ ) dose. Hepatic perfusion was significantly decreased within 18 minutes and renal perfusion within 24

minutes of the lethal dose, and at the sublethal dose, hepatic perfusion was significantly reduced by 39 and renal perfusion by 51 minutes postdosing. Between 12 and 24 minutes after the lethal dose, aortic mean pressure and central venous pressure decreased significantly, while portal venous pressure significantly increased.

The livers of the lethal dose animals were markedly enlarged, dark red-purple, and readily exuded blood on cut surface. Edema of the gallbladder was severe, and there was straw- to brown-colored fluid in the peritoneal cavity. Liver weights (as percent of body weight), liver iron, and liver hemoglobin were significantly elevated in the high dose animals as compared to the control and toxic-sublethal groups. An average of almost 38% of the estimated total blood volume had been lost into the livers of the high dose animals. Other effects included increased serum concentrations of bile acids, bilirubin, and lactate and increased serum activities of liver enzymes and creatinine phosphokinase. There were also increases in  $pO_2$  and decreases in  $pCO_2$ , hematocrits, and platelet counts. Terminally, marked hypoglycemia and hyperkalemia were commonly observed. Serum arginase was demonstrated to be a liver specific enzyme in swine with short half-life such that it should be of value in conjunction with other liver enzymes to predict the reversibility of hepatic injury. Marked increases in the serum arginase activities were seen in swine given MCLR.

Acute death of swine with MCLR toxicosis is most notably associated with reduced perfusion of the liver, lethal hemorrhage into the damaged liver, and terminal hypoglycemia, hyperkalemia, and hypovolemic shock.

## Neurotoxins from *Anabaena flos-aquae*

### Anatoxin-a

The toxicity of racemic anatoxin-a (antx-a) was compared to that of (+)antx-a and (-)antx-a mice dosed IV. LD<sub>50</sub> values (95% CI) for racemic antx-a were 913 (846 to 985) and for (+)antx-a, 386 (365 to 408) µg/kg BW. No deaths were noted in mice given the highest dose, 73 mg/kg, of (-)antx-a. These results seem to indicate that the naturally occurring (+) isomer is highly toxic, whereas the (-) isomer conveys little either in terms of inherent toxicity or in ability to inhibit the toxicity of the (+) isomer when both forms are present in a synthetic racemic mixture.

Neurophysiologic studies with anatoxin-a involved the use of indirectly evoked compound action potentials (ECAP) in the plantar muscles of anesthetized rats following single and repetitive stimulations of the posterior tibial nerve. No changes in maximal motor nerve conduction velocities or latency of the ECAP were noted following IV administration of (+)antx-a at 100 µg/kg. The ED<sub>50</sub> (95% CI) for depression of the ECAP was 47 µg/kg (39 to 57). Rats given (+)antx-a at 200 µg/kg or less displayed a 75% or greater return of the pretoxin amplitude of the ECAP within 93 minutes. At 800 µg/kg, however, rats did not have return of neuromuscular function, and the animals died despite mechanical ventilation, indicating a lethal mechanism(s) of action in addition to respiratory paralysis. Following administration of antx-a at 0, 50, 100, and 200 µg/kg, the percent decrements (± SD) in the amplitudes of the fourth ECAP following repeated stimulation of the tibial nerve at 10 Hz were 6 (± 5), 13 (± 22), 46 (± 18), and 59 (± 8), respectively.

Overall, these studies indicate that antx-a causes a depolarizing blockade of the peripheral muscles, but the decrement following repetitive stimulation studies are indicative of an additional, presynaptic mechanism of action in agreement with earlier reports. These studies suggest that therapy for animals with antx-a toxicosis should include not only general detoxification measures such as evacuation of the digestive tract and the use of adsorbents but also artificial respiration. Nevertheless, toxic effects in addition to respiratory paralysis may result in failure of this approach following sufficiently high exposure to antx-a.

#### Anatoxin-a(s)

A stability study was conducted with the cholinesterase inhibitor anatoxin-a(s) [antx-a(s)]. Stability of the toxin stored at -20°C under gaseous nitrogen was assessed by its ability to inhibit human plasma cholinesterase *in vitro*. The study revealed that the toxin would tolerate storage under these conditions for at least 9 months without significant degradation.

Studies with mice and rats revealed that antx-a(s) inhibited cholinesterases in blood and peripheral tissues but not in whole brain or in individual regions of the brain or cervical spinal cord. The ability of the toxin to inhibit blood cholinesterase exceeded that of the other cholinesterase inhibitors evaluated and the duration of the inhibition was more similar to that of the irreversible inhibitor, paraoxon, than to the reversible carbamate inhibitors. Overall antx-a(s) resembled the polar carbamate, pyridostigmine, in terms of its tendency to inhibit only peripheral cholinesterases and paraoxon in terms of the duration of its effects. This is consistent with the highly polar nature of the molecule and with its recently elucidated organophosphorus structure.

When anesthetized rats were continuously infused with antx-a(s), there was a rapid and marked decline in heart rate and blood pressure, which occurred before a large decrease in

respiratory minute volume. This seemed to suggest the importance of muscarinic effects of antx-a(s) on the circulatory system in the lethal syndrome. Subsequent studies, however, demonstrated that atropine could counteract these effects, but atropine-treated rats still died after being given only approximately 25% more antx-a(s) than those given the toxin alone. In addition, rats given antx-a(s) consistently exhibited increased phrenic nerve activity despite reductions in tidal and minute volumes and, ultimately, a lack of coordinated diaphragmatic electromyographic activity. In addition, rats provided artificial respiration survived a dose of antx-a(s) that was 4.7 times the lethal dose for positive control rats. Thus, although the muscarinic effects of antx-a(s) are of importance in the lethal toxicosis, and atropine is recommended, a highly important aspect in lethality from this syndrome is nicotinic paralysis of the muscles of respiration, and atropine alone is unlikely to sustain survival when this occurs. It would appear that an appropriate therapeutic protocol for antx-a(s) toxicosis would include evacuation of the digestive tract, the use of an adsorbent such as activated charcoal, and administration of atropine and provision of artificial respiration as needed.



## PEPTIDE HEPATOTOXINS

### INTRODUCTION

Adverse health effects and deaths in domestic animals and wildlife have commonly been reported following ingestion of cyanobacteria (Carmichael, 1988; Codd and Poon, 1988). Hepatic dysfunction in humans has also been associated with cyanobacterial contamination of drinking water (Falconer et al., 1983).

Microcystin-LR (MCLR, cyanoginosin-LR) is one of a series of potent monocyclic peptide hepatotoxins called microcystins (Carmichael et al., 1988b) produced by the cyanobacterium *Microcystis aeruginosa*. The complete structure, including the absolute stereochemistry, of MCLR was recently established (Rinehart et al., 1988). This compound is a heptapeptide containing: a characteristic and unusual C<sub>20</sub> amino acid, (2S,3S,8S,9S) 3-amino-9-methoxy-2,6,8-trimethyl-10-phenyl-4,6-decadienoic acid (Adda); D-glutamic acid (D-Glu) linked through its carboxyl; the unsaturated amino acid, N-methyldehydroalalanine; D-alanine; L-leucine (L-Leu); D-β-methylaspartic acid linked through its β-carboxyl; and L-arginine (L-Arg). Unsaturated amino acids, D-Glu, and Adda are common to nearly all cyanobacterial cyclic peptide hepatotoxins described to date.

The most severe and consistent toxic effects of MCLR are related to hepatocyte degeneration. There is associated sinusoidal endothelial distraction and resultant hemorrhage into the liver, shock, and often death (Adams et al., 1985; Falconer et al., 1981; Runnegar et al., 1981). The observed toxicity of a lethal dose is rapid and effects are remarkably hepatospecific with death in parenterally dosed mice typically occurring within 3 hours of administration. The

rapidity of death in affected mice would appear to be incompatible with death due to metabolic insufficiency from hepatic dysfunction (Adams et al., 1988).

Although studies on the fate in and effects of MCs on animals had been performed previous to the presently reported work, many questions remained to be answered at the onset of these studies. Questions of toxin structure, purification, appropriate radiolabelling methodology, fate in intact animals and animal cells, pathophysiology including pathogenesis of hepatic, pulmonary and renal lesions, and primary cellular effects were all insufficiently characterized.

## I. CYCLIC PEPTIDE HEPATOTOXIN PURIFICATION AND ANALYSIS AND TOXIN STABILITY

### A. Purification and Analysis

#### 1. Statement of the Problem

The goals of these studies included: ensuring toxin purity and stability for dosing studies; detecting and quantifying toxins in algal bloom material; detecting toxin in animal tissues and body fluids; improving methods to increase toxin purity and efficiency of purification from algal bloom material.

#### 2. Background and Review of Literature

Toxic blooms of cyanobacteria are a common occurrence in many nutrient-rich fresh and brackish waters. When dense blooms of cyanobacteria occur in recreational or drinking waters, animals may ingest toxic or potentially lethal amounts of algal cells and/or contaminated water (Beasley et al., 1983; Carmichael, 1988; Galey et al.,

1987; Mahmood et al., 1988). Adverse effects on human health have also been noted following ingestion of cyanobacteria-contaminated water (Falconer et al., 1983; Bourke and Hawes, 1983; Schwimmer and Schwimmer, 1968; Steyn, 1945). In addition, profound toxic effects are observed when relatively small quantities of extracts or purified toxins are injected into laboratory animals (Falconer et al., 1981; Runnegar et al., 1988).

Two species of cyanobacteria, *Microcystis aeruginosa* and *Nodularia spumigena*, have long been implicated in poisoning of domestic animals (Edler et al., 1985; Stowe et al., 1981; Francis, 1878). Hepatotoxins from *Microcystis* and *Nodularia* have been subsequently isolated from field collections and laboratory cultures and characterized as monocyclic peptides of low molecular weight ( $\approx 1000$  daltons) (Rinehart et al., 1988; Carmichael et al., 1988a; Eriksson et al., 1988; Kusumi et al., 1987; Botes et al., 1985). The hepatotoxins produced by *M. aeruginosa* are heptapeptides called microcystins (MCs; cyanoginosins) (Carmichael et al., 1988b), and the toxin produced by *N. spumigena* is a pentapeptide called nodularin (NL) (Rinehart et al., 1988).

Their toxins have been isolated and purified, and the fate and effects of the compounds partially characterized. The principal species under investigation, *Microcystis aeruginosa*, has apparently caused more animal poisoning incidents than any other freshwater cyanophyte (Carmichael, 1981; Galey et al., 1987) and the primary toxin of interest from this species, microcystin-LR (MCLR) (Figure 1), is a low-molecular-weight (994 daltons) peptide of high toxicity ( $LD_{50}$ : 35 to 50  $\mu\text{g/kg}$  IP mouse). Human toxicosis has also been implicated following contamination of

municipal water supplies with *Microcystis* spp. (Hawkins et al., 1985; Falconer et al., 1983).

MCs and nocularin display very steep dose/effect curves between a dose which will not cause toxic effects and a potentially lethal dose. Consequently, methods for isolation and purification of cyclic peptide toxins as well as methods to determine toxin purity are essential to ensure the validity of trials which assess such parameters as minimal lethal dose (MLD), no effect dose (NED), LD<sub>50</sub>, and pathophysiologic effects.

Early methods for isolation and partial purification of cyclic peptide hepatotoxins from lyophilized cyanobacteria relied upon organic extraction followed by size exclusion chromatography (Botes et al., 1982a,b; Elleman et al., 1978; Kungsuwan et al., 1987). More recent methods (Brooks and Codd, 1986; Krishnamurthy et al., 1986a; Siegelman et al., 1984) have involved solvent extraction, adsorption onto octadecylsilane (ODS) columns, gel filtration column chromatography, and reverse phase high performance liquid chromatography (HPLC). Reversed phase HPLC had also been used to quantify toxins present in lyophilized algae (Siegelman et al., 1984; Brooks and Codd, 1986). All of these methods utilized detection by mouse bioassay and/or ultraviolet light (UV) absorption: The conjugated diene located in the ADDA group gives algal peptide hepatotoxins a UV absorbance maximum near 238 nm. Such methods had enabled production of toxin with relatively high purity from field material and laboratory cultures; however, the lack of specificity of the detection methods sometimes resulted in failure to recognize non-UV-absorbing impurities in

purified toxin specimens. Also, although effective, most of these methods were tedious and contained steps not needed for rapid analysis of cells, and/or they were incapable of separating certain commonly encountered microcystins (MCs) (Harada et al., 1988a,b). Another HPLC method utilized extraction methods similar to those described above, but liquid chromatographic separations in the protocol relied upon weak anion exchange columns instead of ODS (Gathercole and Thiel, 1987). Although this method did not offer any time savings, it was capable of separating all of the MCs tested. Finally, an additional method had been developed which offered savings in time over the above mentioned ones; however, it was unclear whether it would separate the MCs, and it required an expensive HPLC column (Meriluoto and Eriksson, 1988).

Trace level analysis for MCs has been achieved using monoclonal antibodies (Kfir et al., 1986). To stimulate differentiation of antibody producing cells, mice were injected ip with complexes consisting of MC, muramyl dipeptide, and polylysine. Cells were derived for the production of monoclonal antibodies that proved specific for the MCs, and antibodies were produced for screening of drinking water for trace levels of toxin. No analytical methods of any type were known for detection of nonradiolabeled cyanobacterial peptide toxins in exposed animals.

### 3. Rationale Used in the Current Study

In order to standardize toxin material obtained for dosing studies and to improve the capability to recognize other compounds which occur as contaminants of toxin, a thin-layer chromatography (TLC) method was developed. In collaboration with others

at the University of Illinois, and at Meijo, Japan, various methods were investigated and a less time consuming method for purification of peptide toxins from lyophilized cyanobacteria was developed. This method relies upon extraction using aqueous acetic acid and ODS reversed phase silica gel, silica gel chromatography, and HPLC separations with detection at 238 nm. Confirmation of purity utilized TLC with UV detection and iodine vapor and mass spectrometry (MS) (Harada et al., 1988b). In a subsequent study, similar methods (excluding MS) were refined for the analysis of cyanobacterial peptide hepatotoxins (Harada et al., 1988a).

A second hepatotoxin producing cyanophyte being studied is *Nodularia spumigena*. This algae was collected by the research group of M. H. G. Munro from a toxic bloom in Christchurch, New Zealand, and the toxic principle is under structural investigation by the spectroscopy group of Dr. Kenneth Rinehart with Dr. Ken-Ichi Harada and Dr. Michio Namikashi in the Department of Chemistry at the University of Illinois. As in the case of MCLR, we have found that nodularin is a low-molecular-weight toxin of high toxicity ( $LD_{50}$ : 50 to 80  $\mu$ g/kg IP mouse) and the compound has many structural similarities to the toxin from *Microcystis aeruginosa*.

#### 4. Experimental Methods

##### Organisms

Microcystins were extracted from two different strains of *Microcystis aeruginosa*, by two different methods. One of the *Microcystis* strains had been grown in the laboratory of coinvestigator Dr. Wayne Carmichael and was designated as strain PCC-7820. The other *Microcystis* cell material was from a spontaneously occurring

bloom in a farm pond in Monroe, Wisconsin, and was designated as the Monroe strain. Cells from both strains of *Microcystis* were lyophilized prior to toxin extraction.

#### Toxin Extraction and Purification

The procedure used for toxin extraction of the 7820 strain (Figure 1) was developed in the laboratory of coinvestigator Dr. Wayne Carmichael as a modification of the Siegelman method and had been described by Krishnamurthy et al. (1986a).

The procedure developed in our laboratories for toxin extraction of the Monroe strain is shown in Figure 2.

#### Thin-Layer Chromatography

Microcystin which had been extracted from algae cells and found to be of greater than 90% purity by HPLC with UV detection was dried by lyophilization or under a nitrogen stream. Sufficient HPLC grade methanol was then used to redissolve the toxin to a final concentration of 5 µg/µl. Samples of 5, 10, and 25 µg were applied to high-performance silica TLC plates and application was verified by observation under short-wave UV prior to development (toxin absorbs short-wave UV). The TLC plates were placed in preequilibrated TLC chambers. The solvent path was 13 cm.

#### TLC mobile phase

- a. *System 1*—Ethyl acetate-isopropyl alcohol-water (4:3:7). This system forms two phases, and the upper (organic) layer was used for TLC separations.

- b. *System 2*—Chloroform-methanol-water (65:35:10). This solvent system also forms two layers, and in this case, the lower (organic) layer was used for TLC separation.

Detection. The developed TLC plate was heated at 105°C for 5 minutes to evaporate remaining solvents. The plate was visualized under short-wave UV light and the UV absorbing eluted toxin and contaminants were marked with pencil on the silica surface. The plate was then placed in a chamber with sublimed iodine vapor, and after 5 minutes, the positions of the toxin and impurities were again evaluated and similarly marked. The iodine was then driven from the TLC plate by heating at 105°C for 5 to 10 minutes. Finally, the TLC plate was sprayed with 30% H<sub>2</sub>SO<sub>4</sub> in methanol, and heated for 10 minutes at 105°C. The locations of toxin (R<sub>f</sub> 0.25) and impurities were determined by observation of the TLC plate under long-wave UV light and again recorded.

Purity evaluation. The purity of the toxin was subjectively evaluated by observing the relative size and intensity of the spot accounted for by toxin with respect to those produced by impurities at each of the concentrations applied to the TLC plate.

## 5. Results

The TLC method described offers a normal phase separation method and two spray reagents which serve as detectors in addition to the UV detection used in reverse-phase toxin purification. This additional TLC method has proven valuable for the description of toxin material. Purified toxin which had appeared to be of greater



than 95% purity by HPLC with UV detection alone was shown to contain up to 20% contamination when examined using these TLC methods.

6. Discussion and Conclusions

The method developed for purification of the Monroe stain eliminates costly and time-consuming gel filtration steps and reduces toxin extraction time by eliminating the time necessary to evaporate large volumes of water. It has been used to produce only small quantities of purified toxin but has the advantage of isolating the toxin in organic solvents which can be directly applied to silica gel TLC plates to test toxin purity.

UV detection is a valuable tool which can be used in evaluating the concentration and purity of compounds under investigation; but UV alone does not detect some contaminants of purified toxin material, and for this reason, other methods of detection and analysis were needed.

**B. Stability Evaluation of Microcystin in Aqueous Solution**

1. Statement of the Problem, Background, and Rationale

The authors were unaware of any reports on the stability of MCs and were concerned that studies involving dose response would be invalidated if unrecognized toxin degradation occurred over time.

2. Experimental Methods

Stability of purified toxin material was investigated concurrently with development of toxin purification methods. Purified toxin was dissolved in aqueous solution and evaluated periodically to determine the concentration of the toxin present.

Toxin concentration was assessed by comparing the HPLC chromatograms of a freshly prepared toxin standard solution with those of toxin solutions stored under conditions of freeze/thaw, refrigerate/warm, or constant room temperature.

3. Results and Discussion

Degradation of toxin was noted only after exposure to extreme conditions such as repeated freeze/thaw or after storage of toxin at room temperature in excess of 1 week.

Figure 1. Microcystin extraction procedure used in the laboratories of Dr. Wayne W. Carmichael.

- 1) 1 GM CELLS + 200 ML 5% BUTANOL-20% METHANOL-75% WATER  
STIR 1 TO 3 HOURS AT 4°C  
CENTRIFUGE 100,000 X G—1 HOUR AT 4°C  
REPEAT 3 TIMES WITH CELL PELLETT
- 2) COMBINE SUPERNATANTS  
REDUCE VOLUME TO 300 TO 350 ML BY AIR DRYING
- 3) SUPERNATANT PASSED THROUGH ANALYTICHEM BOND  
ELUTE C-18 COLUMN  
ELUTE TOXIC FRACTION WITH 3 TO 5 ML 100% MeOH  
REPEAT PROCESS 3 TO 4 TIMES (3 TO 4 X)
- 4) DRY COMBINED METHANOL EXTRACT WITH NITROGEN  
DISSOLVE RESIDUE IN 5 ML WATER  
PASS THROUGH 3.0-MICRON MILLIPORE FILTER
- 5) K-26 PHARMACIA COLUMN (26 MM X 80 CM)  
WITH 100 GM SEPHADEX G-25  
ELUTE IN 5% METHANOL WATER  
MONITOR AT 240 NM  
TOXIN IS FIRST LARGE PEAK OFF THE COLUMN
- 6) HPLC-ALTEX C-18 9.4 MM X 25 CM  
0.01 AMMONIUM ACETATE IN 26% ACETONITRILE/WATER  
FLOW RATE 3 ML/MINUTE  
MONITOR AT 240 NM
- 7) LYOPHILIZE TOXIC PEAK  
DESALT TOXIN BY HPLC  
AS IN STEP 6—USING 26% ACETONITRILE/WATER
- 8) STORE TOXIN AT -80°C UNTIL USE

Figure 2. Modified extraction method for microcystin developed at the University of Illinois and used for Monroe strain.

- 1) 1 GM CELLS + 200 ML METHANOL  
STIR 1 TO 3 HOURS AT 21°C  
CENTRIFUGE AT 3,000 X G FOR 10 MINUTES  
REMOVE SUPERNATANT
- 2) EVAPORATE SUPERNATANT IN ROTARY EVAPORATOR TO DRYNESS  
REDISSOLVE RESIDUE IN APPROXIMATELY 10 ML OF H<sub>2</sub>O
- 3) RESIDUE PASSED THROUGH PRECONDITIONED ANALYTICHEM BOND ELUTE  
C-18 COLUMN  
C-18 COLUMN WITH TOXIN RINSED WITH APPROXIMATELY 5 µL OF H<sub>2</sub>O  
ELUTE TOXIN IN 3 ML OF METHANOL  
EVAPORATE METHANOLIC TOXIN SOLUTION UNDER NITROGEN STREAM
- 4) SLURRY PACK SILICA GEL COLUMN WITH CHCl<sub>3</sub>:MeOH:H<sub>2</sub>O  
65:35:10 (BOTTOM LAYER)  
50 GRAMS OF FLASH SILICA IS PACKED INTO 30 CM X 2.55 CM GLASS COLUMN  
TOXIN-CONTAINING RESIDUE IS DISSOLVED IN COLUMN MOBILE PHASE AND  
INTRODUCED INTO COLUMN  
THE TOXIN IS ELUTED UNDER ISOCRATIC CONDITIONS AND MONITORED  
BY TLC
- 5) SILICA COLUMN TOXIN-CONTAINING FRACTIONS ARE COMBINED AND  
THE ORGANIC SOLVENT EVAPORATED
- 6) HPLC—C-18—ALTEX 4.6 MM X 25 CM  
METHANOL:0.05% TRIFLUOROACETIC ACID IN H<sub>2</sub>O (70:30)  
FLOW RATE = 2.0 ML/MINUTE, TOXIN ABSORBS AT 240 MINUTES
- 7) COMBINE FRACTIONS CONTAINING TOXIN
- 8) DESALT WITH KRPTOFIX 221B POLYMER AND KRPTOFIX 222B POLYMER  
(E. MERCK, DARMSTADT, FRG)  
  
STORE TOXIN AT -80°C UNTIL USE

## II. STRUCTURE ACTIVITY RELATIONSHIPS WITH MICROCYSTIN-LR AND NODULARIN

### A. Structure/Toxicity Relationships of Dehydro Amino Acids of Microcystin-LR and Nodularin

#### 1. Statement of the Problem

The specific components of algae cyclic peptides responsible for toxicity had not been explored prior to the present research.

#### 2. Background and Review of Literature

The first moiety explored with regard to its importance in toxicity in MCLR and nodularin were the dehydro amino acids. In fact, the presence of dehydro amino acids is a uniform characteristic of all algal peptide hepatotoxins described to date. Unsaturated amino acids of this type have been found in other peptides, usually of microbial origin, and are closely linked to their associated bioactivities. For example, the antibiotics nisin and subtilin, produced by bacteria, contain  $\alpha,\beta$ -unsaturated amino acids believed to be essential to their antibiotic activity (Gross, 1975). The toxic agents phomopsins A and B are cyclic hexapeptides produced by the fungus *Phomopsis leptostromiformis* which contain didehydro amino acids and cause lupinosis (characterized by liver damage) in Australia.

In fact, most of the dehydro amino acids identified to date have been encountered in relatively low molecular weight cyclic peptides from microbial sources that have a variety of biological activities (Noda et al., 1983). Biologically active

$\alpha,\beta$ -dehydro peptides may be divided into two classes: 1) those that lose their activity upon saturation of the double bond, for example, by hydrogenation or by mercaptan addition, as in the case of AM-toxin, an alternariolide (Shimohigashi et al., 1978); and 2) those that retain a major portion of their activity following saturation, as in the case of nisin (Gross, 1975). In the first group, the double bonds of the dehydro peptides may play important direct roles in the expression of activity, whereas in the second group the  $\alpha,\beta$ -double bonds are assumed to provide overall stability to the peptides, possibly resulting in rigidity, increased hydrophobicity, or resistance to enzymatic degradation (Noda et al., 1983). A working hypothesis for the biological action of cyclic peptides containing dehydro amino acids suggests that the toxins may exert biological effects by reacting with essential sulfhydryl groups in enzymes. Another possible explanation is that sites of  $\alpha,\beta$ -unsaturation stimulate the release of lysozymes leading to architectural breakdown (Shimohigashi et al., 1978). The importance of  $\alpha,\beta$ -unsaturated amino acids has been investigated via the chemical synthesis of dehydro analogs of peptide hormones, peptide antibiotics, and other bioactive peptides in order to elucidate their contributions to interactions with receptors and thus to develop therapeutically useful pharmaceuticals (Noda et al., 1983).

In the present study, the dehydro amino acids of the MCLR and NL were selectively reduced in order to assess the changes in toxicities *in vivo*. The dihydro MCLR products were compared with the parent toxin in whole animal toxicity trials

in order to assess the role of the dehydro amino acid units in the hepatotoxicity and overall lethality of the peptide toxins.

### 3. Rationale Used in Current Study

To begin to determine which structural aspects are responsible for the high toxicity of algal peptide toxins, we conducted numerous investigations into the structure/toxicity relationships of functional moieties of MCLR. In addition, in conjunction with Dr. Kenneth Rinehart's group, nodularin from *Nodularia spumigena* was isolated, purified, structurally characterized, and structurally modified for similar structure activity determinations. In microcystins, the dehydro amino acid is commonly N-methyldehydroalanine (Botes et al., 1982a; Kungsuwan et al., 1987; Painuly et al., 1988), and in NL it is N-methyl-Z-dehydrobutyrine (Rinehart et al., 1988). In addition to these dehydro amino acids, both compounds also possess the unusual C20 amino acid, 3-amino-9-methoxy-2,6,8-trimethyl-10-phenyl-4,6-decadienoic acid (Adda), as well as D-glutamic acid (D-Glu), L-arginine (L-Arg), and D-β-methylaspartic acid (Figure 1). Nodularin has two fewer amino acid residues than the microcystin and yet has approximately the same toxicity.

### 4. Experimental Methods

#### Chemicals and Toxins

All chemicals were reagent grade or, in the case of solvents, HPLC grade. NL was extracted from a toxic bloom of *N. spumigena* collected near Christchurch, New Zealand, and purified as previously described (Rinehart, et al., 1988). MCLR was extracted from laboratory cultured *M. aeruginosa* strain PCC-7820 and purified as

reported previously (Krishnamurthy et al., 1986a). All toxins and derivatives were determined to be > 99% pure by HPLC (Harada et al., 1988a) and TLC (Harada et al., 1988b) prior to chemical reactions or studies with laboratory animals.

Synthesis of Dihydromicrocystin-LR (2H-MCLR) and Dihydronodularin (2H-NODLN)

The dihydro derivatives were formed by hydrogenation of the dehydro amino acid contained in the cyclic peptide. NL (4.9 mg) was reduced with an excess of sodium borohydride ( $\text{NaBH}_4$ ) (23.5 mg) in methanol/water (1:1) for 24 hours at room temperature ( $23^\circ\text{C}$ ) with continuous stirring. The reaction mixture was monitored periodically by silica TLC (NL Rf: 0.27, 2H-NL Rf: 0.29, 0.31) using a solvent system consisting of the organic phase of a mixture of ethyl acetate-2-propanol- $\text{H}_2\text{O}$  (4:3:7). Additional  $\text{NaBH}_4$  was added in excess (total of 22.5 mg) as needed followed by additional stirring at room temperature to complete the conversion to the dihydro products (Figure 2). When parent toxin could no longer be detected in the reaction mixture, the reaction was stopped by addition of 10% acetic acid (0.5 ml, pH 4). Finally, products were evaporated to dryness *in vacuo* on a rotary evaporator.

In the conversion of MCLR, toxin (5.2 mg) was reacted with an excess of  $\text{NaBH}_4$  (21 mg) in methanol (2.0 ml) at room temperature for 24 hours, then the reaction product was monitored on TLC (MCLR Rf: 0.30, 2H-MCLR Rf: 0.31, 0.33) by the same method as described for NL. No parent toxin was detected at the end of 24 hours, so the reaction was stopped with 10% acetic acid (0.5 ml, pH 4). The reaction product was then evaporated to dryness *in vacuo* on a rotary evaporator.



### Thin-Layer Chromatography

Reaction products were spotted on high-performance silica gel TLC plates. The elution solvent was chloroform-methanol-water (65:35:10). This mixture forms two phases and the lower phase (organic) was used. The toxin derivative was observed under short-wave UV light, and iodine vapor was used as a detection reagent.

### Purification of 2H-MCLR or 2H-NL and Characterization by HPLC

Primary purification of reaction mixtures was achieved by placing the products dissolved in 0.5 ml of water on preconditioned 1 g C<sub>18</sub> cartridges (Analytichem International, Harbor City, CA, USA), rinsing with water (3 x 2 ml) followed by 3 ml of 10% methanol, and eluting with methanol (3 x 2 ml).

Final purification was by reversed-phase HPLC with an Alltech C<sub>18</sub> column ( $\phi$  4.6 x 250 mm) or a Nucleosil-5 C<sub>18</sub> ( $\phi$  4.6 x 150 mm) column, using a mobile phase of methanol and 0.05% trifluoroacetic acid in water (70:30). A mobile phase of methanol and 0.05 M phosphate buffer (pH 3) (58:42) also provided good separations of reaction products. Detection was achieved by UV absorbance at 238 or 254 nm.

Typical HPLC chromatograms of parent MCLR and its dihydro products are shown in Figure 3. The chromatogram of purified toxin shows the presence of a small peak (arrow). These small peaks are often present both in purified MCLR and purified NL. These components share the same molecular weights as their respective larger peaks (Harada et al., 1988a). The chromatogram of 2H-MCLR shows the presence of two primary peaks which are epimers resulting from borohydride

reduction (arrows). A total of 4.5 mg of purified 2H-NL and 4.6 mg of 2H-MCLR was produced.

#### Confirmation of Structural Alterations

Mass spectral confirmation of the reaction product was accomplished with fast atom bombardment mass spectroscopy (FAB-MASS) using a ZAB-SE 10 kV mass spectrometer. The compounds were mixed with magic bullet matrix (1:3, dithiothreitol-dithioerythritol) and analyzed using a source temperature of 30°C, and an acceleration potential of 8 kV.

#### Mouse Bioassay

Adult female Balb/c mice (Harlan Sprague-Dawley, Indianapolis, IN) were used for all toxicity trials. In two separate experiments, one involving MCLR and the other involving NL, animals were dosed intraperitoneally with either the saline vehicle, parent toxin, or the respective dihydro derivative and monitored for 24 hours (Table 1). Mice dosed with parent NL received either 25, 50, 100, 200, or 300 µg/kg of toxin to serve as positive controls. Mice dosed with the vehicle (physiologic saline) alone were injected with volumes of 0.25, 0.50, 0.75, or 1.0 ml to serve as negative controls. Mice given 2H-NL were dosed at 100, 200, 300, 400, 500, or 1,000 µg/kg body weight in less than 1.0 ml of the vehicle. Mice given parent MCLR were dosed at 25, 50, or 100 µg/kg and mice given 2H-MCLR were given 25, 50, 100, 200, 300, or 400 µg/kg.

Survival times of animals were recorded along with liver, kidney, and whole body weights. Animals which survived 24 hours after toxin administration were killed

by cervical dislocation. Negative control animals were killed at times within the study where numerous toxin-produced deaths were occurring or at 24 hours when toxin-dosed survivors were killed. Tissues (liver, kidneys, lungs, spleen, stomach, small intestine, large intestine, heart) were examined grossly for lesions. Selected tissues including liver and kidney were fixed by immersion in 10% neutral-buffered formalin, routinely processed, embedded in paraffin, sectioned at 4 to 6  $\mu\text{m}$ , and stained with hematoxylin and eosin.

## 5. Results

### Structural Contamination

Specifically, in low-resolution FABMS, characteristic pseudomolecular ions of 995 and 997 ( $M + H$ )<sup>+</sup> were observed for MCLR and 2H-MCLR and ions of 825 and 827 ( $M + H$ )<sup>+</sup> were observed (Figure 4) for NL and 2H-NL, respectively. High-resolution FABMS confirmed structural formulas of  $C_{49}H_{74}N_{10}O_{12}$  ( $M + H$ ,  $\pm 0.6$  mmu) and  $C_{49}H_{76}N_{10}O_{12}$  ( $M + H$ ,  $\pm 1.6$  mmu) for MCLR and 2H-MCLR, and  $C_{41}H_{61}N_8O_{10}$  ( $M + H$ ,  $\pm 3.2$  mmu) and  $C_{41}H_{63}N_8O_{10}$  ( $M + H$ ,  $\pm 1.2$  mmu) for NL and 2H-NL, respectively.

Thus, sodium borohydride treatment selectively added two hydrogen atoms across the double bond of the dehydroamino acid (n-methyl-Z-dehydrobutyrine) of the toxins resulting in formation of the dihydro derivatives. The identity of the dihydro toxins were confirmed by FABMS and found to be equal to the mass of the parent toxin plus two mass units (from the two hydrogen atoms added).

### Statistical Analysis

Within each of the two experiments, one-way analyses of variance (ANOVA) were used to compare the relative organ weight data from all groups and the differences in survival times between nonsurvivors of the different treatment groups. Similarly, within each experiment, ANOVAs were used to compare organ weights among the groups of each experiment and, similarly, to compare the organ weights of survivors with those of nonsurvivors for each compound. A level of  $\alpha = 0.05$  was chosen to detect differences among groups with those of nonsurvivors for each compound.

### MCLR and 2H-MCLR

Survival rates and times. All mice dosed with MCLR at 100  $\mu\text{g/kg}$  or 2H-MCLR at 200, 300, or 400  $\mu\text{g/kg}$  died within 3 hours of administration of the test agent. All control animals, animals dosed with MCLR at 25 or 50  $\mu\text{g/kg}$  and 2H-MCLR at 25, 50, and 100  $\mu\text{g/kg}$  survived the 24-hour observation period. No significant differences were found in survival times between groups of nonsurvivors given MCLR ( $102 \pm 16$  minutes) or 2H-MCLR ( $114 \pm 22$  minutes, mean  $\pm$  SD).

Lesions. No lesions were noted in tissues of control mice or those given MCLR at 25  $\mu\text{g/kg}$  or in mice given 2H-MCLR at 25, 50, or 100  $\mu\text{g/kg}$ . Livers from mice dosed with MCLR at 50  $\mu\text{g/kg}$  were characterized by occasional, scattered, single cell necrosis of hepatocytes immediately adjacent to the central vein. Mice dosed with MCLR at 100  $\mu\text{g/kg}$  and those given with 2H-MCLR at 200, 300, or 400  $\mu\text{g/kg}$  had similar gross and microscopic hepatic lesions. Lethally affected animals had swollen

dark red livers at the time of death. Other organs appeared normal. Histologically evident hepatic lesions included severe, widespread centrilobular and midzonal hepatocyte dissociation, rounding, degeneration, and necrosis with massive intralesional hemorrhage. In more mildly affected adjacent areas, many hepatocytes contained one to several large, clear intracytoplasmic vacuoles. Renal lesions included only vascular congestion and accumulation of small amounts of granular material in lumens of cortical tubules.

Liver and kidney weights. The mean liver and kidney weights for each group of treated animals are shown in Figures 5 and 6. When relative liver and kidney weights were compared among groups of nonsurvivors, no significant differences were detected. Similarly, no significant differences were detected when relative liver and kidney weights were compared among groups of survivors including controls. However, when the survivors of MCLR were grouped and compared with grouped nonsurvivors of MCLR; significantly greater relative liver weights were detected in grouped nonsurvivors. Similarly when survivors of 2H-MCLR were grouped and compared with nonsurvivors of 2H-MCLR, significantly higher relative liver and kidney weights were detected in the nonsurvivors.

#### NL and 2H-NL

Survival rates and times. All mice given doses of NL at 25 or 50  $\mu\text{g/kg}$  or 2H-NL at 100, 200, 300, and 400  $\mu\text{g/kg}$  survived. All mice given NL at 100, 200, or 300  $\mu\text{g/kg}$  and mice treated with 2H-NL at 500 or 1000  $\mu\text{g/kg}$  died within 4 hours of

administration. No significant differences were detected in survival times of groups of nonsurvivors (NL:  $118 \pm 49$  minutes, 2H-NL:  $125 \pm 34.9$  minutes).

Lesions. No lesions were seen in control mice or those given NL at 25 or 50  $\mu\text{g/kg}$ . Mice which died within 3 hours of dosing in both groups had markedly enlarged, dark red livers. Animals which survived after being given 2H-NL had liver lesions unlike those of survivors of sublethal doses of NL. On gross examination, the outer portions of livers of the survivors of 200, 300, and 400  $\mu\text{g/kg}$  of 2H-NL were extremely pale, whereas the inner portions appeared dark and congested. The livers of mice given 2H-NL at 100  $\mu\text{g/kg}$  were normal in color but friable.

Microscopically, hepatic lesions in mice that died from either NL or 2H-NL included severe, widespread centrilobular and midzonal hepatocyte disassociation, rounding, and degeneration and necrosis involving all regions except for a rim of periportal hepatocytes three to six cells wide. Massive intrahepatic hemorrhage was also present in association with the disassociated and necrotic areas. Some of the periportal hepatocytes exhibited varying degrees of degeneration. In addition, the livers of mice surviving 2H-NL administration had extensive subcapsular hepatocellular necrosis and hemorrhage in peripheral areas that grossly were pale. The lesions occurred in a dose-dependent fashion with animals given higher doses having more severe subcapsular hemorrhage. Renal cortical tubules were mildly dilated and contained moderate amounts of eosinophilic to basophilic granular material. No adverse effects of vehicle administration were detected.

Liver and kidney weights. The relative liver and kidney weights for treated animals are shown in Figures 5 and 6, parallelling those of the MCLR/2H-MCLR already discussed. Increases in liver weights were not significantly different among groups of nonsurvivors; and similarly, there were no significant differences among liver and kidney weights of groups of survivors. As in the case of 2H-MCLR, increases in kidney weights were detected in nonsurvivors of 2H-NL. Increases in kidney weights were also noted in mice that died following NL administration.

6. Discussion and Conclusions

The responses to MCLR observed in this study such as rapid deaths, hemorrhagic livers with increased weights, and steep dose response curves with minimal toxic effects at sublethal doses were consistent with previous reports for toxins produced by *Microcystis* (Elleman et al., 1978; Runnegar and Falconer, 1981; Adams et al., 1988). The toxicity and predominant toxic effects of NL were similar to those of MCLR and to other reports of structurally unknown toxins extracted from *Nodularia* (Runnegar et al., 1988). Increases in relative liver and kidney weight are a sensitive indicator of the toxic effects of these cyclic peptide toxins (Lovell, et al., 1989). The absence of a significant increase in the kidney weights in the MCLR treated animals in this study was therefore unusual and probably was, in part, a result of considerable variation in kidney weights of animals in the control group.

The lethal doses of 2H-MCLR and 2H-NL produced effects similar to those of their parent compounds: Survival times were not affected, and the narrow threshold between doses which cause almost no effect and potentially lethal doses was retained.

Thus, with all doses of either parent or dihydro toxin, the effects seemed to be nearly "all or nothing," with only mild changes observed in sublethally dosed animals and marked lesions in lethally dosed animals. In addition, liver lesions, liver weights, and survival times did not become progressively more severe after the lethal threshold for the toxins had been crossed.

The fact that lesions and subcapsular hemorrhage were noted in animals given sublethal doses of 2H-NL and not noted in survivors of NL administration is not easily explained. Previous reports of subcapsular hemorrhage resulting from the administration of *Nodularia* extracts (Runnegar et al., 1988) and *Microcystis* toxins presumed that this hemorrhage was evidence of direct absorption through the capsule (Runnegar et al., 1986). Perhaps 2H-NL is more readily absorbed directly through the capsule than the other compounds examined in this study.

Both MCLR and NL possess Adda, two acidic amino acids in the stereospecific "D" configuration involved in isolinkages, L-Arg, and one dehydro amino acid. MCLR contains two more amino acids than NL yet nearly identical lethal potency is seen. It is concluded, therefore, that the D-alanine and L-leucine contained in MCLR contribute little to the toxic action of these molecules since their absence in NL does not greatly influence lethal toxicity or hepatospecificity.

Remaining portions of the molecules which appear to contribute to the overall toxicity of these compounds include: D-amino acids and peptide linkages which do not involve the  $\alpha$ -carboxyl group and which retard normal enzymatic degradation, and also the unusual hydrophobic amino acid Adda. Perhaps the role of the dehydro



amino acid in these cyclic peptides is to provide overall stability to the peptide structure through increased rigidity, increased hydrophobicity, or resistance to enzymatic degradation. The present study indicates that, while the dehydro amino acids appear to contribute to the overall toxigenic potential of the molecule, they are not essential for the hepatotoxic and apparently hepatospecific properties of these compounds.

Figure 1. Structures of microcystin-LR and nodularin: two monocyclic peptide hepatotoxins from cyanobacteria.

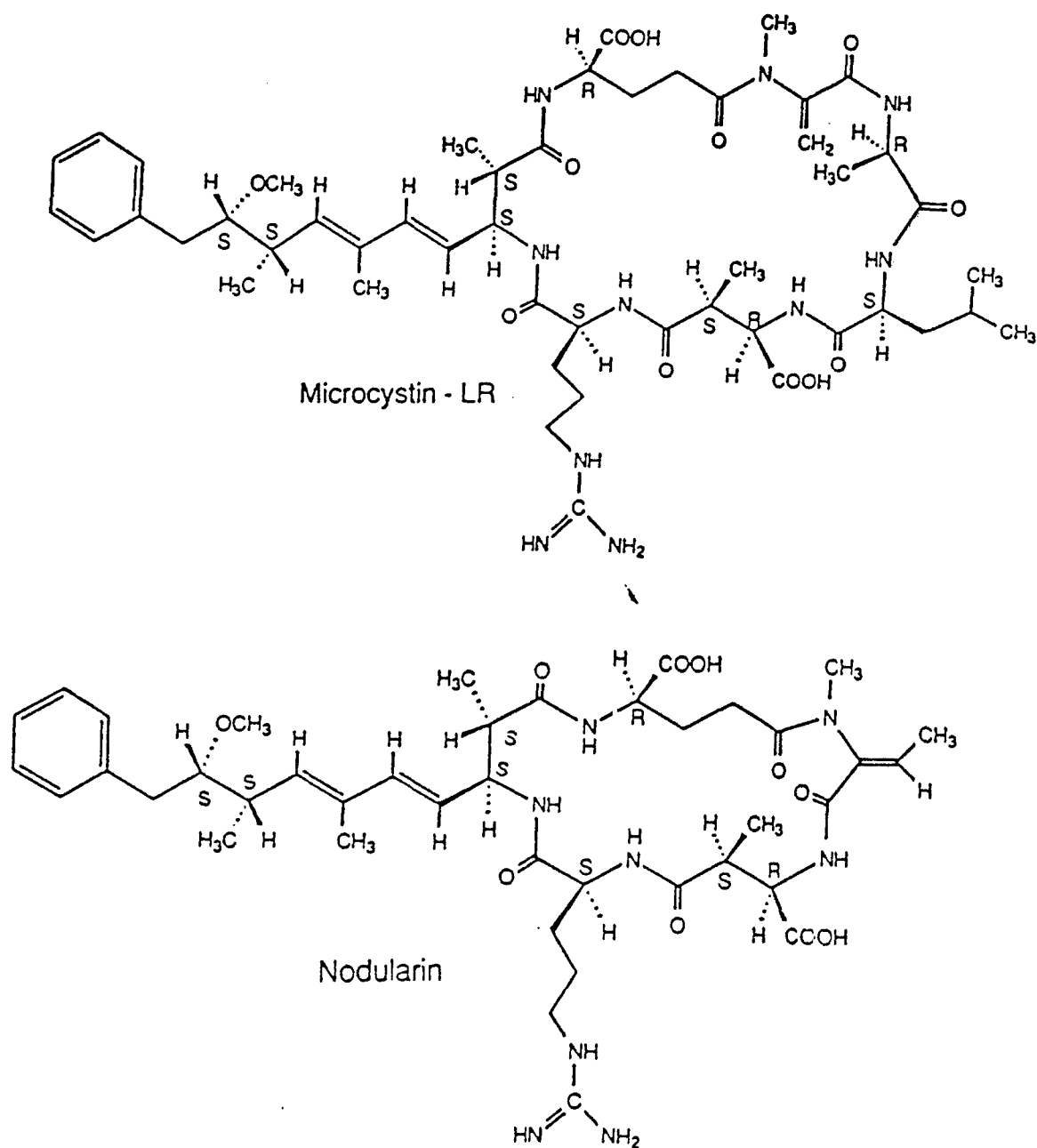
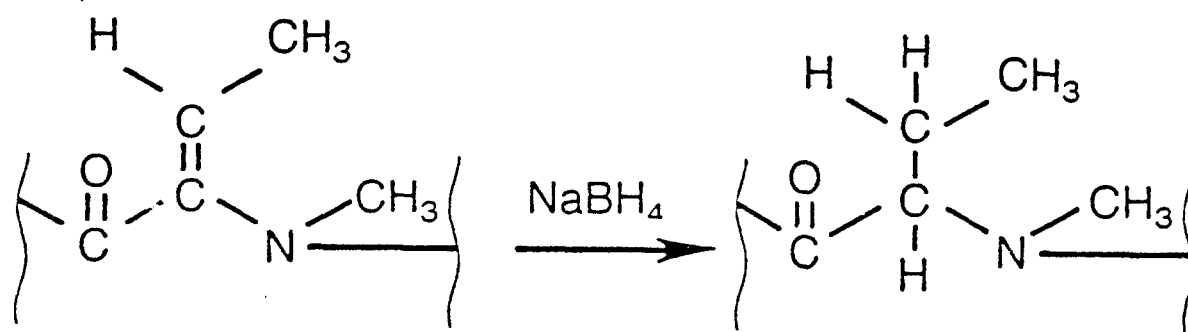


Figure 2. Sodium borohydride reduction of: A) N-methyl-Z-dehydrobutyrine from nodularin and B) N-methyldehydroalanine from microcystin-LR.

**A.**



**B.**

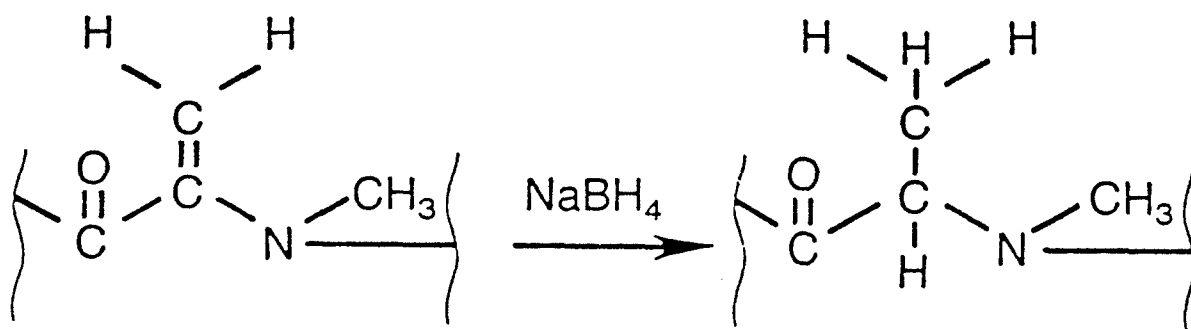


Figure 3. Typical HPLC chromatograms of: A) Purified microcystin-LR and B) dihydromicrocystin-LR. Arrows in A indicate small peak associated with purified parent toxins and in B identify the epimers which result from borohydride reduction.

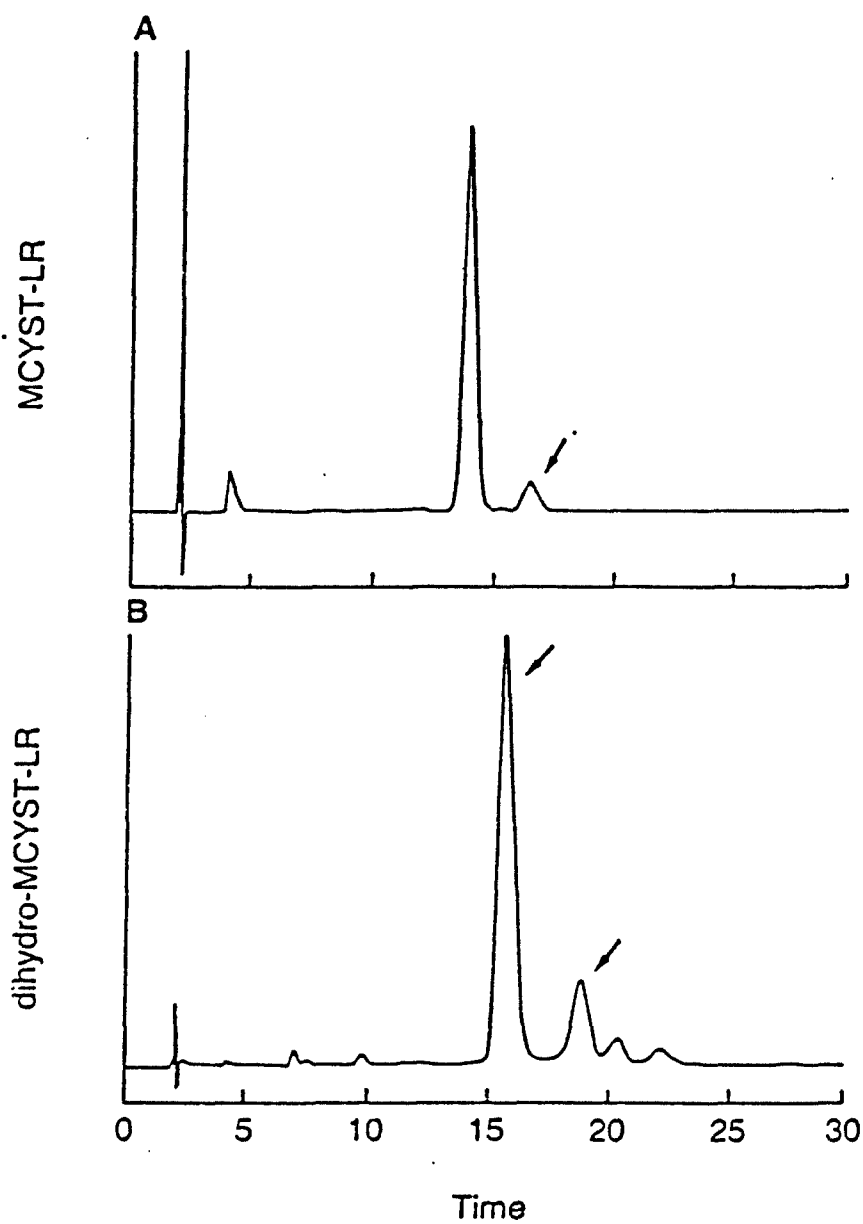


Figure 4. a. Fast atom bombardment mass spectrometric analysis of: microcystin-LR and dihydromicrocystin-LR. MB = magic bullet matrix (1:3, dithiothreitol-dithioerythritol).

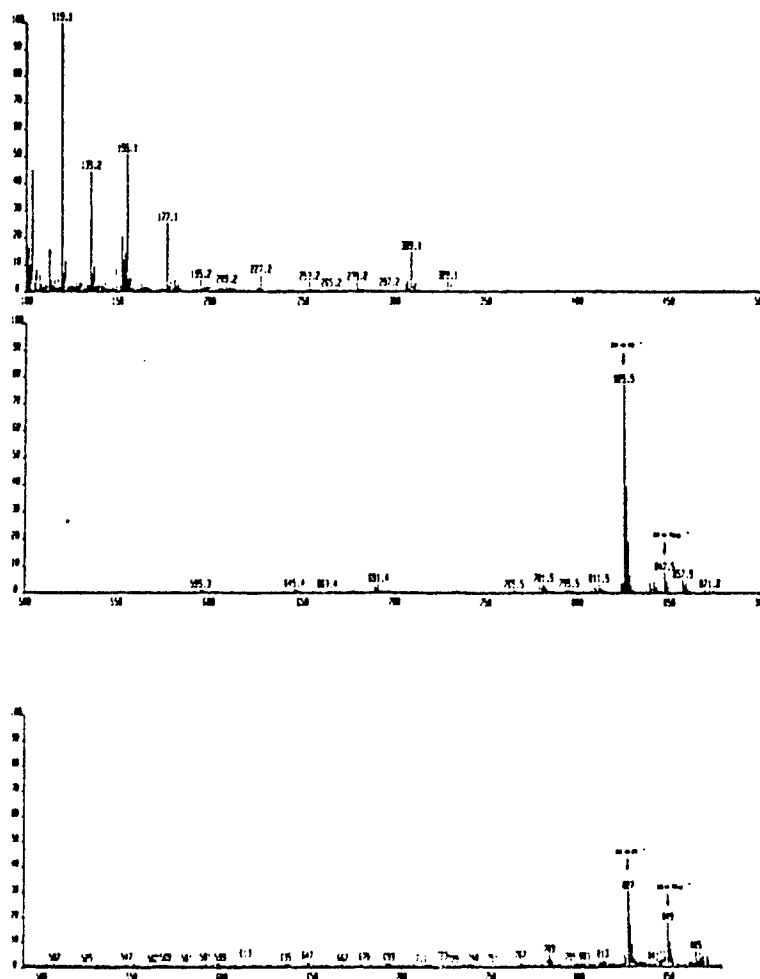


Figure 4. b. Fast atom bombardment mass spectrometric analysis of: nodularin and dihydronodularin. MB = magic bullet matrix (1:3, dithiothreitol-dithioerythritol).

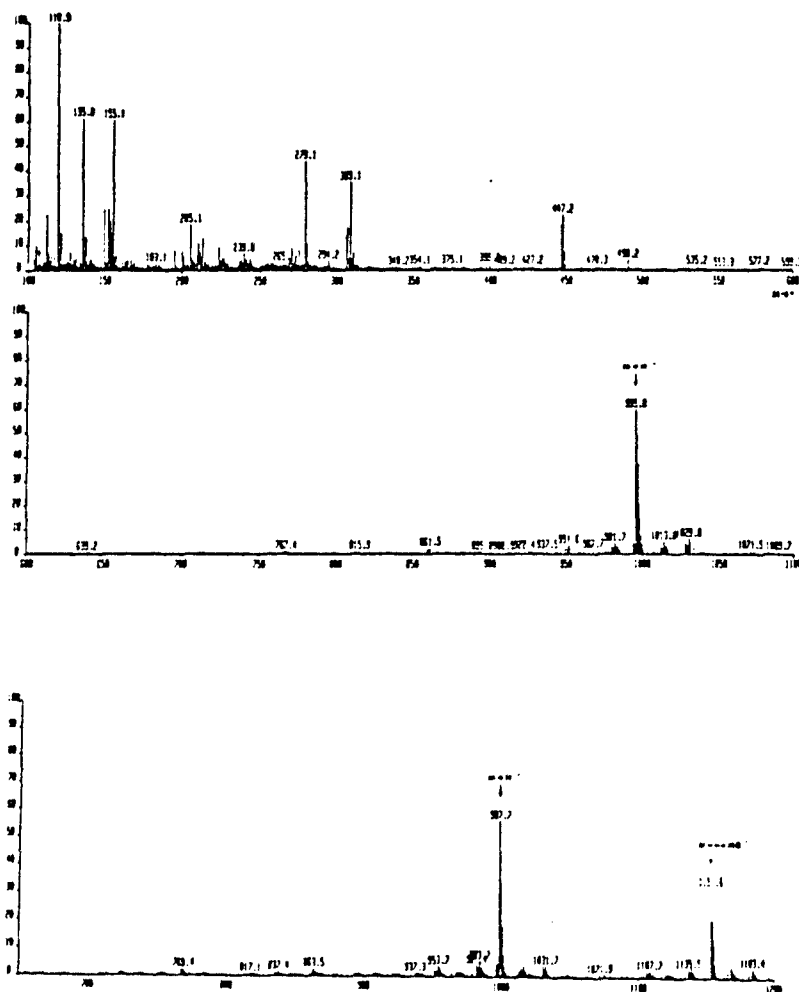


Figure 5. Relative liver weights of toxin treated mice. Mean  $\pm$  standard deviation. N = 3 mice/group for nodularin and dihydronodularin, and N = 6 mice/group for microcystin-LR and dihydromicrocystin-LR.

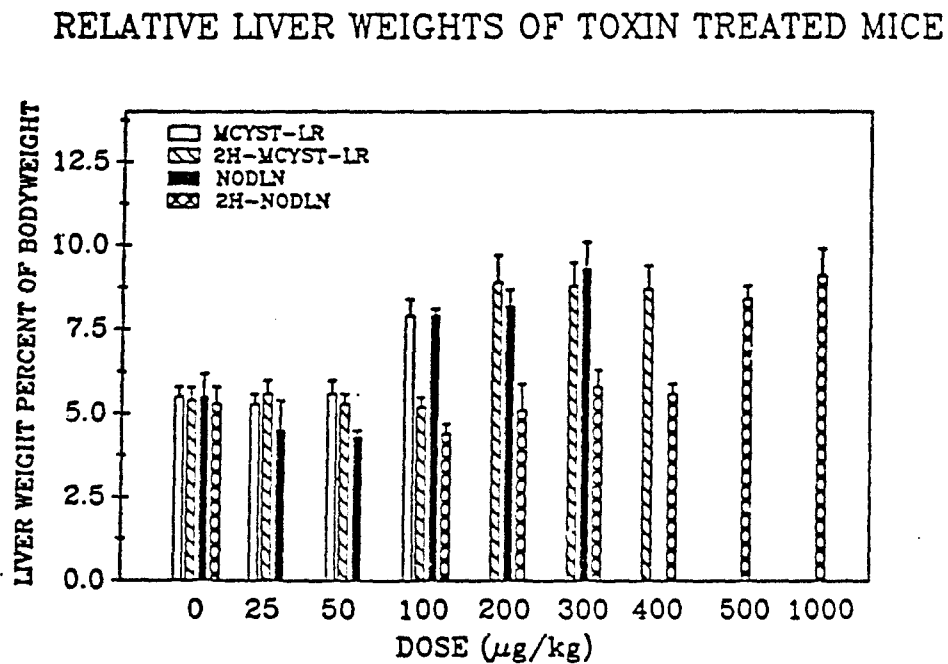
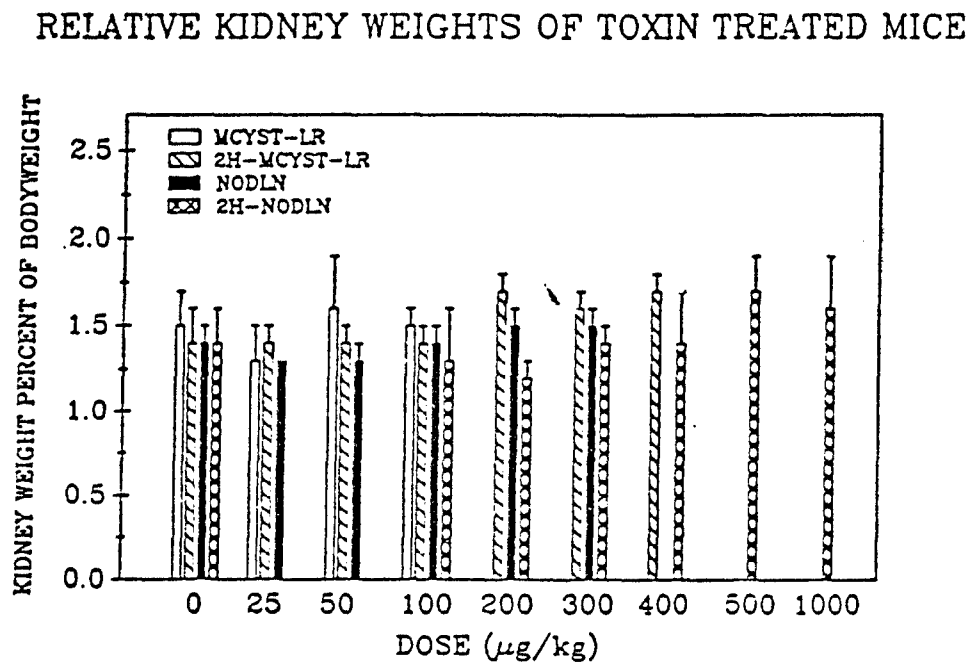


Figure 6. Relative kidney weights of toxin treated mice. Mean  $\pm$  standard deviation. N = 3 mice/group for nodularin and dihydronodularin, and N = 6 mice/group for microcystin-LR and dihydromicrocystin-LR.





## B. The Contribution of Amino Methoxy Trimethyl Phenyldeca-dienoic Acid (Adda) to the Toxicity of Microcystin-LR and Nodularin

### 1. Statement of the Problem under Study, Background, and Rationale

The structures (Figure 1) of both MCLR and NL have in common: the unusual hydrophobic amino acid, 3-amino-9-methoxy-2,6,8-trimethyl-10-phenyldeca-4,6-dienoic acid (Adda), two acidic amino acids in the stereospecific "D" configuration, and involved in peptide linkages which do not involve the  $\alpha$ -carboxyl, L-Arginine, and one dehydro amino acid.

Structural aspects of MCLR and NL not investigated above but believed to be likely to contribute to the overall toxicity of these compounds include: 1) the D-amino acids and the isolinkages of the acidic amino acids which probably retard normal enzymatic degradation (Botes et al., 1986), 2) the absence of N and C terminal amino acids due to the cyclic nature of the compound which is also likely to retard enzymatic degradation, and 3) the unusual hydrophobic amino acid Adda which is consistently present in cyanobacterial cyclic peptide hepatotoxins. Here, we investigated the toxicological significance of the Adda moiety in MCLR and NL.

### 2. Experimental Methods

#### Compounds

MCLR or NL (1 mg) was placed in sealed vessels and reduced with excess hydrogen gas and a palladium catalyst. This reaction causes the addition of a total of six hydrogen atoms to the toxin by saturating both the dehydro amino acid and the

double bond of the hydrophobic tail of the adda moiety. The identity of the reaction products were evaluated using fast atom bombardment mass spectroscopy (FABMS).

In addition, MCLR was modified such that the bulk of the hydrophobic portion of Adda was removed but the molecule retained its basic structure (Third Annual Report, pp. 42-48). In the first of these experiments, MCLR was subjected to ozonolysis for 30 minutes then reduced with excess sodium borohydride to yield a cyclic peptide structure which lacked all points of unsaturation (Figure 2).

MCLR was also first reduced with sodium borohydride to form the [ $^3\text{H}$ ]-2H-MCLR derivative which results from hydrogen addition to the N-methyl dehydroalanine, then subjected to ozonolysis and reduced with sodium borohydride to yield another cyclic product which lacked points of unsaturation (Figure 3).

Finally, Adda was synthesized and confirmed to have the same stereochemistry as the natural product (Namikoshi and Rinehart, unpublished data). The toxin derivatives were purified and separated from parent compounds and confirmed by fast atom bombardment mass spectrometry as described by Rinehart et al. (1988). The toxicities of both the free amino acid and the protected amino acid (Figure 4) were then compared with parent MCLR by mouse bioassay.

#### Animals and Dosing Procedures

Male Swiss Webster mice (Harlan Sprague-Dawley, Indianapolis, IN) were dosed intraperitoneally with either the appropriate toxin derivative, the parent toxin, or the saline vehicle and monitored for 24 hours. Animals which survived the observation period were killed by cervical dislocation. Survival times and whole body, liver, and

kidney weights were determined. Tissues (liver, kidneys, spleen, small intestine, large intestine, heart) were examined grossly for lesions. Sections of tissue were then fixed by immersion in 10% neutral-buffered formalin for histologic examination. After fixation, the sections were routinely processed, embedded in paraffin, cut at 4 to 6  $\mu\text{m}$ , and stained with hematoxylin and eosin.

### 3. Results

Approximate minimum  $\text{LD}_{100\text{s}}$  for these compounds are given in Table 1. At the doses examined, the cyclic peptide compounds with Adda removed through ozonolysis or with Adda saturated exhibited none of the toxicity associated with parent MCLR. These data indicate that the hydrophobic portion of Adda, in the correct configuration, is essential for bioactivity. Nevertheless, Adda by itself in either the protected or the deprotected form did not produce the toxic effects associated with either MCLR or NL.

Animals which survived for 24 hours after toxin, derivative, or vehicle administration did not show any gross or histologic lesions associated with MCLR, and organ weights were not notably different from vehicle controls. Positive control animals given MCLR at 100  $\mu\text{g/kg}$  had elevated liver weights and severe liver lesions including: widespread centrilobular and midzonal hepatocyte dissociation, rounding, degeneration, and necrosis of hepatocytes with massive intralesional hemorrhage.

### 4. Discussion and Conclusions

The structural variations explored to date in the dehydro amino acids, as well as the variable L-amino acids in a range of microcystins do result in altered toxicity, but

these component changes do not affect the hepatospecific nature of the toxicosis. By contrast, alterations in the Adda moiety produce marked reductions in lethal toxicity and hepatic damage. These data demonstrate that the hydrophobic portion of Adda is likely to play an active role either in the transport of algal peptides into the cell or in the basic biochemical mechanism. Moreover, the hydrophobic portion of Adda must be in the correct stereo configuration.

Table 1. Comparative toxicity of synthetic derivatives of cyclic peptide toxins from cyanobacteria.

Toxin	LD <sub>100</sub> (minimum)
Nodularin	97 nM/kg
Microcystin-LR	90 nM/kg
Hexahydro-Microcystin-LR <sup>2</sup>	> 2,000 nM/kg
Hexahydro-Nodularin <sup>2</sup>	> 2,000 nM/kg
O <sub>3</sub> Product 1 of Microcystin-LR <sup>2</sup>	> 16,000 nM/kg
O <sub>3</sub> Product 2 of Microcystin-LR <sup>2</sup>	> 16,000 nM/kg
Protected Adda*	> 1,600 nM/kg
Adda (Free Amino Acid)*	> 1,600 nM/kg

\*Adda = 3-amino-9-methoxy-2,6,8-trimethyl-10-phenyl-4,6-decadienoic acid.

**Figure 1. Structures of Microcystin-LR (a) and Nodularin (b).**

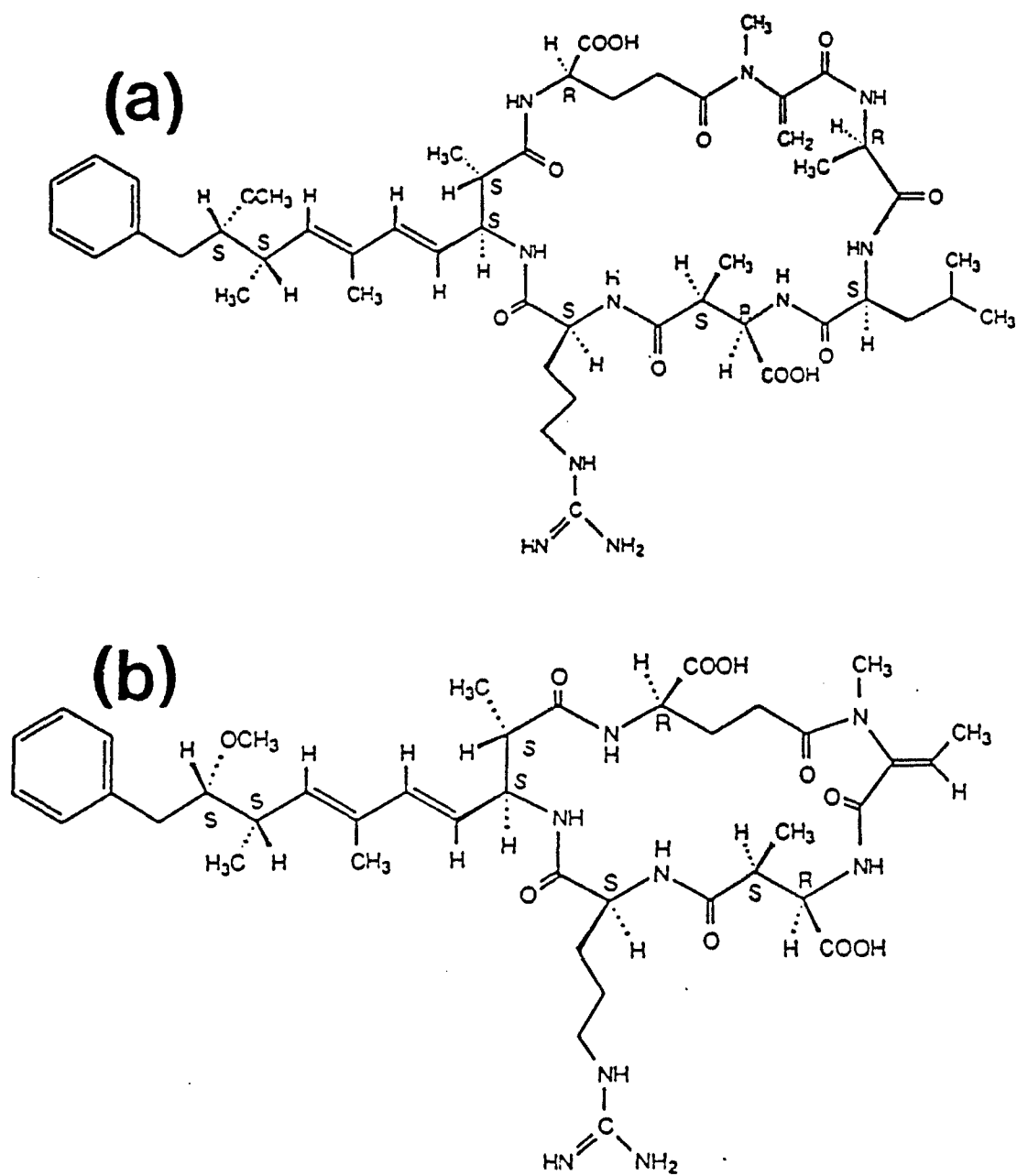


Figure 2. Microcystin-LR ozonolysis product formed by reaction with ozone followed by reduction with sodium borohydride.

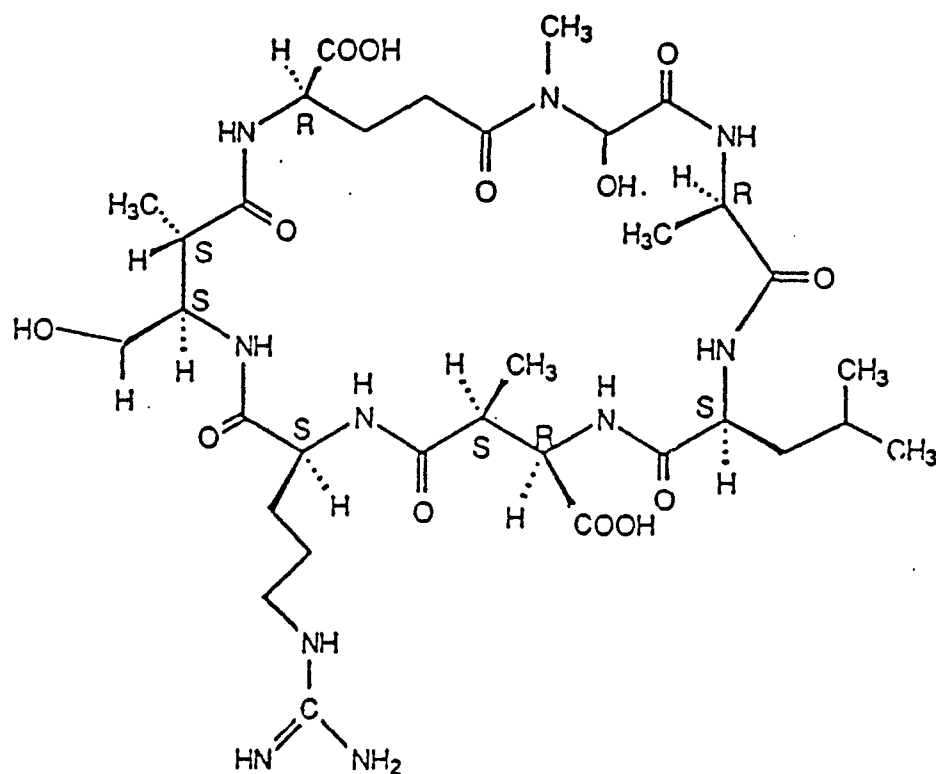


Figure 3. Microcystin-LR ozonolysis product formed by reduction with sodium borohydride, then reaction with ozone and finally reduction with sodium borohydride again.

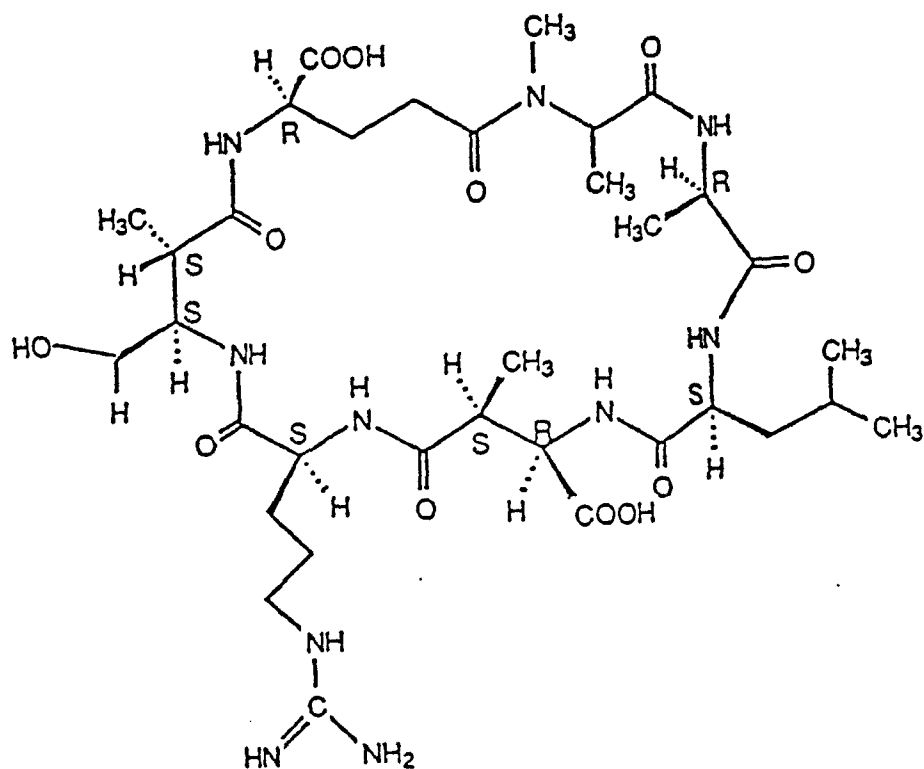
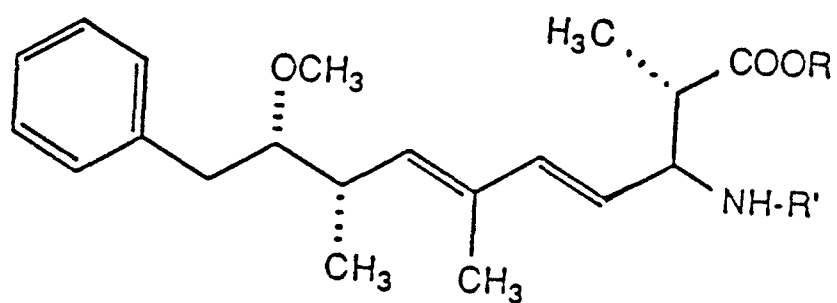




Figure 4. Structures of: 1) free amino decadienoic acid (Adda);  $R = R' = H$ , and 2) protected Adda;  $R = -CH_2CH_3$ ,  $R' = -CO_2CH_2C_6H_5$ .



**C. Pilot Study on the Influence of Glutathione Depletion on Microcystin-LR Toxicity and the Toxicity of Glutathione-Bound Microcystin-LR**

**1. Statement of the Problem, Background, and Rationale**

Little is known about MCLR metabolism in mammals. No effects of MCLR were noted with regard to lipid peroxidation or activities of  $P_{450}$  or  $P_{448}$  *in vitro* (Côté et al., 1986). Pretreatment with phenobarbital,  $\beta$ -naphthoflavone, or 3-methylcholanthrene, however, afforded partial protection against liver damage in mice given an algal extract believed to contain MCLR (Brooks and Codd, 1986). It seems that, since the primary structure of the toxin includes both glutamic and  $\beta$ -methylaspartic acids, it is ionized at biological pH and thus unlikely to undergo membrane bound (i.e., microsomal) metabolism.

Detoxification of xenobiotics by glutathione (GSH) is a critical protective mechanism *in vivo*. GSH is a tripeptide consisting of glycine, cysteine, and glutamic acid which can bind spontaneously with electrophiles, but more commonly serves as a cofactor and binds via the activity of glutathione-S-transferases (Igwe, 1986). Substrates for these enzymes share three common characteristics: 1) they must be hydrophobic to some degree, 2) they must contain an electrophilic carbon atom, and 3) they must react nonenzymatically with GSH at some measurable rate. Factors which affect the rate of inactivation of reactive compounds by GSH can alter the toxicity of certain xenobiotics. Cellular protection by GSH may be diminished by xenobiotics in at least two ways: 1) by binding GSH and thus promoting its

excretion, or 2) by inhibition of synthesis of glutathione. Since GSH is also a cofactor for glutathione peroxidase, its depletion can promote lipid peroxidation.

A dietary source of cysteine or methionine is also important for the synthesis of GSH which normally follows a cyclical pattern associated with photoperiods and times of feeding. Cysteine can alternatively be supplied in the form of pro-drugs which contain cysteine in a bound state such as N-acetyl-L-cysteine (NAC). NAC is often used therapeutically to encourage detoxification both via its direct binding with toxic agents and by serving as a precursor to increase the biological pool of GSH. Despite these benefits, immediately following administration, NAC tends to decrease hepatic GSH in rats (Estrela et al., 1983; Vina et al., 1980).

Diethylmaleate (DEM) depletes GSH pools by conjugating with GSH and promoting excretion of bound GSH into bile and urine. L-buthionine sulfoximine (BSO) lowers tissue GSH concentrations by inhibiting gamma-glutamylcysteine synthetase, an enzyme essential for GSH synthesis (Drew and Miners, 1984; Sun et al., 1985).

GSH conjugation does not always represent detoxification since some compounds are of enhanced toxicity following conjugation (Green and Lock, 1984; Igwe, 1986). For example, dichloroethane is believed to be more mutagenic after binding to GSH. The glutathione transferase-catalyzed reaction yields sulfur half-mustard, which may be the putative electrophilic alkylating agent responsible for DNA adduct formation (Igwe, 1986).

The structure of MCLR (Figure 1) contains N-methyldehydro alanine, an  $\alpha,\beta$ -unsaturated amino acid believed to be susceptible to glutathione (GSH) conjugation (Dahlem et al., 1987). GSH binding reactions occur principally within the cytosol where the MCLR molecule likely resides. In these studies, we investigated the role of GSH on the toxicity of MCLR.

## 2. Experimental Methods

### Formation and Purification of the Glutathione Adduct of MCLR

MCLR (3.12  $\mu$ mole) of greater than 95% purity was dissolved in 0.8 ml of an aqueous solution of 5%  $K_2CO_3$  (pH 10). Glutathione (31.2  $\mu$ mole) was added slowly to the toxin solution and stirred continuously for 2 hours. The solution was neutralized with 0.2 N HCl and placed onto a preconditioned Baker C-18 cartridge and rinsed with 2.0 ml of  $H_2O$ . The reaction product was eluted with 2.0 ml of methanol and evaporated to dryness under a stream of nitrogen. The glutathione adduct of MCLR was then purified via isocratic reversed-phase HPLC using a Nucleosil 5C<sub>18</sub> column and a mobile phase of methanol and 0.05 M dibasic phosphate buffer 58:42 (pH 3).

### Structural Characterization

The identities of purified toxins and reaction products were confirmed by secondary ion mass spectrometry (SIMS) at Meijo University, Nagoya, Japan, using a double focusing Hitachi M-80B mass spectrometer fitted with a high field magnet, SIMS source, and M-0101 data system (Figure 2). Operating conditions were: primary ion  $Xe^+$ ; accelerating voltage, 8 kV (primary) and 3 kV (secondary); source

temperature, 35°C. Samples were dissolved in methanol at a concentration of 10 µg/µL. The sample (10 µg) was then loaded on a silver target. Approximately 1 µl of matrix, glycerol with 1 N HCl, was then added to the sample on the target.

The specific location of GSH addition was confirmed by <sup>1</sup>H-nuclear magnetic resonance spectroscopy using a 270 MHz JEOL GX-270 spectrometer with tetramethylsilane as an internal standard. The compound was dissolved in methanol and reduction of the dehydroamino acid was confirmed by the loss of the proton signal from the olefinic protons at 4.7 and 5.8 ppm (Figure 3).

#### Chemicals used to Alter GSH Status

The L-isomer of BSO was obtained from Chemical Dynamics Co., Plainfield, NJ, USA, dissolved in saline (40 mg/mL), and administered at a dose of 1 g/kg body weight. DEM and NAC were purchased from Sigma Chemical Company, St. Louis, MO, USA. DEM was mixed with corn oil (1:19; V/V) and given at a dose of 0.2 mg of DEM/kg body weight. All other chemicals were reagent grade, and all solvents were distilled in glass.

#### Animals and Treatments

Experiment 1. Hepatic GSH of control fed animals was compared with that of fasted, fasted + buthionine sulfoximine with diethyl maleate, and fasted + N-acetylcysteine treated animals. Hepatic glutathione was thus depleted by both chemical and dietary means, and randomly selected animals from each group were killed to measure the extent of GSH depletion. The remaining animals in each group were then given an LD<sub>50</sub> dose (55 µg/kg BW) of MCLR intraperitoneally. Male Swiss

Webster mice (20 to 25 g, Harlan Sprague-Dawley, Indianapolis, IN) were assigned to the treatment groups shown in Table 1. Ninety minutes following the treatments to modify GSH status, five to seven animals from each group of approximately 22 mice were killed by decapitation for measurement of hepatic GSH content. The remaining animals in each group were dosed intraperitoneally with MCLR (55 µg/kg body weight) and their liver weights and survival times were monitored for 4 hours. Animals which survived the observation period were killed by cervical dislocation. The livers were removed from all animals blotted dry and weighed, and liver weights as a percentage of animal body weights were calculated.

Experiment 2. Male Swiss Webster mice were randomly assigned to one of two treatment groups and given either the GSH-adduct of MCLR in the saline vehicle at 200, 400, 600, 800, or 1,000 µg/kg body weight, or vehicle alone. Animals were killed and livers were collected as described above. Kidneys were also removed, blotted dry, and a combined kidney weights as a fraction of body weight were determined.

Determination of hepatic glutathione concentrations. The liver was removed and homogenized with 5 ml of 4% sulfosalicylic acid. The homogenate was centrifuged at 20,000 x g for 20 minutes, and an aliquot of the protein-free supernatant fraction was used for GSH determination using the glutathione-S-transferase method described by Asaoka and Takahashi (1981).

### 3. Results

The effect of GSH depletion on the apparent survival times of animals dosed with MCLR following fasting and treatment is shown in Figure 4. The absolute survivability was similar for the test groups, but there was an apparent difference in the mean survival times of groups of nonsurvivors. There were no marked significant differences in liver weights as a percentage of whole body weights among animals that died, indicating a similar lethal action in the animals given toxin alone and the GSH depleted, toxin-treated mice.

The goal of this study was to assess the toxicological importance of GSH status of the livers of mice at the time of exposure to MCLR. GSH concentrations in livers of mice were not measured after toxin administration because hemorrhage into the damaged liver would be likely to yield anomalous GSH values.

In the present study, NAC-treatment depleted hepatic GSH to a lesser extent than did DEM + BSO (Table 2). Despite altered GSH status, lethal toxicity of MCLR was not markedly altered among groups (Figure 4).

The binding of GSH to MCLR results in a product with slightly reduced toxicity but which remains potent and highly hepatotoxic (Figure 5). Animals which died acutely following dosing with the GSH-adduct of MCLR had liver weights similar to those of animals which died acutely after MCLR administration. Animals which survived for 24 hours after being given the GSH adduct had organ weights similar to those of survivors given either MCLR or the vehicle alone.

No treatment associated lesions were found in any of the tissues examined in mice given the GSH adduct of MCLR at 0 to 400  $\mu\text{g/kg}$ . In mice dosed with this derivative at 600 to 1,000  $\mu\text{g/kg}$ , treatment-associated lesions were similar and were present in all of the mice which died. Liver lesions were characterized by severe, widespread, centrilobular and midzonal hepatocyte disassociation and rounding which frequently extended into periportal regions. These were accompanied by breakdown of the sinusoidal endothelium resulting in severe hemorrhage in affected areas. These lesions appeared identical to those in the mice given doses of MCLR. The liver of the one mouse which survived the 600  $\mu\text{g/kg}$  dose had numerous, large, centrilobular to midzonal areas of hemorrhage with hepatocyte disassociation and necrosis. Small numbers of neutrophils were intermixed with the cellular debris. Lesions were also present in the lungs of two of the four mice at 600  $\mu\text{g/kg}$  and in the lungs of all of the mice at 800 and 1,000  $\mu\text{g/kg}$ . Lung lesions consisted of variably sized clumps of eosinophilic material within pulmonary capillaries. This material occasionally contained pyknotic nuclei and/or a few small, clear intracytoplasmic vacuoles and it appeared to be hepatocyte debris.

#### 4. Discussion

The intermediate degree of GSH depletion by NAC was accompanied by an intermediate increase in mean survival time, as compared to the greater increase in mean survival time in the BSO + DEM treated animals and the shorter survival in the fed + NAC mice. These trends are consistent with a hypothesis that a decrease in GSH content would prolong survival in MCLR treated animals.



The results of these experiments also show that the GSH adduct of MCLR is a potent hepatotoxic compound. When administered intraperitoneally to mice, it is less toxic than parent MCLR, but the derivative remains highly toxic and hepatospecific.

In our initial experiments, we found that GSH depletion seemed to cause slight prolongation of survival in toxin-treated mice but differences in survival time were not marked.

Altered delivery of MCLR to the target cell in the liver may be the reason for the reduction in the toxicity of the GSH derivative as compared with MCLR. Conjugation of xenobiotics to GSH occurs primarily in the cytosol or mitochondria of the cell and conjugation before uptake into hepatocytes probably results in reduced membrane solubility. Consequently, it is uncertain whether the affinity of the MCLR conjugate for receptors of hepatocytes is either diminished or enhanced as compared to the unaltered compound.

In a previous study, hepatocyte GSH concentrations were decreased following administration of MCLR, but morphologic changes in cells occurred before large depletions of GSH were observed (Runnegar et al., 1987). Thus, the authors concluded that, if GSH within the cell is critical for cytoskeletal maintenance, then the pool involved may be somewhat distinct from the total GSH pool.

These results show that conjugation of MCLR with GSH does not result in substantial detoxification of the toxin molecule. Whether the GSH-adduct of MCLR is itself toxic or enzymatic deconjugation reactions in the animal quickly act to free the parent toxin, the observed effects occur rapidly and can be lethal. The extent of

conjugation *in vivo* has yet to be determined in independent studies, but toxicity of the GSH adduct predicts that GSH conjugation may not result in effective detoxification.

As previously mentioned, conjugation of toxic species by GSH may on occasion potentiate toxicity rather than the more common detoxification effect (Green and Lock, 1984; Igwe, 1986). In fact, the data from the present studies *in vivo* could be interpreted to suggest that GSH conjugation may play a role in enhancement of the toxicity observed with MCLR.

Table 1. Feeding status and treatment of animals in glutathione depletion study.

Group	Feeding Status	Treatment	Trial Day
I	Fed	Saline	2
II	Fasted	Saline	1
III	Fasted	NAC	3
IV	Fasted	DEM + BSO	1

Table 2. Hepatic glutathione (GSH) concentrations in mice prior to microcystin-LR treatment.

Treatment Group Used Determination	GSH Concentration <sup>1</sup> ( $\mu$ mole/g liver)	Number of Animals for GSH
Fasted	5.68 $\pm$ 0.68	5
Fed	6.80 $\pm$ 0.30	7
NAC	3.21 $\pm$ 0.38	7
BSO + DEM	0.24 $\pm$ 0.10	6

<sup>1</sup>Mean  $\pm$  standard error.

**Figure 1.** Structure of microcystin-LR from the cyanobacterium *Microcystis aeruginosa*.

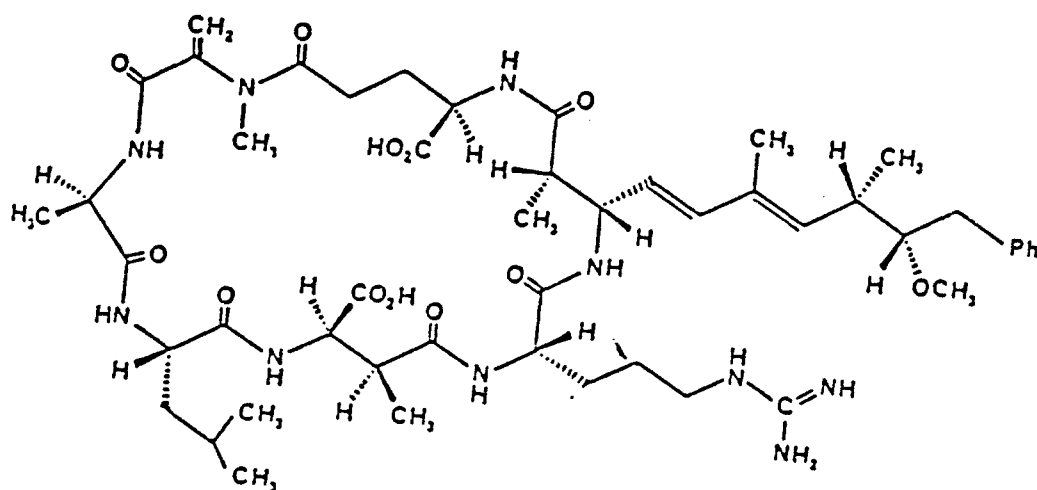


Figure 2. Fast atom bombardment mass spectrum of glutathione-bound microcystin-LR.

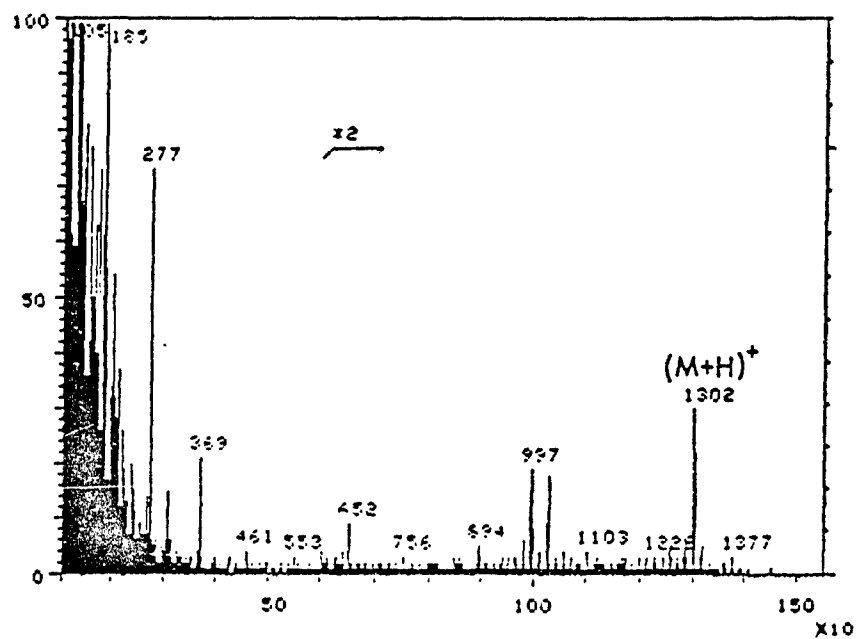


Figure 3. Proton nuclear magnetic resonance spectrum of glutathione-bound microcystin-LR. Loss of proton signal from the dehydroamino acid confirmed addition of glutathione to the microcystin molecule.

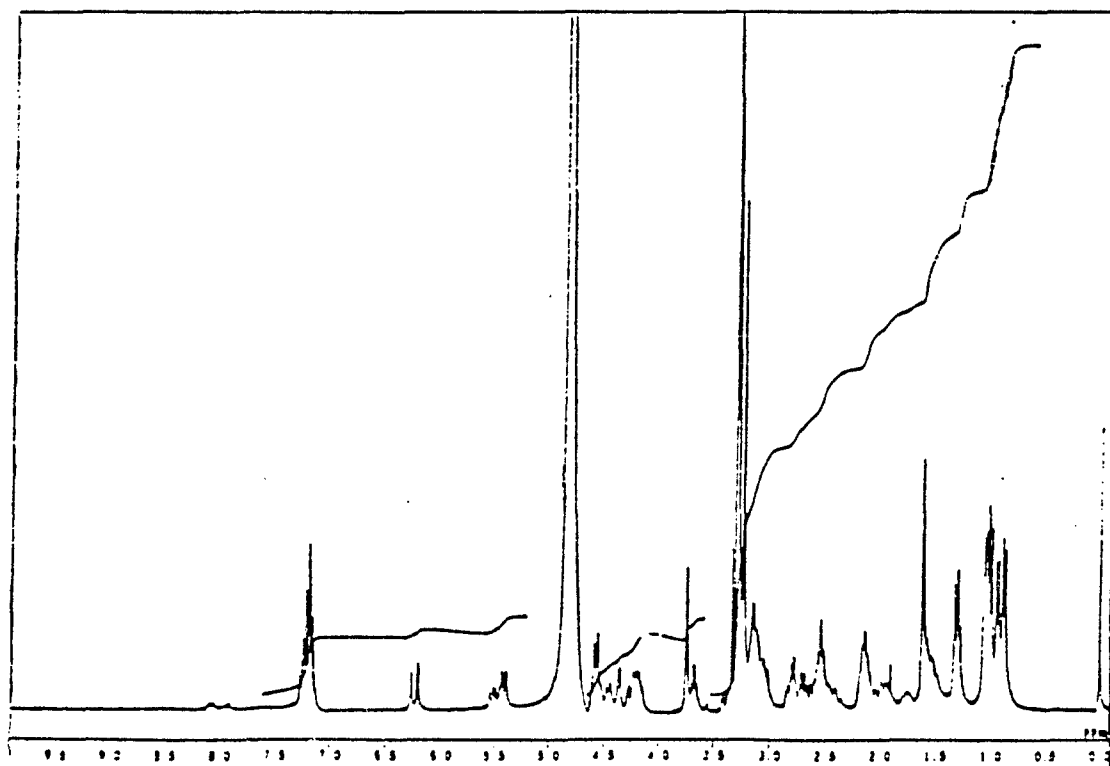
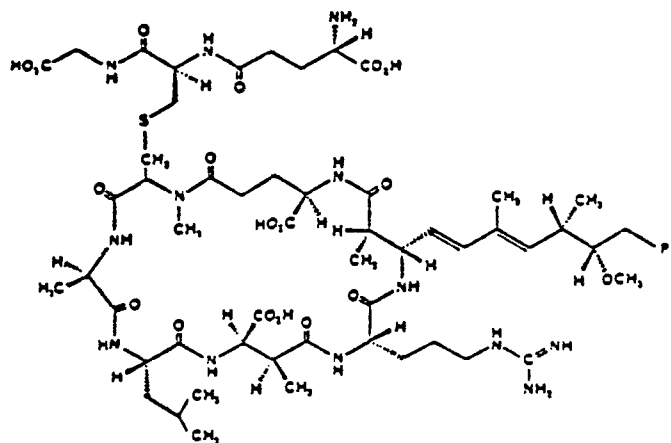


Figure 4. Relative survival over time of glutathione depleted, toxin-treated mice. (N = 16 animals/group with the exception of N-acetyl cysteine treated animals where N = 10.) NAC = N-acetyl cysteine, DEM = diethylmaleate, BSO = buthionine sulfoximine.

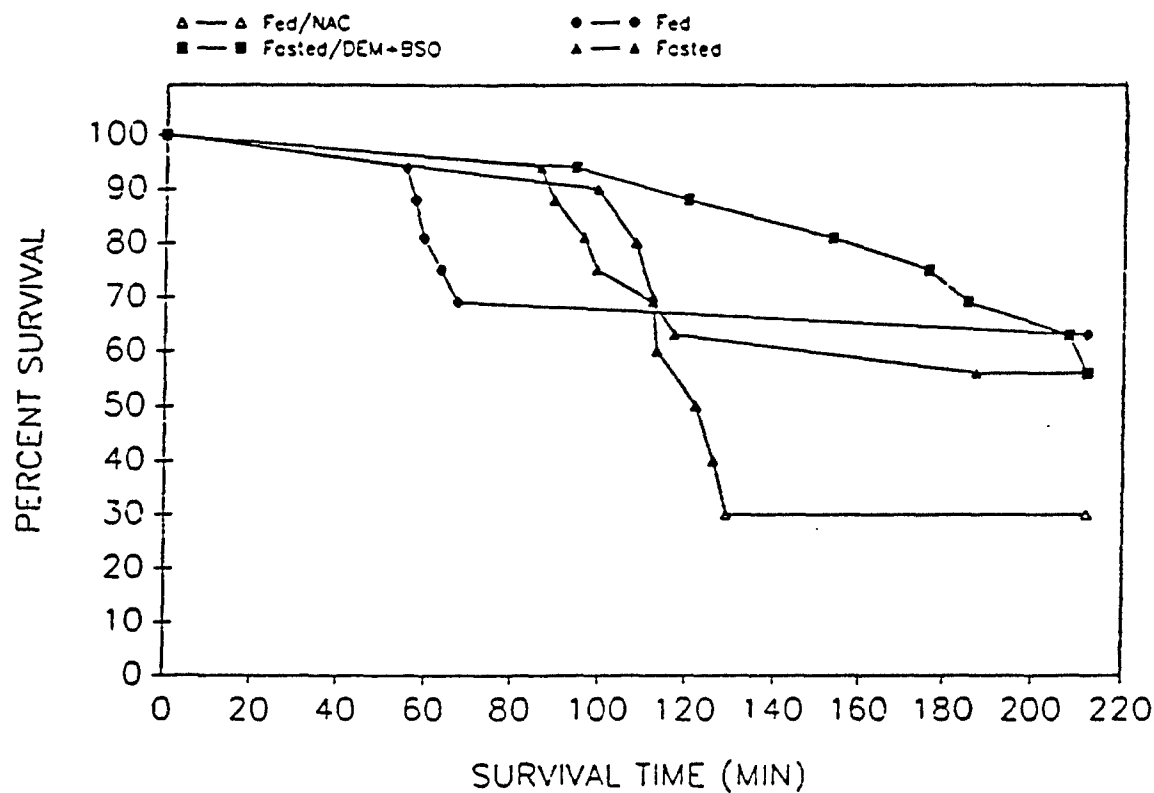
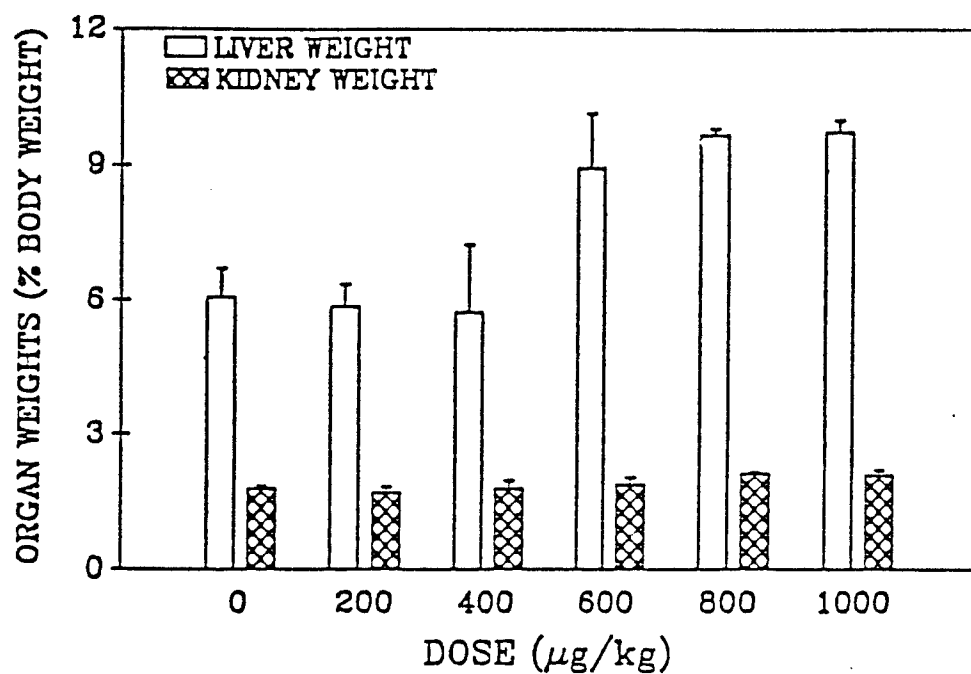




Figure 5. Liver and kidney weights as a fraction of body weight in animals treated with the glutathione-adduct of microcystin-LR.

MOUSE LIVER AND KIDNEY WEIGHTS AS A PERCENTAGE OF BODY WEIGHT  
AFTER TREATMENT WITH MC-LR/GSH ADDUCT



### III. METHODS FOR PRODUCTION OF ISOTOPICALLY LABELLED MICROCYSTIN-LR

#### A. Statement of the Problem

Problems associated with the UV absorption as a method for detection of toxin material can be circumvented through the use of radiolabelled toxin. Radiolabelled toxin is of value for analytical methods development, and especially for studies assessing absorption, distribution, metabolism, and excretion. It is generally most desirable to impart an easily detectable isotopic label, which will remain a part of the parent toxin and of any toxin metabolite. In this way, the labelled compound can be expected to behave in a manner most like the parent toxin, and the radiolabel should serve as a reliable marker even if the toxin becomes structurally altered or protein bound and thereby difficult to detect by other methods, such as UV absorption.

#### B. Background

The potent toxicity of cyclic peptides from cyanobacteria makes radiolabeling of the compounds essential for experiments to characterize toxin fate in biological systems. Radiolabeled algal peptide hepatotoxins have been produced both biosynthetically (Brooks and Codd, 1986,1987) and synthetically (Runnegar et al., 1986; Falconer et al., 1986). The biosynthetic method utilized  $^{14}\text{C}$ -labeled bicarbonate to produce toxin of extremely low specific activity (2.6  $\mu\text{Ci/mg}$ ). The identity of the toxin used in these experiments were not reported, but the strain of algae used in their experiments (PCC-7820) is known to produce both MCLR and a related monodesmethylated toxin (Carmichael, unpublished data). Toxin

labeled by this method was subsequently given intraperitoneally (injection volumes not specified) to mice at sublethal doses. Seventy-six percent of the radioactivity was localized in the liver after 1 minute and 90% of the administered dose was localized in the liver at 3 hours postdosing. The injection volumes used for toxin administration were not mentioned in this report and may have played a role in the extremely rapid uptake of the toxin by the liver. Radioactive residues were also found in the kidneys, urine, and lungs of toxin-treated animals. No data were reported beyond the 3-hour observation period, and no information was given concerning the chemical or biological stability of the label.

Synthetic radiolabelling involved addition of  $^{125}\text{I}$  to microcystin-YM (MCYM) (Runnegar et al., 1986). This method utilized the mild lactoperoxidase method of iodination to produce toxin of rather high specific activity. Microcystin-YM is structurally similar to MCLR except it has L-tyrosine substituted for L-Arg and L-methionine substituted for L-leu. The lactoperoxidase method of iodination would be expected to produce a mixture of at least four nonisotopically labeled compounds. The semipurified toxin was then administered either IP to mice or intravenously (IV) to rats. This experiment again demonstrated rapid localization of most of the toxin in the livers of both species. The major drawback of iodination is that iodine is a nonisotopic label which is known occasionally to change the observed biological activity of xenobiotics. In this case, however, iodination by this method did not appear to change the hepatotoxicity or hepatospecific lesions associated with microcystin-YR. As in the studies of Brooks and Codd (1986,1987), the chemical and biological stability of the labeled products were not reported. With MCYR, the label was incorporated into tyrosine, one of the variable

L-amino acids, but this method will not work for microcystin-LR (MCLR) and other closely related cyclic peptide toxins (MCs and nodularin) which do not contain tyrosine or methionine. For these reasons, alternate methods for synthetic labeling of cyanobacterial peptide toxins were investigated.

### C. Rationale

#### 1. Biosynthetic Radiolabelling

In order to produce biosynthetically labelled toxin, we provided  $^{14}\text{C}$ - or  $^3\text{H}$ -labelled amino acids as raw materials for the growing algae, in the hope that the labelled precursor amino acids would be incorporated into the peptide structure of the toxin.

#### 2. Synthetic Radiolabelling

Production of synthetically labelled toxin was attempted by utilizing the free  $\alpha$ -carboxyl moieties present in glutamic acid and B-methyl aspartic acid to substitute  $^3\text{H}$  for hydrogen on the adjacent alpha carbon. Botes et al. (1985) utilized a related technique to prove isolinkages of these moieties in the peptide structure which involved a tritium labelling of C-terminal amino acids.

### D. Experimental Methods

#### 1. Biosynthetic Radiolabelling

A culture of *Microcystis aeruginosa* strain 7820 provided by Dr. Carmichael was continuously grown in our laboratory. The identity of purified MCLR from this culture was established by fast atom bombardment mass spectroscopy (FAB-MASS), gas chromatography (GC), and mouse bioassay.

We attempted biosynthetic radiolabelling of MCLR in three ways. First, 10  $\mu\text{Ci}$  of  $^{14}\text{C}$ -glutamic acid (with a specific activity of 40 to 60  $\mu\text{Ci}/\text{mmole}$ ) was added to a growing culture of *Microcystis aeruginosa* strain PCC-7820. Secondly, 100  $\mu\text{Ci}$  in 10 aliquots of 10  $\mu\text{Ci}$  of a  $^{14}\text{C}$ -labelled racemic mixture of D- and L-glutamic acid was added to a similar growing culture every other day. Finally, 100  $\mu\text{Ci}$  of purified  $^3\text{H}$ -labelled L-glutamic acid was added in 10 aliquots of 10  $\mu\text{Ci}$  each, every other day (to see if it would be converted to the D-form and ultimately incorporated into the MCLR molecule).

## 2. Synthetic Radiolabelling

### a. Procedure 1. Specific tritium exchange, pilot study

Tritiated water was purchased from New England Nuclear (NEN) Research Products Company, Boston, MA, USA. The specific activity was 1  $\mu\text{Ci}/\mu\text{l}$ . All solvents were distilled in glass.

The peptide toxin (0.1  $\mu\text{mole}$ ) was mixed with  $^3\text{H}_2\text{O}$  (5  $\mu\text{l}$ , 5  $\mu\text{Ci}$ ) and pyridine (10  $\mu\text{l}$ ). Acetic anhydride (10  $\mu\text{l}$ ) was then added to the same tube which was then sealed with parafilm and held in an ice water bath at  $0^\circ\text{C}$  for 5 minutes. The tube was subsequently placed in a room-temperature ( $23^\circ\text{C}$ ) water bath for 15 minutes. Another volume (20  $\mu\text{l}$ ) of pyridine was then added, followed by acetic anhydride (20  $\mu\text{l}$ ), and the mixture was again held at  $0^\circ\text{C}$  for 5 minutes followed by a room-temperature water bath for an addition hour. Another aliquot (5  $\mu\text{l}$ ) of tritiated water was then added and the mixture placed in a room-temperature water bath for 1 hour to decompose the excess acetic

anhydride. The solution was then evaporated to dryness. Removal of exchangeable tritium was accomplished by addition of 10% acetic acid (100  $\mu$ l) followed by evaporation. The addition of acetic acid followed by evaporation was repeated five times.

b. Procedure 2. General tritium exchange: Synthetic labeling with Rh/A1<sub>2</sub>O<sub>3</sub> and tritiated water

In this method undertaken at the initiative of New England Nuclear Company (and contrary to our previously agreed upon protocol based on the above method), 10 mg of MCLR was dissolved in 0.3 ml of anhydrous dimethylformamide. To this solution, 10 mg of 5% Rh/A1<sub>2</sub>O<sub>3</sub> and 25 Ci of tritiated water were added and the mixture was stirred overnight at 50°C. Labile tritium was then removed with ethanol and the sample was shipped to us in ethanol. Mass spectral analysis revealed the presence of dimethylformamide solvent adducts to MCLR. The compound was therefore subjected to rotary evaporation under a high vacuum with intermittent washing using 1.0 ml volumes of water for 18 hours. After these evaporation steps, the material was transferred with methanol from the evaporation flask to a tared vial and 5  $\mu$ g of the product was submitted for mass spectroscopy.

A portion of the labelled toxin was also applied to Whatman 60A-K6F silica thin-layer chromatography (TLC) plates which were developed using a mobile phase consisting of the organic layer of a mixture of 65:35:10 chloroform-methanol-water. Bands of silica were scraped from the plate at the

relative retention (Rf: 0.23) of MCLR and subjected to liquid scintillation counting (LSC) to quantify the radioactivity remaining with the toxin following removal of the solvent adduct. The TLC band corresponding to MCLR was found to contain substantial radioactivity after removal of the dimethylformamide so the purification process was continued.

After TLC and LSC confirmation of the toxin identity and radioactivity, respectively, the material was subjected to gel filtration using TSK Toyopearl HW-40F gel (Supelco Inc., Bellefonte, PA). The column size was 90 cm x 2.0 cm ID and the solvent system was 100% methanol at a flow rate of 2.0 ml/minute. Toxin was detected by UV absorbance at 238 nm. Fractions (10.0 ml) were collected and those corresponding to MCLR were combined and dried on a rotary evaporator. The residue was then transferred with methanol to a tared vial and again evaporated to dryness. The mass of the toxin was determined and a fraction of the material again subjected to LSC.

c. Procedure 3. Specific tritium exchange scale up: Synthetic labeling with pyridine and tritiated water

In this case, New England Nuclear Company Inc. followed the procedure designated by our laboratory. MCLR (10 mg) was placed in a reaction vessel with 25 curies of tritiated water and pyridine (5 µl). A clear solution was observed. Acetic anhydride (15 µl) was added at 0°C and stirred for 5 minutes followed by stirring for 20 minutes at room temperature. Thirty µl of pyridine was then added followed by 30 µl of acetic anhydride at 0°C, and the mixture

was stirred for 5 minutes at 0°C, then stirred for an hour at room temperature. Labile components were removed by repeated evaporation with 10% acetic acid, and the compound was shipped to us in water.

In this case, 10 mg of > 95% pure MCLR resulted in production of 450  $\mu$ Ci of activity following removal of labile tritium. The first shipment of this material accounted for 25  $\mu$ Ci. It was initially examined on TLC using Whatman silica gel 60A-K6F plates with the organic layer of a mixture of chloroform-methanol-water (65:35:10) as the solvent system. Bands of silica (0.5 cm) were scraped from the TLC plate and the silica rinsed with methanol (100  $\mu$ l). Aliquots were then counted on LSC and the resultant radioactivity plotted.

The remaining compound was subjected to purification using Bond Elut C-18 cartridges. The cartridge was first rinsed with 2 x 2.0 ml of methanol followed by 2 x 2.0 ml of water. The material believed to correspond to labelled toxin was applied to the cartridge in water, which was then rinsed with 3 x 2.0 ml of water. Elution from the cartridge relied upon 100% methanol. The toxin in methanol was evaporated to dryness on a rotary evaporator, then transferred to a silica column (22 x 1.0 cm). The silica column chromatography step was performed using Whatman flash silica and the solvent system already described for TLC. Fractions (0.5 ml) were collected and an aliquot was applied to TLC as already described. Bands of silica were again scraped and counted on LSC.



An additional shipment of this reaction product (50  $\mu$ Ci) was obtained from NEN and investigated in our laboratories. TLC was performed as described above. Purification on TSK Toyopearl HW-40F was employed in place of the silica column.

## E. Results, Discussion, and Conclusion

### 1. Biosynthetic Radiolabelling

The radiolabelled glutamic acid was utilized by *M. aeruginosa* in the production of MCLR and the degree of labelling was proportional to the specific activity of the toxin, however, specific activity was nevertheless low. The highest specific activity was obtained with the second of the three methods attempted and, even here, it was only 420 to 450 cpm/ $\mu$ g of toxin. In view of a) the low specific activity obtained, b) the expense of purified D-glutamic acid, and c) the fact that the location of label insertion could not be entirely controlled through the use of biosynthetic methods, studies using solely the D isomer were not undertaken. Instead, we decided to concentrate on methods for synthetic labelling.

### 2. Synthetic Radiolabelling

#### a. Procedure 1. Specific tritium exchange, pilot study

The toxin was successfully labelled synthetically by our research group using tritiated water and purified toxin as precursors. This experiment utilized the unusual isolinkage of glutamic acid and B-methyl aspartic acid which results in a free  $\alpha$ -carboxyl in each moiety that would otherwise be involved in peptide bonding. This free  $\alpha$ -carboxyl allows tritium incorporation on the adjacent

carbon by the method of Matsuo (Matsuo and Norita, 1975), which is customarily used to provide information about the C-terminal amino acid of noncyclic peptides. This process is dependent upon all reactants except the tritiated water being anhydrous, so that as little extraneous water as possible is available which can interfere with toxin labelling.

b. Procedure 2. General tritium exchange: Synthetic labelling with Rh/Al<sub>2</sub>O<sub>3</sub> and tritiated water

Prior to removal of the dimethyl formamide adduct, it was unclear whether the toxin was actually labeled. Removal of the dimethylformamide adduct and subsequent LC revealed that radioactivity was present both in the toxin and in the adduct. Figure 1 shows the mass spectrum obtained after the high vacuum evaporation process and in this case the major ion obtained was 995 (M + H). Other ions present are attributable to sodium and/or FAB matrix adducts. Using Toyopearl gel chromatography, the toxin was eluted in approximately 170 minutes and was well separated from identifiable impurities (Figure 2).

This exchange reaction is normally used in the case of very complex molecules for which more specific methods of tritium labelling are impractical. Such reactions typically result in the addition of tritium atoms throughout the molecule. In the present study, the specific activity of the material obtained was calculated to be approximately 0.5  $\mu\text{Ci/mg}$ .

An additional concern with preparation of labeled MCLR by this method was that catalytic tritium replacement can result in saturation of double bonds,

which we have shown to be important in toxin bioactivity. Another concern is that the dihydro product, reduced at the N-methyldehydroalanine moiety, exhibits HPLC retention times very similar to those of the unreduced parent toxin so that care is needed to resolve the two compounds.

c. Procedure 3. Specific tritium exchange scale up: Synthetic labelling with pyridine and tritiated water

The TLC results with the original shipment of compound were promising. Twenty percent of the applied radioactivity was accounted for by the TLC band corresponding to the  $R_f$  of MCLR (Figure 3). Also, mass spectral analysis of the toxin showed a molecular ion of 995 corresponding with authentic MCLR ( $MH^+$ ) standard. Consequently, a large amount of labeled material was subjected to the silica purification method we had developed for MCLR. In the case of the labeled molecule, however, decomposition appeared to have occurred, since following silica column clean-up, the toxin could no longer be detected (Figure 4).

Subsequently, we found that the peak observed on Toyopearl chromatography, along with the radioactivity found on TLC at the  $R_f$  of microcystin, were not attributable to labeled toxin. Also, the peak observed under Toyopearl chromatography was not reproducible, and did not show the same UV spectrum as authentic toxin. When the reaction product was subjected to C-18 reverse phase chromatography, the only peaks observed in the chromatogram eluted before MCLR. Thus, examination of the reaction product

showed no compounds which structurally resembled the parent compound. Apparently the toxin had been degraded as a result of the synthetic labeling procedure employed by NEN.

A possible explanation for the degradation observed under the experimental conditions employed by NEN is that the extremely high specific activity of tritiated water (much higher than used in the pilot study) resulted in sufficiently greater molecular energy to bring about destruction of peptide bonds and associated hydrolysis of the parent peptide toxin. Although Amersham Company subsequently utilized this method, or one very similar to it, to produce isotopically labelled  $^3\text{H}$ -MCLR, their initially successful effort was reportedly not reproducible. Consequently, it is our understanding that other groups which initially utilized this material (Robinson et al., 1988) have begun to employ tritiated dihydro MCLR for subsequent trials (see next section). It is not known why NEN was unsuccessful in this method or why Amersham had an initial success followed by subsequent failures.

Figure 1. Mass spectrum of tritium labelled microcystin after removal of dimethylformamide adduct.

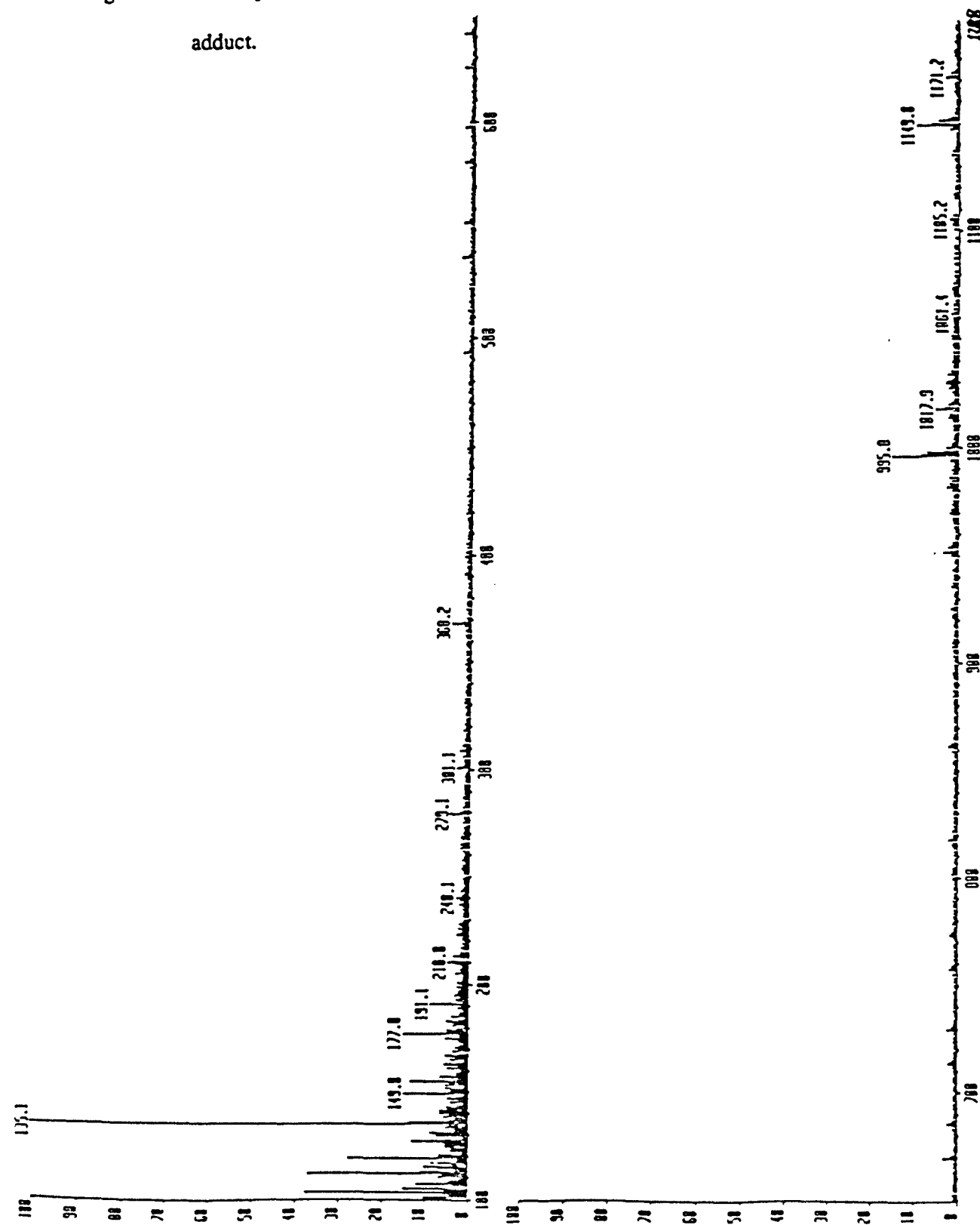
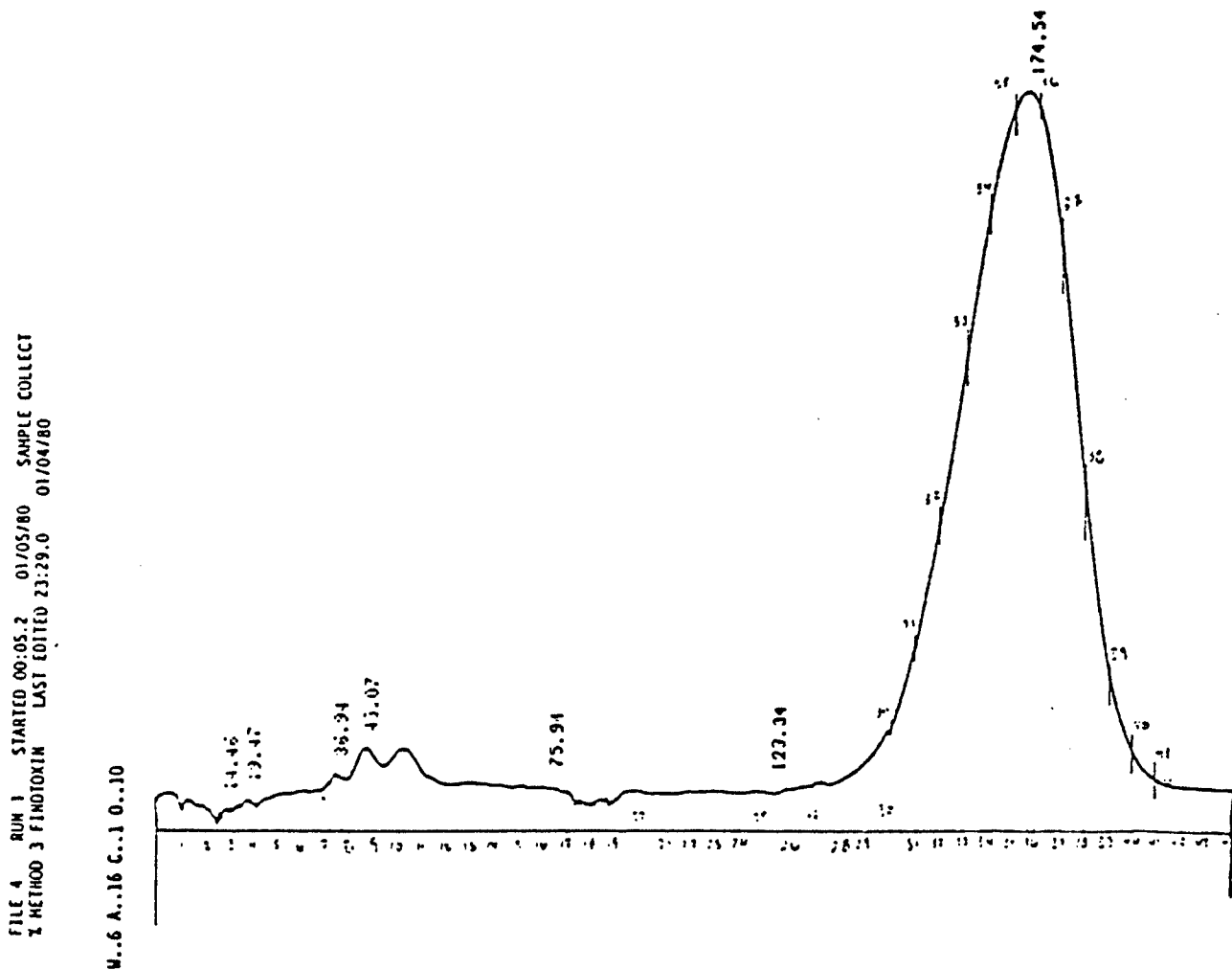


Figure 2. Chromatogram of Toyopearl purification of tritium labelled microcystin.



FILE 4 RUN 1 STARTED 00:05.2 01/05/80 SAMPLE COLLECT  
% METHOD 3 FINOTOXIN LAST EDITED 23:29.0 01/04/80

RT	AREA	HEIGHT	BC	AREA PERCENT	HEIGHT PERCENT
14.46	192024		T	0.1004	
19.47	491004		V	0.2567	
36.94	109709		V	0.0578	
43.07	338545		V	0.1770	
75.94	759129		V	0.3968	
123.84	61460		V	0.0321	
174.54	189355920	155.7579		98.9797	100.0000

7 PEAKS > AREA REJECT 191307776 TOTAL AREA  
1 PEAK > HEIGHT REJECT 115.7579 TOTAL HEIGHT

KEYBOARD DIRECTED EVENTS  
TIME EVENT VALUE  
220.619 Stop Data

Figure 3. TLC radiochromatogram of crude reaction product.

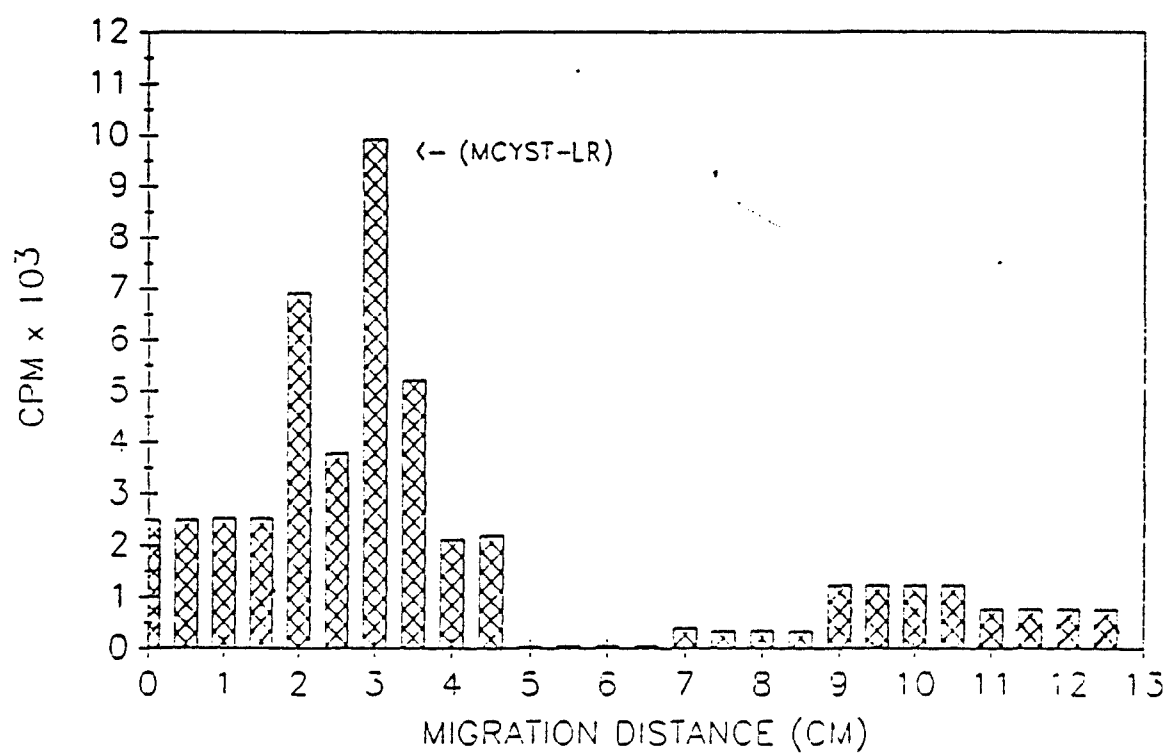
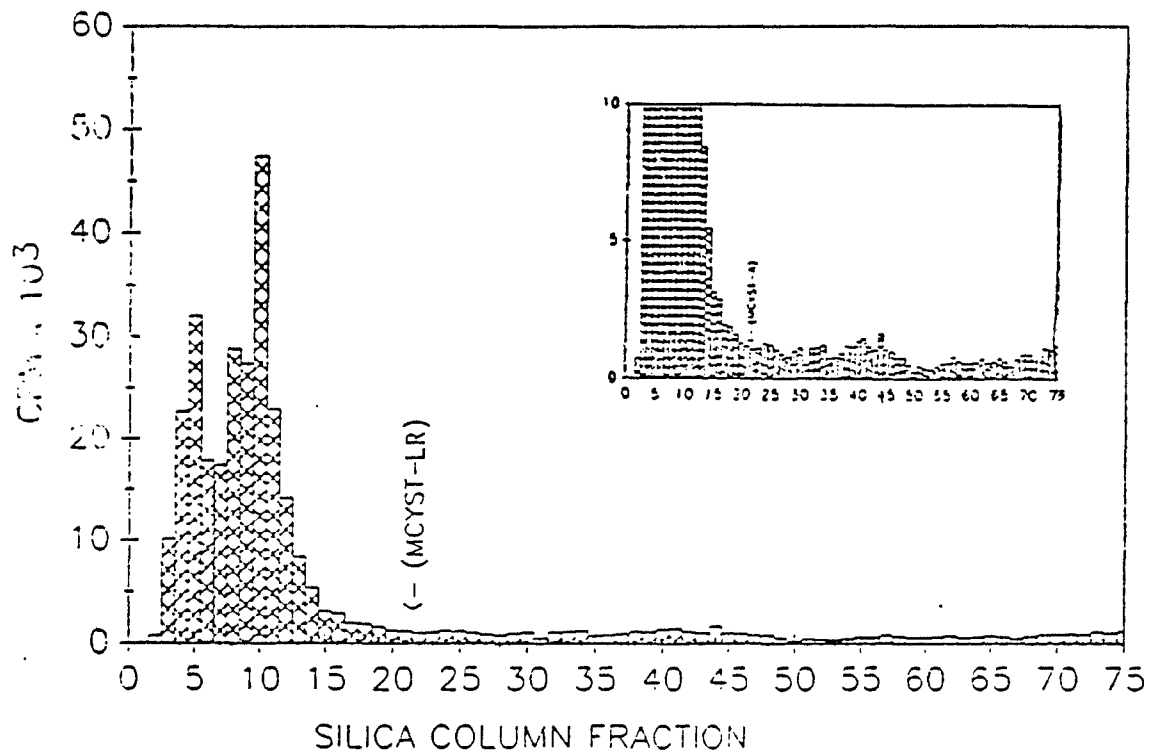


Figure 4. Radiochromatogram of fractions from silica column.





**IV. PRODUCTION AND CHARACTERIZATION OF THE FATE OF  
TRITIATED DIHYDROMICROCYSTIN-LR IN MICE,  
ISOLATED PERFUSED RAT LIVERS, AND RAT HEPATOCYTES  
IN SUSPENSION**

**A. Production and Purification of Tritiated-[<sup>3</sup>H]-2H-MCLR: Fate in Mice Dosed Intraperitoneally**

**1. Statement of the Problem, Background, and Rationale**

Although we had developed a method for the production of (isotopically labelled) tritiated microcystin-LR ([<sup>3</sup>H]-MCLR), and this method was successfully employed by USAMRIID workers (Robinson et al., 1988), when utilized by New England Nuclear, the toxin was degraded (Third Annual Report, pp. 9-19, previous section of this report). Methods for production of [<sup>3</sup>H]-2H-MCLR (2H-MCLR) and its toxicity assessment (Second Annual Report, pp. 44-52; Dahlem et al., 1990) have also been previously reported, and it is clear that nonlabeled 2H-MCLR remained a potent hepatospecific derivative. Lethal toxicity of the compound was reduced by only 50%; and lesions were essentially the same as those caused by the parent compound. The goals of the present study were: 1) to produce highly purified, tritiated (dihydromicrocystin-LR ([<sup>3</sup>H]-2H-MCLR)), 2) to confirm the biological stability of [<sup>3</sup>H]-2H-MCLR, 3) to characterize the tissue distribution and rates of elimination of the radiolabel in response to a lethal and sublethal dose of

[<sup>3</sup>H]-2H-MCLR, and 4) to characterize the cellular distribution of [<sup>3</sup>H]-2H-MCLR when added to the perfusate of isolated rat livers or to rat hepatocytes in suspension.

## 2. Experimental Methods

### Toxin

MCLR was produced in the laboratory of W. Carmichael at Wright State University in Dayton, OH. Purity evaluation relied upon Whatman K6F normal phase high performance silica TLC plates (Baxter Scientific Products, McGaw Park, IL; Harada et al., 1988b) and HPLC with UV detection at 238 nm (Harada et al., 1988a). MCLR was found to be > 99% pure by each method prior to use in labelling procedures.

### Other Chemicals

Tritium-labelled sodium borohydride ([<sup>3</sup>H]-NaBH<sub>4</sub>; specific activity = 14 Ci/mole) was obtained from ICN Radiochemicals (Division of ICN Biomedicals, Irvine, CA) and was found to be > 97% radiochemically pure by TLC. Other chemicals were reagent grade or, in the case of solvents, HPLC grade.

### Synthesis of Nonlabelled 2H-MCLR

MCLR (2.0 mg) was mixed with an excess of NaBH<sub>4</sub> (10 mg) in 70% 2-propanol (1.0 ml, aqueous) at room temperature (22°C) for 24 hours. The reaction was subsequently quenched with 10% acetic acid (0.5 ml, pH 4) and evaporated to dryness *in vacuo* using a rotary evaporator. Silica TLC with a solvent system comprised of the organic (upper) phase of a mixture of ethyl acetate, 2-propanolol, and water (4:3:7) was used to characterize reaction products (MCLR R<sub>f</sub> = 0.30;

2H-MCLR Rf = 0.31, 0.33). Since parent MCLR was no longer detectable, the reaction was determined to have gone to completion.

#### Synthesis of [ $^3\text{H}$ ]-2H-MCLR

MCLR (2.5 mg) was mixed with [ $^3\text{H}$ ]- $\text{NaBH}_4$  (12.5 mCi) in 70% 2-propanol (1.0 ml) at room temperature for 24 hours then quenched with 10% acetic acid (0.5 ml, pH 4). The reaction product was then evaporated to dryness *in vacuo* using a rotary evaporator.

#### Purification of 2H-MCLR and [ $^3\text{H}$ ]-2H-MCLR

The reaction mixture in water (0.5 ml) was loaded onto preconditioned 1 g  $\text{C}_{18}$  cartridges (Analytichem International, Harbor City, CA). The column was rinsed with water (3 x 2 ml) and 10% methanol (3 ml) and the toxin derivatives eluted with 100% methanol (3 x 2 ml). In the case of radiolabelled production, this step removed the bulk of the excess tritium.

Isolation and purification of a single enantiomer from the mixture was accomplished by reversed-phase HPLC using a Spectra Physics 8800 HPLC system equipped with a Whatman Partisphere  $\text{C}_{18}$  column (4.6 x 120 mm), a mobile phase of 0.05 M dibasic potassium phosphate and methanol at a flow rate of 1.0 ml/minute (58:42, pH 3), and detection at 238 nm. Fractions containing the [ $^3\text{H}$ ]-2H-MCLR-toxin were dried *in vacuo* and purified using the same  $\text{C}_{18}$  method described previously to remove the involatile buffer from the mobile phase.

### Confirmation of Reaction Products

Identities of the purified reaction products were confirmed on both low and high resolution fast atom bombardment mass spectrometry (FABMS) using a VG ZAB-SE 10 kV mass spectrometer. Compounds were mixed with magic bullet matrix (1:3, dithiothreitol-dithioerythritol) and 10% oxalic acid (1 ml) and analyzed using a source temperature of 30°C, and an acceleration potential of 8 kV. The HPLC and TLC profiles of [<sup>3</sup>H]-2H-MCLR were also compared to those of previously characterized 2H-MCLR. Chemical stability of the tritium label in [<sup>3</sup>H]-2H-MCLR was monitored at weekly intervals for 2 weeks by means of replicate injections of aliquots on the HPLC system described above.

### Mice

Male Swiss Webster mice weighing 20 to 22 g were obtained from Harlan Sprague-Dawley, Inc., Indianapolis, IN.

### Toxicity Assessment of Diastereomers of 2H-MCLR

The toxicity of diastereomers were compared by IP administration to mice.

### Distribution Study

In the first study, mice were provided food and water *ad libitum* and allowed 1 week to become acclimated. Animals were then randomly assigned to one of four treatment groups. Groups were dosed IP (as described by Codd and Carmichael, 1982) with one of the following: 2H-MCLR (200 mg/kg), [<sup>3</sup>H]-2H-MCLR + 2H-MCLR (total of 100 mg/kg), [<sup>3</sup>H]-2H-MCLR + 2H-MCLR (total of 200 mg/kg), or the saline vehicle. Each mouse given [<sup>3</sup>H]-2H-MCLR received 0.2 µCi of total

radioactivity regardless of the toxin dose. The mice were then housed individually and killed by decapitation at predetermined time intervals ( $N = 3/\text{time interval}$ ).

Following euthanasia, abdominal cavities were opened via a midline incision and fluids in the cavity were blotted onto absorptive paper. Organs were removed, blotted dry, weighed, homogenized, and stored at  $-20^{\circ}\text{C}$ . Aliquots of tissue (approximately 100 mg) were removed and placed in preweighed glass scintillation vials, reweighed, and suspended in 500  $\mu\text{l}$  of Protosol Tissue and Gel Solubilizer (New England Nuclear Research Products, Boston, MA). Tissue suspensions were then mixed on a vortexer, heated at  $55^{\circ}\text{C}$  for 18 hours with intermittent gentle shaking. After cooling to room temperature, samples were decolorized by adding 100  $\mu\text{l}$  of 30% hydrogen peroxide. Finally, Aquasol liquid scintillation cocktail (6 ml, New England Nuclear, Boston, MA) was added, and samples were placed in the dark for 72 hours prior to counting on a Packard Tri-carb Model 300 M liquid scintillation counter (Downers Grove, IL). Cpm were converted to dpm for all calculations of organ distribution of radioactivity.

#### Elimination Study

In the second study, mice were housed individually in metabolism cages (Nalge Company, Rochester, NY) for 24 hours prior to dosing. Urine and feces were separated during this acclimation period and subsequently served as control material for the study. Animals ( $N = 6$ ) were administered [ $^3\text{H}$ ]-2H-MCLR + 2H-MCLR (total of 100 mg/kg) and their fecal and urinary excreta were collected separately at 12-hour intervals for 72 hours. Feces were weighed and urine volumes recorded, and samples

of each were stored at  $-20^{\circ}\text{C}$  until assayed. Animals were killed as described above at 72 hours postdosing and tissues were collected as described above. Feces were diluted with water (5 ml/g feces), digested, and processed as described above for tissues. Urine was diluted with water to a volume of 20 ml and counted directly in liquid scintillation cocktail. Biological stability of the tritium label was assayed by evaporating subsamples of the urine and measuring the tritium associated with the distillate.

#### Statistical Analysis

Analyses of variance for a factorial design (F-ANOVA) were used to compare radioactivity in organs of the animals of the various treatment groups and to compare the radiolabel in the first 10 cm of small intestine with that in the remainder of the intestines in the two toxin-treated groups. Fixed variables in this design included dose of radiolabeled material and time elapsed between toxin administration and euthanasia. The response variables were accumulations of radiolabel in specific organs. Additional F-ANOVA analyses were used to compare the liver weights of various treatment groups over time. When statistically significant differences between groups were found for radiolabel uptake over time, linear contrasts were used within the F-ANOVA analyses to compare the radioactivity in livers and small intestines of various treatment groups at specific times. A level of  $\alpha = 0.05$  was chosen to detect statistically significant differences.

### 3. Results

#### Toxin

In low resolution FABMS, characteristic pseudomolecular ions of 995 and 997 ( $M + H$ )<sup>+</sup> were observed for MCLR and 2H-MCLR, respectively. High resolution FABMS confirmed structural formulae of  $C_{49}H_{74}N_{10}O_{12}$  ( $M + H$ ,  $\pm 1.6$  mmu) and  $C_{49}H_{76}N_{10}O_{12}$  ( $M + H$ ,  $\pm 1.6$  mmu), respectively. The 2H-MCLR obtained was determined to be > 99% chemically pure by HPLC and TLC methods, and the [<sup>3</sup>H]-2H-MCLR was found to be > 99% chemically pure and > 98% radiochemically pure by HPLC and TLC (Dahlem, 1989).

NaBH<sub>4</sub> treatment of MCLR followed by purification on HPLC yielded 1.4 mg of 2H-MCLR. [<sup>3</sup>H]-NaBH<sub>4</sub> treatment of MCLR followed by purification yielded 0.24 mg of purified labeled product with a specific activity of 5.3  $\mu$ Ci/mmol. The reaction of sodium borohydride with MCLR formed a mixture of diastereomers which were epimeric at the  $\alpha$ -carbon of the dehydro amino acid. These reduction products were separable from each other and from unreacted parent toxin by HPLC.

No spontaneous loss of radiolabel was detected in toxin stored at 1  $\mu$ g/ $\mu$ l in 0.1% ethanol at a temperature of -20°C for 2 weeks. Biological loss of radioactivity to form tritiated water was < 0.01% in all of the urine samples analyzed.

#### Toxicity Assessment of Diastereomers of 2H-MCLR

One of the diastereomers (the one with the shortest retention under the HPLC conditions described) retained approximately one-half of the original toxicity of the parent compound. The toxic effects of this diastereomer and the time course of

toxicity were found virtually identical to those of the parent compound in related studies (Dahlem et al., 1989a). Unfortunately, the configuration of the specific isomeric structure used in these studies could not be directly determined.

#### Distribution Study

A dose of 2H-MCLR which had been uniformly sublethal in preliminary studies (100 µg/kg) was compared with a dose of toxin which had been uniformly lethal (200 µg/kg) in animals (whether given as either the labeled or unlabeled dihydro derivative). The calculated total amounts of toxin equivalents and the concentrations of toxin equivalents detected in each organ are shown in Table 1. Fractions of the doses of toxin present in each organ over time are shown in Figure 1. Greater than 99% of the low dose and > 90% of the high dose were accounted for by the 60-minute time point.

A total of  $94.7 \pm 3.3\%$  (mean  $\pm$  SD) of the low dose was found in the liver at 60 minutes following administration and  $57.8\% \pm 5.2\%$  of the total radiolabel given remained in the liver of these animals at 72 hours postdosing. The high dose animals accumulated a lesser fraction, approximately 50% of the radiolabel administered in the liver with peak concentrations occurring at approximately 30 minutes postdosing. Although the fraction of the administered radioactivity taken up by the livers of high dose group was less, the concentrations of toxin equivalents in the liver were still significantly higher than in the low dose group at both 30 and 60 minutes. In addition, the relative liver weights of the high dose group ( $8.9\% \pm 0.8$ ) were also significantly greater than those of the low dose group at 60 minutes ( $6.7\% \pm 0.6$ ;



mean  $\pm$  standard deviation), and thus the total toxin uptake at the lethal dose was even higher than reflected in the concentration figures.

At most time points, the second highest concentration of toxin equivalents was found in the first (the most oral) 10 cm of the small intestine. In this portion of intestine, radiolabel initially increased, then tended to decline, and finally became elevated again over time. Nevertheless, significantly higher concentrations of label were found in the first 10 cm, as compared to the remainder of the small intestine, at 10, 30, and 60 minutes in both high and low dose groups.

At 60 minutes, concentrations of toxin equivalents became elevated in the kidneys and lungs of the high dose animals. In the kidneys,  $< 2\%$  of the administered dose at 30 minutes increased to  $> 4\%$  at 60 minutes, and lung concentrations increased from less  $< 0.3\%$  to  $> 0.8\%$  over the same period.

#### Elimination Study

In the second study, radioactivity above background was detected in urine for only the first 12 hours postdosing (Table 2). After administration of a total of 100  $\mu\text{g/kg}$ , urine volumes at the 12-hour point were uniformly consistently  $< 100 \mu\text{l}$ . Subsequently, urine volumes increased to the predosing range (0.5 to 1.0 ml) at every 12-hour sampling interval for the duration of the study. Elimination of radiolabel in the feces of the low dose mice was minimal during the first 12 hours postdosing, but elimination in feces ultimately accounted for 34% of the administered dose. As urinary elimination decreased, fecal elimination increased and was maintained at a relative high level throughout the 72-hour observation period.

#### 4. Discussion and Conclusions

Further studies will be necessary to compare the toxicity of the two diastereomers of 2H-MCLR, but it is clear that at least one bears similar lethal toxicity and causes the same spectrum of lesions as the parent compound. A steep threshold for toxicity is observed for MCLR between doses which cause minimal toxic effects and acutely lethal doses (First Annual Report, pp. 131-144; Lovell et al., 1989). This threshold was also observed in animals treated with 2H-MCLR in these preliminary experiments. The doses compared in the formal studies on elimination and distribution were selected in order to evaluate the fate of toxin in mice at doses that bracket this critical threshold of toxicity.

The liver is the major target organ for MCs (Falconer et al., 1981; Hooser et al., 1989a), and this would appear to be related to the fact that, as demonstrated in the present study, the liver accumulated the majority of the doses, and moreover, a large fraction of the radiolabel was retained by the liver for up to 72 hours after dosing. A larger percentage of the dose of toxin was taken up by the livers of animals in the sublethal group, but at 30 minutes, the lethal dose group had accumulated higher absolute concentrations of the compound than did the sublethal dose group even at 60 minutes. This seems to suggest that, at the higher dose, saturation of sites of uptake occurred and/or that damaged hepatocytes lost their ability to take up additional toxin.

This study indicated that the liver plays a major role in the elimination of 2H-MCLR. The high concentrations of radioactivity in the most oral portion of the small intestine was compatible with elimination via biliary excretion as were the

higher overall concentrations of radioactivity in feces than in urine. It seems likely that the high concentrations of radiolabel in the intestines shortly after dosing in both groups was probably a result of the intraperitoneal administration of toxin and association with the intestine prior to absorption into the portal circulation.

The increase in radiolabel in the kidneys and lungs of the lethal dose group at the 60-minute time point would appear to be related to lesions in these organs as documented in separate studies (Hooser et al., 1989a). Eosinophilic debris in the arterioles of the kidneys and lung at 60 minutes postdosing appeared to be intact or fragmented, degenerative or necrotic hepatocytes. The increase in the radioactivity associated with these organs of the lethal dose groups was therefore presumed to transport of toxin bound to hepatocytes and/or hepatocyte debris rather than a result of direct binding of 2H-MCLR to the kidney or lung.

Most studies on the fate of labeled algal peptide hepatotoxins performed before these trials had significant shortcomings. They failed to determine the structure of the labeled compound, to identify the specific location of the label(s) within the peptide structure, or to establish the stability of labeled compounds (Falconer et al., 1986; Runnegar et al., 1986; Brooks and Codd, 1987). In the absence of such information, the validity of the studies was uncertain. By contrast, in the present study, the identity of the MC derivative used, the site of label incorporation, and the stability of the radiolabel were established.

Brooks and Codd (1987) found accumulation of radiolabel in the livers of sublethally dosed animals reached 75% of the administered dose within 1 minute of

intraperitoneal administration of toxin. In the present study, however, accumulation was shown to be dose dependent and absorption in sublethal groups did not reach 75% of the dose until more than 30 minutes after toxin administration. Runnegar et al. (1986) found no more than 63% of the administered dose of radiolabel from  $^{125}\text{I}$ -labeled MC in the liver either following an acutely lethal dose or when animals were killed at the end of a 24-hour observation period. By contrast, a much higher fraction of the dose was accounted for by the livers of mice in the present study. Differences in the extent of reported hepatic uptake of the various toxin(s) may be related to differences in polarity of the compounds. Regardless of differences in the absolute uptake or time course of accumulation, all known reports to date have identified the liver as the target organ, and the site of primary toxin accumulation.

Elimination of radiolabel from toxin via the urine was limited to the first 12-hour observation period, whereas fecal elimination began within 12 hours of dosing and continued through the 72-hour observation period. Fecal mass was decreased slightly in the first 12 hours but increased to predosing rates within 24 hours of dosing. Whether the reduced fecal output was a response to stress caused by the dosing procedures or to the effects of the toxin remains uncertain.

Several groups have provided indirect evidence for the involvement of a bile acid transport system(s) in the uptake of MCs into isolated hepatocytes. Studies by our group involving administration of MCLR into jejunum and ileum were deemed compatible with a possible role of bile acid transport systems in the uptake of MCLR from the ileum (Dahlem et al., 1989b). Biliary excretion is likely to play a major role

in removing toxin from the liver since toxin appears rapidly in the duodenum of toxin-treated animals presumably from the bile. The terminal increase in radiolabel in the most oral portion of the small intestine is compatible with enterohepatic recirculation but this remains to be confirmed. These results are also largely in agreement with those of Robinson et al. (1989) who employed isotopically labelled [ $^3\text{H}$ ]-MCLR. Six hours after [ $^3\text{H}$ ]-MCLR was injected IP into mice, 56% of the dose was present in the liver, 10% was in the carcass, and 7% was in the intestine.

It is concluded from these studies that: 1) saturation of the dehydro portion of MCLR with tritium-labeled sodium borohydride is practical and the resultant material retains toxicity and organ specificity, 2) the labeled toxin has reasonable chemical and biological stability, 3) accumulation of toxin by the liver is rapid and elimination occurs slowly probably via the bile, 4) accumulation of toxin in the liver is a dose-dependent phenomenon and hepatic toxin uptake reaches a maximum after administration of a lethal dose, 5) accumulation of radiolabel from the toxin occurs in the lungs and kidneys to a greater degree when lethal doses are administered, which is compatible with passage of toxin bound to hepatocytes and hepatic debris from the damaged liver, and 6) toxin initially leaves via the urine but soon this virtually ceases and fecal elimination predominates.

Table 1. Tissue concentrations of toxin equivalents based on tritium-labeled dihydro microcystin-LR (mean  $\pm$  SD) over time. N = 3 animals/treatment/time in all groups with the exception of the 4,320-minute group where N = 6.

Tissue	Dose ( $\mu\text{g/kg}$ )	Time (min)	Total toxin equivalents ( $\mu\text{g/organ}$ )	Concentration of toxin equivalents ( $\mu\text{g/g}$ )
Liver	100	1	$0.44 \pm 0.03$	$0.39 \pm 0.02$
		5	$0.90 \pm 0.12$	$0.72 \pm 0.12$
		10	$1.64 \pm 0.28$	$1.41 \pm 0.18$
		30	$3.56 \pm 0.82$	$2.79 \pm 0.82$
		60	$4.73 \pm 0.16$	$3.86 \pm 0.48$
		4,320	$2.89 \pm 0.26$	$1.92 \pm 0.09$
	200	1	$0.64 \pm 0.06$	$0.52 \pm 0.06$
		5	$1.30 \pm 0.27$	$1.16 \pm 0.27$
		10	$2.20 \pm 0.51$	$1.82 \pm 0.37$
		30	$5.36 \pm 0.68$	$4.15 \pm 0.52$
		60	$5.02 \pm 0.38$	$2.93 \pm 0.27$
Kidneys	100	1	$0.07 \pm 0.03$	$0.22 \pm 0.10$
		5	$0.10 \pm 0.01$	$0.26 \pm 0.03$
		10	$0.15 \pm 0.05$	$0.43 \pm 0.12$
		30	$0.11 \pm 0.02$	$0.30 \pm 0.06$
		60	$0.07 \pm 0.01$	$0.19 \pm 0.03$
		4,320	$0.06 \pm 0.01$	$0.14 \pm 0.02$
	200	1	$0.10 \pm 0.01$	$0.30 \pm 0.03$
		5	$0.15 \pm 0.02$	$0.43 \pm 0.07$
		10	$0.18 \pm 0.03$	$0.50 \pm 0.07$
		30	$0.16 \pm 0.03$	$0.49 \pm 0.11$
		60	$0.42 \pm 0.04$	$1.16 \pm 0.05$
Spleen	100	1	$0.04 \pm 0.01$	$0.56 \pm 0.05$
		5	$0.03 \pm 0.01$	$0.44 \pm 0.03$
		10	$0.04 \pm 0.01$	$0.46 \pm 0.13$
		30	$0.02 \pm 0.01$	$0.19 \pm 0.08$
		60	$0.01 \pm 0.01$	$0.09 \pm 0.01$
		4,320	$0.01 \pm 0.01$	$0.04 \pm 0.01$

Tissue	Dose ( $\mu\text{g/kg}$ )	Time (min)	Total toxin equivalents ( $\mu\text{g/organ}$ )	Concentration of toxin equivalents ( $\mu\text{g/g}$ )
Small Intestine (first 10 cm)	200	1	$0.06 \pm 0.02$	$0.82 \pm 0.20$
		5	$0.07 \pm 0.01$	$0.87 \pm 0.08$
		10	$0.06 \pm 0.01$	$0.73 \pm 0.16$
		30	$0.02 \pm 0.01$	$0.29 \pm 0.05$
		60	$0.02 \pm 0.01$	$0.25 \pm 0.04$
	100	1	$0.93 \pm 0.27$	$2.71 \pm 0.85$
		5	$0.74 \pm 0.13$	$1.44 \pm 0.24$
		10	$0.45 \pm 0.07$	$1.23 \pm 0.13$
		30	$0.61 \pm 0.26$	$1.79 \pm 0.91$
		60	$1.06 \pm 0.04$	$1.64 \pm 0.38$
		4,320	$0.16 \pm 0.03$	$0.32 \pm 0.09$
		1	$1.13 \pm 0.07$	$2.61 \pm 0.41$
		5	$1.18 \pm 0.37$	$2.55 \pm 0.50$
		10	$0.92 \pm 0.13$	$2.32 \pm 0.45$
		30	$0.92 \pm 0.12$	$1.79 \pm 0.77$
		60	$1.29 \pm 0.25$	$2.32 \pm 0.43$
		1	$0.33 \pm 0.05$	$0.59 \pm 0.12$
Small Intestine (remainder)	100	5	$0.31 \pm 0.02$	$0.44 \pm 0.05$
		10	$0.29 \pm 0.06$	$0.48 \pm 0.13$
		30	$0.34 \pm 0.06$	$0.50 \pm 0.10$
		60	$0.28 \pm 0.07$	$0.41 \pm 0.14$
		4,320	$0.18 \pm 0.05$	$0.17 \pm 0.06$
	200	1	$0.61 \pm 0.10$	$0.95 \pm 0.18$
		5	$0.53 \pm 0.08$	$0.77 \pm 0.11$
		10	$0.54 \pm 0.01$	$0.80 \pm 0.03$
		30	$0.60 \pm 0.09$	$0.80 \pm 0.07$
		60	$0.52 \pm 0.07$	$0.94 \pm 0.11$
Stomach	100	1	$0.20 \pm 0.03$	$0.96 \pm 0.26$
		5	$0.23 \pm 0.04$	$0.85 \pm 0.14$
		10	$0.20 \pm 0.05$	$0.92 \pm 0.20$
		30	$0.22 \pm 0.05$	$1.09 \pm 0.27$
		60	$0.14 \pm 0.02$	$0.59 \pm 0.13$
		4,320	$0.14 \pm 0.02$	$0.77 \pm 0.11$

Tissue	Dose ( $\mu\text{g/kg}$ )	Time (min)	Total toxin equivalents ( $\mu\text{g/organ}$ )	Concentration of toxin equivalents ( $\mu\text{g/g}$ )
	200	1 5 10 30 60	$0.32 \pm 0.07$ $0.35 \pm 0.03$ $0.34 \pm 0.06$ $0.32 \pm 0.07$ $0.45 \pm 0.12$	$1.43 \pm 0.31$ $1.47 \pm 0.22$ $1.65 \pm 0.46$ $1.33 \pm 0.37$ $2.00 \pm 0.70$
Large Intestine	100	1 5 10 30 60 4,320	$0.51 \pm 0.09$ $0.45 \pm 0.07$ $0.43 \pm 0.11$ $0.30 \pm 0.05$ $0.25 \pm 0.04$ $0.16 \pm 0.03$	$0.92 \pm 0.15$ $0.69 \pm 0.14$ $0.81 \pm 0.20$ $0.47 \pm 0.08$ $0.45 \pm 0.09$ $0.18 \pm 0.03$
	200	1 5 10 30 60	$0.65 \pm 0.06$ $0.85 \pm 0.27$ $0.50 \pm 0.08$ $0.60 \pm 0.12$ $0.54 \pm 0.13$	$1.12 \pm 0.09$ $1.37 \pm 0.40$ $0.98 \pm 0.19$ $0.88 \pm 0.15$ $0.91 \pm 0.18$
Brain	100	1 5 10 30 60 4,320	$0.00 \pm 0.00$ $0.01 \pm 0.00$ $0.01 \pm 0.00$ $0.01 \pm 0.00$ $0.01 \pm 0.00$ $0.00 \pm 0.00$	$0.01 \pm 0.00$ $0.02 \pm 0.00$ $0.01 \pm 0.00$ $0.01 \pm 0.00$ $0.01 \pm 0.00$ $0.01 \pm 0.00$
	200	1 5 10 30 60	$0.01 \pm 0.00$ $0.01 \pm 0.00$ $0.01 \pm 0.00$ $0.01 \pm 0.00$ $0.02 \pm 0.00$	$0.02 \pm 0.00$ $0.02 \pm 0.00$ $0.03 \pm 0.01$ $0.02 \pm 0.00$ $0.04 \pm 0.01$
Heart	100	1 5 10 30 60 4,320	$0.01 \pm 0.00$ $0.01 \pm 0.00$ $0.01 \pm 0.00$ $0.01 \pm 0.00$ $0.01 \pm 0.00$ $0.00 \pm 0.00$	$0.07 \pm 0.01$ $0.07 \pm 0.01$ $0.09 \pm 0.03$ $0.07 \pm 0.02$ $0.06 \pm 0.02$ $0.03 \pm 0.00$



Tissue	Dose ( $\mu\text{g/kg}$ )	Time (min)	Total toxin equivalents ( $\mu\text{g/organ}$ )	Concentration of toxin equivalents ( $\mu\text{g/g}$ )
Lung	200	1	$0.01 \pm 0.00$	$0.12 \pm 0.02$
		5	$0.01 \pm 0.00$	$0.13 \pm 0.03$
		10	$0.01 \pm 0.00$	$0.12 \pm 0.02$
		30	$0.01 \pm 0.00$	$0.13 \pm 0.02$
		60	$0.03 \pm 0.00$	$0.29 \pm 0.03$
	100	1	$0.02 \pm 0.00$	$0.12 \pm 0.02$
		5	$0.01 \pm 0.00$	$0.08 \pm 0.01$
		10	$0.03 \pm 0.01$	$0.17 \pm 0.07$
		30	$0.02 \pm 0.01$	$0.11 \pm 0.04$
		60	$0.01 \pm 0.00$	$0.05 \pm 0.01$
		4,320	$0.10 \pm 0.22$	$0.56 \pm 1.21$
	200	1	$0.06 \pm 0.05$	$0.36 \pm 0.32$
		5	$0.04 \pm 0.02$	$0.23 \pm 0.11$
		10	$0.03 \pm 0.01$	$0.18 \pm 0.06$
		30	$0.03 \pm 0.01$	$0.16 \pm 0.03$
		60	$0.08 \pm 0.01$	$0.44 \pm 0.05$

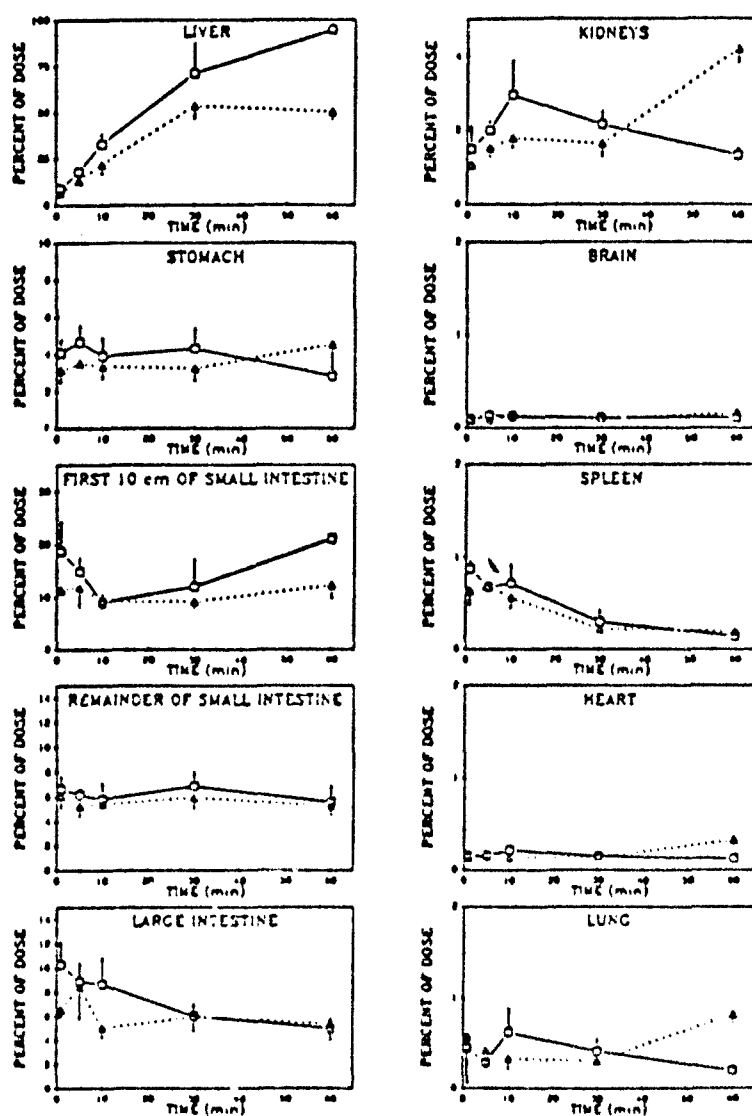
\*Mean  $\pm$  standard deviation.

Table 2. Elimination of tritium-labeled dihydromicrocystin-LR as a function of time in the urine and feces of mice dosed intraperitoneally.

Sample	Time	Percent of Dose*
Urine	0 to 12 hours	$3.63 \pm 2.25$
	12 to 24 hours	$< 0.10$
	24 to 36 hours	$< 0.10$
	36 to 48 hours	$< 0.10$
	48 to 60 hours	$< 0.10$
	60 to 72 hours	$< 0.10$
Feces	0 to 12 hours	$2.51 \pm 2.37$
	12 to 24 hours	$7.18 \pm 6.48$
	24 to 36 hours	$6.89 \pm 6.77$
	36 to 48 hours	$9.70 \pm 9.35$
	48 to 60 hours	$13.87 \pm 5.51$
	60 to 72 hours	$13.56 \pm 12.87$

\*Mean  $\pm$  standard deviation.

Figure 1. Fraction of the administered sublethal (100  $\mu\text{g/kg}$ ) (squares) or lethal (200  $\mu\text{g/kg}$ ) (triangles) doses of labeled + nonlabeled toxin in mouse tissues over time.  $N = 3$  animals  $\cdot$  treatment $^{-1}$   $\cdot$  time $^{-1}$ .



**B. Uptake and Subcellular Localization of Tritiated Dihydromicrocystin-LR in Rat Liver****1. Statement of the Problem, Background, and Rationale**

Ultrastructurally, MCLR causes hepatocyte plasma membrane invagination, blebbing, and loss of microvilli prior to cell death (Hooser et al., 1990a). In cell suspensions, MCLR causes plasma membrane blebbing in hepatocytes but not in sinusoidal endothelial or Kupffer cells (Hooser et al., 1990b). In contrast to the hepatocyte necrosis induced by microcystins *in vivo*, hepatocytes in suspension remain viable (Runnegar and Falconer, 1982).

It has been suggested that the hepatocyte specificity of MCs is related to transport into these cells by a hepatocyte-specific bile acid carrier. When suspensions of isolated hepatocytes were preincubated with noncompetitive inhibitors of hepatocyte specific bile acid carriers (rifampicin and bromosulfophthalein) (Ziegler and Frimmer, 1986), there was marked reduction in microcystin-induced plasma membrane blebbing (Runnegar et al., 1981; Runnegar and Falconer, 1982).

Both cultured hepatocytes and hepatocyte suspensions exhibit aggregations of actin filaments following treatment with MCLR, and these changes seem to be related to plasma membrane blebbing (Eriksson et al., 1989; Hooser et al., 1990b). However, a significant change in the ratio of polymerized to unpolymerized actin was not detected in microcystin-treated hepatocytes (Runnegar and Falconer, 1986; Eriksson et al., 1989).

The objectives of our studies were to: 1) characterize the rate and extent of uptake of [<sup>3</sup>H]-2H-MCLR in hepatocytes in suspension, with and without pretreatment

with rifampicin; 2) characterize the nature of intracellular distribution of [ $^3$ H]-2H-MCLR using subcellular fractionation of hepatocytes; 3) determine whether [ $^3$ H]-2H-MCLR binds directly to hepatocyte proteins, particularly those of the cytoskeleton; and 4) confirm findings from hepatocyte suspensions by repeating these studies in isolated perfused livers.

## 2. Experimental Methods

### Animals

Male, 175 to 250 g, Sprague-Dawley rats (Harlan Sprague-Dawley, Inc., Indianapolis, IN) were allowed to acclimatize to their cages for 2 weeks or longer before use. Animals had free access to a commercial laboratory animal ration and water and were maintained on a 12-hour light-dark cycle.

### Toxin

Microcystin-LR (MCLR) (approximately 95% pure) from *Microcystis aeruginosa*, laboratory strain PCC-7820 was produced and purified in the laboratory of W. W. Carmichael using techniques previously described (Krishnamurthy et al., 1986a). Purified toxin was dissolved in phosphate-buffered saline (PBS) prior to use. Dihydromicrocystin-LR and tritiated dihydromicrocystin-LR ([ $^3$ H]-2H-MCLR) were prepared and purified as previously described.

### Hepatocyte Isolation

Rat hepatocytes were isolated using a two-step collagenase perfusion technique (Kuhlenschmidt et al., 1982). Cell viability was 85 to 90%, as determined by Trypan blue exclusion. Cell pellets were resuspended in Ham's F-10 medium (complete

medium), containing (per 500 ml) 100 ml of fetal bovine serum (FBS) and 0.3 ml of insulin (100 U/ml), and placed on ice.

#### Uptake of Dihydromicrocystin-LR into Hepatocytes

Uptake of [ $^3\text{H}$ ]-2H-MCLR into suspensions of hepatocytes was determined at 0°C, 37°C, and following a 10-minute preincubation with 50 µg/ml of rifampicin at 37°C using modifications of previously described methods (Eaton and Klaassen, 1978; Kuhlenschmidt et al., 1984). Hepatocytes in complete medium were centrifuged at 70 x g for 2 minutes and the pellets were resuspended in 2.5 ml of Ham's F-10 media without FBS but with insulin (incomplete medium) to a final concentration of  $1.5 \times 10^7$  hepatocytes/ml, placed in capped plastic culture tubes (12 x 75 mm), and incubated at 0°C or 37°C under constant end-over-end rotation at 6 rpm. Rifampicin preincubation was achieved by adding rifampicin in PBS to the suspension 10 minutes before toxin addition. Cold 2H-MCLR (37.5 µg), premixed with [ $^3\text{H}$ ]-2H-MCLR (12.5 µg,  $9.8 \times 10^5$  dpm), was added to PBS at 37°C so that the toxin concentration was 20 µg/ml. This mixture was then added to the hepatocyte suspension such that the final toxin concentration was 10 µg/ml (cold plus tritiated,  $2 \times 10^4$  dpm/µg), and the final hepatocyte concentration was  $7.5 \times 10^6$  hepatocytes/ml in 5 ml of medium.

At time 0, 20, 40, and 60 seconds and at 2, 4, 6, 8, 10, 15, and 30 minutes, two 100 µl aliquots of each suspension were removed, layered over 500 µl of Dow Corning 550 silicone oil:light mineral oil (5:1) (Kuhlenschmidt et al., 1984), and microfuged for 15 seconds to separate cells from the supernatant. The supernatant and oil from each tube were then removed and 100 µl of 1% Triton X-100 (TX-100) was

used to solubilize each pellet. The 100  $\mu$ l pellet (in TX-100) was placed in 10 ml LSC. All cell pellets in LSC were counted on a Packard 460 Tri-Carb scintillation counter.

Following removal of the last two 100  $\mu$ l aliquots at 30 minutes, the remainder of each suspension culture was placed in an ice bath for less than an hour until subcellular fractionation was begun.

#### Uptake of [ $^3$ H]-2H-MCLR into Isolated, Perfused Liver

Two rats were anesthetized and their portal veins catheterized in the same manner as that used to isolate hepatocytes, except that the flow rate of perfusate was 25 ml/minute (Berg et al., 1988). Once catheterized, the livers were perfused for 15 minutes with complete medium containing (per 500 ml) 1.2 g HEPES, pH 7.35. Since the minimum IP LD<sub>100</sub> for MCLR in rats is 180  $\mu$ g/kg (Hooser et al., 1989a), while the minimum LD<sub>100</sub> for 2H-MCLR is approximately two times that of MCLR (Dahlem et al., 1990), 172.4  $\mu$ g of toxin (two parts of cold 2H-MCLR:one part [ $^3$ H]-2H-MCLR, 12.5  $\mu$ g,  $9.8 \times 10^5$  dpm) was added to 100 ml of media (final specific radioactivity was  $5.68 \times 10^3$  dpm/ $\mu$ g). After a 15-minute perfusion of the isolated liver with medium not containing toxin, the perfusate was changed to the 100 ml of medium containing toxin and drained from the liver to allow recirculation of the toxin. One 200  $\mu$ l aliquot was removed from the container of recirculating medium from the first rat liver at 0, 20, 40, and 60 seconds, at 2, 4, 6, 8, and 10 minutes, and then every 5 minutes until 120 minutes. Aliquots (200  $\mu$ l) in 5 ml of LSC were counted as described above. At 120 minutes, the liver was perfused with 100 ml of complete

medium without toxin and then placed on ice in 0.25 M sucrose (4°C) for subcellular fractionation. At 15, 30, 45, and 120 minutes, small pieces of liver were tied off with surgical suture, removed, and placed in 10% neutral buffered formalin for histologic examination.

Since maximal uptake of toxin in the liver of the first rat had occurred at approximately 45 minutes, perfusion of the second liver with toxin was ended at 45 minutes, and liver samples for histologic examination were taken at 0, 15, 30, and 45 minutes.

#### Subcellular Fractionation of Hepatocytes and Perfused Liver

The 2.8 ml of hepatocyte suspension obtained from the uptake studies described above and the two perfused livers were fractionated using a modification of a previously described subcellular fractionation method (Reid and Williamson, 1974). This technique yields five fractions: crude nuclear (which also contains plasma membrane fragments), heavy mitochondrial, light mitochondrial (which also contains lysosomes), microsomal, and cytosolic. Isolated hepatocytes were resuspended in cold 0.25 M sucrose and homogenized by passage through a 26-gauge needle 20 to 40 times. Cell disruption was verified by microscopic examination. All pellets of the various subcellular fractions were resuspended in 1 ml of PBS and aliquots were placed in LSC (Aquasol II, containing detergent) for scintillation counting.

#### Extraction of Isolated Hepatocytes Following Exposure to [<sup>3</sup>H]-2H-MCLR

Suspensions of hepatocytes in incomplete Ham's F-10 medium were prepared as described above. A combination of 2H-MCLR (37.5 µg) and [<sup>3</sup>H]-2H-MCLR (12.5



µg) were added to PBS so that the total toxin concentration was 20 µg/ml. This mixture was added to the 2.5 ml of hepatocyte suspension resulting in a final toxin concentration of 10 µg/ml. Cells were incubated at 37°C for 30 minutes, placed on ice, and subsequently pelleted by centrifugation at 70 x g for 2 minutes at 4°C.

The supernatant was removed and saved for subsequent counting. For extraction, 10 ml of 1% TX-100 buffer (10 mM EDTA, 0.1 M Tris-Cl, pH = 7.4) was mixed with the cell pellet, and the mixture was placed on ice and periodically agitated to allow for solubilization over a 2-hour period. The solubilized cells were centrifuged at 150,000 x g for 45 minutes at 4°C using a Beckman LS-50 ultracentrifuge (Fox et al., 1984). Detergent soluble components in the supernatant were removed and saved for scintillation counting. Insoluble components in the pellet (predominantly actin, other cytoskeletal elements, and histones) were added to 1.5 ml of 3 N HCl and warmed until dissolved. An equal amount of 3 M KOH was added and the samples saved for liquid scintillation counting.

#### Trichloroacetic Acid Precipitation of Cytosolic Fractions

Two hundred microliters of 30% (w/v) trichloroacetic acid (TCA) was mixed with 400 µl of the cytosolic fraction from each of the two isolated liver perfusions and the six isolated hepatocyte suspensions for a final TCA concentration of 10%. Samples were placed on ice for 1 hour and microfuged for 10 minutes. Subsequently, 500 µl of the supernatant was placed in 4.0 ml of LSC. Pellets were mixed with 500 µl of LSC (Aquasol II, containing detergent) and held over night in an oven at 53°C, such that only a small amount of detergent insoluble material remained. Samples

were again microfuged for 10 minutes and the supernatant removed and placed in 4.0 ml of LSC. The residual insoluble pellet was mixed with 250  $\mu$ l of 3 M KOH and dissolved overnight at 53°C. To this material, 250  $\mu$ l of 3 N HCl was added; this was mixed with 4.5 ml of LSC for liquid scintillation counting.

#### Histologic Examination

To determine the extent of plasma membrane blebbing, unfixed hepatocyte suspensions were examined by light microscopy. Specimens from the isolated perfused livers were fixed in 10% neutral buffered formalin, embedded in glycol methacrylate, sectioned at 2 microns, stained with hematoxylin and eosin, and examined by light microscopy.

### 3. Results

#### Uptake of [ $^3$ H]-2H-MCLR by and Morphologic Changes in Hepatocytes

Hepatocytes in suspension at 37°C rapidly incorporated [ $^3$ H]-2H-MCLR during the first 4 minutes. Thereafter, uptake was more gradual and it began to level off after 15 minutes (Figure 1). At 30 minutes, the average radioactivity taken up by the 100  $\mu$ l aliquot of hepatocytes ( $7.5 \times 10^5$  hepatocytes per 100  $\mu$ l) was 1,752 dpm, which is equivalent to 87.6 ng (88 pmole) of total toxin per  $7.5 \times 10^5$  hepatocytes.

Incubation of hepatocytes at 0°C, or preincubation with rifampicin at 37°C, markedly slowed and reduced the total uptake of [ $^3$ H]-2H-MCLR (Figure 1). After 30 minutes at 0°C, uptake of [ $^3$ H]-2H-MCLR was reduced by 50% as compared to 37°C. Preincubation with rifampicin reduced uptake over the same time period by 64%.

Microscopic examination following incubation with [ $^3\text{H}$ ]-2H-MCLR at 37°C for 30 minutes revealed that almost all hepatocytes had numerous large plasma membrane blebs. By contrast, less than 50% of the hepatocytes preincubated with rifampicin or incubated at 0°C had multiple large plasma membrane blebs.

#### Uptake of Dihydromicrocystin-LR by Perfused Livers

Uptake of [ $^3\text{H}$ ]-2H-MCLR by perfused liver at 37°C was rapid. In the first experiment, there was rapid uptake of radiolabel for the first 10 minutes, then uptake plateaued for approximately 40 minutes, and this was followed by a release of radioactivity from the liver into the perfusion medium beginning at 50 minutes and continuing until the end of the experiment at 120 minutes (Figure 2). At the time of maximal hepatic uptake (50 minutes), a total of 83.5  $\mu\text{g}$  2H-MCLR were present in this 11.58 g liver, which is equivalent to an uptake of 7.2  $\mu\text{g}$  (7.3 nmoles) per g liver. Assuming  $1.2 \times 10^8$  hepatocytes per g of liver (Doust, 1958), this is equivalent to an uptake of 45 ng (45.6 pmole) of total toxin per  $7.5 \times 10^5$  hepatocytes which may be compared to 87.6 ng taken up by this number of cells in suspension.

The second experiment was technically superior to the first due to better perfusion. Uptake in this liver was even more rapid, with near maximal uptake occurring by 4 minutes (Figure 3). After 4 minutes, however, uptake virtually stopped and radioactivity in the perfusion media remained essentially constant until 40 minutes, when hepatic radioactivity began to decrease, i.e., radioactivity in the perfusate began to increase. At the time of maximal uptake (40 minutes), 230  $\mu\text{g}$  of 2H-MCLR were present in this 12.62 g liver. This is equivalent to an uptake of 118

$\mu\text{g}$  (119 pmoles) of total toxin per  $7.5 \times 10^5$  hepatocytes, which compares favorably to the 87.6 ng taken up by the same number of hepatocytes in suspension.

### Lesions

In each of the perfused livers, microscopic lesions were first evident beginning at 15 minutes after perfusion with [ $^3\text{H}$ ]-2H-MCLR was begun and then became progressively more severe thereafter. Initial lesions were located periportally and were characterized by hepatocyte vacuolization followed by hepatocyte disassociation and rounding. By 45 minutes, necrosis characterized by cell fragmentation, nuclear pyknosis, and karyorrhexis was observed periportally and midzonally, and hepatocyte disassociation and rounding were noted in centrilobular regions. In the liver perfused for 120 minutes, necrosis was more severe at 120 minutes than at 45 minutes, but even at this time point it was still less severe than the necrosis in the second liver which had been perfused for a total of 45 minutes.

### Subcellular Fractionation of Hepatocytes from Suspension Cultures

In hepatocyte suspensions, the majority of radioactivity remained in the medium and was not incorporated into hepatocytes. Incubation of hepatocytes at  $37^\circ\text{C}$  resulted in an uptake of 2.5% of the total [ $^3\text{H}$ ]-2H-MCLR added to the medium. When fractionated, the largest percentage of radioactivity was present in the cytosolic fraction, followed by nuclear/plasma membrane fraction. In hepatocytes incubated at  $37^\circ\text{C}$ , 70.0 and 13.5% were found in the cytosolic and plasma membrane/nuclear fractions, respectively. Although the total uptake of [ $^3\text{H}$ ]-2H-MCLR was reduced by incubation at  $0^\circ\text{C}$  or by pretreatment with rifampicin, the distribution of the total

cellular radioactivity ultimately found in various fractions was similar to that in the hepatocytes incubated at 37°C.

#### Subcellular Fractionation of Specimens of Isolated Perfused Livers

In the first liver, perfused for 120 minutes, 10.5% of the radioactivity was incorporated into the liver. When fractionated, 71.0% of the radiolabel was in the cytosolic fraction, while 7.0 and 15.7% was present in the nuclear/plasma membrane and microsomal fractions, respectively (Figure 4). In the perfused liver preparations, a significantly greater percentage of the added toxin was taken up. In the liver perfused for 45 minutes, 13.1% of the radioactivity was taken up. When fractionated, 77.8% of the radiolabel was present in the cytosolic fraction, while 0.7 and 15.8% was present in the nuclear/plasma membrane and microsomal fractions, respectively.

#### Extraction of Hepatocytes in Suspensions Following Uptake of [<sup>3</sup>H]-2H-MCLR

The detergent extractable portions of isolated hepatocytes contained 97.5% of the radioactivity associated with the cells, whereas only 2.5% was associated with the insoluble pellet.

#### Trichloroacetic Acid Precipitation of Proteins in Cytosolic Fractions from Hepatocyte Suspensions

Following treatment with TCA, 92.4% of the radioactivity was present in the supernatant. In cytosolic fractions of hepatocytes incubated at 37°C for 30 minutes, 59.1% of the tritium was present in the precipitated pellet and 40.9% was in the supernatant (Figure 5). In cytosolic fractions from hepatocytes preincubated with

rifampicin or incubated at 0°C for 30 minutes, approximately 50% of the radiolabel was present in the precipitated pellet and 50% remained in the supernatant.

#### Trichloroacetic Acid Precipitation of Proteins in Cytosolic Fractions from Isolated Perfused Livers

In the liver perfused for 120 minutes, 78.5% of the radiolabel was found in the precipitate and 21.5% was present in the supernatant (Figure 5). The precipitated pellet of the cytosolic fraction of the liver perfused for 45 minutes contained 88.3% of the radiolabel, while the supernatant contained 11.7%.

#### 4. Discussion and Conclusion

In hepatocyte suspension, the uptake of [ $^3\text{H}$ ]-2H-MCLR was rapid, plateauing after 4 to 10 minutes. Such a plateau could result from saturation of hepatocyte receptors, microcystin-induced alteration which prevents further uptake, or the establishment of a steady-state where uptake is balanced by toxin or metabolite efflux. Cessation of uptake could be due to: 1) disruption of actin filaments and/or their plasma membrane connections, 2) a direct effect on the plasma membrane receptor or carrier itself, or 3) another MCLR-intracellular protein interaction which then secondarily affects the carrier (or receptor). Further studies are needed to rigorously define the mechanism of hepatic uptake of microcystin and to identify its cellular target site. However, it now seems likely that the primary biochemical effect of MCs is inhibition of protein phosphatase activity (see subsequent section).

Uptake of [ $^3\text{H}$ ]-2H-MCLR also took place very rapidly in isolated perfused livers. The difference in total amount of toxin taken up and time required to reach

maximal uptake in the two preparations was presumably due to technical difficulties in the 120-minute preparation. The severity of necrosis was greater in the 45-minute preparation which had taken up a greater amount of toxin and had reached plateau quite early. Additional studies are needed to confirm these preliminary data.

The release of radioactivity from the isolated perfused liver preparation at 40 minutes following the onset of toxin perfusion was likely to have been due to cellular necrosis and fragmentation which was observed histologically within 45 minutes of the introduction of toxin into the system. Although less likely, some of the release may also be due to biliary excretion of the toxin. Although the main route of excretion of microcystins is in the bile (Falconer et al., 1986; Dahlem, 1989), bile flow may cease within 45 minutes of perfusion with a toxic dose of microcystin (Berg et al., 1988).

The reduction in the rate and total amount of [ $^3$ H]-2H-MCLR associated with incubation of the exposed cells at 0°C suggests that the uptake of [ $^3$ H]-2H-MCLR into hepatocytes is an energy-dependent process (Frimmer, 1982). Preincubation of hepatocytes with rifampicin caused an even larger decrease in toxin uptake, presumably via noncompetitive inhibition of hepatocyte bile acid carriers responsible for MC uptake (Ziegler and Frimmer, 1986). This is in agreement with the studies of Runnegar and Falconer (1982), in which pretreatment of hepatocytes in suspension with rifampicin prevented or greatly reduced microcystin-induced plasma membrane blebbing.

Uptake of [ $^3\text{H}$ ]-2H-MCLR into hepatocytes at 37°C or into perfused liver was only 2.5% or up to 13.1%, respectively, of the total in the medium. When calculated on a nanogram/hepatocyte basis, however, the uptake in each system was very similar. Although the amount taken up was very small, it was nevertheless sufficient to induce lesions in hepatocytes and in the perfused liver which were virtually identical to those caused by MCLR. At 0°C or with rifampicin preincubation, uptake was slowed and morphologic changes were delayed. It seems that a critical but only very small amount of microcystin must enter the cell before damage occurs.

The difference in lesion distribution in this study, may be due to changes in perfusion or oxygen tension in the artificial perfusion system used.

In hepatocyte suspensions and perfused livers, the major fraction of radioactivity from toxin taken into the cells was present in the cytosolic fraction, and a smaller percentage was in the plasma membrane/nuclear fraction. It is uncertain if a portion of the [ $^3\text{H}$ ]-2H-MCLR is specifically associated with the plasma membrane or the nucleus. One might speculate that some of the toxin is likely to be associated with the plasma membrane bile acid carrier because at 0°C and with rifampicin preincubation, the percentage in this fraction increases at the expense of the cytosolic fraction, and this would be compatible with the slower uptake.

When cytosolic fractions from cells in suspension were treated with trichloroacetic acid, 40 to 50% of the radiolabel was found in the supernatant, presumably as free or degraded toxin. However, 50 to 60% of the [ $^3\text{H}$ ]-2H-MCLR was in the precipitated pellet suggesting that it was bound to cytosolic protein. Larger



fractions of incorporated radiolabel (78.5 and 88.3%) were present in the cytosolic precipitate of cells from the isolated, perfused livers. This may reflect increased reaction with a specific cytosolic binding protein made possible as a result of the later times of fractionation (45 and 120 minutes) as compared to the hepatocyte suspensions (30 minutes).

Based on the detergent-extraction experiments, it would appear unlikely that [ $^3\text{H}$ ]-2H-MCLR preferentially binds to actin, since only 2.5% of the radiolabel was bound to the insoluble pellet (actin and other detergent insoluble elements). This finding is unlike the case of phalloidin which binds directly to actin filaments and thus elicits its toxic effect (Weiland, 1977). Although MCs do not cause a change in the polymerization state of actin (Runnegar and Falconer, 1986; Eriksson et al., 1989), MCLR does cause morphologic alterations in the actin filaments of hepatocytes both *in vitro* and *in vivo* (Eriksson et al., 1989; Hooser et al., 1990b). It is possible that MCs interact with or otherwise activate a cytosolic protein(s) which results in cross-linking of actin filaments which are already polymerized, so that the polymerization state remains constant. Alternately, MCLR may bind to a cytosolic protein which interacts with a protein responsible for actin-plasma membrane binding. Either or both mechanisms may cause actin microfilaments to detach from the plasma membrane and collapse into the interior of the cell.

The present study in the context of previous reports supports the hypothesis that MCs are taken up by hepatocytes via an energy-driven, hepatocyte-specific bile acid carrier-dependent system (Runnegar and Falconer, 1982; Weiland et al., 1984; Hooser

et al., 1990b). Once inside the hepatocyte, the tritium appears to bind to cytosolic protein that directly or indirectly causes aggregation of polymerized actin filaments (Hooser et al., 1990b), plasma membrane alterations, breakdown of the hepatic architecture, hemorrhage, and death of the animal (Runnegar and Falconer, 1982; Hooser et al., 1989a). These observations seem to be compatible with inhibition of protein phosphatases and cytoskeletal damage which is presumed to be a direct result of excessive phosphorylation of intracellular proteins (see later section).

Figure 1. Kinetics of uptake of 2H-MCLR by hepatocytes in suspension. Hepatocytes ( $7.5 \times 10^6$  cells/ml) were incubated with [ $^3$ H]-2H-MCLR ( $2 \times 10^4$  dpm/ $\mu$ g) and analyzed for toxin uptake. Each point represents the mean of four replicates (two from each of two rats)  $\pm$  SEM. (O-O), uptake at 37°C; ( $\diamond$ - $\diamond$ ), uptake at 37°C by rifampicin (rif)-treated (50  $\mu$ g/ml) hepatocytes; ( $\Delta$ - $\Delta$ ), uptake at 0°C.

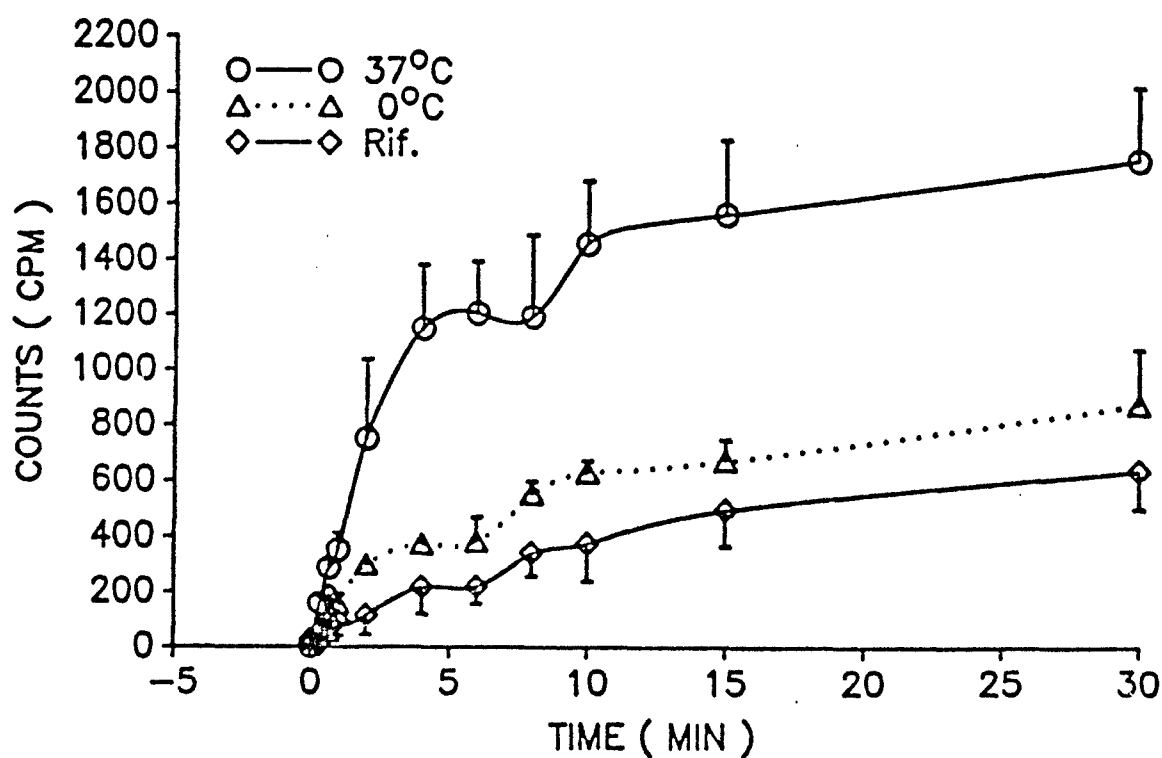


Figure 2. Kinetics of uptake of 2H-MCLR by perfused liver. Intact rat livers were perfused with [ $^3\text{H}$ ]-2H-MCLR (172.4  $\mu\text{g}$ ,  $5.68 \times 10^3$  dpm/ $\mu\text{g}$ ) and analyzed. "Counts" is the total number of counts taken up by the liver (from the media) at each time point.

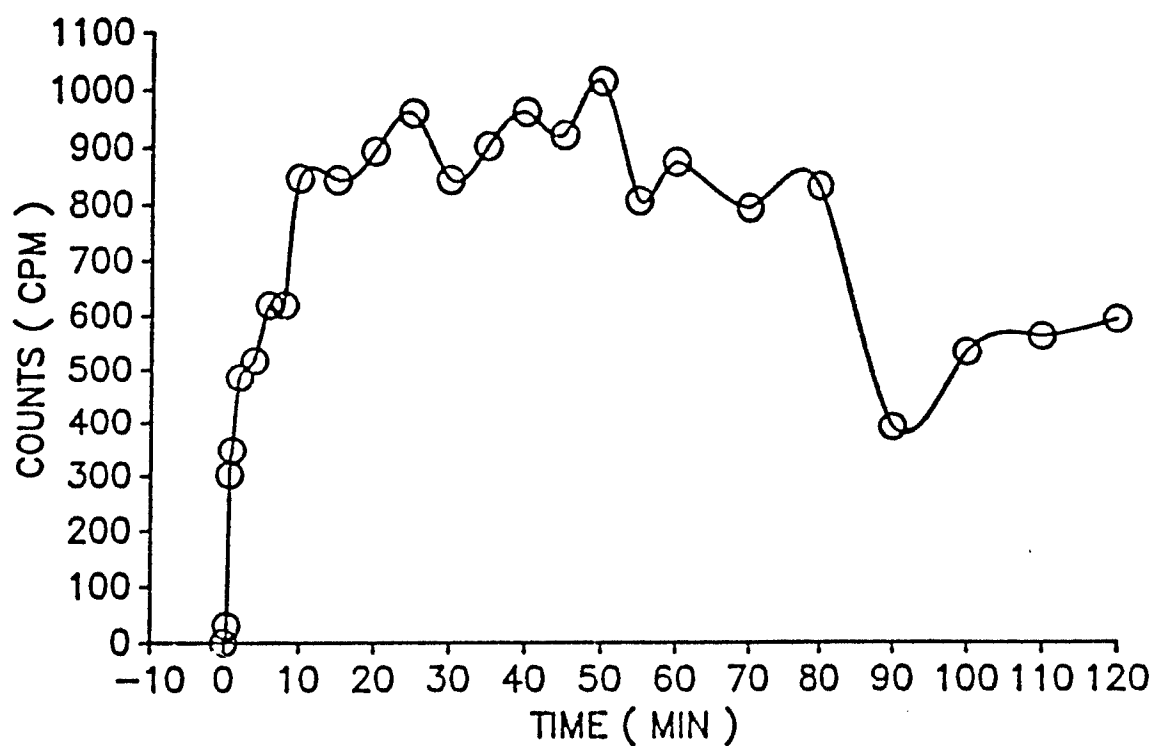


Figure 3. Kinetics of uptake of 2H-MCLR by perfused liver. Intact rat livers were perfused with [ $^3\text{H}$ ]-2H-MCLR and analyzed. "Counts" is the total number of counts taken up by the liver (from the media) at each time point.

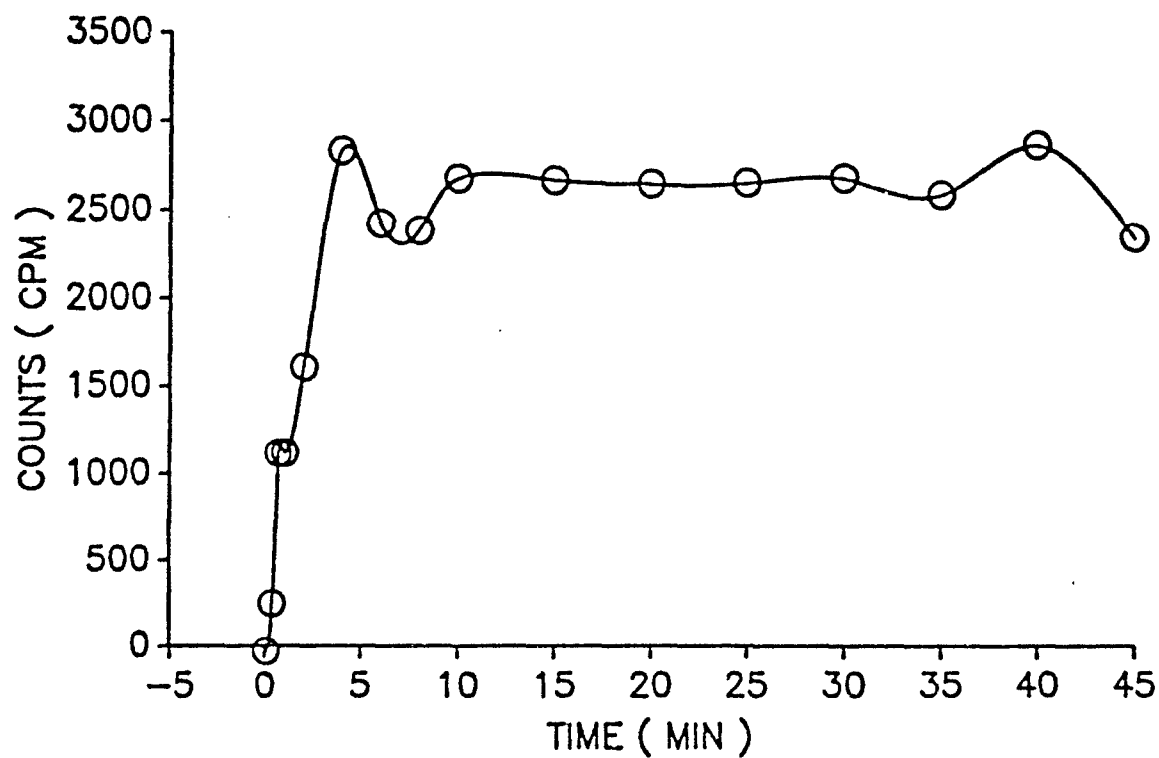


Figure 4. Subcellular distribution of 2H-MCLR in hepatocytes in suspension and during liver perfusion. Data are presented as the mean percentage  $\pm$  SEM of total incorporated radioactivity found in each subcellular fraction, except for the 45-minute and 120-minute perfused livers which represent one animal for each perfusion. PM/NUC, plasma membrane plus nuclear fraction; H. MIT, heavy mitochondrial fraction; L. MIT, light mitochondrial fraction; MICRO, microsomal fraction; CYTO, cytosolic fraction.

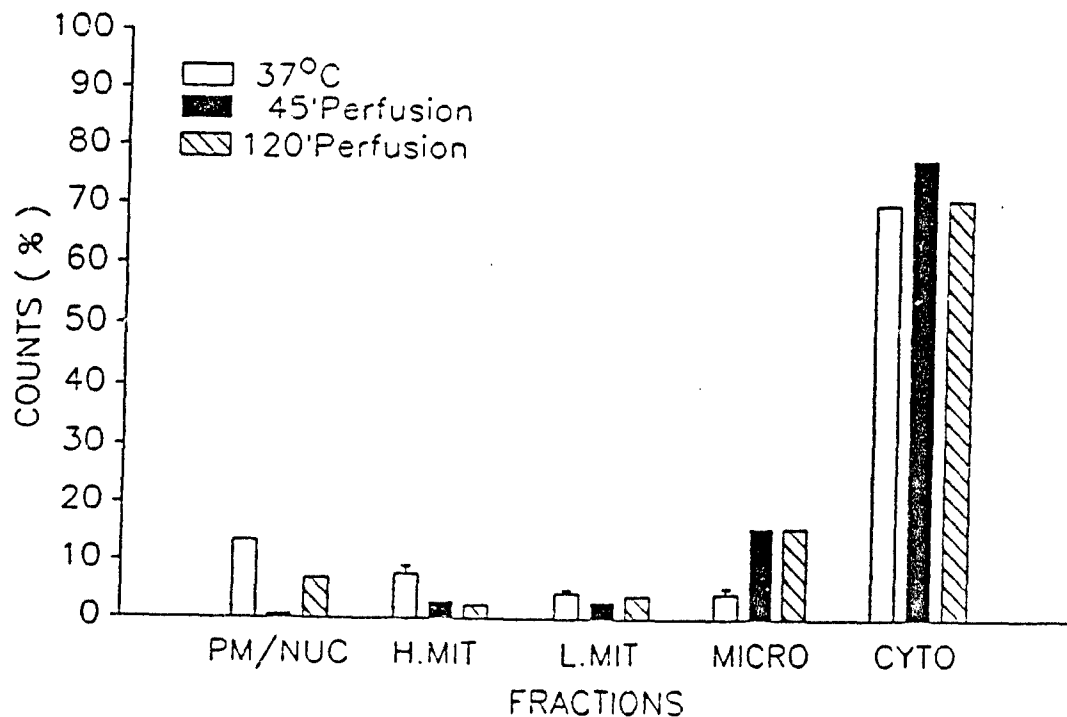
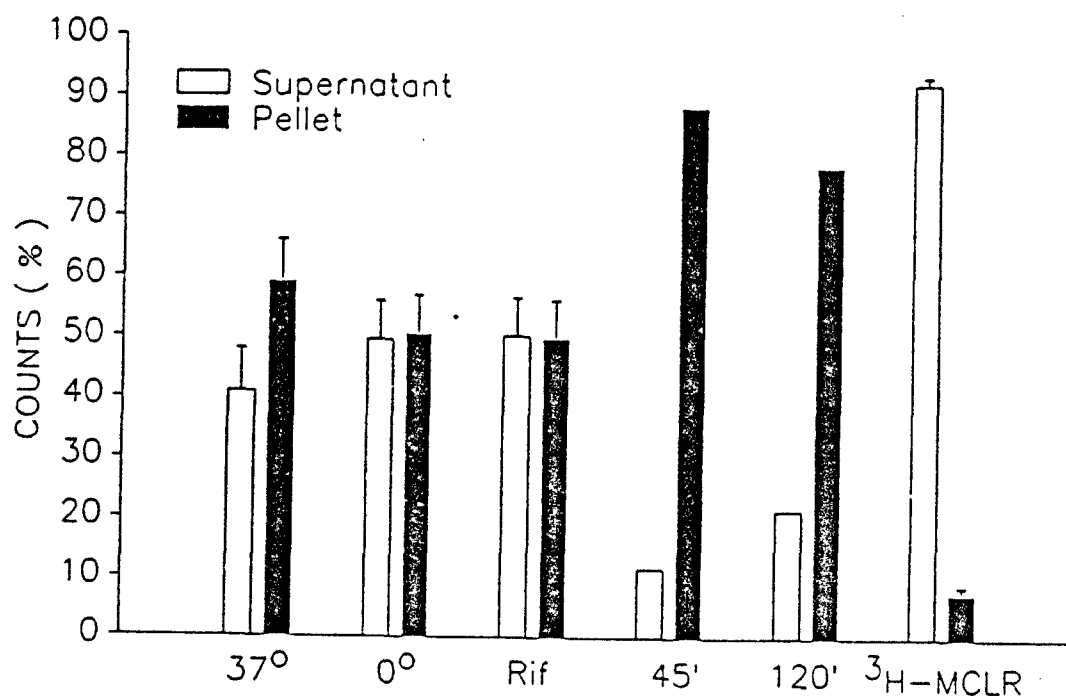


Figure 5. Effect of trichloroacetic acid on the solubility of  $^3\text{H}$ -MCLR in hepatocyte cytosolic fractions. Data are expressed as percent of the total cytosolic radioactivity subjected to TCA treatment which partitioned in the TCA precipitated pellet (protein fraction) and the supernatant.



## V. LESIONS INDUCED IN INTACT ANIMALS EXPOSED TO PEPTIDE HEPATOTOXINS

### A. Mice

#### Toxicity of Single and Repeated Intraperitoneal Doses of Microcystin-LR in Two Strains of Male Mice

##### 1. Statement of the Problem, Background, and Rationale

There is little published data on the effects that a sublethal dose of microcystin has upon susceptibility to a subsequent potentially lethal dose of the hepatotoxin. In one report, a marked tolerance to *M. aeruginosa* extracts developed following repeated IP administration to albino rats (Ashworth and Mason, 1946). Rabbits given sublethal oral doses of *M. toxica* Stephens developed a marked resistance to the toxin (Louw and Smit, 1950). Fasted rats were more susceptible to MCLR than nonfasted rats, and rats fasted prior to a sublethal dose were more likely to be protected when subsequently challenged with a "consistently lethal" dose than were similarly exposed nonfasted rats.

Here we examined whether a parenteral dose of MCLR would protect against a second, higher dose of MCLR. The major goals of study A were to determine the 24-hour LD<sub>50</sub> and the approximate LD<sub>0</sub> maximum and LD<sub>100</sub> minimum of MCLR and to determine whether a sublethal dose of MCLR would protect mice from a subsequent "consistently lethal" dose of the toxin. Study B was designed to verify and better characterize the protective effect observed in study A. Clinical signs, survival time,



liver and combined kidney weights, and lesions were monitored in the mice of each study following one or two IP doses of MCLR.

## 2. Experimental Methods

### First Study (Study A)

Sixty male Balb/c mice ranging from 20 to 35 g BW were fed a commercial rodent ration, provided water *ad libitum*, and placed on a 12-hour light/12-hour dark cycle. After 2 weeks for acclimation, the mice were randomly assigned one of six beginning treatment regimens: tap water (control) or 20, 25, 30, 35, or 40 µg of approximately 75% pure MCLR/kg (N = 10 for each group). The lesser purity in this study related to the fact that this is one of the initial studies performed during the time of simultaneous toxin characterization and development of improved methods for purification. Testing of high doses of the impurities by IP administration to mice failed to demonstrate significant toxicity.

On day 0, all mice were given the appropriate IP dose. Mice that died within 24 hours (treatment groups A, B, and C; Table 1) were examined postmortem and comprised the single dose lethal response (SingLeth) group. In addition, five randomly chosen control mice (treatment group F) were killed and similarly examined. On day 1, 12 mice were randomly chosen from groups C, D, and E, each of which contained more than five survivors. The mice were killed and subjected to necropsy and comprised the single dose sublethal response (SingSubl) group. One animal given MCLR at 35 µg/kg which died unexpectedly during the night of day 1 (survival time

36 to 46 hours) was counted as alive for the 24-hour LD<sub>50</sub> calculations, but its organ weights are not included in Table 1.

On day 2, 48 hours after the initial MCLR dosing, the 17 surviving hepatotoxin-treated mice were given MCLR at 40 µg/kg, and the five remaining control mice were again given tap water in a volume equivalent to that of the 40 µg/kg dose. All mice that died (moribund animals were assessed as dead) within 24 hours after the second IP dose of MCLR were examined at postmortem and comprised the second dose lethal response (SecoLeth) group (treatment groups H, I, J, and K). The five remaining control mice (treatment group G) were also killed and necropsied. On day 3, all mice still alive at 32 hours after the second dose of hepatotoxin were killed and examined. These mice (treatment group I) comprised the second dose sublethal response (SecoSubl) group.

Animals were monitored for clinical signs for 10 hours following the administration of hepatotoxin on both day 0 and day 2. Clinical signs in survivors were recorded on days 1 and 3.

Mice were killed by cervical dislocation and necropsies performed within 30 minutes of either spontaneous death or euthanasia. Liver and combined kidney weights were obtained as a percentage of live body weight (% BW). The gall bladder was considered part of the liver weight. Sections of kidneys, liver, heart, lung, and spleen were fixed in 10% neutral-buffered formalin, processed routinely, embedded in paraffin, cut at 5 to 6 microns and stained with hematoxylin and eosin.

Second Study (Study B)

One hundred forty-four male, 6-week-old, Swiss-Webster mice weighing 22 to 28 g were obtained from the Charles River Company (Shaver Road, Portage, MI). The animals were allowed to become acclimated and maintained as described above.

MCLR of > 95% purity (Harada et al., 1988a,b) was dissolved in a vehicle of 0.9% saline and 0.1% ethanol. Preliminary trials with 30 mice established 55 µg of MCLR/kg as an approximate IP LD<sub>50</sub> dose and 75 µg/kg as an approximate LD<sub>100</sub> minimum.

On day 0, 48 mice were given MCLR at 55 µg/kg IP. At the same time, 36 additional mice were given an equivalent volume of vehicle, and 30 mice remained untreated.

Three days later, the 37 MCLR-dosed mice that survived the day 0 hepatotoxin dosing, 24 of the day 0 vehicle-dosed mice, and 24 of the mice given no day 0 treatment were given MCLR IP at 75 µg/kg. At this time, the remaining 12 mice, given only the vehicle on day 0, and the six mice given no treatment on day 0 were administered the vehicle.

Six mice given the vehicle on days 0 and 3, and all six mice given the vehicle solely on day 3 were killed on day 4. All surviving preliminary and formal study mice and the remaining six mice given the vehicle on days 0 and 3 were killed on day 7. Two mice were disqualified from this study as a result of improper dosing (1) and microkidney (1). Monitoring for clinical signs was conducted for 10 hours immediately following the day 0 and day 3 dosings and every 4 hours thereafter.

Mice were classified as survivors and the experiment was terminated at approximately 96 hours following MCLR administration on day 3. This time was selected because all mice still alive had been observed: (a) eating, (b) drinking, and (c) rearing (which was not observed postdosing in any mouse that died). Mice were killed and organ weights were obtained as described above. Necropsies were performed within 4 hours of death. Sections of liver and kidney were fixed in 10% formalin.

#### Statistical Methods

Study A. The Student's t-test was used to compare: 1) the liver and combined kidney weights (as % BW) of treatment group F with treatment group G, and 2) the survival times (minutes) and rank of survival time of mice of the SingLeth vs SecoLeth groups. Covariate analysis was performed on the liver weight (LIVWT) data from the 34 mice which died following MCLR administration(s). In this analysis, mice were grouped by number of doses (#DO) and the following model was used:  $LIVWT = CONSTANT + \#DO + LST$  where LST = natural log of survival time in minutes. One-way analyses of variance were used to compare liver and combined kidney weight (% BW) of the various treatment groups within the same response group. Equations were developed which related kidney weight to fractional polynomials of survival time when a significant treatment effect was discovered within a response group. When the trend in organ weight with survival time was significant, kidney weights were detrended using the 4253H compound smoother (Tukey, 1977), as described by Velleman and Hoaglin (1981). The smoothed kidney weight data was

then reanalyzed using a one-way analysis of variance. The Student-Newman-Keuls multiple comparison test (SNK MCT) of means with unequal sample sizes and the Bartlett Test for homogeneity of group variance (Winer, 1971) were used to compare liver and combined kidney weights among the five response groups. Yates corrected Chi square analysis (Winer, 1971) was used to test for differences in survivability between groups of mice given MCLR at 40  $\mu\text{g/kg}$ . For these tests, a level of significance of  $\alpha = 0.05$  was chosen. The method of Miller and Tainter (1944) was used to calculate the  $\text{LD}_{50}$  and its standard error.

Study B. Covariate analyses were performed on the natural logarithms of the relative liver weight (LLIVWT) data and kidney weight (LKIDWT) data. Mice were grouped according to their day 0 and day 3 treatments (TRT; Table 2), and the following models were used:

- a.  $\text{LLIVWT} = \text{CONSTANT} + \text{TRT} + \text{LST}$ .
- b.  $\text{LLIVWT} = \text{CONSTANT} + \text{TRT} \times \text{RES}$ .
- c.  $\text{LKIDWT} = \text{CONSTANT} + \text{TRT} \times \text{LST}$ .
- d.  $\text{LKIDWT} = \text{CONSTANT} + \text{TRT} \times \text{RES}$ .

LST and RES served as the covariate: LST = natural log of survival time in minutes, and RES = a response variable chosen on the basis of clinical signs and gross lesions in mice which survived for similar periods of time. If survival time was  $< 5.5$  hours, then RES = peracute death; if survival time was  $\geq 5.5$  hours and  $< 48$  hours, then RES = acute death; if survival time was  $\geq 48$  hours and  $< 96$  hours, then RES =

subacute death; if survival time was  $\geq 96$  hours, then RES = survivor; if mice were administered vehicle on day 3, then RES = control.

The SNK MCT for means from unequal sample sizes and the Bartlett Test for homogeneity of group variances were also used to check for differences in:

- a. LLIVWT and LKIDWT among the three vehicle control groups.
- b. LLIVWT among the 11 TRT x RES groups (Table 3).
- c. LKIDWT among the five RES groups (Table 4).
- d. Rank of survival time among the four TRT groups (Table 5); only mice which died were used in this comparison.

The cumulative probability for the binomial (CPB; Fleiss, 1981) was used to test for significant differences (outside the 95% confidence interval) in survival between TRT groups 55/75, veh/75, and no TRT/75 on day 3 (Table 6). Student's t-test was used to compare the LLIVWT and LKIDWT of the 17 formal vehicle control mice with those of the 18 preliminary mice that survived 10 to 12 days after a single dose of MCLR (Table 7).

### 3. Results

#### Study A

The 24-hour IP  $LD_{50}$  for 75% pure MCLR was determined to be  $32.5 (\pm 1.2)$   $\mu\text{g/kg}$ , the 24-hour approximate  $LD_{100}$  minimum 40  $\mu\text{g/kg}$ , and the 24-hour approximate  $LD_0$  maximum 25  $\mu\text{g/kg}$ . No significant differences in survival time or rank of survival time were detected between the SingLeth and the SecoLeth groups. In addition, no significant differences in survival were detected when treatment group

A (zero of 10) was compared with all mice (three of 17) in the protective effect portion of this study (treatment groups H, I, J, and K) after both groups were given 40  $\mu\text{g/kg}$  IP. A significant difference ( $p = 0.040$ ) in survival was evident, however, between treatment group A (zero of 10) and treatment group I (three of five).

Clinical signs in mice which died from MCLR toxicosis began no sooner than 20 minutes postdosing and included reduced activity and responsiveness, piloerection, pallor, and sternal recumbency, followed by moribund appearance and death.

Survival times are shown in Table 1, which also illustrates the organ weight data of the 11 treatment groups (A to K) and the five response groups. No significant differences were detected between the two control groups (F and G) for liver ( $p = 0.068$ ) and combined kidney weights (% BW); therefore, these data were pooled to provide the best estimate of control values.

Survival times did not significantly influence the liver weights of mice that died during study A. In addition, no significant differences were detected among treatment groups within response groups for liver weight (SingLeth group,  $p = 0.0735$ ). A significant difference ( $p = 0.0047$ ) was detected, however, among treatment groups within the SingLeth group for kidney weight. However, when the significant trend in kidney weights related to survival time was accounted for, differences among the three treatment groups in the SingLeth group for kidney weights were no longer significant ( $p = 0.498$ ). Consequently, the 20 mice which died within 24 hours following the initial IP hepatotoxin administration were combined into the single dose lethal response group, the 12 mice which survived for 24 hours following the initial

IP hepatotoxin dose were combined into the single dose sublethal response group, and the 14 mice which died within 24 hours after the second IP hepatotoxin administration were combined into the second dose lethal response group.

Toxin-related lesions were not detected in the lungs, kidneys, heart, or spleen of any of the mice on gross examination, and grossly evident lesions were not found in livers of the control and SingSubl group. In the livers of the three mice in the SecoSubl group and the mice of the SingLeth and SecoLeth groups, multifocal pinpoint reddened areas were evident especially near the margins of the liver lobes. The livers were greatly swollen, dark red in color, and exuded blood when cut.

Histologically evident lesions were detected in the livers and kidneys of mice that died, including mild dilation of renal cortical tubules. Deeply eosinophilic granular to fibrillar material was often present in affected tubules and was noted occasionally in Bowman's space and in glomerular capillaries. Hepatic lesions were similar to those described below.

#### Study B

Survival times and overall survival are presented in Tables 5 and 6. In mice that died peracutely (survival time  $\leq 5.5$  hours), decreased responsiveness/movement was the first noted adverse effect occurring 35 to 40 minutes postdosing. Piloerection, limited movement, increased respiratory rate, and mild pallor of the extremities followed. Within 45 minutes of death, mice became recumbent and inactive, with eyes closed. Periodically, a whole body tremor, opening of the eyes, and a "hop" of up to several cm in height would occur, followed by a return to the eyes closed,



recumbent position. Marked pallor, weakness (inability to stand), and increased rate and depth of respiration preceded death.

In mice that died acutely (survival time 5.5 to 48 hours), decreased responsiveness/movement became apparent at 50 to 75 minutes postdosing. These mice were able to walk around the cage for several hours following the initial ill effects. The development of piloerection, decreased movement, increased respiratory rate, and pallor of the extremities progressed much more slowly in these mice. No attempts to eat or drink were noted following the onset of clinical signs. "Hopping movements" occurred sporadically but were less marked and not consistently associated with impending death.

In mice that died subacutely (survival time 48 to 96 hours), decreased responsiveness/movement was evident within 90 minutes postdosing. These mice would walk slowly when gently urged for 40 hours postdosing but often lay still. Icterus and an enlarged abdomen developed between 48 hours postdosing and death in several mice of this group. "Hopping" occurred sporadically beginning 36 hours postdosing in two of these mice.

Of nine mice that survived the second dose of MCLR, three exhibited no ill effects during the 96-hour postdosing observation period; two of these mice had been given the vehicle on day 0 and one had received MCLR at 55 µg/kg on day 0.

Of six mice that survived after being given MCLR at 55 µg/kg on day 0, decreased responsiveness/movement was evident within 2 hours of the second dosing, but these animals never lost the ability to walk slowly, and no "hopping movements"

were observed in these mice. For 48 hours postdosing, these mice lay still, and then from 60 hours postdosing until the time of euthanasia (96 hours postdosing), gradual improvement in appetite, strength, and responsiveness was observed. These mice also developed mild to severe jaundice and one developed marked enlargement of the abdomen from 48 to 96 hours postdosing.

At 24 hours after the day 0 treatment, no clinical signs were observed in any of the surviving mice. Clinical signs were never observed in any mouse administered the vehicle alone.

Organ weights. In both LLIVWT models, there was a significant difference ( $p < 0.001$ ) in mean liver weight among the four treatment (TRT) groups administered MCLR. The covariates, RES and LST, had a significant influence ( $p < 0.001$ ) on liver weight (Table 3). In both LKIDWT models, there were no significant differences ( $p > 0.60$ ) in mean kidney weight among the four treatment (TRT) groups administered MCLR. In contrast, the covariate, either RES or LST, had a significant influence ( $p < 0.001$ ) on kidney weight (Table 4).

Grossly evident lesions. Mice that died peracutely had markedly swollen, hemorrhagic, dark red livers and severe pallor of the carcass. Mice that died acutely had severely swollen, hemorrhagic, mottled reddish-brown livers and moderate to severe pallor of the carcass. Mice that died subacutely had moderately swollen, extremely red and white mottled livers with mild to severe jaundice and moderate pallor of the carcass. The six survivors that displayed clinical signs had moderately to severely enlarged, firm, solid white to mottled pink-white livers and mild to

moderate pallor of the carcass. Grossly evident lesions were not found in the kidneys of any of the mice. Gross lesions were not observed in either the three survivors that displayed no adverse effects or the 17 vehicle control mice.

Histologically evident lesions. Treatment-associated lesions were restricted to the liver. Mice that died peracutely (< 5.5 hours) all had similar lesions, including severe centrilobular hepatocyte disassociation, rounding, degeneration, and necrosis, which frequently extended into midzonal regions. In severely affected areas, there was marked hepatocyte loss, breakdown and loss of sinusoidal endothelium, disruption of normal architecture, and severe hemorrhage. In midzonal and periportal areas, hepatocytes often contained single or multiple intracytoplasmic vacuoles. In most lobules, all hepatocytes were affected except for a rim of periportal hepatocytes from one to six cell layers deep. These liver lesions were identical to those observed in mice which died peracutely in study A.

The livers of mice surviving 5.5 to 24 hours were similar to those described above except hepatocyte disassociation and necrosis in the most severely affected centrilobular regions were more marked, and prominent cellular shrinkage, nuclear pyknosis, and karyorrhexis were evident. Small numbers of neutrophils and lymphocytes had infiltrated these areas. Cellular swelling in periportal and midzonal hepatocytes had compressed sinusoidal lumina.

The livers of mice surviving 24 to 48 hours were characterized by severe centrilobular and variable midzonal hemorrhage and infiltration of moderate numbers of neutrophils and lesser numbers of lymphocytes and macrophages. Hepatocytes in

these areas had undergone coagulative necrosis and were frequently replaced by cellular debris. Intact, midzonal, and periportal hepatocytes were moderately swollen causing obliteration of numerous sinusoids. In scattered areas, these hepatocytes often contained one to several large, clear, intracytoplasmic vacuoles.

The livers of mice surviving 48 to 96 hours appeared similar to those above or were characterized by severe infiltration of macrophages into the centrilobular areas in addition to small numbers of neutrophils, lymphocytes, and fibroblasts. There appeared to have been a marked reduction in erythrocytes and cellular debris. Hepatocytes adjacent to centrilobular areas were packed together and the normal architecture of hepatic plates was largely inapparent. These hepatocytes contained abundant, streaming, slightly basophilic cytoplasm, and large, pale nuclei often with several prominent nucleoli. Midzonal and periportal hepatocytes were enlarged and formed sheets of cells which obscured almost all sinusoids in these areas. The cytoplasm of these cells was often pale and contained numerous very small cytoplasmic vacuoles.

The livers of the six mice which survived after showing clinical signs were characterized by marked disorganization of the centrilobular and midzonal hepatic architecture. Irregularly shaped regions that had previously contained central veins were filled with erythrocytes. Hepatocytes in these areas were frequently elongated with a streaming cytoplasm. One to two mitotic figures per high-power field were noted in centrilobular and midzonal areas.

The liver of one of the surviving mice (given vehicle on day 0) which showed no clinical signs also had no histologic lesions. The livers of the remaining two surviving mice which showed no clinical signs had mild centrilobular hepatocyte disassociation and disorganization.

#### 4. Discussion and Conclusion

In study A, the approximate  $LD_0$  maximum was 76.9% of the  $LD_{50}$ , which is largely in agreement with the responses of sheep following intraruminal administration of *M. aeruginosa* cells in which the consistently sublethal dose was greater than 90% of the  $LD_{50}$  (Jackson et al., 1984).

In study A, a "protective effect" was observed in three of five mice which survived a  $LD_{30}$  dose of MCLR at 30  $\mu\text{g/kg}$  and 2 days later survived a  $LD_{100}$  minimum dose of 40  $\mu\text{g/kg}$ . Because of the small number of animals, however, the protective effect in this study was considered inconclusive.

In study B, the  $LD_{23}$  dose of MCLR conclusively provided a "protective effect" from a  $LD_{100}$  minimum dose administered 3 days later. Both increased survival time and survival were observed (Tables 5 and 6). Although "resistant" individuals were selected in the 55/75 group, there was a highly significant increase in rank of survival time in the 55/75 group even when compared to the survival times of the most "resistant" 77% of the mice in the other three treatment groups. The sublethal effects of MCLR at 55  $\mu\text{g/kg}$  would appear to be responsible for the increase in survival time. Dose also influenced rank of survival time since the 24 mice given no TRT/75 died at a significantly earlier time than the 11 mice which died following a dose of 55

µg/kg. Increased survival in the 55/75 group cannot be attributed to prevention of increases in final liver weight (Table 3) or solely to the primary effects of MCLR administered on day 0, since mice given veh/75 also had survivors. Indeed, pharmacologic doses of hydrocortisone prevented deaths in mice given "lethal" doses of MCLR (Adams et al., 1985), and thus the stresses of handling, the administration of vehicle (ethanol and physiologic saline), and the sublethal effects of MCLR may all play a role in increased survival. The "protective effect" of the LD<sub>23</sub> of MCLR in this study may be similar to the "protective effect" of a sublethal dose of carbon tetrachloride (CCl<sub>4</sub>) on mice subsequently given MCLR (Adams et al., 1985). Thus, the protective effect induced by CCl<sub>4</sub> and MCLR against a subsequent "consistently lethal" dose of MCLR could be a result of less efficient uptake of MCLR by bile acid carriers of damaged hepatocytes (Runnegar et al., 1981) or related to less severe hemorrhage into an already disrupted and distended liver. This protective effect is not likely to be mediated by effects on MFO activities because prior induction with phenobarbital (Lovell et al., 1985) or inhibition with piperonyl butoxide (Lovell et al., 1985), SKR-525A, or cobaltous chloride (Adams et al., 1985) did not affect the 5-hour survival rate of microcystin-treated mice.

The sublethal (55 µg/kg) dose of MCLR caused a slight increase in liver weight prior to the lethal dose, similar to the findings in study A. Unlike study A, however, there was a definite inverse relationship between survival time and liver weight in the mice of study B that ultimately died. This inconsistency between the two phases of

this study is probably due to the larger number of mice that died with survival times of more than 10 hours in study B as compared to study A (19 vs. two).

The no TRT/75 mice that died peracutely had significantly higher liver weights as compared to the mice that died peracutely after the 55  $\mu\text{g/kg}$  dose (Table 3). Although dose would appear to be the most logical explanation for this difference, the possibility that more susceptible mice died with lower liver weights could not be ruled out. Based on gross and histologic lesions, it appears that the markedly increased liver weights in mice that died following MCLR administration were caused primarily by hemorrhage, and the extreme pallor of the carcass would be compatible with death from hemorrhagic shock.

The fact that seven of the 10 mice in study A with the shortest survival times had "normal" kidney weights seems to indicate that acute death in mice caused by hepatotoxin administration is not necessarily associated with a significant increase in kidney weight. At least with Balb/c mice, the longer an animal lived following a lethal dose of MCLR (survival time < 240 minutes), the greater was the increase in kidney weight.

In the Swiss-Webster mice of study B, kidney weights decreased in relation to increasing survival time (peracute death > acute death > subacute death > survivors) (Table 4). The time course of changes in organ weights and gross/histologic findings in these two trials suggests that the liver is the primary target organ and that the kidneys are secondarily affected following administration of MCLR. Renal lesions and the increase in kidney weight seem to be a product of embolic hepatic debris

(Ashworth and Mason, 1946; Hooser et al., 1988), hypoxia, edema, and/or decreased glomerular filtration rate (increased solute retention).

The liver and kidney weight data of the 18 preliminary mice of study B (Table 7), when compared to the 17 study B control mice, suggest that recovery from a single sublethal dose of MCLR is accompanied by a significant dose-dependent decline in liver weight and gain in kidney weight by 10 to 12 days postdosing.

There were marked gross differences between the dark red, enlarged, hemorrhagic livers of mice which died peracutely and the livers of most 55/75 survivors which were swollen, firm, and nearly solid white. Prior to this study, we had observed no significant variation in lesions and no subacute or chronic lesions in the livers of animals that died spontaneously following a single MCLR administration. Mice and rats either survived with no gross or histologic liver lesions or they died with extensive hepatic necrosis and hemorrhage.

When lyophilized suspensions of *M. toxic* were given intragastrically to vervet monkeys at 100, 200, or 500 mg/kg/week, periodic liver biopsies and postmortem examinations revealed: 1) panlobular hepatocytic necrosis and degeneration with hemorrhages, 2) foci of inter- and intralobular connective tissue proliferation, 3) primitive bile duct formation, and 4) disturbances of normal architecture (Tustin et al., 1973). Similarly, when mice were dosed daily with MCYM at 0.75, 0.50, or 0.25 of the LD<sub>100</sub> minimum, lesions included: 1) generalized hepatocyte degeneration with scattered necrosis, 2) progressive fibrosis and mononuclear cellular infiltration, and 3) numerous mitotic figures in hepatocytes (Elleman et al., 1978). Thus, in the



present study, the histologic liver lesions in mice which survived for at least 48 hours were similar (hepatocyte degeneration and necrosis, fibroblast infiltration, architectural disturbances, and several mitotic figures) to those previously observed as a result of exposure to a greater number of doses of microcystins.

The results of this study indicated that: 1) an acutely toxic dose of MCLR would protect against a potentially lethal dose of the toxin when administered 2 to 3 days later, and 2) subacute lesions may occur in the livers of mice following repeated MCLR administration, and 3) active repair (including hepatocyte mitosis, neovascularization, and phagocytosis of necrotic debris) proceeds rapidly after exposure ceases.

Table 1. Treatment, survival, organ weight, and survival time data for the Balb/c mice of the First Study (Study A). Data are presented for both the 11 treatment and five response groups.

TRT Group	IP Dose of 75% Pure		No. Died	No. Killed	Surv. Time (minutes) Mean ± SD	Liver Wt. (% BW) Mean ± SD	SNK MCT <sup>a</sup>	Kidney Wt. (% BW) Mean ± SD	SNK MCT <sup>a</sup>
	MCLR Day 0	(µg/kg) Day 2							
Single Dose Lethal Response Group									
A	40	--	10	--	131 ± 32	8.66 ± .44		1.80 ± .15	
B	35	--	7	--	308 ± 106	8.26 ± .21		1.67 ± .17	
C	30	--	3	--	107 ± 8	8.24 ± .33		1.41 ± .12	
Combined Group Response									
			20		189 ± 129	8.45 ± .40	D	1.70 ± .20	B
Single Dose Sublethal Response Group									
C	30	--	--	2	<sup>b</sup> 1554 ± 105	5.40 ± .14		1.32 ± .10	
D	25	--	--	5	<sup>b</sup> 1572 ± 49	5.62 ± .25		1.35 ± .13	
E	20	--	--	5	<sup>b</sup> 1601 ± 50	5.59 ± .48		1.46 ± .15	
Combined Group Response									
				12	<sup>b</sup> 1581 ± 56	5.59 ± .33	B	1.40 ± .10	A
Control Group									
F	0	--	--	5	<sup>b</sup> 270 ± 80	5.31 ± .30		1.34 ± .14	
G	0	0	--	5	<sup>b</sup> 342 ± 9	4.99 ± .17		1.39 ± .04	
Combined Group Response									
				10	<sup>b</sup> 306 ± 66	5.15 ± .28	A	1.36 ± .10	A

TRT Group	IP Dose of 75% Pure		No. Died	No. Killed	Surv. Time (minutes) Mean $\pm$ SD	Liver Wt. (% BW) Mean $\pm$ SD	SNK MCT <sup>a</sup>	Kidney Wt. (% BW) Mean $\pm$ SD	SNK MCT <sup>a</sup>
	MCLR Day 0	( $\mu$ g/kg) Day 2							
Second Dose Lethal Response Group									
H	35	40	2	--	227 $\pm$ 206	9.01 $\pm$ .96		1.46 $\pm$ .36	
I	30	40	2	--	839 $\pm$ 965	8.93 $\pm$ .40		1.70 $\pm$ .13	
J	25	40	5	--	529 $\pm$ 558	8.95 $\pm$ .71		1.83 $\pm$ .15	
K	20	40	5	--	142 $\pm$ 58	8.74 $\pm$ .39		1.74 $\pm$ .26	
Combined Group Response									
			14		392 $\pm$ 488	8.88 $\pm$ .54	E	1.72 $\pm$ .24	B
Second Dose Sublethal Response Group									
I	30	40	--	3	<sup>b</sup> 1934 $\pm$ 6	6.67 $\pm$ .29	C	1.33 $\pm$ .06	A

<sup>a</sup>Means with different letters were significantly different from each other based on the Student-Newman-Keuls multiple comparison test [SNK MCT] ( $\alpha = 0.05$ ). The Bartlett Test for homogeneity of response group variances did not detect significant differences ( $\alpha = 0.05$ ).

<sup>b</sup>Killed by cervical dislocation.

SD = standard deviation.

Table 2. Days 0 and 3 treatments (TRT) with microcystin-LR in the 6-week-old male Swiss-Webster mice used in the Second Study (Study B).

Day 0 Treatment IP Dose MCLR	Day 3 Treatment IP Dose MCLR	N	Representation of TRT in the Text
55 µg/kg	--	11	55/--
55 µg/kg	75 µg/kg	37	55/75
Vehicle	75 µg/kg	23	veh/75
No treatment	75 µg/kg	24	no TRT/75

--Mice died following day 0 treatment.

Table 3. Means and standard deviations (SD) of the natural logs of liver weight (% live body weight) in the Second Study (Study B) mice. Data are grouped according to treatment (TRT) and response (RES).

Day 0 TRT	Day 3 TRT	RES	N	Natural Log Liver Weight $\pm$ SD	SNK MCT*
no TRT/veh	vehicle	survivor	17	1.674 $\pm$ 0.068	A
vehicle	75 $\mu$ g/kg	survivor	2	1.799 $\pm$ 0.048	B
55 $\mu$ g/kg	--	acute death	2	1.871 $\pm$ 0.023	B,C
55 $\mu$ g/kg	75 $\mu$ g/kg	subacute death	8	1.893 $\pm$ 0.088	B,C
vehicle	75 $\mu$ g/kg	acute death	2	1.901 $\pm$ 0.059	B,C
55 $\mu$ g/kg	75 $\mu$ g/kg	survivor	7	1.984 $\pm$ 0.115	C,D
55 $\mu$ g/kg	75 $\mu$ g/kg	acute death	7	2.017 $\pm$ 0.021	D,E
55 $\mu$ g/kg	--	peracute death	9	2.023 $\pm$ 0.057	D,E
vehicle	75 $\mu$ g/kg	peracute death	19	2.056 $\pm$ 0.054	E,F
no TRT	75 $\mu$ g/kg	peracute death	24	2.085 $\pm$ 0.057	F
55 $\mu$ g/kg	75 $\mu$ g/kg	peracute death	15	2.151 $\pm$ 0.054	G

\*Mean with different letters are significantly different from each other based on Student-Newman-Keuls multiple comparison test [SNK MCT] ( $\alpha = 0.05$ ). The Bartlett Test for homogeneity of group variances did not detect significant differences ( $p = 0.054$ ).

--Mice died following day 0 treatment.

Table 4. Means and standard deviations (SD) of the natural logs of kidney weight (% live body weight) in the Second Study (Study B) mice. Data are grouped according to response (RES).

RES	N	Natural Log Kidney Weight Mean $\pm$ SD	SNK MCT*
survivors	9	0.178 $\pm$ 0.101	A
vehicle control	17	0.187 $\pm$ 0.081	A
subacute death	8	0.248 $\pm$ 0.102	A
acute death	11	0.339 $\pm$ 0.080	B
peracute death	67	0.372 $\pm$ 0.084	B

\*Means with different letters are significantly different from each other based on the Student-Newman-Keuls multiple comparison test [SNK MCT] ( $\alpha = 0.05$ ). The Bartlett Test for homogeneity of group variances did not detect significant differences ( $\alpha = 0.054$ ).

Table 5. Means and standard deviations of the natural logs of survival time in minutes and the rank of survival time for the 86 mice which died following microcystin-LR administration in mice of the Second Study (Study B). Data are grouped according to treatment (TRT).

Day 0 TRT	Day 3 TRT	N	Natural Log Survival Time Mean $\pm$ SD	Survival Time Rank Mean $\pm$ SD	SNK MCT*
no TRT	75 $\mu$ g/kg	24	4.919 $\pm$ 0.185	21.9 $\pm$ 16.2	A
vehicle	75 $\mu$ g/kg	21	5.198 $\pm$ 0.655	31.8 $\pm$ 19.2	A
55 $\mu$ g/kg	--	11	5.415 $\pm$ 0.702	48.5 $\pm$ 21.2	B
55 $\mu$ g/kg	75 $\mu$ g/kg	30	6.501 $\pm$ 1.293	71.5 $\pm$ 17.3	C

\*Rank of survival time means with different letters are significantly different from each other based on the Student-Newman-Keuls multiple comparison test [SNK MCT] ( $\alpha = 0.05$ ). The Bartlett Test for homogeneity of group variances of rank of survival time did not detect significant differences ( $\alpha = 0.05$ ). No comparison between groups based on natural log of survival time in minutes was performed since the Bartlett Test for homogeneity of group variances was significant ( $p < 0.001$ ). The geometric mean of survival times is given by the antilog of the natural log of survival time. Transformed confidence limits were obtained by taking the antilog of the natural log of survival time  $\pm$  SD. Rank transformations were used for analysis since neither the raw data nor natural logs of the transformed data met the assumptions of ANOVA (i.e., homogeneous variances). The rank transformation (Conover and Inman, 1981) was therefore used to provide immediate information as to whether there was a genuine difference among treatment groups.

--Mice died following day 0 treatment.

Table 6. Number and percentage of mice surviving an LD<sub>100</sub> minimum of MCLR. Data from these mice of the Second Study (Study B) are grouped according to treatment (TRT).

Day 0 TRT	Day 3 TRT	Total N	Number of Survivors	Percent Survivors	CPB*	95% Confidence Interval
55 µg/kg	75 µg/kg	37	7	18.9	A	7.96 to 35.16%
vehicle	75 µg/kg	23	2	8.7	A,B	1.07 to 28.04%
no TRT	75 µg/kg	24	0	0.0	B	0.00 to 14.25%

\*Percent survivors with different letters are significantly different (outside the 95% confidence interval of the cumulative probability of the binomial-CPB) from each other.



Table 7. Means and standard deviations (SD) for the natural log of liver (LLIVWT) and kidney (LKIDWT) weights (% live body weight) for mice in first phase of the Second Study (Study B) surviving various IP doses of MCLR for 10 to 12 days.

Dose	Survival Time	N	LLIVWT Mean $\pm$ SD	LKIDWT Mean $\pm$ SD
35 $\mu\text{g/kg}$	12 days	1	1.452	0.392
50 $\mu\text{g/kg}$	10 to 12 days	8	1.542 $\pm$ 0.030	0.299 $\pm$ 0.065
55 $\mu\text{g/kg}$	10 to 22 days	3	1.568 $\pm$ 0.056	0.276 $\pm$ 0.064
60 $\mu\text{g/kg}$	10 days	4	1.586 $\pm$ 0.054	0.260 $\pm$ 0.017
65 $\mu\text{g/kg}$	10 days	2	1.637 $\pm$ 0.080	0.255 $\pm$ 0.000
35 to 65 $\mu\text{g/kg}$	10 to 12 days	18	1.562 $\pm$ 0.057	0.287 $\pm$ 0.058

## B. Mice and Rats

### Toxicity of Microcystin-LR, a Cyclic Heptapeptide Hepatotoxin from *Microcystis aeruginosa*, to Rats and Mice

#### 1. Statement of the Problem, Background, and Rationale

Published theories suggest that MCLR induced hepatic damage may be due to: 1) a direct hepatotoxic effect (Falconer et al., 1981; Jackson et al., 1983), 2) venous hypertension attributable to massive pulmonary thrombosis (Adams et al., 1985; Slatkin et al., 1983), or 3) stimulation of the sympathetic nervous system leading to vasoconstriction with subsequent hepatic pooling of blood and peripheral anoxia (Oishi and Watanabe, 1986). Death may be due to hypovolemic shock associated with hepatic necrosis and hemorrhage or to pulmonary embolism with subsequent venous hypertension, reduced cardiac output, and circulatory collapse (Adams et al., 1985; Slatkin et al., 1983). The goals of the present studies included characterization of the acute toxicity of MCLR and the associated lesions in mice and rats, as well as the clinical pathologic changes in rats.

Using MCLR, we evaluated and compared the toxic effects in: 1) male versus female rats, 2) male rats at minimal lethal doses versus doses greatly in excess of the minimum lethal dose, and 3) mice versus rats. In addition, we characterized the sequential morphologic and clinical pathologic changes occurring in male rats at a minimally lethal dose of the hepatotoxin.

## 2. Experimental Methods

### Animals

Male and female Sprague-Dawley rats (175 to 200 g) were obtained from Harlan Sprague-Dawley, Inc. (Indianapolis, IN), and allowed to become acclimated to their cages for 2 weeks or longer before use. Adult female Balb/c mice, raised in our own colony, were also used. A commercial laboratory chow and water were given *ad libitum* and animals were maintained on a 12-hour light:dark cycle. Rats and mice were randomly assigned to the various dose groups immediately before dosing and given free access to food and water thereafter until the end of the study.

### Toxin

MCLR, approximately 95% pure, was produced and purified in the laboratory of W. W. Carmichael as described above (Krishnamurthy et al., 1986a). The toxin was dissolved in 0.9% NaCl prior to use.

### Preparation for Gross and Histologic Studies

Animals that did not die spontaneously were anesthetized with ether, killed by exsanguination, weighed, and subjected to necropsy. For the sequential kill studies, livers, kidneys (with adrenals), and spleens were weighed. Lungs were fixed by intratracheal instillation of 10% neutral-buffered formalin. Sections of liver, lungs, kidneys, spleen, and thymus from all animals as well as brain, heart, adrenal glands, small and large intestine, pancreas, urinary bladder, skeletal muscle, and eyes of rats from the acute toxicity study were fixed by immersion in 10% neutral-buffered formalin. Tissues were routinely processed, embedded in paraffin, cut at 4 to 6  $\mu\text{m}$ ,

and stained with hematoxylin and eosin (HE) for examination by light microscopy. Selected sections of kidney from the sequential kill study were stained for fibrin deposition with phosphotungstic acid hematoxylin, Martius scarlet blue trichrome, Martius yellow scarlet red analine blue, or Carstairs' stains, or for calcium deposition with Vos Kossa's stain or Alizarin red stain.

#### Acute Toxicity Study in Rats

Male rats (two to eight per group [Table 1]) were dosed intraperitoneally (IP) with MCLR at one of the following doses: 20, 40, 80, 120, 160, 180, 200, 240, or 400  $\mu\text{g/kg}$ . The volume of toxin solution administered ranged from 0.1 to 1.0 ml. Animals were then observed continuously for clinical signs of toxicosis for 12 hours and periodically thereafter. Similarly, female rats (three per group) were dosed IP with MCLR at 40, 80, 120, or 160  $\mu\text{g/kg}$ . Surviving animals were killed 5 days after treatment.

Male rats (three per group) were dosed IP with MCLR at one of the following doses: 0, 400, 800, or 1,200  $\mu\text{g/kg}$ . Surviving animals were killed at 24 hours following toxin administration.

#### Sequential Kill Study with Rats

Male rats (two to seven per group) were dosed IP with a lethal dose of MCLR (160  $\mu\text{g/kg}$ ) and killed with ether at one of the following times: 5, 10, 20, 30, 40, 50, or 60 minutes or 3, 6, 9, 12, 18, or 24 hours. None of these animals died spontaneously. Control rats (three per group) were dosed IP with 0.5 ml of 0.9% NaCl and killed at 60 minutes or 12 or 24 hours. Immediately before necropsy, blood

samples were collected by cardiac puncture, placed in plain tubes or tubes containing EDTA as an anticoagulant, and put on ice. Serum samples were routinely prepared and kept frozen until analyzed. Serum biochemical parameters included: creatinine, blood urea nitrogen, total protein, albumin, calcium, phosphorus, sodium, potassium, chloride, glucose, alkaline phosphatase, alanine aminotransferase (ALT = serum glutamic-pyruvic transaminase), gamma glutamyl transferase, and total bilirubin.

#### Sequential Kill Study with Mice

Female mice were dosed IP with MCLR at 100 µg/kg and killed (two per group) at 15, 30, 60, and 90 minutes postdosing. In addition, three mice that died from 90 to 120 minutes postdosing were also subjected to necropsy immediately. Control mice given 0.9% NaCl were killed at 120 minutes postdosing.

#### Statistical Methods

Serum biochemical data were analyzed using a one-way analyses of variance (SAS Institute, SAS Circle, Cary, NC) in conjunction with Tukey's tests to evaluate differences between individual times. Controls were not included at every time point, and thus, all control data were pooled to compare with observations from treated rats. A level of  $\alpha = 0.05$  was chosen to identify significant differences.

### 3. Results

#### Acute Toxicity Study in Rats

Male rats given 20, 40, or 80 µg/kg and female rats given 40 µg/kg did not display clinical signs of toxicosis. Some of the animals dosed with MCLR at 80 µg/kg (females) or 120 µg/kg (males) were affected (Table 1). No lesions were

identified in clinically unaffected animals. By contrast, all clinically affected animals in all dose groups died and had similar gross and histologic lesions irrespective of sex or dose. Affected animals displayed lethargy and ruffled fur beginning several hours following dosing. Survival time following dosing with hepatotoxin ranged from 20 to 32 hours in males and females given MCLR at 240 µg/kg. All rats given MCLR at 400 to 1,200 µg/kg died between 6 and 8 hours postdosing (Table 1).

Gross lesions were evident only in the liver. Livers from all rats which died were dark red and enlarged, and these changes were most marked in rats given the higher doses. Centrilobular and midzonal necrosis was severe and degenerate and necrotic hepatocytes were sometimes noted in central veins. Pulmonary capillaries and larger vessels were often dilated and contained globular eosinophilic debris or intact cells which appeared to be hepatocytes.

Fibrillar to homogeneous eosinophilic material was noted in glomerular capillaries. Proximal tubular epithelial cells were moderately vacuolated. Scattered tubules were mildly dilated and contained moderate amounts of homogeneous, basophilic to eosinophilic material. At the highest doses, multifocal tubular epithelial necrosis was present along with small amounts of luminal necrotic debris. No other lesions were detected.

#### Sequential Kill Study in Rats

Clinical signs were similar to those seen in the acute studies. Livers from rats killed as early as 40 minutes following MCLR administration were dark red and enlarged. No other gross lesions were noted. Liver weights (as a fraction of body

weight) of treated rats were significantly ( $p = 0.01$ ) greater than those of controls over the 24-hour time period (Figure 1). Kidney weights (as a fraction of body weight) increased progressively beginning at 3 hours postdosing (Figure 2).

Lesions were first noted in the liver at 20 minutes postdosing and consisted of mild disassociation and rounding of centrilobular hepatocytes. By 60 minutes, severe hepatocyte disassociation, degeneration, and necrosis with marked loss of hepatocytes and hemorrhage (Figure 3) were present, except for outer areas of the lobule approximately six to seven cells wide (adjacent to the portal regions). Disassociated hepatocytes, cellular debris, and erythrocytes were often present in place of central veins by 3 hours (Figure 4), and where central veins were intact, they often contained hepatocytes or hepatic debris (Figure 5). Between 9 and 24 hours postdosing, there was a progressive reduction in the number of intact cells and cellular debris became intermingled with red blood cells (Figure 6).

Pulmonary capillaries and arterioles were found to contain eosinophilic granular debris or intact rounded cells much larger than leukocytes beginning 1 hour postdosing (Figures 7 and 8). The rounded cells had abundant eosinophilic cytoplasm, occasional binucleate and frequently pyknotic nuclei. The cells in the pulmonary capillaries became increasingly degenerate between 12 and 24 hours with nuclear karyolysis and intracytoplasmic vacuolation and these changes were highly correlated with similar hepatocyte degeneration and necrosis in the liver at the same time points.

Scattered renal cortical tubules contained progressively increasing amounts of homogeneous, basophilic material beginning 60 minutes postdosing. In glomerular

capillaries, small accumulations of eosinophilic, fibrillar material which did not stain for fibrin with phosphotungstic acid hematoxylin, Martius scarlet blue trichrome, Martius yellow scarlet red analine blue, or Carstairs' stains were first noted at 9 hours postdosing. Scattered basophilic areas within this fibrillar material did not stain for calcium with Von Kossa's or Alizarin red stains. At 18 hours after toxin administration, proximal tubular epithelial cells often contained one to several variably sized, clear, intracytoplasmic vacuoles.

Significant increases occurred in serum alanine aminotransferase (ALT) (Figures 9 and 10) and alkaline phosphatase (ALP) (Figure 11) activities and in blood urea nitrogen (BUN) and creatinine from treated animals as compared to controls. Total bilirubin (Figure 12) was elevated beginning 360 minutes postdosing and BUN increased to 70 mg/dl over the 24-hour period. Serum glucose decreased by 67% over time.

#### Sequential Kill Study in Mice

Mice killed at 15 minutes had no observable lesions. In mice killed at 30 minutes postdosing, livers were dark red and markedly enlarged, and thereafter, liver and kidney weights increased with time. In mice killed at 30 minutes postdosing, mild centrilobular disassociation of hepatocytes was noted.

By 60 minutes, severe centrilobular congestion, disassociation and rounding of hepatocytes, and scattered hepatocyte necrosis were present such that one-third to one-half of each lobule was affected, and free hepatocytes were present in several central veins.



Dilation of renal cortical tubules was mild when first noted at 60 minutes postdosing and became more severe by 90 minutes. Many tubules contained eosinophilic granular to fibrillar material, and occasionally, similar material was observed in Bowman's space and glomerular capillaries. No pulmonary lesions were noted.

#### 4. Discussion and Conclusion

Severe hepatocyte disassociation and necrosis noted in the rats and mice in our experiments are similar to effects in mice and sheep given whole cells or toxin extracts and in animals exposed in the field (Elleman et al., 1978; Falconer et al., 1981, 1983, 1986; Galey et al., 1987; Jackson et al., 1983, 1984; Konst et al., 1965; Zin and Edwards, 1979). No notable differences were noted in the response of male rats as compared to females. Essentially, no effects were noted at doses less than 80 µg/kg and virtually 100% lethality occurred at doses greater than 160 µg/kg. Rats given MCLR at 80 to 160 µg/kg were either clinically affected and died with massive liver destruction and hemorrhage or were clinically unaffected and had no gross or microscopic lesions. Microscopic lesions in exposed rats and mice were evident in the liver as early as 20 to 30 minutes postdosing. At 60 minutes, the histologic lesions in rats were comparable to those in mice. Nevertheless, although mice died at 60 to 90 minutes postdosing, rats survived for 20 to 32 hours. Even at doses of MCLR greater than 240 µg/kg, rats still survived 6 to 8 hours. No explanation is presently available for this species difference.

As might be expected, the initial hepatocyte lesions seen at 30 minutes nearly coincided with the initial increase in alanine aminotransferase (ALT) at 40 minutes postdosing. Increases in alkaline phosphatase (ALP) and total bilirubin are often correlated with biliary obstruction but may reflect cell rupture with release of cytosolic components into the circulation. The increase in hepatic enzyme release noted *in vivo* contrasts with the effects of *M. aeruginosa* toxin extracts when added to hepatocyte suspensions. Although morphologic changes (plasma membrane blebbing) in isolated hepatocytes occur within 5 to 10 minutes of release, intracellular enzyme release does not occur for 60 to 100 minutes (Aune and Berg, 1986; Runnegar and Falconer, 1982, 1986; Runnegar et al., 1981). Whether hepatocytes become less susceptible to enzyme release as a result of isolation, some contributing factor present *in vivo* is not present *in vitro*, or the number of hepatocytes damaged *in vivo* is sufficiently large to allow an increase in ALT to be detected earlier than *in vitro* remains to be addressed. The decline in serum glucose may be a result of damage to the liver causing a loss of the ability to convert glycogen to glucose and/or to synthesize glucose from precursor molecules.

The massive intrahepatic hemorrhage and loss of central veins and sinusoidal architecture is compatible with endothelial damage. The data of this study do not clearly discern whether the initial effect was on the endothelial cells or on hepatocytes. It is apparent, however, that the breakdown in hepatic sinusoidal endothelial integrity and the massive hepatocyte disassociation allows intact hepatocytes and necrotic cellular debris into the venous circulation, subsequently into

the pulmonary artery, and eventually into the lungs. It appears that this debris is subsequently deposited as eosinophilic fibrillar material in the renal glomerular capillaries. In rats, necrotic debris and intact cells closely resembling hepatocytes were present in the pulmonary vasculature as early as 1 hour postdosing. Nevertheless, marked hepatic lesions preceded the movement of intact hepatocytes and necrotic cellular debris into the pulmonary vasculature. Consequently, the hypothesis that pulmonary thrombosis is responsible for microcystin-induced hepatic damage should be discounted. Although present in many pulmonary vessels, the hepatocyte microemboli did not appear to cause significant pulmonary or extrapulmonary damage. Perhaps similar findings by others lead to the assumption that pulmonary thrombosis and embolism in response to microcystin exposure was a result of acellular material (Adams et al., 1985; Slatkin et al., 1983).

On light microscopy, the renal tubular lesions in mice and rats given MCLR were suggestive of glomerular damage with leakage of protein into cortical tubules. The kidney lesions were more extensive in rats than mice, perhaps as a result of the short survival time in the latter. The considerable eosinophilic material in glomerular capillaries of rats at 18 and 24 hours coincided with the presence of increased amounts of eosinophilic to basophilic material within the lumens of renal cortical tubules, and this would be compatible with the passage of hepatic debris into the renal circulation. Renal damage could also be due in part to ischemia from hypovolemic shock with damage to glomerular capillaries. Proximal tubular necrosis was evident

in rats given the highest doses of MCLR. The time at which renal lesions were seen was roughly correlated with the elevations in blood urea nitrogen and creatinine.

Death in MCLR-dosed rats and mice appears to be a result of massive hepatic destruction and hemorrhage resulting in a loss of liver function and severe circulatory shock.

Table 1. Mortality of male and female rats following intraperitoneal administration of microcystin-LR.

Dose ( $\mu\text{g/kg}$ )	Number Dead/Number Treated	
	Males	Females
20	0/3	--
40	0/3	0/3
80	0/3	1/3
120	2/3	2/3
160	7/8	3/3
180	3/3	--
200	3/3	--
240	1/2	--
400	3/3	--
800	3/3	--
1,200	3/3	--

Table 2. Liver and kidney weights (as % body weight [BW]) of mice dosed intraperitoneally with microcystin-LR at 100 µg/kg.\*

Time after Dosing (minutes)	Liver (% BW)	Kidney (% BW)
Saline controls (120)	5.37	0.76
15	5.37	0.75
30	5.63	0.75
60	9.01	0.82
90	10.48	0.97
90 to 120†	9.69	1.00

\*Mean of two mice per group.

†Spontaneous death.

Figure 1. Liver weights (as % body weight) (mean  $\pm$  SEM) in rats ( $N = 2$  to 7) dosed intraperitoneally with microcystin-LR at 160  $\mu\text{g/kg}$ . The value plotted and the time 0 observation is the mean value for the control animals.

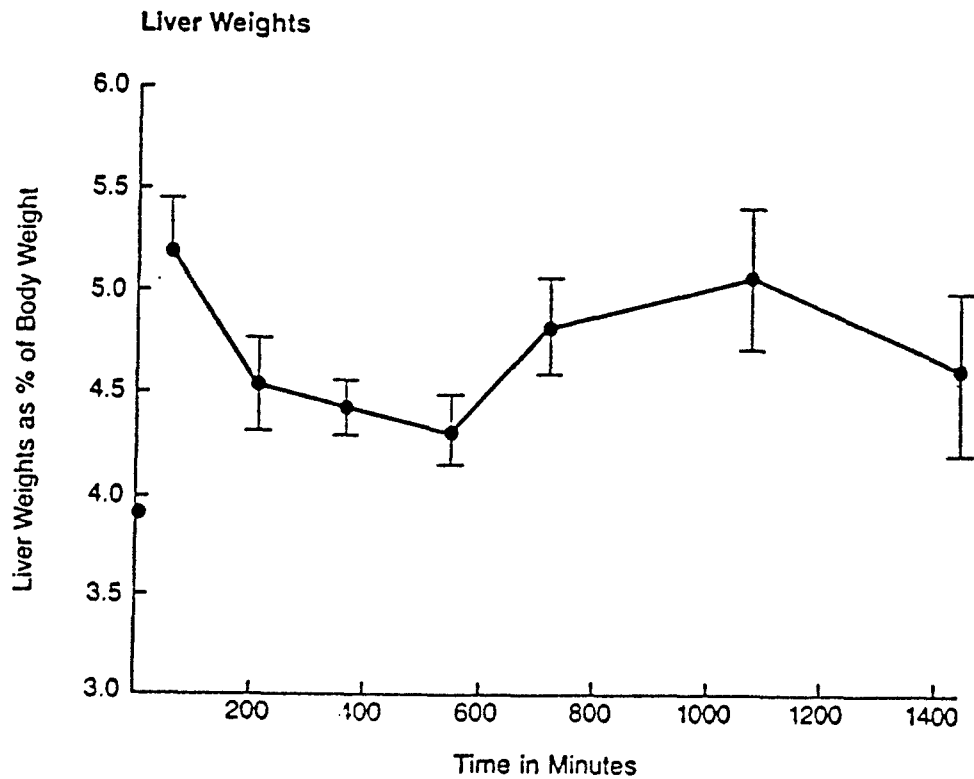


Figure 2. Kidney weights (as % body weight) (mean  $\pm$  SEM) in rats (N = 2 to 7) dosed intraperitoneally with microcystin LR at 160  $\mu\text{g}/\text{kg}$ . The value plotted as the time 0 observation is the mean value for the control animals.

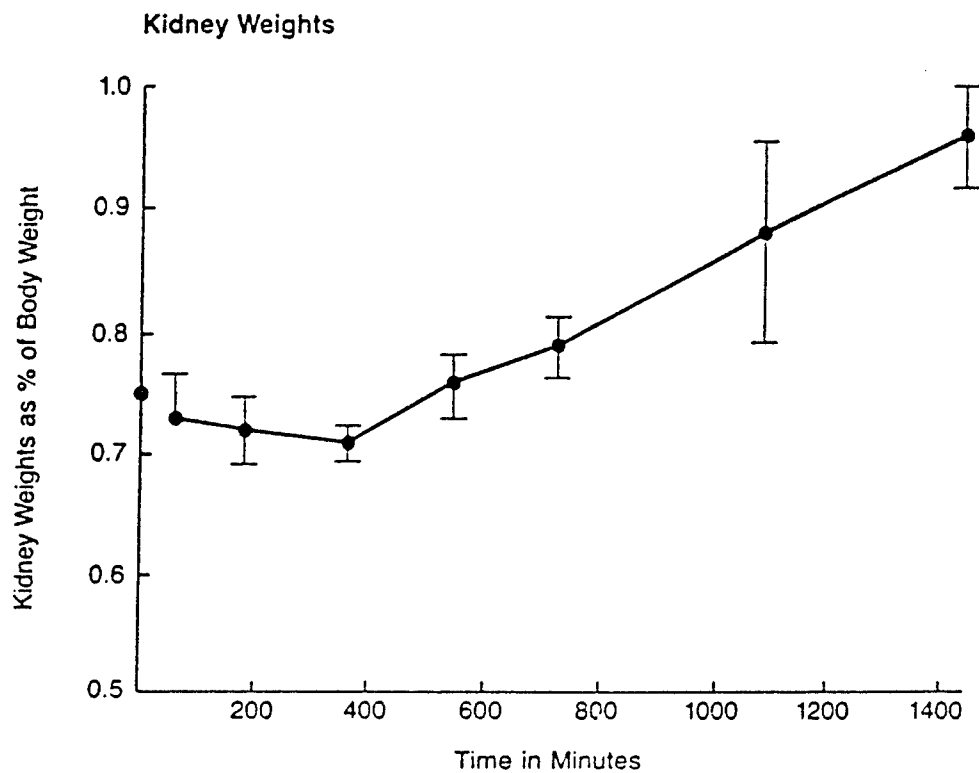




Figure 3. Liver from a rat dosed intraperitoneally with microcystin-LR at 160  $\mu\text{g/kg}$ . Centrilobular hepatocyte degeneration, disassociation, and rounding with small areas of hemorrhage at 1 hour postdosing. HE.

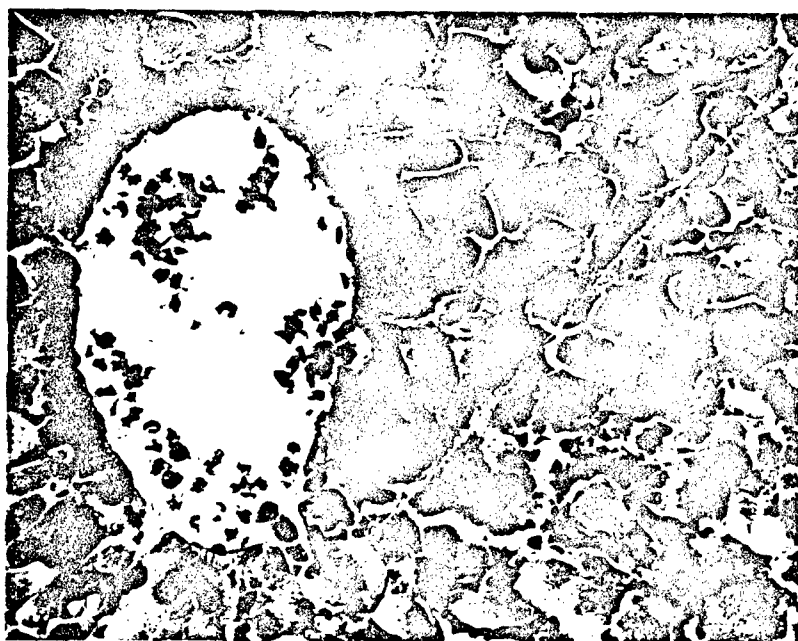


Figure 4. Liver from rat dosed intraperitoneally with microcystin-LR at 160  $\mu\text{g/kg}$ .  
Loss of centrilobular architecture with destruction of a central vein and marked  
hepatocyte degeneration and necrosis at 3 hours postdosing. HE.

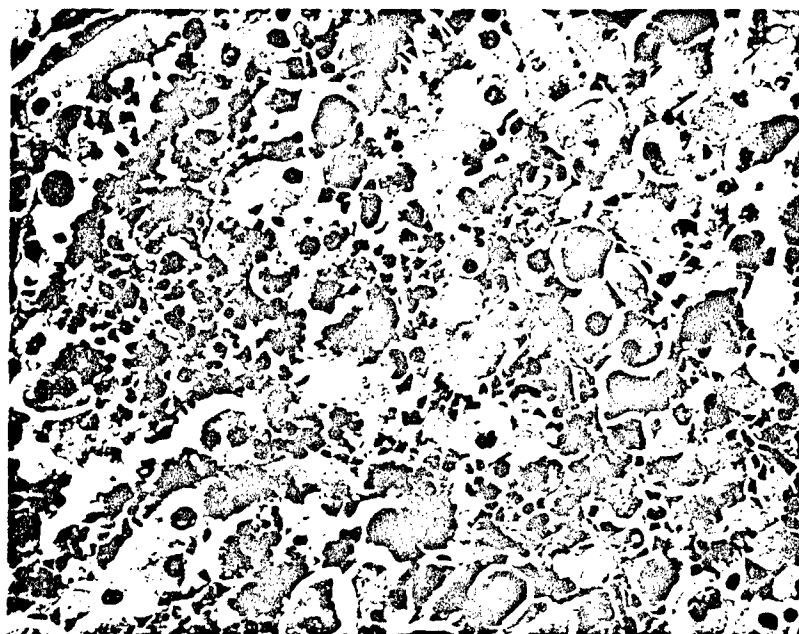


Figure 5. Liver from a rat dosed intraperitoneally with microcystin-LR at 160  $\mu\text{g/kg}$ .

Hepatocytes in central vein at 1 hour postdosing. HE.

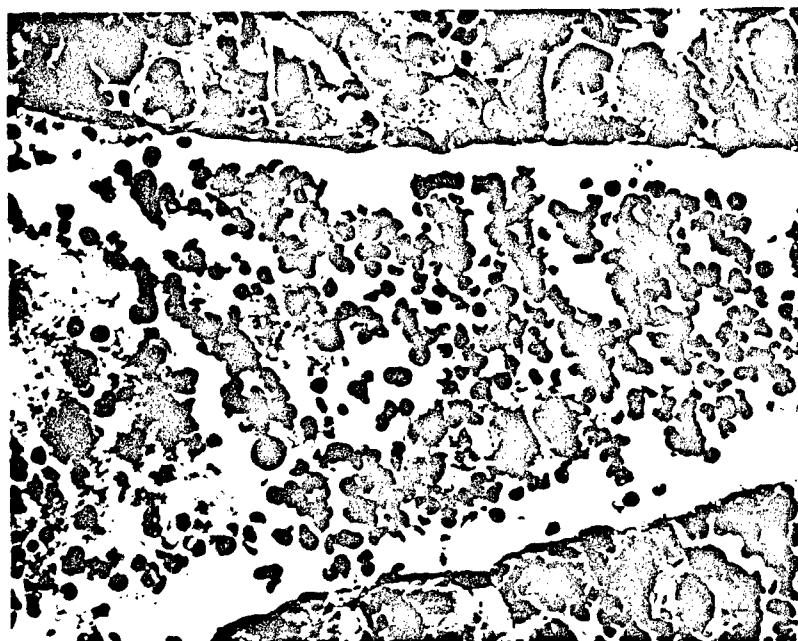


Figure 6. Liver from a rat dosed intraperitoneally with microcystin-LR at 160  $\mu\text{g/kg}$ . Most hepatocytes, except for a rim periportally, have been replaced by necrotic debris and erythrocytes at 24 hours postdosing. HE.

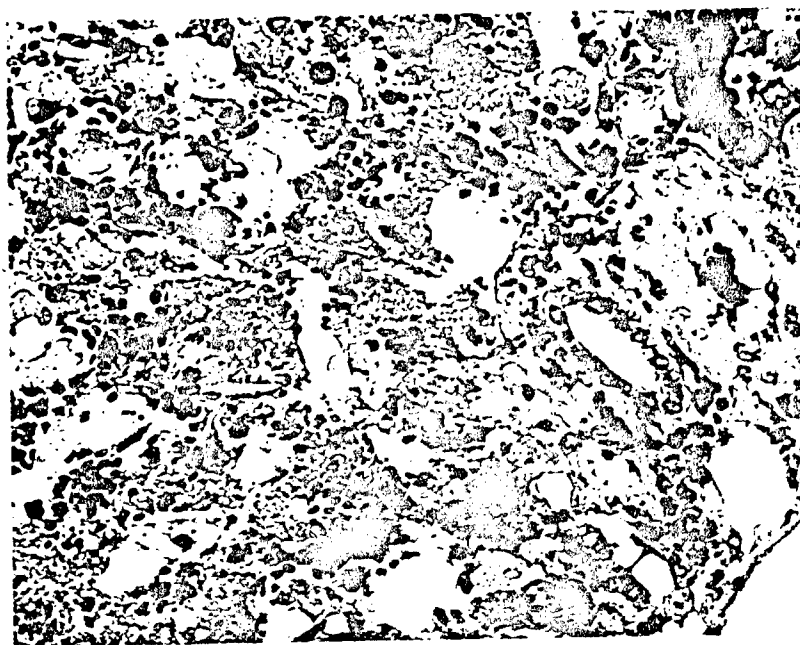


Figure 7. Lung from a rat dosed intraperitoneally with microcystin-LR at 160  $\mu\text{g/kg}$ . Pulmonary capillaries containing intact hepatocytes and erythrocytes. One hepatocyte is binucleate at 3 hours postdosing. HE.

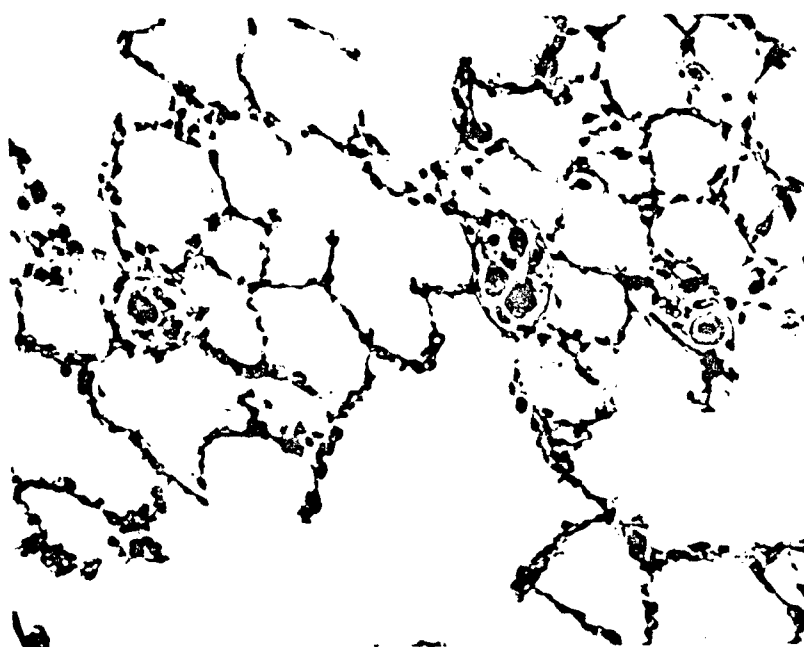


Figure 8. Lung from a rat dosed intraperitoneally with microcystin-LR at 160  $\mu\text{g/kg}$ . Pulmonary vessel containing several hepatocytes and erythrocytes. One hepatocyte is binucleate at 6 hours postdosing. HE.

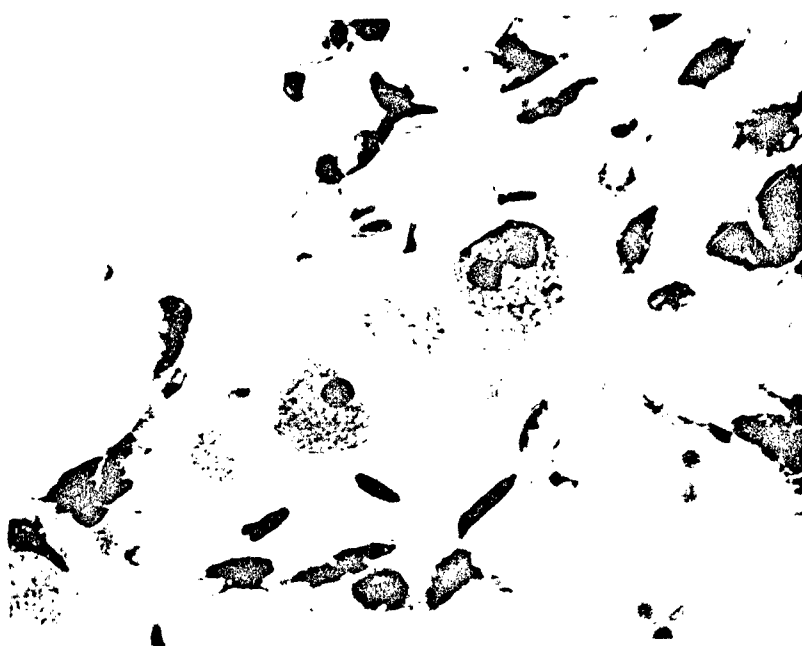


Figure 9. Alanine aminotransferase (mean  $\pm$  SEM) of rats ( $N = 2$  to  $7$ ) over the first 60 minutes after intraperitoneal administration of microcystin-LR at  $160 \mu\text{g/kg}$ . The value plotted as the time 0 observation is the mean value for the control animals.

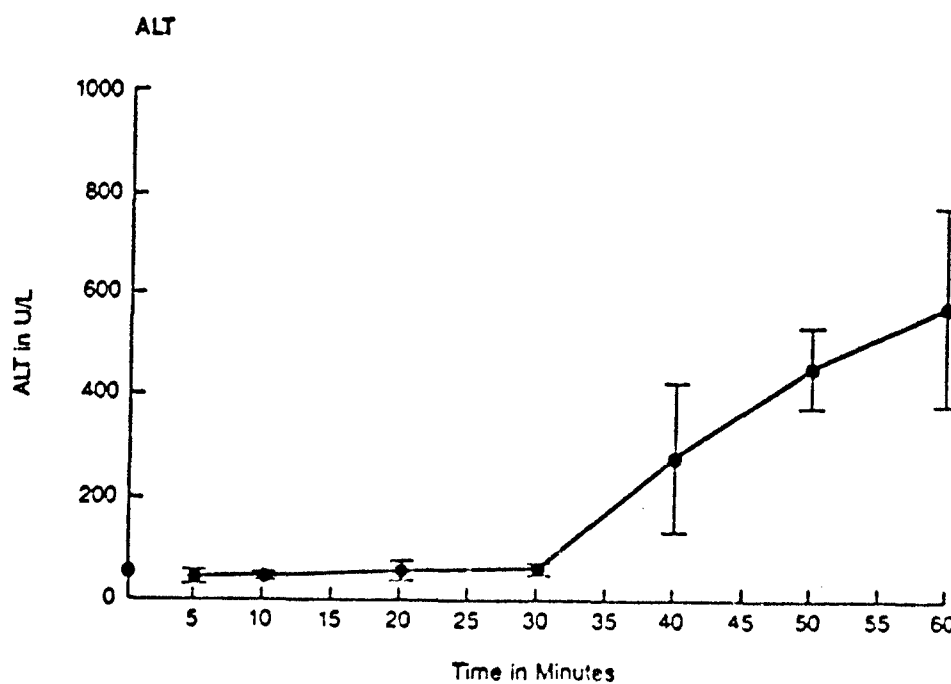


Figure 10. Alanine aminotransferase of rats ( $N = 2$  to  $7$ ) over 1,440 minutes after intraperitoneal administration of microcystin-LR at  $160 \mu\text{g/kg}$ . The value plotted as the time 0 observation is the mean value for the control animals.

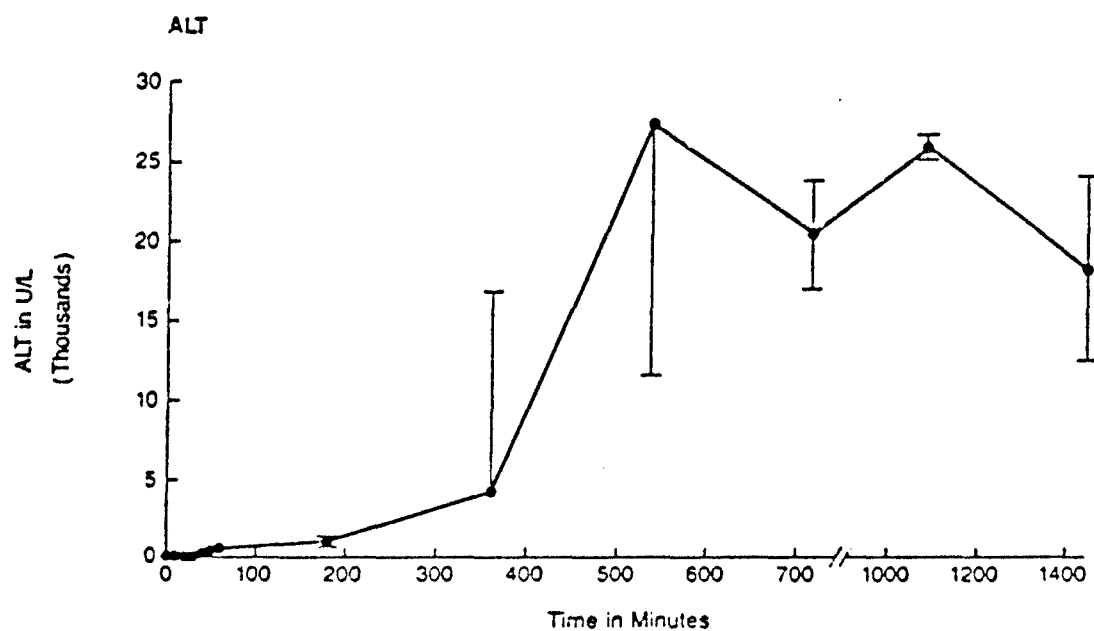




Figure 11. Serum alkaline phosphatase (mean  $\pm$  SEM) of rats (N = 2 to 7) after intraperitoneal administration of microcystin-LR at 160  $\mu$ g/kg. The value plotted as the time 0 observation is the mean value for the control animals.

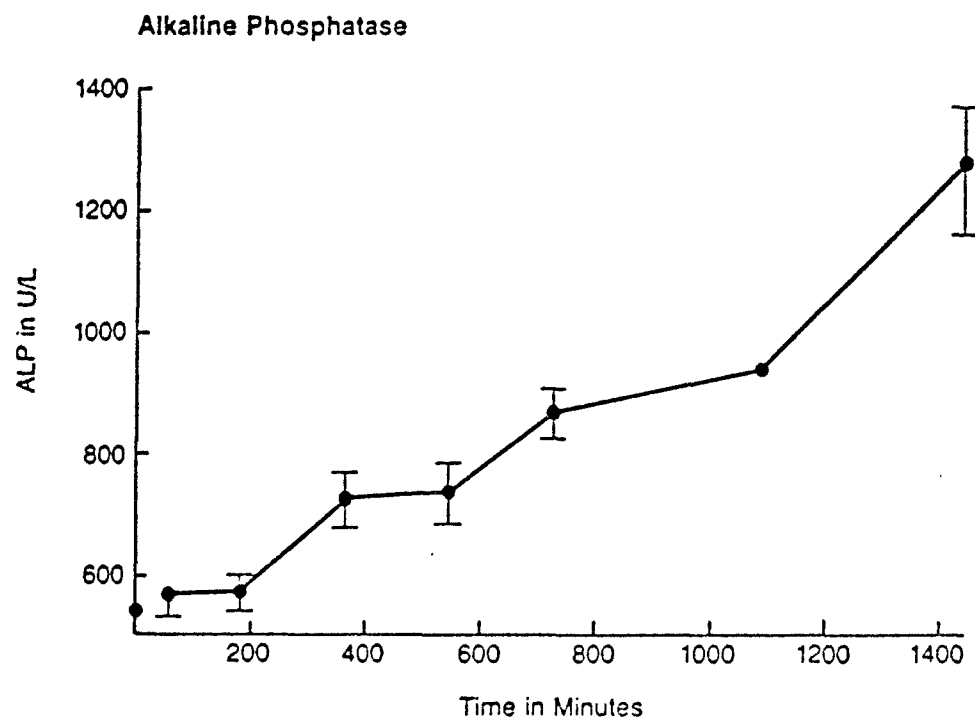
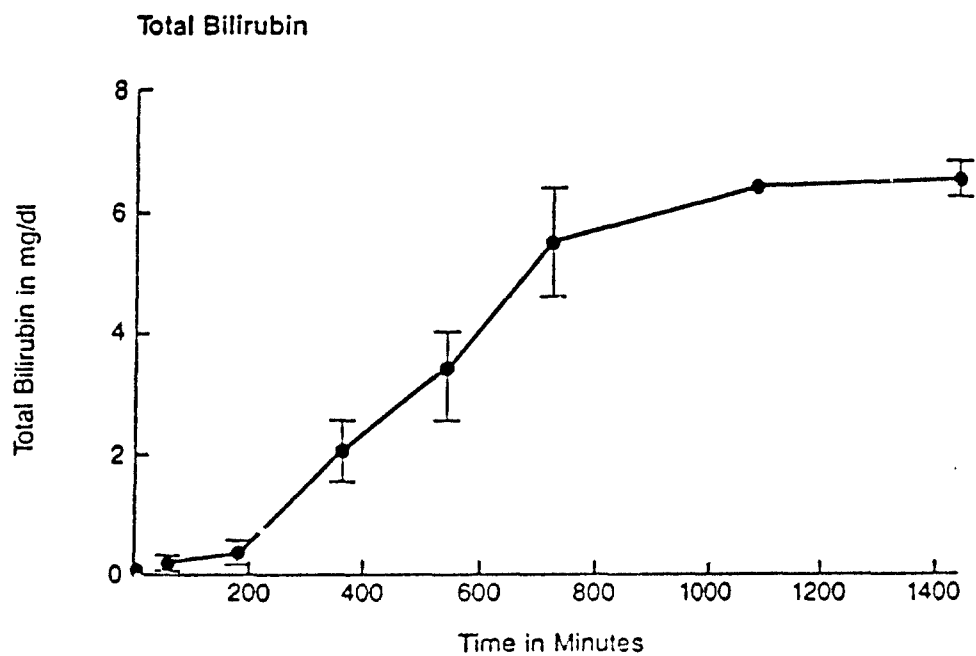


Figure 12. Total bilirubin (mean  $\pm$  SEM) of rats (N = 2 to 7) after intraperitoneal administration of microcystin-LR at 160  $\mu$ g/kg. The value plotted as the time 0 observation is the mean value for the control animals.



## C. Rats

### Microcystin-LR-Induced Ultrastructural Changes in Rats

#### 1. Statement of the Problem, Background, and Rationale

Only a limited number of studies have involved characterization of the ultrastructural effects of microcystin-LR (MCLR) or similar algal peptides. Scanning electron microscopy (SEM) of rat hepatocyte suspensions revealed dose-dependent deformation and blebbing within 5 minutes of toxin administration (Runnegar and Falconer, 1982; Runnegar et al., 1981). SEM and transmission electron microscopy (TEM) of mouse liver following intraperitoneal administration of an aqueous extract of *Microcystis aeruginosa* revealed progressive breakdown of sinusoidal endothelium, disappearance of the space of Disse, damage to hepatocyte membranes, and necrotic changes in hepatocyte cytoplasm (Falconer et al., 1981). This report is the only one known in which lesions began periportally and progressed centrilobularly.

When sheep were given aqueous extracts of *M. aeruginosa*, TEM of liver at 20 hours postdosing demonstrated centrilobular hepatic necrosis with aggregation of the endoplasmic reticulum, peripheral displacement of cellular organelles, and vacuolation of severely affected cells (Jackson et al., 1984). A sequential TEM study involving purified MCLR at 10 and 100 µg/kg intraperitoneally in mice revealed vesiculation and degranulation of the rough endoplasmic reticulum and mitochondrial swelling. At the 100 µg/kg dose, an increase in intracytoplasmic membranous whorls was also present (Dabholka and Carmichael, 1987).

There are marked differences in the responses of mice and rats to MCLR. In mice, massive, centrilobular to midzonal hemorrhage and death occurred within 60 to 90 minutes. In rats, although hepatic necrosis and hemorrhage were present within 60 minutes, the hemorrhage was not as severe as in mice, and rats survived 20 to 32 hours (Hooser et al., 1989a).

This study was intended to: 1) characterize ultrastructural hepatic, pulmonary, and renal changes in rats following intravenous administration of MCLR; 2) correlate these changes with previously described light microscopic changes to determine the sequence of lesion development in rats; and 3) begin localization of the subcellular site(s) of MCLR toxicity.

## 2. Experimental Methods

Male Sprague-Dawley rats (175 to 200 g) were obtained from Harlan Sprague-Dawley, Inc., Indianapolis, IN, provided commercial rat chow and water *ad libitum*, kept on a 12-hour light/12-hour dark cycle, and allowed 2 weeks to become acclimated before use.

Microcystin-LR (MCLR) was produced and purified (approximately 95% pure) in the laboratory of W. W. Carmichael as previously described (Krishnamurthy et al., 1986a). MCLR was dissolved in 0.9% NaCl prior to use.

Rats were dosed intraperitoneally with MCLR at a lethal dose of 160 µg/kg or with 0.9% NaCl (control). At 5, 10, 20, 30, and 60 minutes postdosing, two MCLR-treated rats (for a total of 10) were anesthetized with ether (control rats were anesthetized at 60 minutes after administration of 0.9% NaCl), the thorax was opened,

and a cannula was placed in the left ventricle. Whole body perfusion and fixation were achieved using Tyrode's solution at 37°C, followed by cool 2.5% glutaraldehyde in 0.1 M isotonic cacodylate buffer and 3% sucrose (pH 7.2). The Tyrode's solution and fixative were kept at a constant perfusion pressure of 102 mmHg through the use of a Cole-Palmer masterflex pump (Cole-Palmer Instrument Co., Chicago, IL). Samples of perfusion-fixed liver, lung, and kidney were minced into 1-mm cubes and placed in 2.5% glutaraldehyde with 0.1 M isotonic cacodylate buffer and 3% sucrose (pH 7.2) until subsequent processing was done (at least 7 days following perfusion). Tissue samples were washed in 0.1 M isotonic cacodylate buffer and 3% sucrose, postfixed in 1% osmium tetroxide, rinsed, and dehydrated in a graded ethanol series of 10 to 100%. Final dehydration with 100% propylene oxide was followed by infiltration and embedding with epoxy. Thin sections of specimens were mounted on copper grids, stained with uranyl acetate and lead citrate, and viewed with a JEOL 100-CS transmission electron microscope.

### 3. Results

No ultrastructural changes were seen in the livers of controls or in toxin-dosed rats at 5 minutes postdosing (Figures 1 and 2). Ten minutes postdosing, mild widening of intercellular spaces between centrilobular hepatocytes was apparent with occasional invaginations of the plasma membrane; these lesions became progressively more severe and widespread over time. By 20 minutes postdosing, the changes in centrilobular hepatocyte plasma membranes consisted of invaginations with formation of variably sized cytoplasmic vacuoles. Blebbing as well as invagination of the entire

hepatocyte plasma membrane and loss of microvilli along the sinusoidal face were often noted, and hepatocyte separation was pronounced and widespread. In severely affected areas, widening of sinusoidal endothelial fenestrae was also present (Figure 3). Lesions in Kupffer and bile ductular cells were not evident at this time.

At 30 minutes postdosing, marked widening of the space of Disse was noted in centrilobular regions as was a further loss of hepatocyte sinusoidal microvilli, blebbing, invagination of hepatocyte plasma membranes, and widening of intercellular spaces. Bile canaliculi in affected areas were frequently dilated, and microvilli were often shorter than normal or lost altogether. Despite these changes, the tight junctions surrounding bile canaliculi appeared to remain intact.

At 60 minutes postdosing, centrilobular areas were characterized by a loss of sinusoidal endothelium and necrotic hepatic cells. Such cells had lost portions of plasma membranes but the organelles nevertheless appeared relatively normal. Free-floating, but intact, organelles (nuclei, mitochondria, and rough endoplasmic reticulum) together with erythrocytes and platelets were also seen in these areas (Figure 4). In the less affected midzonal and periportal regions, the severity of the lesions seen at 30 minutes had increased and prominent hepatocytic rounding, and accumulation of erythrocytes within the space of Disse (Figure 5) were noted. There was a moderate, focal loss of the sinusoidal endothelium and occasional hepatocyte necrosis in these areas. Moderate whorling of the rough endoplasmic reticulum around normal-appearing mitochondria was occasionally present (Figure 6). Also at 60 minutes postdosing, the pulmonary microvasculature contained cellular debris,

including relatively intact cells with recognizable mitochondria, rough endoplasmic reticulum, and nuclei similar to that resulting from the hepatocyte destruction already noted (Figure 7). Finally, at 60 minutes postdosing, the renal cortical glomerular and peritubular capillaries contained relatively intact cells identical to those in the pulmonary vasculature and small amounts of necrotic cellular debris, including cytoplasmic fragments and mitochondria (Figure 8). In fact, the mitochondria and the whorled rough endoplasmic reticulum that were noted in the pulmonary and renal capillary debris and in intact cells in these locations were virtually identical to the mitochondria and whorled rough endoplasmic reticulum noted in hepatocytes of the liver at 60 minutes. Pulmonary or renal damage associated with these microemboli was not apparent.

#### 4. Discussion and Conclusion

The ultrastructural lesions first detected in rats following administration of microcystin-LR (MCLR) consisted of alterations in the plasma membrane of hepatocytes. Such changes were recognizable as early as 10 minutes postdosing. Lesions seen in this study were highly compatible with the hepatocyte disassociation and rounding previously characterized by light microscopy (Hooser et al., 1989a).

The decrease in hepatocyte cell-to-cell contact, loss of sinusoidal microvilli, plasma membrane blebbing and invagination, and rounding of hepatocytes are compatible with effects on the plasma membrane and/or the hepatocyte cytoskeleton. As described later in this report, we have also demonstrated marked alterations in actin filaments in primary cultures of hepatocytes exposed to MCLR (Hooser et al.,

1989b). The fact that hepatocyte disassociation and rounding seen with light microscopy and hepatocyte disassociation, loss of microvilli, and plasma membrane invagination seen ultrastructurally are all compatible with structural changes caused by alterations in actin filaments, and the fact that no other hepatocyte degenerative changes (nuclear, mitochondrial, or endoplasmic reticular) were seen until a considerable time following the onset of plasma membrane shape changes supports the hypothesis that actin filament changes precede other hepatocyte changes.

From previous studies, it was uncertain whether the changes in the sinusoidal endothelium and the space of Disse were secondary to hepatocyte changes or if there was also a direct effect on sinusoidal endothelial cells (Falconer et al., 1981; Runnegar and Falconer, 1982). In our study, however, hepatocyte changes preceded all other changes, supporting a hypothesis that MCLR affects primarily hepatocytes and that sinusoidal endothelial damage occurs secondarily.

Evidence for a direct effect on hepatocytes is also derived from the fact that cholate, deoxycholate, bromosulphophthalein, and rifampicin provided protection to isolated rat hepatocytes exposed to MCLR (Runnegar et al., 1981). This observation seems to suggest that MCLR preferentially enters cells by binding to a hepatocyte-specific, bile-acid carrier as do certain other low-molecular-weight cyclic peptides, such as phalloidin and somatostatin (Ziegler and Frimmer, 1986).

Despite the severe plasma membrane damage, most hepatocyte mitochondria did not appear swollen; rough endoplasmic reticulum had not degranulated; nuclear chromatin was not clumped and nuclei had not undergone pyknosis. These findings



were in contrast to those reported with regard to microcystin-dosed mice in which changes in intracellular organelles were among the earliest lesions described (Dabholkar and Carmichael, 1987).

The presence of hepatocytes in the pulmonary vasculature, as deduced by light microscopy at 60 minutes (Hooser et al., 1989a), was confirmed on TEM. Accumulation of hepatocyte debris in pulmonary capillaries would appear to account for a previous report describing atypical pulmonary thrombosis seen in mice given microcystin (Slatkin et al., 1983).

Pulmonary damage secondary to passage of hepatocyte debris into the pulmonary vascular was not evident in rats. However, in animals with pulmonary intravascular macrophages, such as sheep and pigs, phagocytosis of such particulate matter could potentially bring about the release of macrophage enzymes with resultant damage to the microvasculature. This is compatible with the fact that sheep given lethal doses of toxic cells of *M. aeruginosa* developed pulmonary edema, although hepatocyte microemboli were not reported (Jackson et al., 1984).

Hepatic debris in renal cortical glomerular and peritubular capillaries was observed by TEM as early as 60 minutes postdosing by electron microscopy, despite the fact that it was not evident on light microscopy until 9 hours postdosing (Hooser et al., 1989a). In summary, ultrastructural lesions identified with TEM in rat hepatocytes following a lethal dose of MCLR develop rapidly but are initially confined to changes in the hepatocyte plasma membrane. As discussed in a subsequent section of this report, we believe that the plasma membrane changes are

a result of altered organization of hepatocyte actin filaments. Hepatocyte rounding and disassociation apparently leads to breakdown of sinusoidal endothelium and hepatic architecture including disruption of the sinusoidal endothelium. This, in turn, seems to result in severe intrahepatic hemorrhage and permits release of hepatocyte microemboli into the hepatic vein, the pulmonary vasculature, and then into the systemic circulation. Deaths in rats given MCLR appear to be a result of loss of hepatic function, intrahepatic hemorrhage, and eventual circulatory collapse.

Figure 1. Normal hepatocytes and endothelium lining sinusoid(s). Hepatocyte microvilli are present in the space of Disse. 9,000 X.

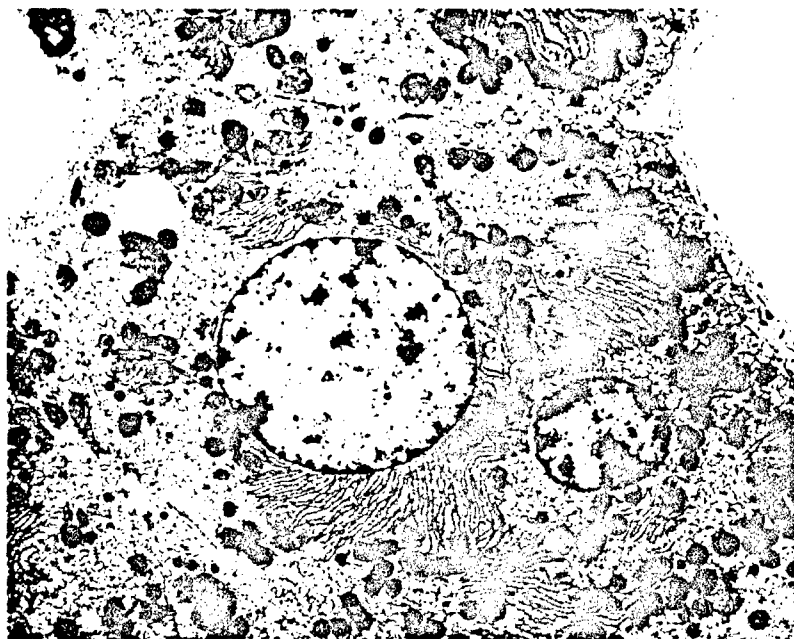


Figure 2. Normal hepatocytes, bile canaliculus (B) with adjacent tight junctions. 20,000 X.



Figure 3. Hepatocytes and sinusoidal endothelium at 20 minutes postdosing. Organelles appear essentially normal; however, lesions include separation of hepatocytes from one another, plasma membrane invagination, loss of hepatocyte microvilli in space of Disse, formation of intracytoplasmic vacuoles, and widening of sinusoidal endothelial fenestrae. 15,000 X.

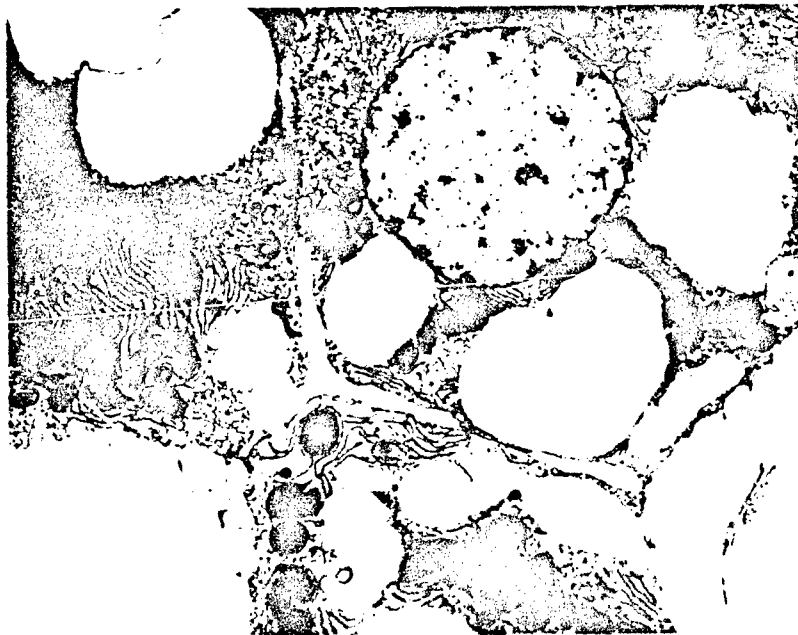


Figure 4. Centrilobular hepatocytes and debris are intermingled with erythrocytes at 60 minutes postdosing. Hepatocyte nuclei, mitochondria, and rough endoplasmic reticulum appear normal. 9,000 X.

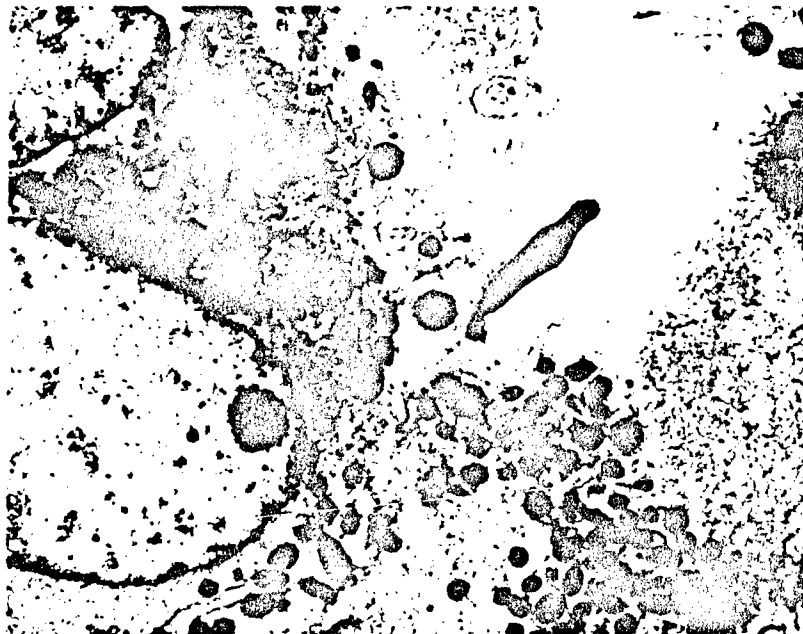


Figure 5. Rounding and disassociation of hepatocytes at 60 minutes postdosing. Erythrocytes and platelets are present in the space of Disse (D). 6,500 X.

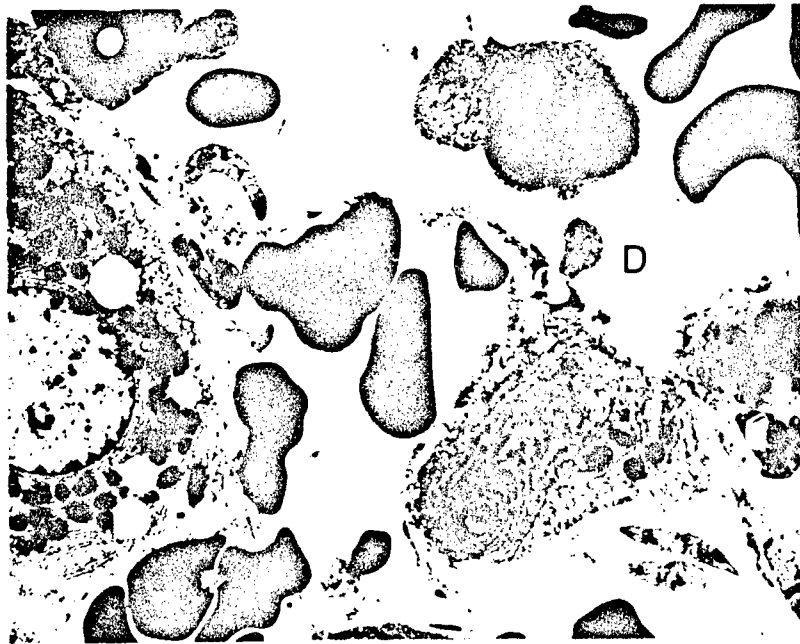


Figure 6. Blebbing of hepatocyte plasma membranes and whorling of rough endoplasmic reticulum around mitochondria at 60 minutes postdosing. 23,000 X.





Figure 7. Hepatocyte debris with whorled rough endoplasmic reticulum and mitochondria in pulmonary vessel at 60 minutes postdosing. 12,000 X.



Figure 8. Hepatocyte debris in a glomerular capillary at 60 minutes postdosing. The rough endoplasmic reticulum and mitochondria appear similar to those in Figures 5, 6, and 7. 13,000 X.



## VI. LESIONS IN HEPATOCYTES INDUCED BY MICROCYSTIN-LR *IN VITRO*

### A. Statement of the Problem, Background, and Rationale

Studies with purified microcystin-LR (MCLR) in rats and mice have demonstrated that it is specifically toxic to the liver and that toxicosis is characterized by rapid, progressive, centrilobular hepatocyte rounding, dissociation, and necrosis, as well as breakdown of the sinusoidal endothelium. This is followed by massive intrahepatic hemorrhage and death (Falconer et al., 1981; Hooser et al., 1989a); however, the specific cell type(s) targeted by MCLR and the mechanism of action of MCLR were unknown at the onset of these studies. In mice given an aqueous extract of *M. aeruginosa* IP, breakdown of the sinusoidal endothelium was the earliest ultrastructural change recognized (Falconer et al., 1981). In rats given purified MCLR, however, injury to sinusoidal endothelium did not precede hepatocyte changes (Hooser et al., 1989a). It was not clear, therefore, whether the hepatocytes or the nonparenchymal hepatic cells (particularly sinusoidal endothelial cells) are the primary cells affected by MCLR.

In suspension cultures, hepatocytes exposed to MCLR undergo rapid plasma membrane deformation (blebbing) without cell death, as determined by morphologic change, enzyme release, and trypan blue uptake (Prentki et al., 1979; Runnegar and Falconer, 1982, 1986). Similar blebbing has been described following treatment of hepatocytes with phalloidin and cytochalasin B which specifically affect the cytoskeleton (Prentki et al., 1979; Weiland, 1986). We have shown that early hepatocyte changes in response to a parenteral dose of MCLR *in vivo*, include plasma membrane invagination, blebbing, and

loss of microvilli (Hooser et al., 1990a). Based on these morphologic findings, we and others have proposed that cytoskeletal alteration may be an early intracellular event following MCLR treatment (Hooser et al., 1990a; Runnegar et al., 1981).

The hepatocyte cytoskeleton consists largely of actin filaments, intermediate filaments, and microtubules, which are important in cellular structural stability, intracellular transport, and endocytosis (Sager et al., 1986). These components interact with each other and with other cellular proteins and are modulated by intracellular conditions such as pH and calcium concentration. Actin occurs in two forms, the monomeric (G, unpolymerized) form and the filamentous (F, polymerized) form. Disruption of the equilibrium between these two forms, such as occurs following phalloidin or cytochalasin B treatment, can cause profound alterations in cell morphology and function. Phalloidin binds directly to filamentous actin preventing its depolymerization, while cytochalasin B stops the polymerization of actin into its filamentous form (Weiland, 1986). Reorganization of actin filaments unassociated with a change in actin polymerization, and therefore unlike that induced by phalloidin or cytochalasin B, has recently been demonstrated in isolated suspensions of hepatocytes treated with microcystin (Runnegar and Falconer, 1986; Eriksson et al., 1989). Actin filament and cytoskeletal organization in hepatocytes in suspension are different from those in culture or *in vivo*.

The objectives of this study were to: 1) identify the primary hepatic cell type(s) affected by MCLR, 2) determine whether alterations in the arrangement of actin filaments occur in association with other MCLR-induced morphologic changes both *in vitro* and *in*

*vivo*, and 3) compare MCLR-related actin filament alterations to those caused by phalloidin and cytochalasin B.

## **B. Experimental Methods**

### Animals

Male Sprague-Dawley rats (175 to 200 g) (Harlan Sprague-Dawley, Inc., Indianapolis) were allowed to become acclimated to their cages for 2 weeks or longer before use. The rats had free access to a commercial laboratory animal ration and water, and were maintained on a 12-hour light/12-hour dark cycle prior to use.

### Toxin

MCLR (approximately 95% pure) was purified in the laboratory of W. W. Carmichael using techniques described previously (Krishnamurthy et al., 1986a) and dissolved in phosphate buffered saline (PBS) prior to use.

### Hepatic Parenchymal and Nonparenchymal Cells

Parenchymal (hepatocytes) and nonparenchymal (primarily sinusoidal endothelial and Kupffer) cells were isolated from livers of rats using a two-step collagenase perfusion method (Kuhlenschmidt et al., 1982). Hepatocytes were separated by centrifugation. Pronase digestion of the supernatant and metrizamide gradient centrifugation were used to isolate nonparenchymal cells (Lafranconi et al., 1986; Wanson and Mosselmans, 1980). Nonparenchymal cells were identified by their size and morphologic characteristics. The cell pellets were resuspended in Ham's F-10 medium containing (per 500 ml) 100 ml of fetal bovine serum and 0.3 ml of insulin. For culturing, 1.0 ml of gentamicin (50 mg/ml) and 6 ml of a combination of penicillin (10,000 U/ml) and streptomycin (10 mg/ml) were

added to the medium. Duplicate samples from three rats were used to prepare the hepatocyte suspensions and cultures.

Toxin Exposures of Cell Suspensions and Cultures; Fixation Methods

For cell suspension studies, 2 ml of the cell suspensions ( $1 \times 10^6$  cells/ml) were placed in cell suspension tubes to which were added 2 ml of PBS (pH = 7.4) or 2 ml of a solution of PBS containing MCLR at a final concentration of 0.1, 1.0, or 10.0  $\mu\text{g/ml}$ . The cells were incubated at 37°C with mild agitation. The addition of PBS or MCLR was designated time 0. At 10, 20, and 30 min, aliquots of cells were removed for immediate microscopic examination or fixed in 10% neutral-buffered formalin for subsequent microscopic examination (Aune and Berg, 1986; Falconer et al., 1981; Runnegar and Falconer, 1982). The percent of cells with plasma membrane blebbing was estimated and the progression of morphologic changes determined.

For cell culture studies, hepatocytes suspended in complete Ham's F-10 medium were added to Lux 8-well tissue culture plates, each of which contained a collagen-coated 22 mm square glass coverslip. The cells were seeded at a subconfluent concentration of  $1 \times 10^5$  cells/ml and media was changed daily. The hepatocytes were incubated in a water-jacketed incubator at 37°C in air:CO<sub>2</sub>, 95:5 (Kuhlenschmidt, et al., 1982).

Seventy-two-hour monolayer cultured hepatocytes were treated with PBS or MCLR in PBS at a final concentration of 0.1, 1.0, or 10.0  $\mu\text{g/ml}$ . At 6 hours (0.1 and 1.0  $\mu\text{g/ml}$ ) and at 1, 2, 3, 4, 5, and 6 hours (10.0  $\mu\text{g/ml}$ ) posttreatment, the medium was removed, and the cells were washed with PBS, fixed with fresh 3.7% paraformaldehyde in PBS, and permeabilized with 0.5% Triton X-100 in PBS (Zand and Albrecht-Beuhler, 1989).

### Comparison of the Effects of MCLR with Those of Phalloidin and Cytochalasin

Twenty-four-, 48-, and 72-hour cultured hepatocytes were treated with MCLR at 10.0 µg/ml, phalloidin at 10.0 µg/ml, or cytochalasin B at 10.0 µg/ml or unamended PBS. At 6 hours after addition of toxin, the medium was removed from each replicate, and the cells were washed, fixed, and permeabilized as above.

### Studies with Intact Rats

Twenty-one rats were randomly assigned to seven groups of three animals each. Six of the groups were given a lethal dose of MCLR IP (180 µg/kg), and the seventh was given PBS (controls). Rats were killed by ether inhalation at 60 minutes following PBS administration (controls) or at 5, 10, 20, 30, 45, and 60 minutes following MCLR treatment. Sections of liver were covered with optimal cutting temperature fluid (a cryoprotectant), frozen in liquid nitrogen, and subsequently cryosectioned. Adjacent liver sections were fixed in 10% neutral-buffered formalin, routinely processed, paraffin embedded, cut at 4 to 6 µ, and stained with hematoxylin and eosin.

### Rhodamine-Labelled Phalloidin Visualization of Actin

Frozen liver sections and fixed, permeabilized cultured hepatocytes were stained with rhodamine-labelled phalloidin (Molecular Probes, Eugene, OR) and examined by fluorescence (epiluminescent) microscopy and by direct luminescence light microscopy (Zachary et al., 1986). Morphologic changes were recorded and the fraction of cultured hepatocytes with plasma membrane blebbing was estimated for each timepoint after treatment and for each dose of MCLR. Photomicrographs were taken with an Olympus

BH2 fluorescent and incandescent illumination photomicroscope using Kodak Tri-MAX 400 black and white film.

### C. Results

#### Effects on Hepatocytes and Nonparenchymal Cells in Suspension

Hepatocytes in phosphate-buffered saline (PBS) were unaffected, whereas plasma membrane blebbing developed in response to MCLR. The blebs increased in number and size in a time-dependent manner until they coalesced to form large blebs. At 10 minutes after addition of MCLR at 10.0  $\mu\text{g/ml}$ , over 90% of the cells had multiple medium to large plasma membrane blebs. At 30 minutes, the blebs had increased in size and many had coalesced to form a rim around the original cell border. Fewer and smaller blebs were observed at the lower doses of 1.0 or 0.1  $\mu\text{g}$  of MCLR/ml. Plasma membrane blebbing was not observed in similarly treated hepatic nonparenchymal cells.

#### Effects on the Plasma Membrane and Actin Filaments of Cultured Hepatocytes

In pilot studies, after 24 hours in culture, hepatocytes were still rounded and staining with rhodamine-labelled phalloidin revealed that actin filaments were not yet organized. After 72 hours, hepatocytes had spread out and actin filaments were well organized. We therefore chose to study the effects of MCLR primarily in hepatocytes cultured for 72 hours.

Hepatocytes cultured for 72 hours and treated with PBS exhibited no abnormalities in the plasma membrane or actin filaments (Figure 1a). Following 1 hour of treatment with MCLR at 10  $\mu\text{g/ml}$ , approximately 50% of hepatocytes had one or several small plasma membrane blebs, and filamentous actin was aggregated at the base of these blebs. After



3 hours of MCLR exposure, approximately 75% of hepatocytes had multiple plasma membrane blebs, and the blebs typically contained filamentous actin which appeared as thickened linear "rays" extending to the tip of the bleb and/or as focal aggregates at the base of these blebs (Figures 1b and c). After 6 hours of toxin exposure, more than 95% of hepatocytes were affected. These hepatocytes were rounded, with blebbed plasma membranes which occasionally coalesced to form a rim around the original cell border, and filamentous actin in these cells was aggregated into a single, intensely staining locus (Figure 1d). Similar but less marked increases in numbers of hepatocytes affected, as well as in the severity of effects were observed over time at lower concentrations of MCLR. Thus, with MCLR at 1  $\mu\text{g/ml}$ , approximately 10% of hepatocytes were affected at 1 hour, 20% at 3 hours, and 50% at 6 hours.

The numbers of hepatocytes with plasma membrane blebbing increased with the dose of MCLR at each of the time points examined, i.e., 1, 3, and 6 hours (data not shown). Thus, at 3 hours, the number of hepatocytes affected was 0% at 0  $\mu\text{g/ml}$  and approximately 5% at 0.1  $\mu\text{g/ml}$ , 20% at 1.0  $\mu\text{g/ml}$ , and 75% at 10  $\mu\text{g/ml}$ .

#### Comparison of the Effects of MCLR with Those of Phalloidin and Cytochalasin

The numbers of hepatocytes developing plasma membrane blebbing in response to phalloidin exposure was related to the age of the cells: approximately 50% were affected in 24-hour cultures, 10 to 20% in 48-hour cultures, and less than 5% in 72-hour cultures. By contrast, neither MCLR nor cytochalasin B showed this age dependency. Since phalloidin had little effect on hepatocytes cultured for 72 hours, only that data obtained with 24-hour cultured hepatocytes is presented.

After 6 hours of exposure to PBS, no change was observed in 24-hour cultured hepatocytes; they remained rounded and stained diffusely with rhodamine-phalloidin with few linearly organized actin filaments. However, 6 hours after exposure of 24-hour cultured hepatocytes to MCLR at 10.0 µg/ml, cell blebbing and aggregation of filamentous actin into a single, intensely staining locus was identical to that described above with regard to 72-hour cultured hepatocytes. Treatment of 24-hour cultured hepatocytes for 6 hours with phalloidin at 10.0 µg/ml or with cytochalasin B at 10.0 µg/ml also caused numerous plasma membrane blebs, but when stained with rhodamine-phalloidin, the actin aggregates were variable in size and scattered throughout the cytoplasm thus differing from changes induced by MCLR (Figures 2a and b).

#### Morphologic and Cytoskeletal Effects of MCLR in Livers of Intact Rats

Lesions in formalin-fixed, hematoxylin and eosin stained sections of liver, were similar to those reported previously (Jackson et al., 1984). At 30 minutes after dosing with MCLR at 180 µg/kg, disassociation and rounding of hepatocytes was evident adjacent to central veins, and mild hemorrhage was seen in some areas (Figure 3). Lesions became progressively more widespread and severe until, at 60 minutes after dosing, hepatocyte fragmentation and necrosis with hemorrhage involved entire liver lobules except for a rim of periportal hepatocytes 10 to 15 cells wide.

In rhodamine-phalloidin stained, frozen liver sections from control (PBS-treated) rats, actin was normally distributed in hepatocytes with margination occurring along the plasma membrane. Random cytoplasmic stippling was evident in these cells (Figure 4a). Random cytoplasmic stippling was also noted at 5 and 10 minutes after dosing rats with MCLR. By

20 minutes after dosing, however, multiple (5 to 15) discrete aggregates of actin were observed in the cytoplasm of centrilobular and a few midzonal hepatocytes. By 45 minutes after dosing, centrilobular and some midzonal hepatocytes contained distinct aggregates of filamentous actin (Figure 4b), and the lesions progressed in extent and severity until, at 60 minutes, the majority of periportal hepatocytes were also affected. The intracytoplasmic filamentous actin aggregates in most centrilobular and midzonal hepatocytes appeared as dense foci.

#### D. Discussion and Conclusion

These studies demonstrated that the morphology of hepatocytes in suspension cultures is affected by MCLR but that of nonparenchymal cells is not. In cultured hepatocytes, MCLR caused time- and dose-dependent alterations in both the plasma membrane and actin filaments suggesting that the loss of integrity in the membrane may result from cytoskeletal dysfunction. The actin reorganization associated with plasma membrane changes in cultured hepatocytes exposed to MCLR was unlike that induced by either phalloidin or cytochalasin B. Previous studies had shown that phalloidin and cytochalasin B cause a change in the polymerization state of actin, whereas microcystin does not (Eriksson et al., 1989; Runnegar and Falconer, 1986). Finally, we have demonstrated that MCLR induces actin filament alterations both *in vitro* and *in vivo* and that these alterations are associated with hepatocyte rounding and degeneration seen histologically.

The development of MCLR-induced plasma membrane blebbing in hepatocytes, but not in sinusoidal endothelial or Kupffer cells in suspension, is presumably due to the hepatocyte-specific bile acid carrier uptake of the toxin which is similar to that responsible

for phalloidin uptake into hepatocytes (Faulstich and Münter, 1986; Frimmer, 1982). Hepatocytes in suspension are protected from MCLR-induced toxicity when certain competitors of bile acid carriers are added prior to toxin administration (Runnegar et al., 1981). The lack of such plasma membrane carriers in other cell types apparently accounts for their resistance to MCLR and phalloidin. The variation in susceptibility of hepatocytes of different ages to phalloidin was in contrast to the similar susceptibility to MCLR. This may suggest differences either in bile acid carriers involved in transport or in carrier function involved with these two toxins.

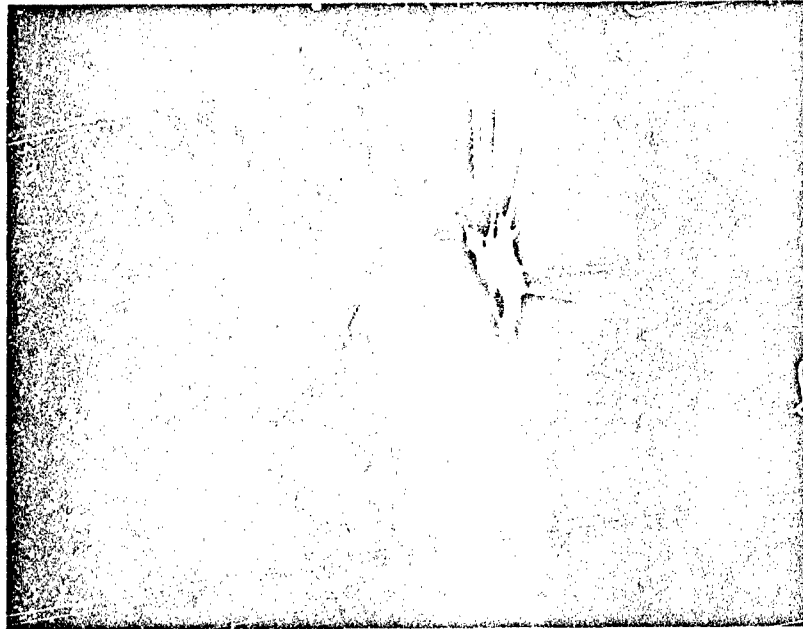
Although cytoskeletal alterations have been suspected to be responsible for the cell deformation induced by MCLR, only recently has MCLR-induced actin filament alteration been demonstrated in hepatocyte suspensions (Eriksson et al., 1989). In the present study, we have demonstrated MCLR induced a rearrangement of filamentous actin within hepatocytes both in cultured hepatocytes and *in vivo*. Cultured hepatocytes, in contrast to suspended hepatocytes, have actin filament and cytoskeletal organization more closely resembling that found *in vivo*. Alterations in the filamentous actin of hepatocytes occurred *in vivo* at the same time or slightly before lesions were observed by routine histologic examination. The fact that MCLR-induced actin filament rearrangement was distinctly different from that caused by phalloidin or cytochalasin B supports the work of others showing that the effects of MCLR are distinct from those of phalloidin or cytochalasin B (Prentki et al., 1979; Weiland, 1986).

Figure 1. Fluorescent micrographs. Seventy-two-hour cultured hepatocytes. Rhodamine-labeled phalloidin.

- a. Control, 6 hours after treatment with phosphate-buffered saline. The cells are flattened and contain numerous, thin, well-organized actin filaments. 250 X.



Figure 1. b. One hour after treatment with microcystin-LR at 10.0  $\mu\text{g/ml}$  of medium. Several plasma membrane blebs contain large, thick actin filaments that extend from the bases to the tips of the blebs. 500 X.



- Figure 1. c. Three hours after treatment with microcystin-LR at 10.0  $\mu\text{g/ml}$  of medium. Actin is aggregating beneath the plasma membrane with thickened actin filaments extending out to the tips of the blebs. As the cells undergo blebbing, they round up and appear smaller. 500 X.

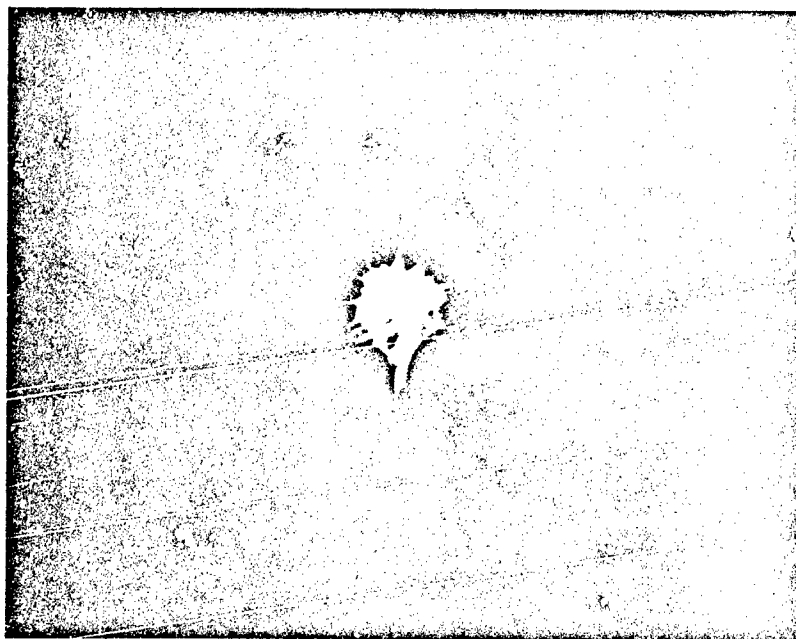


Figure 1. d. Six hours after treatment with microcystin-LR at 10.0  $\mu\text{g/ml}$  of medium. Most of the intracellular actin in each of these hepatocytes has aggregated into a single locus and there is some blebbing of the plasma membranes. 500 X.

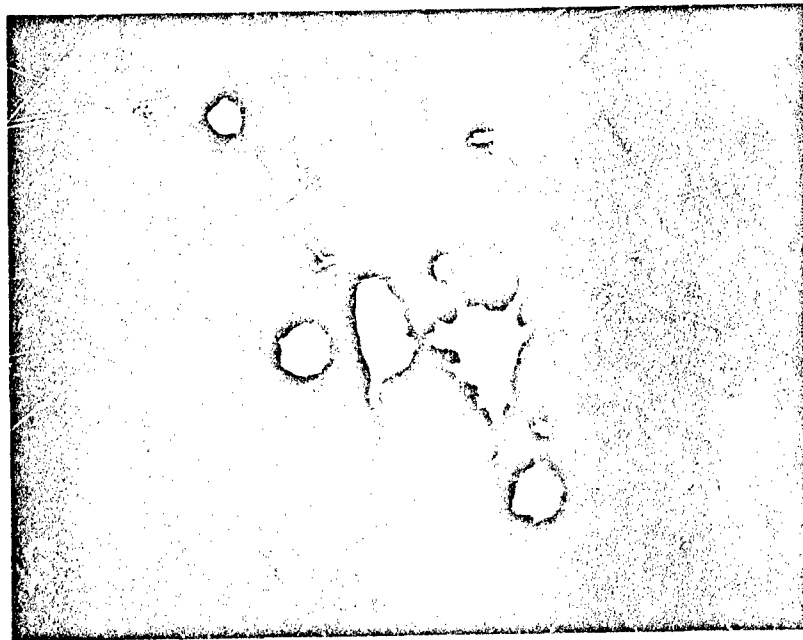




Figure 2. Fluorescent micrographs. Twenty-four-hour cultured hepatocytes 6 hours after treatment. Rhodamine-labeled phalloidin.

- a. Treated with phalloidin at 10.0  $\mu\text{g/ml}$  of medium. In this cell, intracellular actin has aggregated into many, variable-sized foci located throughout the cytoplasm. 500 X.

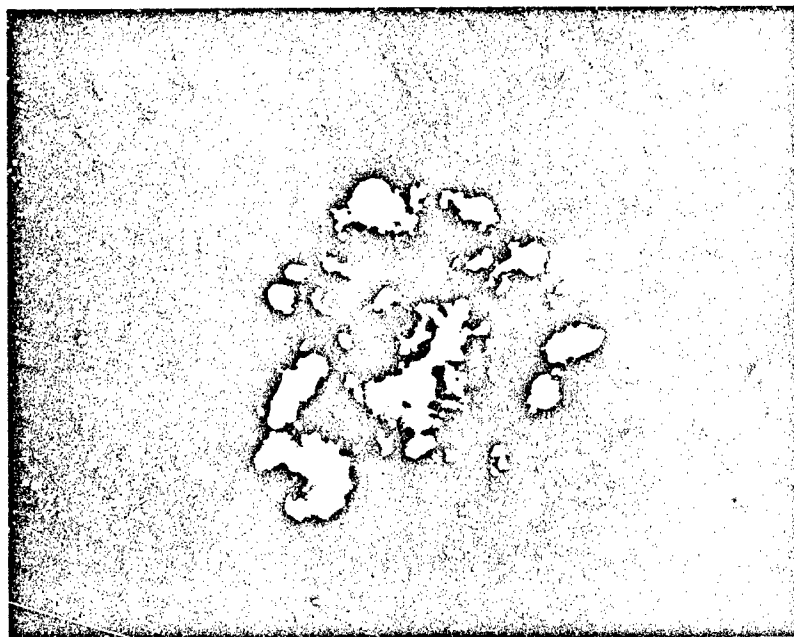


Figure 2. b. Treated with cytochalasin B at 10.0  $\mu\text{g/ml}$  of medium. In this cell, intracellular actin has aggregated into many, small foci located throughout the cytoplasm. 500 X.

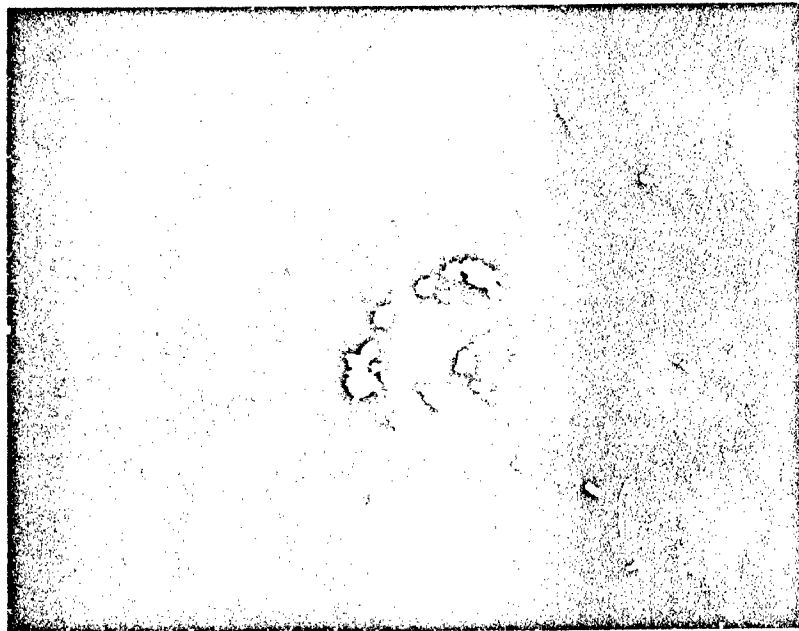


Figure 3. Liver 30 minutes after dosing of a rat with microcystin-LR at 180  $\mu\text{g/kg}$ . There is rounding of hepatocytes and sinusoidal congestion adjacent to the central vein (top right). HE. 500 X.

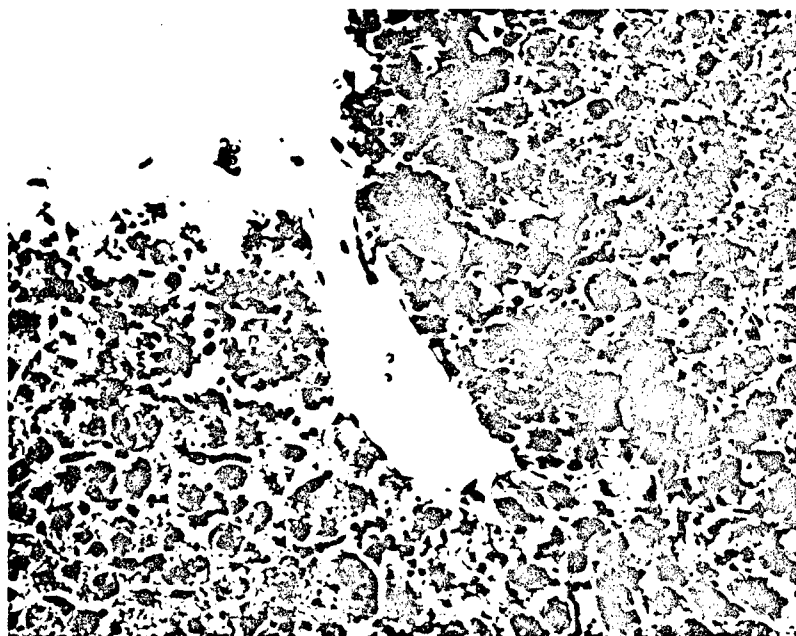


Figure 4. Fluorescent micrographs. Frozen liver sections, rhodamine-labeled phalloidin.

- a. Control, 60 minutes after dosing with phosphate-buffered saline. There is a normal pattern of actin staining at the margins of the hepatocytes as well as randomly distributed stippling. 500 X.



Figure 4. b. Forty-five minutes after dosing with microcystin-LR at 180  $\mu\text{g/kg}$ . Actin within centrilobular (top) and some midzonal hepatocytes is aggregated into variably sized foci. Periportal (bottom) and some midzonal hepatocytes have lost the random actin stippling observed in livers from untreated rats. 500 X.



**VII. MICROCYSTIN-LR TOXICOSIS IN SWINE: HEPATIC AND RENAL  
PERFUSION, HEMODYNAMIC, HEMATOLOGIC, AND SERUM BIOCHEMICAL  
EFFECTS FOLLOWING INTRAVENOUS ADMINISTRATION**

**A. Arginase Activity in Swine: Tissue Distribution, Serum Half-life, and Serum Changes  
after Microcystin-LR Administration**

1. Statement of the Problem, Background, and Rationale

Serum activities of liver specific enzymes are sensitive and reliable indicators of hepatocellular damage and biliary obstruction. However, certain fundamental characteristics of an enzyme must be determined in order for serum enzyme activity to provide insight into the location, duration, severity, and mechanism involved in a particular hepatopathy. The development of analytical techniques for (Mia and Koger, 1978) and studies on arginase activity (ARG) in specific tissues (Cornelius et al., 1963; Porembska et al., 1971; Boyd, 1981) have served to increase its use as an aid in the diagnosis of liver disease in numerous species. In accordance with its liver specificity in ureotelic animals (Greenberg, 1960; Cornelius, 1970), and cytoplasmic location in hepatic parenchymal cells (Skrzypek-Osiecka et al., 1980; Sumitani, 1977), arginase has been shown to be a reliable indicator of hepatic necrosis induced by carbon tetrachloride (CCl<sub>4</sub>) (Cornelius et al., 1963; Cacciatore and Antoniello, 1971; Cargill and Shields, 1971; Mia and Koger, 1978). The present study was undertaken to assess the utility of serum ARG as an indicator of microcystin-LR-induced hepatic damage in swine.

## 2. Experimental Methods

### Animals, Serum, and Tissues for Arginase Determinations

The tissues of six Yorkshire cross-bred pigs (two gilts and four barrows, weighing 80 to 100 kg) were analysed. The four barrows had been subjected to splenectomy, and all six animals had participated in an 8-week-long study addressing immunologic aspects of eperythrozoonosis. Serum biochemistry parameters were not monitored in this earlier trial since no alterations in parameters indicative of hepatic damage were observed in a preliminary study. Halothane<sup>1</sup> (barrows only) and oxytetracycline<sup>2</sup> (two doses at 2.2 mg/kg given intramuscularly 3 weeks apart) were the only known hepatotoxic agents to which these pigs had been exposed in the earlier trial. Swine were fed a standard corn/soybean based diet during the earlier trial and during an acclimation period prior to the present study. Before qualifying for use in the ARG study, each animal was required: a) to have gained more than 40 kg since the start of the previous research trial 58 days earlier, b) to have had no known exposure to any hepatotoxic agent in the past 30 days (over 100 days had elapsed between halothane exposure and the current study), c) to be judged as clinically healthy throughout the earlier formal research trial and the 2-day-long acclimation period prior to the present study, and d) to bear no gross lesions during tissue collection.

---

<sup>1</sup>Halothane USP, Halocarbon Laboratories, Inc., Hackensack, NJ.

<sup>2</sup>Liquamycin, LA-200, Pfizer Inc., New York, NY.

Blood samples were collected from the anterior vena cava, placed on ice, and allowed to clot; serum was harvested following centrifugation at 500 x g for 10 minutes at 4°C. Animals were then killed by captive-bolt stunning followed by exsanguination. Within 40 minutes of death, the following tissues were sealed in plastic bags and placed on ice: liver (cross sections from multiple lobes, excluding the gallbladder), kidneys (cortex, medulla and pelvis), adrenals (entire), pancreas (entire), lung (left diaphragmatic lobe), jejunal mucosa (mid-jejunum), brain (right or left hemisphere, excluding the pituitary), heart (right and left ventricles), salivary glands (parotid and/or maxillary), spleen (two gilts), diaphragm (one barrow), and quadriceps femoris. Tissues were diced into 1 cm cubes, sealed in plastic bags, frozen, and held at -12°C.

#### Tissue Processing and ARG Determination

Within 2 days of collection, the tissue specimens were placed in liquid nitrogen and blended into a fine homogenous powder, resealed in plastic bags, and returned to -12°C storage.

All samples were analyzed for ARG between 12 and 14 days after collection. On the day of analysis, 1.00 g of the frozen tissue powder was placed into a pulverizer, and 9.0 ml of normal saline was added to aid in tissue disruption by manual force using a glass rod. Following disruption of visible tissue structure to remove erythrocytes, nuclei, connective tissue, and residual intact cells, the homogenate was centrifuged for 10 minutes at 500 x g and 4°C. For all tissues except liver, kidney, and pancreas, 20 µl of tissue homogenate supernatant was used in the



arginase analysis. For kidney and pancreas a 1:10 and for liver a 1:50 dilution of the supernatant with normal saline was required to obtain enzyme activity in the dynamic range of our procedure. Reagents were prepared and the assay for ARG activity performed as previously described (Mia and Koger, 1978).

#### Standard Curve

Five standard curves were obtained over 3 days. A linear regression of ornithine concentration versus absorbance provided five estimates of the correlation coefficient, slope and y-intercept. The mean of the five estimates of the slope and y-intercept were an overall estimate of these parameters. The means of the slope and y-intercept were utilized to calculate tissue and serum ARG.

#### Arginase Half-Life Determination

Animals. Three swine (two gilts and one barrow) were purchased from the University of Illinois College of Veterinary Medicine Research Farm (UICVMRF). The animals had been raised under specific-pathogen-free conditions and were fed the same corn/soybean based ration that they had received while at the UICVMRF. Upon arrival, the animals were intramuscularly administered vitamin K<sup>1</sup> at 1.5 mg/kg, vitamin E<sup>4</sup> at 1.1 mg/kg, and selenium<sup>4</sup> at 55 µg/kg.

A liver extract solution was derived from one of the gilts purchased from the UICVMRF. The animal was killed by electrocution and the liver placed on ice within 10 minutes of death and then held at 0 to -5°C for 1 week until the day prior to

---

<sup>3</sup>Veta-K1, Professional Veterinary Laboratories, Minneapolis, MN.

<sup>4</sup>E-SE, Burns-Biotec Laboratories, Inc., Omaha, NB.

dosing. The liver was homogenized after thawing and centrifuged for 30 minutes at 500 x g and 4°C. A portion of the supernatant was diluted 1:120 with normal saline and analyzed for ARG as described above. The diluted liver extract solution had an ARG activity of 145 IU/L.

Animal Dosing. Two 12-week-old Yorkshire cross littermates (a gilt and a barrow) were dosed with the undiluted liver extract. Following a 24-hour fast, ketamine<sup>5</sup> (20 mg/kg, IM) followed by thiamylal<sup>6</sup> (to effect, IV) were administered to induce and maintain anesthesia. A 16-gauge catheter<sup>7</sup> was placed into the anterior vena cava via the external jugular vein. The catheter was capped, filled with heparin,<sup>8</sup> and buried subcutaneously. Following a 6-day recovery period, 3 ml of a 2% lidocaine<sup>9</sup> solution was infiltrated around the buried catheter to facilitate its exteriorization. The pigs were then returned to their stall and their normal daily feeding routine was followed.

At 2 hours after catheter exteriorization, 2 ml/kg of the undiluted liver extract solution (17.55 IU of ARG/ml) was administered IV over a 2.5-minute period to the gilt (32.3 kg) and barrow (33.9 kg). Catheters were flushed with 20 ml of normal saline after the liver extract administration. Blood samples (7 ml) were collected 10

---

<sup>5</sup>Ketaset, Bristol Laboratories, Syracuse, NY.

<sup>6</sup>Biotol, Boehringer Ingelheim Animal Health, Inc., St. Joseph, MO.

<sup>7</sup>Tygon, Norton Company, Akron, OH.

<sup>8</sup>LyphoMed, Lyphomed, Inc., Rosemont, IL.

<sup>9</sup>Butler Lidocaine Injectable, The Butler Company, Columbus, OH.

minutes before and 5, 8, 13, 20, 30, 45, 60, 90, 120, 180, 240, 300, 390, and 480 minutes after dosing. Catheters were flushed with saline following each blood collection. One blood sample was not collected due to a temporary catheter positioning problem. Blood samples were allowed to clot at room temperature for 90 to 120 minutes, followed by centrifugation for 10 minutes at 500 x g and 4°C. Serum was harvested and immediately refrigerated (0 to 5°C), and ARG was determined between 22 to 30 hours after blood collection using the methods described above.

Data Analysis. Linear regression of the natural log of the serum ARG greater than 30 IU/L versus time postdosing with liver extract was used to determine the y-intercept, slope, and correlation coefficient. The serum ARG half-lives ( $t_{1/2}$ ), apparent volumes of distribution ( $V_d$ ), elimination constants ( $k_{el}$ ), and total body clearances ( $Cl_b$ ) were calculated from the intravenous dose ( $D_{iv}$ ) and the slope and y-intercept (inverse ln of y-intercept = concentration at time 0 [ $C_0$ ]) of the regression lines using the following formulae:  $V_d = D_{iv}/C_0$ ; slope =  $-k_{el}$ ;  $t_{1/2} = 0.693/k_{el}$ ; and  $Cl_b = V_d * k_{el}$  [11]. Analysis of covariance was used to determine differences ( $\alpha = 0.05$ ) in slope of the regression lines and a t-test was used to determine differences ( $\alpha = 0.05$ ) in the y-intercepts (Snedecor and Cochran, 1967).

#### Influence of Microcystin-LR on Serum Arginase

Three Yorkshire cross gilts (24.5 to 29.0 kg) were obtained from the UICVMRF. Following a preanesthetic dose of atropine<sup>10</sup> (0.05 mg/kg, SC) and the use of lidocaine<sup>9</sup> to facilitate endotracheal intubation, anesthesia was induced and maintained

---

<sup>10</sup>Atropine Sulfate, Professional Veterinary Laboratories, Minneapolis, MN.

with halothane.<sup>1</sup> Catheters<sup>7</sup> were placed within the anterior vena cava, aorta, left atrium, and pulmonary artery, filled with heparin,<sup>8</sup> and buried subcutaneously. Following a 2- to 3-week recovery period, 2% lidocaine solution<sup>9</sup> was infiltrated around the buried catheters to facilitate their exteriorization. Three hours later,  $\geq 95\%$  pure microcystin-LR (MCLR) initially dissolved in 100% ethanol<sup>11</sup> and diluted with saline<sup>12</sup> (so that the 16 ml of dosing solution consisted of  $\leq 0.1\%$  ethanol in normal saline [v/v]) was given into the pulmonary artery catheter over 1.5 minutes, followed by flushing with 20 ml of normal saline. One gilt was given a sublethal dose (16  $\mu\text{g}$  of MCLR/kg), a second pig was administered a lethal dose (24  $\mu\text{g}$  of MCLR/kg), and a third was given 16 ml of 0.1% ethanol in normal saline and served as a control.

Blood for of serum ARG and aspartate aminotransferase AST activities was collected periodically from the catheter in the anterior vena cava. This catheter was flushed with 10 ml of normal saline after each collection. ARG was determined as described above, and AST activities were determined photometrically by the rate of NADH oxidation.<sup>13</sup>

#### Pathologic Studies

Gilts given MCLR were subjected to necropsy immediately after death or euthanasia (electrocution). Tissues were fixed in 10% neutral buffered formalin, imbedded in paraffin, sectioned at 5  $\mu\text{m}$ , and stained with hematoxylin and eosin.

---

<sup>11</sup>100% Ethanol, US Industrial Chemicals Co., Tuscola, IL.

<sup>12</sup>0.9% Sodium Chloride Injection, USP, Travenol Laboratories, Inc., Deerfield, IL.

<sup>13</sup>Hatachi 705, Boehringer Mannheim Diagnostics, Indianapolis, IN.

### 3. Results

#### Calibration Curve

The mean  $\pm$  SEM of the slope was  $0.190 \pm 0.0065$  absorbance units/50 IU/L (1 mM ornithine/L = 50 IU/L), and the mean  $\pm$  SEM of the y-intercept was  $0.020 \pm 0.014$  absorbance units. Each of the five standard curves had a correlation coefficient greater than 0.996.

#### Arginase Activity of Tissues and Serum

The means, standard errors, and ranges of ARG for the tissues and serum from the six pigs are presented in Table 1.

#### Serum Arginase Half-Life

Both pigs had a predosing serum ARG of 1 IU/L, and each of the animals vomited twice between 3 and 5 minutes of the administration of liver extract. No other adverse effects were observed, and both pigs ate normally later that morning and afternoon. Figure 1 shows the fit of the simple linear regression lines of the natural log of the serum ARG versus time for the gilt and barrow. Predosing serum ARG activity was 578.4 IU/L in the gilt and 855.9 IU/L in the barrow. The serum  $t_{1/2}$ s for ARG were 128.5 and 85.8 minutes for the gilt and barrow, respectively. The slopes and y-intercepts of the regression lines were different between the gilt and barrow; however, there was no apparent difference in clearance of arginase, which depends on both the elimination constant (calculated from the slope) and apparent volume of distribution (calculated from the y-intercept), between the two pigs.

#### Serum ARG and AST Following a Dose of MCLR

Marked increases in serum ARG and AST occurred between 8 and 14 hours after administration of a sublethal dose (16 µg/kg) of MCLR (Figure 2). Maximal values for ARG (250 IU/L) and AST (1969 IU/L) occurred at 14 and 20 hours after dosing, respectively. By 26 hours postdosing, serum ARG had returned to near baseline (8 IU/L) while AST (834 IU/L) was still markedly increased. Following the lethal dose of MCLR (24 µg/kg), serum enzyme activities increased markedly from 120 minutes until death (325 minutes) when ARG reached 1432 IU/L and AST reached 2090 IU/L. Serum ARG and AST of the gilt administered the 0.1% ethanol-normal saline vehicle remained near predose values over the 24-hour period.

#### Histologic Lesions

Lesions in the two MCLR-treated pigs were similar in character but they were more severe in the animal given the lethal dose. Included were diffuse centrilobular hepatocyte disassociation, degeneration, and necrosis with moderate to severe hemorrhage. In the gilt given the lethal dose, hepatocytes were nearly all affected except for a rim of periportal hepatocytes a few cell layers wide. No lesions were seen in the control gilt.

#### 4. Discussion and Conclusion

Serum ARG was found to be stable for at least 1 week when stored at 0 to 5°C and for 3 months at -20°C (Mia and Koger, 1978). The ARG calibration curve prepared from ornithine standards in our studies was in good agreement with previously published results.

A comparison of the tissue ARG activities (Table 1) demonstrates that liver, pancreas, and kidney contain the greatest amount of enzyme per unit of organ weight. Liver ARG is approximately one order of magnitude greater than the pancreas and kidney, two orders of magnitude greater than the salivary glands and jejunal mucosa, and three to four orders of magnitude greater than the other tissues tested. In addition, the relative mass of the liver is quite large compared to that of the pancreas or kidney. Thus, major increases in serum ARG would most likely reflect hepatocellular damage.

The organ distribution of tissue ARG activities in other species is similar to that observed in the swine of this study. In a comparison of ARG activities in the liver and kidney of 10 species, activities in swine were determined to be 44 IU/g and 1.55 IU/g in liver and kidney, respectively (Porembska et al., 1971), which are similar to the ARG values reported here of 34 IU/g of liver and 3.24 IU/g of kidney. The mean serum ARG in the swine measured here (2.58 IU/L) is also close to the 1 IU/L value reported previously for swine (Mia and Koger, 1978) and falls within the range of mean values (0.50 to 21.30 IU/L) reported in other species (Cornelius et al., 1963). Based on this study and the initial serum ARG obtained shortly after arrival from 20 other animals since this study, we consider normal serum ARG in swine to be <10 IU/L.

The serum ARG  $t_{1/2}$ s of 128.5 and 85.8 minutes in the gilt and barrow of this study are similar to the 80-minute half-life reported for a calf (Cornelius et al., 1963). These values are, however, in contrast to the 18-hour half-life of AST reported in

three 10 kg pigs (Massarrat, 1965). The limited apparent volume of distribution in swine (approximately equal to total blood volume) may account in part for the short serum  $t_{1/2}$  of arginase observed in the two swine of the present study.

Serum ARG activities increase in various species as a result of hepatic damage induced by  $\text{CCl}_4$  and/or metabolic changes associated with starvation and corticosteroids (Mia and Koger, 1978; Cornelius et al., 1963; Cacciatore and Antonello, 1971; Cargill and Shields, 1971). For example, serum ARG activities in pigs ranged from 90 to 584 IU/L between 24 and 48 hours following oral administration of  $\text{CCl}_4$  at 0.2 to 3.0 ml/kg body weight (Mia and Koger, 1978), which can be compared to the maximum serum ARG of 250 and 1432 IU/L after administration of a sublethal and lethal IV dose of MCLR, respectively.

Following induction of acute hepatic necrosis by  $\text{CCl}_4$  in dogs, sheep, horses, and calves, ARG increased significantly within hours and then returned to normal or below normal values within 3 to 4 days (Cornelius et al., 1963). Transaminase activities in these species exhibited the same rapid rise but remained elevated for over a week. Although not conclusively demonstrated by the present study, increases in serum ARG activities in swine given MCLR may also have shorter  $t_{1/2}$  than MCLR-induced increases in AST (Figure 2).

Differences in the duration of increased serum activities of transaminase(s) and ARG in dogs, horses, sheep, and cattle are used to distinguish the nature of a hepatic insult and to evaluate the repair process (Cornelius et al., 1963). Considering the short serum  $t_{1/2}$  of ARG, it seems likely that progressive hepatocellular damage would



be necessary to maintain an increase in serum activity for more than 24 hours in swine. When monitored in conjunction with other liver enzymes, the short  $t_{1/2}$  of serum ARG activities in swine is likely to be of value in differentiating progressive versus nonprogressive hepatocellular damage.

Table 1. Means, standard error of the mean (SEM), and range of arginase activities in tissues and serum of swine.

Tissue	Mean (IU/g)	SEM (IU/g)	Range (IU/g)	Number of Animals
Liver	34.01	10.40	13.68 to 74.89	6
Pancreas	5.43	0.91	2.60 to 9.25	6
Kidney	3.25	0.64	1.12 to 5.79	6
Salivary glands	0.52	0.11	0.27 to 0.97	6
Jejunal mucosa	0.47	0.07	0.23 to 0.63	6
Quadriceps	0.10	0.03	0.00 to 0.18	5
Lung	0.03	0.02	0.00 to 0.08	6
Adrenal	0.03	0.02	0.00 to 0.11	6
Spleen	0.03	0.03	0.00 to 0.06	2
Brain	0.01	0.01	0.00 to 0.03	6
Heart	0.01	0.01	0.00 to 0.03	6
Diaphragm	0.03			1
Serum	2.29*	1.05*	0.00 to 5.24*	6

\* = IU/L.

Figure 1. Linear regression of the natural log of serum arginase (ARG) activity as a function of time in a gilt (O---O) and a barrow (•—•) following IV administration of a swine liver extract containing 17,545 IU of ARG/L at 2.0 ml/kg.

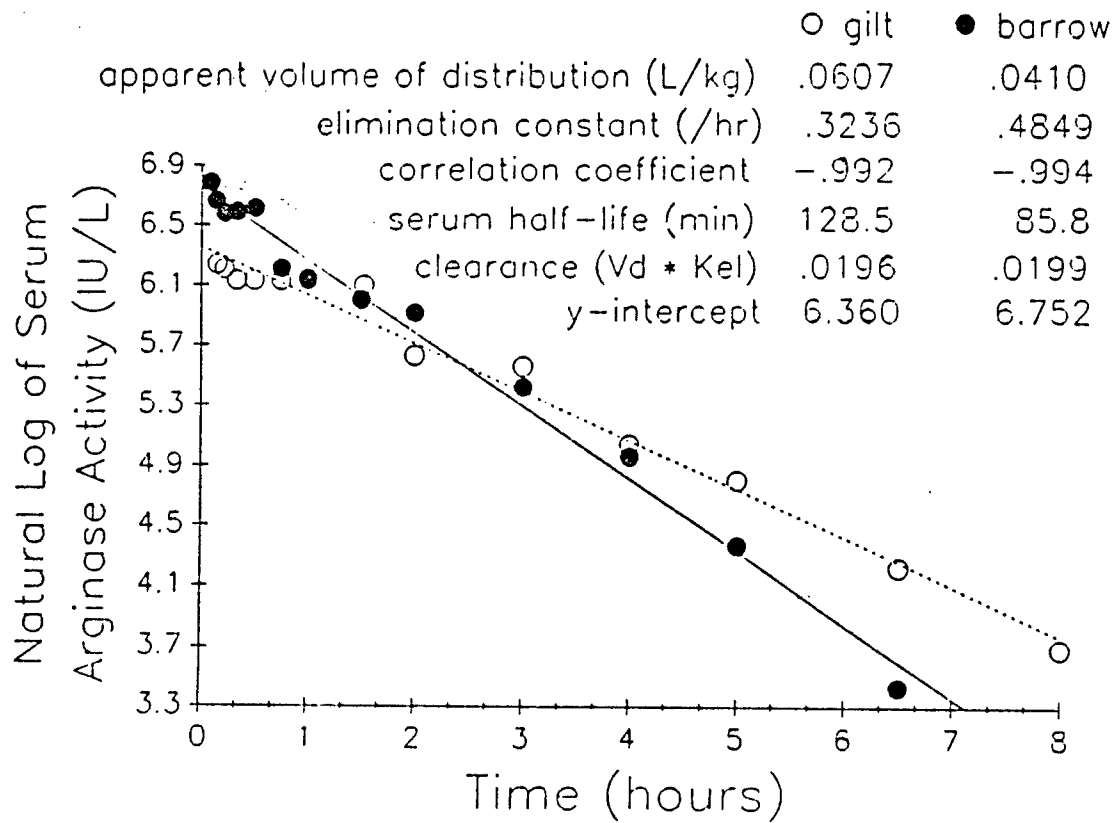
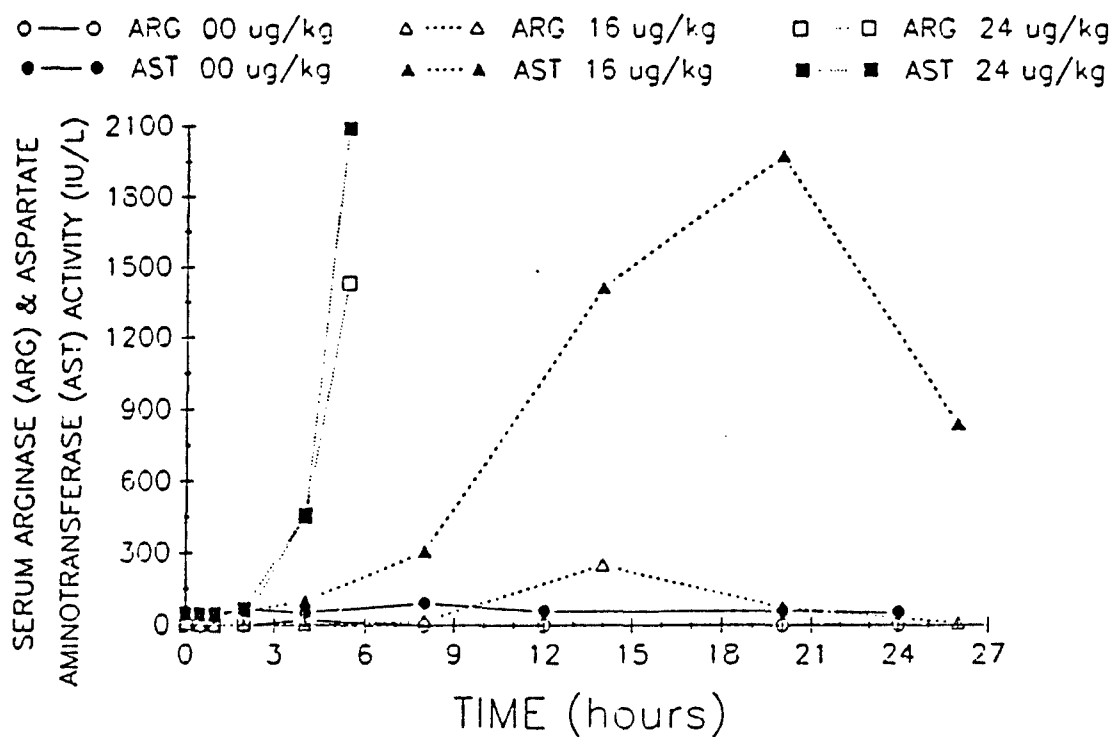


Figure 2. Serum aspartate aminotransferase and arginase activities as a function of time in three gilts dosed intravenously with a toxic-sublethal (16  $\mu\text{g/kg}$ ) or lethal dose (24  $\mu\text{g/kg}$ ) of microcystin-LR or the 0.1% ethanol-saline vehicle.



**B. The Effects of Microcystin-LR on Hemodynamic, Organ Perfusion, Clinical Pathologic, Gross Pathologic, and Blood-Gas Parameters in Swine**

1. Statement of the Problem, Background, and Rationale

Although the cause of acute death following microcystin administration has been attributed to hemorrhagic shock (Ostensvik et al., 1981; Runnegar and Falconer, 1982; Sasner et al., 1984; Theiss and Carmichael, 1986) caused by primary effects of microcystin on the liver, only limited studies involving physiologic measures have been performed. In addition, as mentioned previously, Slatkin et al. (1983) had proposed a theory suggesting that "atypical pulmonary thrombi" lead to pulmonary congestion, right heart failure, and centrilobular hepatic necrosis and hemorrhage in microcystin-dosed animals. The major goals of this study were to characterize the primary cause(s) of death following MCLR administration in swine and to identify processes which differentiate lethal from sublethal toxicoses. To address these goals, a comprehensive battery of assays to determine changes in hemodynamic function, liver and kidney perfusion, and hematologic, blood gas, and serum biochemical values, as well as the development of grossly evident lesions was undertaken.

2. Experimental Methods

Animals

Crossbred gilts (16 to 25 kg), raised under specific pathogen free conditions, were purchased from the University of Illinois, College of Veterinary Medicine Research Farm (UICVMRF), and housed in the College of Veterinary Medicine Laboratory Animal Care Facilities. Upon arrival, blood was drawn from the vena

cava to establish complete blood count and serum biochemistry values; and vitamin K<sup>1</sup> (1.5 mg/kg), vitamin E<sup>2</sup> (1.5 IU/kg), and sodium selenite<sup>2</sup> (55 µg Se/kg) were administered intramuscularly. Gilts were fed a corn- and soybean-based ration, and water was provided ad libitum during the 2- to 7-day acclimation period. Twenty-four hours prior to surgery all feed was removed from the stall.

### Anesthesia

Alpha-chloralose<sup>3</sup> (50 mg/kg; 1% in physiologic saline<sup>4</sup>) followed immediately by ketamine<sup>5</sup> (20 mg/kg; 10% solution) were administered via an ear vein catheter to induce anesthesia. Gilts were then endotracheally intubated after spraying the larynx with 0.75 ml of 2% lidocaine<sup>6</sup> and placed in left lateral recumbency. Anesthesia was maintained by IV supplements of ketamine and α-chloralose during surgical procedures. Anesthesia was later maintained by IV supplements of α-chloralose during the data collection stage which followed. Gilts were required to breathe on their own during the entire data collection period (from 30 to 45 minutes prior to dosing until 5 hours postdosing or death).

---

<sup>1</sup>Veta-K1, Professional Veterinary Laboratories, Minneapolis, MN.

<sup>2</sup>E-SE, Burns-Biotec Laboratories, Inc., Omaha, NB.

<sup>3</sup>α-chloralose No. C-0128, Sigma Chemical Company, St. Louis, MO.

<sup>4</sup>0.9% Sodium Chloride Injection, USP, Travenol Laboratories, Inc., Deerfield, IL.

<sup>5</sup>Ketaset, Bristol Laboratories, Syracuse, NY.

<sup>6</sup>Butler Lidocaine Injectable, The Butler Co., Columbus, OH.

### Surgery and Instrumentation

Incisions in the right jugular furrow and right paracostal-paralumbal area were made with an electrocautery unit,<sup>7</sup> and 16-gauge non-compliant catheters<sup>8</sup> were placed in the cranial vena cava via the external jugular vein and the ascending aorta via the carotid artery. An 18-gauge non-compliant catheter<sup>8</sup> was placed in the portal vein via the mesenteric vein draining the terminal jejunum. Five to eight temperature pulse decay (TPD) probes were inserted into the diaphragmatic surface of the right lateral and medial lobes of the liver. Four to five TPD probes were inserted into the cortex of the right kidney. One ml of heparin<sup>9</sup> (1,000 IU) was sprayed around the TPD probe wires to aid in their removal at the conclusion of the study.

### Toxin Administration

The appropriate doses (toxic-sublethal dose group = 25 µg/kg [n = 6], lethal dose group = 72 µg/kg [n = 6], or control group = 0 µg/kg [n = 4]) of > 95% pure MCLR in 15 ml of physiologic saline<sup>4</sup> were prepared. The dosing solution was placed in a 40°C water bath to warm it to body temperature prior to its administration over 90 seconds via the cranial vena cava followed by 10 ml of warmed, heparinized Ringer's solution.<sup>10</sup>

---

<sup>7</sup>Cameron-Miller Model 265, Cameron-Miller Surgical Instruments Co., Chicago, IL.

<sup>8</sup>Tygon, Norton Co., Akron, OH.

<sup>9</sup>Lyphomed, Lyphomed, Inc., Rosemont, IL.

<sup>10</sup>Ringer's Injection, USP, Abbott Laboratories, North Chicago, IL.

Hematologic, Serum Biochemistry, and Blood Gas Measurements

Arterial blood samples were collected 5 to 15 minutes prior to MCLR dosing and 45, 90, 150, 210, and 300 minutes postdosing and/or immediately prior to death so that complete blood counts (3 ml) (includes red [RBC] and white [WBC] blood cell counts, differential white blood cell counts, platelet counts, hemoglobin and hematocrit), serum biochemistry profiles (10 ml) (includes creatinine [CRE], urea nitrogen [UN], total protein [TP], albumin, calcium, phosphorus [P], sodium, potassium, chloride [Cl], magnesium [Mg], glucose, cholesterol, total bilirubin [TB], alanine aminotransferase [ALT], aspartate aminotransferase [AST], alkaline phosphatase [AP], gamma glutamyl transferase [GGT], lactate dehydrogenase [LDH], creatinine phosphokinase [CPK];<sup>11</sup> arginase [ARG; Mia and Koger, 1978]; and bile acids),<sup>12</sup> blood gases and electrolytes (3 ml; anaerobically collected) (includes pH, pCO<sub>2</sub>, total CO<sub>2</sub>, pO<sub>2</sub>, O<sub>2</sub> saturation, O<sub>2</sub> content, base excess base [BE<sub>B</sub>], base excess extracellular fluid [BE<sub>ECF</sub>], standardized bicarbonate [SBC], bicarbonate [HCO<sub>3</sub><sup>-</sup>], hematocrit [Hct], hemoglobin [Hb], sodium [Na], potassium [K], ionized calcium [iCa], and normalized calcium [nCa]),<sup>13</sup> and blood lactate concentrations<sup>14</sup> (1 ml) could be followed over time. The aortic catheter was flushed as above between blood samples, and all catheters were periodically flushed to maintain patency.

---

<sup>11</sup>Hitachi 705, Boehringer Mannheim Diagnostics, Indianapolis, IN.

<sup>12</sup>Enzabale, NYCOMED AS Diagnostics, Oslo, Norway.

<sup>13</sup>Stat Profile 1 Analyzer, Nova Biomedical, Newton, MA.

<sup>14</sup>Lactate Procedure No. 826-UV, Sigma Diagnostics, St. Louis, MO.



### Hemodynamic and Organ Perfusion Measurements

Hemodynamic pressure signals were obtained using a pressure transducer,<sup>15</sup> recorded on a polygraph,<sup>16</sup> and logged on a hemodynamic analyzer.<sup>17</sup> Mean aortic, central venous, and portal venous pressures were determined predosing and every 20 seconds throughout the study. Perfusion of the liver and kidney was measured by the temperature pulse decay (TPD) system (Arkin et al., 1986,1987) every 3 minutes from 30 minutes predosing until 120 minutes postdosing and every 6 minutes from 120 to 300 minutes postdosing.

### Postmortem Observations

Gilts still alive 5 hours after dosing were killed by exsanguination. A complete gross examination was performed on all gilts. The liver, kidneys, adrenals, and spleen were removed and weighed. The gallbladder was considered part of the liver weight. Portions of the liver were held at -5°C for subsequent iron analysis as previously described (Osheim and Ross, 1985) using atomic absorption spectrophotometry and for liver hemoglobin<sup>18</sup> determinations.

### Statistical Analysis

Before statistical analysis was performed on the hemodynamic and organ perfusion parameters, 6-minute means were obtained from 30 minutes predosing to 60

---

<sup>15</sup>Model P23ID, Gould-Statham, Oxnard, CA.

<sup>16</sup>Model 5/6 H Recorder, Gilson Medical Electronics, Middleton, WI.

<sup>17</sup>Buxco Hemodynamics Analyzer, Buxco Electronics, Inc., Sharon, CT.

<sup>18</sup>DMA Cyanomethemoglobin Procedure, Data Medical Associates, Inc., Arlington, TX.

minutes postdosing and 12-minute means were taken from 60 minutes postdosing until 300 minutes postdosing (or death). The mean of the 6- or 12-minute organ perfusion data as measured using two to four TPD probes in the liver and one to three TPD probes in the kidney were used in the statistical analysis. Each animal served as its own control and the overall predosing mean was subtracted from each postdosing time point.

A nested analysis of variance patterned on a univariate repeated measures analysis (Wilkinson, 1988) was used to identify significant differences ( $\alpha = 0.05$ ) due to treatment, time, or treatment\*time interaction for the hematology, blood-gas, clinical biochemistry, hemodynamic, and organ perfusion data. Prior to statistical analysis, all postdosing values (except electrolytes) were subtracted from the predose mean of that animal. The model used was: corrected response (corresp) = constant + treatment (trt) + subjects in control group (sub1) + subjects in toxic-sublethal dose group (sub2) + subjects in lethal dose group (sub3) + time + trt\*time. Corresp, trt, sub(1 to 3), time, and trt\*time represented the corrected response (postdosing value minus mean predose value), the treatment, the subjects within each treatment, the time after MCLR administration, and the treatment\*time interaction, respectively. Since the major component of any change in the electrolyte data occurred terminally, the electrolyte data was analyzed using both the untransformed data (response replaces corresp in the above model) and the transformed data. Analysis of the untransformed data was chosen because it provided a more conservative estimate of electrolyte changes. The number of surviving animals in the lethal dose group decreased with

time which prevented some uses of the repeated measures analysis. Data from terminal blood samples in the lethal dose group (collected at 57, 60, 85, 138, and 178 minutes, respectively) were analyzed as though they were taken at the next scheduled time point (90, 90, 90, 150, and 210 minutes) for the clinical pathology and blood gas parameters.

Comparisons between treatment groups at postdosing time points were performed using linear contrasts at a level of  $\alpha = 0.05$  (Wilkinson, 1988), except at time points where only one pig was alive in the lethal dose group. These included the 300-minute time point for blood-gas and clinical pathology parameters and the 186-, 198-, 210-, 222-, 236-, 248-, 260-, 272-, 284-, and 294-minute time points for hemodynamic and organ perfusion parameters. The denominator of the F statistic in these contrasts was the error (time) term in the nested ANOVA analysis. At time points where only one pig was alive in the lethal dose group, one-way analyses of variance (Wilkinson, 1988) were used to compare the lethal dose group and the other two groups. Due to the small sample size and a desire to increase power,  $\alpha$  was set at 0.15 in these analyses. A one-way analysis of variance (Wilkinson, 1988) was used to identify statistically significant ( $\alpha = 0.05$ ) differences between treatment groups for organ weights (% live body weight), and liver iron and hemoglobin concentrations.

### 3. Results

#### Hemodynamic and Organ Perfusion Effects

At 15 minutes (12- to 18-minute mean) after MCLR administration, mean central venous pressures (CVP; Figure 1) and mean hepatic perfusions (Figure 2) in pigs of

the lethal dose group were significantly less than in controls. At 21 minutes, mean renal perfusion (Figure 3) and mean aortic pressure (AOM; Figure 4) were significantly decreased, while mean portal venous pressure (PVP; Figure 5) was significantly increased in the lethal dose group when compared to controls. The three pigs in the lethal group with the highest predosing portal venous pressures had the largest increases in portal venous pressure and the shortest survival times.

The CVP, hepatic perfusion, renal perfusion, and AOM of the lethal dose group were decreased significantly as compared to the toxic-sublethal dose group at 15, 15, 21, and 33 minutes, respectively. The PVP of the lethal dose group was significantly increased as compared to the toxic-sublethal dose group at 21 minutes. From 180 to 300 minutes, the PVPs of the toxic-sublethal and lethal dose groups were not significantly different from one another.

Changes in the hemodynamic and organ perfusion parameters of the toxic-sublethal dose group occurred in the same direction as in the lethal dose group, but except the AOM (15 minutes), significant differences from controls (liver perfusion = 39 minutes, renal perfusion = 51 minutes, CVP = 57 minutes, and PVP = 162 minutes) took longer to become established and overall changes were not of as great a magnitude. The AOM of the toxic-sublethal dose group was not significantly different from that of the control group during the last hour of the study.

#### Effects on Hematologic, Serum Biochemistry, and Blood Gas Parameters

Clinical biochemistry, blood-gas, and complete blood count parameters (Table 1) in the lethal dose group which were significantly different from the control group

by 45 minutes included: a) lactate (Figure 6), bile acids (Figure 7), K (Figure 8),  $pO_2$  (Figure 9),  $O_2$  saturation, and TB (all increased); and b) Hct, platelet count (Figure 10),  $HCO_3^-$ ,  $pCO_2$  (Figure 11), and  $BE_b$  (all decreased). By 90 minutes, significant increases in lethal dose group versus control were noted in ARG (Figure 12), UN, P, and CRE; and significant decreases were noted in glucose (Figure 13) and pH (Figure 14). At 150 minutes, ALT, AST (Figure 15), ALP, LDH, and CPK (Figure 16) were significantly increased when the lethal dose group was compared with controls.

At 150 minutes, as compared to controls, the toxic-sublethal group had significantly higher serum bile acid concentrations and significantly lower platelet counts. Significant decreases (lethal dose group versus control dose groups) were observed in serum Hb, SBC,  $BE_{ECF}$  at the five postdosing time points (except serum Hb at 300 minutes).

#### Gross Lesions

The livers of the lethal dose group were markedly swollen, dark red-purple, and readily exuded blood on cut surface. There was severe edema of the gall bladder, marked accumulations of straw-brown colored peritoneal fluid, slight to moderate subendocardial hemorrhage, and a pale carcass. The livers in the toxic-sublethal dose group varied from slightly mottled to dark red and exuded blood on cut surface. Slight to moderate edema of the gall bladder and increased peritoneal fluid was present in the three pigs of this group with the most notable hepatic lesions. No compound-related lesions were evident in the control group.

Significant increases in liver weight, liver iron, and liver hemoglobin were present in the lethal dose group as compared to the toxic-sublethal dose or control groups. The kidney weights of the toxic-sublethal dose group were significantly higher than the lethal dose group and nearly significantly greater than in the control group ( $p = 0.051$ ; Table 2). No differences in spleen or adrenal weights were detected among the groups.

#### 4. Discussion and Conclusion

Three groups (Ostensvik et al., 1981; Berg and Soli, 1985; Theiss and Carmichael, 1986) have measured aortic blood pressure and found that aortic blood pressures steadily declined to values which were less than 50% of predosing values, often by 45 to 60 minutes postdosing. Our findings concerning a fall in aortic blood pressure are in close agreement with these studies using rats, except with the pig the decrease was often more precipitous. Despite these changes, Theiss and Carmichael (1986) found no significant effects on either jugular or portal venous pressures during the course of their study with rats. In the swine of this study, however, the concomitant decrease in central venous pressure and increase in portal venous pressure indicate that partial blockage of blood flow through the liver. Although our central and portal venous pressure findings differ from those of Theiss and Carmichael (1986) and may be due to differences in species, dose, anesthetics, and survival time, the data of neither study is compatible with a backup of pressure from a failing heart (Fox, 1986; Bonagura and Hamlin, 1986) or pulmonary thrombosis as the cause of the hepatic lesions as suggested by Slatkin et al. (1983). Moreover, in preliminary studies

with pigs given MCLR, we measured pulmonary artery pressure and detected no consistent trend indicative of increased pressure. Rather, the findings of all our studies indicate that there is a partial obstruction of blood flow from the liver to the caudal vena cava in swine administered a lethal dose.

No previous studies were found where blood-gas parameters or organ perfusion were measured following microcystin administration. Our findings indicate that the lungs are functioning properly since the lethal dose group had the highest arterial  $pO_2$  and lowest  $pCO_2$  after dosing. Tachypnea observed in the lethal dose group was likely to have been in response to metabolic acidosis (decreased pH,  $HCO_3^-$ , and  $BE_B$ , and increased lactate) and a marked fall in AOM (Brobst, 1983).

Organ perfusion was one of the first parameters affected by MCLR administration. Hepatic perfusion decreased more rapidly than renal perfusion in both the lethal and toxic-sublethal groups, providing additional support for a primary effects of MCLR on the liver. Perfusion to these vital organs did not return to near predose levels for 5 hours postdosing in either the lethal and toxic-sublethal dose groups. The fact that the liver and kidneys are deprived of normal perfusion following a lethal or toxic-sublethal dose of MCLR suggests that hypoxic changes are likely to interact with other toxin-induced processes in these organs.

Serum bile acid concentration was the clinical pathologic parameter in MCLR-dosed swine which provided the most marked, early indication of acute hepatic damage/dysfunction. Bile acids were increased 40X by 45 minutes and 15X by 150 minutes in the lethal and toxic-sublethal dose groups, respectively. Significant

increases in liver-related enzymes (ARG, AST, LDH, AP) in the serum required 90 to 150 minutes to occur, which suggests that hepatocyte membrane disruption occurs after the onset of inadequate liver perfusion. The longer the survival time in the swine of this study, the greater was the magnitude of increase in serum activities of enzymes potentially released from the liver and muscle (AST and LDH) as well as the mild increase in one considered to be muscle specific (CPK). These results suggest that muscle damage as well as liver damage is contributing to the increases in AST and LDH (Duncan and Prasse, 1977). Also, the longer the survival time in pigs of this study, the greater was the decrease in glucose concentrations, and the lesser the decrease in hematocrit. It seems likely that liver dysfunction in the face of continued glucose utilization would account for the trend in serum glucose. Significant decreases in hematocrit and platelet counts and increases in lactate occurred by 45 minutes postdosing in the lethal group and are consistent with hemorrhage and shock. Less severe hemorrhage may account for the lesser reduction in hematocrit and longer survival in individual pigs of the lethal dose group.

Reduced renal perfusion and mild renal damage are the most likely causes of the significant increases in BUN, CRE, and PHOS. Tubular nephrosis has been reported previously in several species exposed to algal peptide hepatotoxins (Ashworth and Mason, 1946; Louw & Smit, 1950; Konst et al., 1965; Edler et al., 1985; Hooser et al., 1989a; Lovell et al., 1989) and is likely secondary to hypoxia and hepatic emboli, although direct effects of microcystin cannot be ruled out. Metabolic acidosis resulting in the exchange of extracellular hydrogen ions for intracellular K, the



reduced ability of the kidney to excrete hydrogen ions, and hepatocyte leakage probably account for the terminal hyperkalemia (Brobst, 1983; Duncan and Prasse, 1977).

Gross lesions in the livers of the pigs in this study were similar to those previously described in other species. Histologic findings typically include centrilobular to panlobular hemorrhage and hepatocyte necrosis, which would probably account for the increase in mean portal venous pressure and contribute to the decline in mean central venous and aortic pressures.

Gross evidence of extrahepatic hemorrhage and enteritis was not observed in pigs in this study. This lack of agreement with some field reports might be explained by differences between iv dosing with purified toxin and ingestion of intact algal cells, the cell walls of which would contain lipopolysaccharides, the time courses of the toxicoses, and/or the animal species involved.

Marked increases in liver weight ( $\geq 8\%$  of total body weight) in mice following parenteral microcystin administration is well documented and is one of the major criteria used in the bioassay of potentially hepatotoxic cyanobacterial blooms (Beasley et al., 1989). Increases in hepatic volume and hemoglobin concentration have lead investigators to estimate that 36% of the estimated blood volume is present in the liver within 3 hours in mice that die following microcystin exposure (Sasner et al., 1984). Using an estimated blood volume for pigs of 8.23% (Bossone and Hannon, 1985) and assuming that this blood contains 11 g Hb/dL, then after accounting for normal liver blood volume (control group), the mean blood volume lost into the livers of the pigs

in the lethal group was 37.9%. This conclusion is based on the following computation:

$$\frac{([4.40\% * 9.19 \text{ g Hb/dL}] - [2.43\% * 2.53 \text{ g Hb/dL}])}{[8.23\% * 11 \text{ g Hb/dL}]} * 100 = 37.9\%$$

The 4.40% and 2.43% represent the mean liver weight (% live body weight) in the lethal dose and control groups; and the 9.19 and 2.53 g Hb/dL represent the mean concentration of hemoglobin in the livers of the lethal and control groups. The acute loss of 25 to 30% of the estimated blood volume has been shown to lead to death in 50% of animals experiencing rapid hemorrhage (Phyllis, 1976).

In conclusion, the hemodynamic, organ perfusion, blood-gas, clinical pathology, and gross pathologic findings of the present study indicate that the liver is the target organ for MCLR. Acute death is caused by hypovolemic shock that results from partial blockage of blood flow through the liver and accumulation of approximately 38% of the estimated blood volume in the liver.

Table 1. Changes in selected clinical pathologic, blood-gas, and complete blood count parameters which had significant ( $p \leq 0.05$ ) treatment or treatment\*time effects.

Parameter	P Values	TRT GRP	Predose Mean $\pm$ SEM	Change from Predose Values				
				45 minutes Mean $\pm$ SEM	90 minutes Mean $\pm$ SEM	150 minutes Mean $\pm$ SEM	210 minutes Mean $\pm$ SEM	300 minutes Mean $\pm$ SEM
Alanine Amino- trans- ferase (IU/L)	trt < 0.001	VEH	26 $\pm$ 4.3	1 $\pm$ 1.7 <sup>a</sup>	2 $\pm$ 1.7 <sup>a</sup>	-3 $\pm$ 2.1 <sup>a</sup>	3 $\pm$ 1.2 <sup>a</sup>	-1 $\pm$ 1.5 <sup>a</sup>
	time < 0.001	TOX	25 $\pm$ 4.6	1 $\pm$ 1.8 <sup>a</sup>	4 $\pm$ 1.8 <sup>a</sup>	11 $\pm$ 6.2 <sup>b</sup>	16 $\pm$ 7.4 <sup>b</sup>	25 $\pm$ 8.2 <sup>b</sup>
	trt*time < 0.001	LET	39 $\pm$ 4.5	1 $\pm$ 1.2 <sup>a</sup>	12 $\pm$ 5.9 <sup>a</sup>	75 $\pm$ 4.7 <sup>c</sup>	120 $\pm$ 31.0 <sup>c</sup>	104 <sup>c</sup>
Alkaline Phospha- tase (IU/L)	trt = 0.043	VEH	274 $\pm$ 44.0	9 $\pm$ 7.6 <sup>a</sup>	26 $\pm$ 14.8 <sup>a</sup>	-6 $\pm$ 17.4 <sup>a</sup>	18 $\pm$ 24.6 <sup>a</sup>	14 $\pm$ 11.3 <sup>a</sup>
	time < 0.001	TOX	383 $\pm$ 34.8	29 $\pm$ 8.3 <sup>a</sup>	81 $\pm$ 30.1 <sup>a</sup>	79 $\pm$ 59.8 <sup>b</sup>	103 $\pm$ 57.0 <sup>b</sup>	180 $\pm$ 65.2 <sup>b</sup>
	trt*time = 0.032	LET	358 $\pm$ 42.5	39 $\pm$ 12.4 <sup>a</sup>	89 $\pm$ 17.0 <sup>a</sup>	147 $\pm$ 14.2 <sup>b</sup>	190 $\pm$ 5.0 <sup>b</sup>	328 <sup>b</sup>
Arginase (IU/L)	trt = 0.059	VEH	0 $\pm$ 0.0	0 $\pm$ 0.0 <sup>a</sup>	1 $\pm$ 0.8 <sup>a</sup>	2 $\pm$ 1.2 <sup>a</sup>	3 $\pm$ 2.0 <sup>a</sup>	3 $\pm$ 1.1 <sup>a</sup>
	time = 0.014	TOX	1 $\pm$ 1.2	-0 $\pm$ 1.6 <sup>a</sup>	3 $\pm$ 3.3 <sup>a</sup>	26 $\pm$ 24.9 <sup>a</sup>	30 $\pm$ 21.9 <sup>a</sup>	36 $\pm$ 23.2 <sup>b</sup>
	trt*time = 0.036	LET	0 $\pm$ 0.0	24 $\pm$ 15.7 <sup>a</sup>	92 $\pm$ 28.1 <sup>b</sup>	103 $\pm$ 27.1 <sup>b</sup>	35 $\pm$ 10.0 <sup>a</sup>	75 <sup>b</sup>
Bile Acids ( $\mu$ m/L)	trt = 0.064	VEH	5 $\pm$ 2.8	4 $\pm$ 2.4 <sup>a</sup>	10 $\pm$ 9.2 <sup>a</sup>	11 $\pm$ 12.0 <sup>a</sup>	4 $\pm$ 4.4 <sup>a</sup>	7 $\pm$ 7.6 <sup>a</sup>
	time < 0.001	TOX	4 $\pm$ 1.8	15 $\pm$ 2.5 <sup>a</sup>	32 $\pm$ 8.1 <sup>a</sup>	61 $\pm$ 16.9 <sup>b</sup>	60 $\pm$ 19.4 <sup>b</sup>	82 $\pm$ 28.7 <sup>b</sup>
	trt*time = 0.041	LET	3 $\pm$ 2.3	120 $\pm$ 82.7 <sup>b</sup>	162 $\pm$ 65.4 <sup>b</sup>	150 $\pm$ 42.8 <sup>c</sup>	179 $\pm$ 19.5 <sup>c</sup>	218 <sup>c</sup>
Total Bilirubin (mg/dl)	trt < 0.001	VEH	0.5 $\pm$ 0.18	0.0 $\pm$ 0.07 <sup>a</sup>	0.0 $\pm$ 0.09 <sup>a</sup>	0.0 $\pm$ 0.07 <sup>a</sup>	-0.0 $\pm$ 0.05 <sup>a</sup>	-0.2 $\pm$ 0.09 <sup>a</sup>
	time = 0.001	TOX	0.4 $\pm$ 0.07	0.1 $\pm$ 0.06 <sup>ab</sup>	0.2 $\pm$ 0.06 <sup>a</sup>	0.2 $\pm$ 0.09 <sup>a</sup>	0.2 $\pm$ 0.10 <sup>b</sup>	0.3 $\pm$ 0.12 <sup>b</sup>
	trt*time < 0.001	LET	0.3 $\pm$ 0.07	0.2 $\pm$ 0.05 <sup>b</sup>	0.4 $\pm$ 0.05 <sup>b</sup>	0.6 $\pm$ 0.07 <sup>b</sup>	0.8 $\pm$ 0.10 <sup>c</sup>	0.9 <sup>c</sup>

Parameter	P Values	TRT GRP	Predose Mean $\pm$ SEM	Change from Predose Values					
				45 minutes Mean $\pm$ SEM	90 minutes Mean $\pm$ SEM	150 minutes Mean $\pm$ SEM	210 minutes Mean $\pm$ SEM	300 minutes Mean $\pm$ SEM	
Aspartate Amino-transferase (IU/L)	trt < 0.001	VEH	40 $\pm$ 10.1	10 $\pm$ 4.0 <sup>a</sup>	18 $\pm$ 6.1 <sup>a</sup>	20 $\pm$ 9.0 <sup>a</sup>	29 $\pm$ 9.1 <sup>a</sup>	37 $\pm$ 13.9 <sup>a</sup>	
	time < 0.001	TOX	41 $\pm$ 8.5	6 $\pm$ 2.8 <sup>c</sup>	50 $\pm$ 22.0 <sup>a</sup>	212 $\pm$ 110 <sup>a</sup>	343 $\pm$ 156 <sup>b</sup>	541 $\pm$ 222 <sup>b</sup>	
	trt*time < 0.001	LET	47 $\pm$ 1.5	53 $\pm$ 24.7 <sup>a</sup>	283 $\pm$ 64.1 <sup>a</sup>	2217 $\pm$ 429 <sup>b</sup>	3065 $\pm$ 234 <sup>c</sup>	4034 <sup>c</sup>	
Lactate Dehydrogenase (IU/L)	trt < 0.001	VEH	446 $\pm$ 63.6	34 $\pm$ 15.4 <sup>a</sup>	54 $\pm$ 25.5 <sup>a</sup>	2 $\pm$ 38.5 <sup>a</sup>	56 $\pm$ 36.2 <sup>a</sup>	55 $\pm$ 48.9 <sup>a</sup>	
	time < 0.001	TOX	460 $\pm$ 68.4	-10 $\pm$ 27.3 <sup>a</sup>	110 $\pm$ 55.6 <sup>a</sup>	248 $\pm$ 125 <sup>a</sup>	367 $\pm$ 216 <sup>a</sup>	628 $\pm$ 350 <sup>b</sup>	
	trt*time < 0.001	LET	460 $\pm$ 68.4	95 $\pm$ 72.9 <sup>a</sup>	282 $\pm$ 85.4 <sup>a</sup>	2136 $\pm$ 360 <sup>b</sup>	2777 $\pm$ 457 <sup>b</sup>	4038 <sup>c</sup>	
Creatinine Phosphokinase (IU/L)	trt = 0.196	VEH	1207 $\pm$ 209	408 $\pm$ 124 <sup>a</sup>	658 $\pm$ 243 <sup>a</sup>	593 $\pm$ 363 <sup>a</sup>	867 $\pm$ 390 <sup>a</sup>	804 $\pm$ 333 <sup>a</sup>	
	time < 0.001	TOX	1466 $\pm$ 307	292 $\pm$ 55 <sup>a</sup>	670 $\pm$ 237 <sup>a</sup>	757 $\pm$ 406 <sup>a</sup>	1196 $\pm$ 403 <sup>a</sup>	2020 $\pm$ 542 <sup>b</sup>	
	trt*time = 0.002	LET	1873 $\pm$ 166	437 $\pm$ 189 <sup>a</sup>	735 $\pm$ 313 <sup>a</sup>	1205 $\pm$ 39 <sup>b</sup>	2256 $\pm$ 333 <sup>b</sup>	3189 <sup>b</sup>	
Glucose (mg/dl)	trt = 0.002	VEH	77 $\pm$ 11.2	0 $\pm$ 3.4 <sup>a</sup>	-1 $\pm$ 8.4 <sup>a</sup>	-2 $\pm$ 11.7 <sup>a</sup>	13 $\pm$ 6.6 <sup>a</sup>	14 $\pm$ 4.5 <sup>a</sup>	
	time = 0.325	TOX	91 $\pm$ 10.6	8 $\pm$ 10.9 <sup>a</sup>	8 $\pm$ 10.2 <sup>a</sup>	10 $\pm$ 8.0 <sup>a</sup>	2 $\pm$ 9.1 <sup>a</sup>	12 $\pm$ 13.3 <sup>a</sup>	
	trt*time = 0.095	LET	98 $\pm$ 11.0	-12 $\pm$ 12.5 <sup>a</sup>	-39 $\pm$ 13.2 <sup>b</sup>	-36 $\pm$ 10.1 <sup>b</sup>	-44 $\pm$ 2.5 <sup>b</sup>	-74 <sup>b</sup>	
Lactate (mg/dl)	trt < 0.001	VEH	8.4 $\pm$ 0.40	1.2 $\pm$ 0.76 <sup>a</sup>	3.2 $\pm$ 1.53 <sup>a</sup>	2.7 $\pm$ 1.36 <sup>a</sup>	1.1 $\pm$ 0.45 <sup>a</sup>	0.3 $\pm$ 0.44 <sup>a</sup>	
	time < 0.001	TOX	10.7 $\pm$ 1.03	0.6 $\pm$ 1.40 <sup>a</sup>	2.7 $\pm$ 1.33 <sup>a</sup>	6.9 $\pm$ 1.84 <sup>a</sup>	14.3 $\pm$ 4.53 <sup>a</sup>	20.9 $\pm$ 6.95 <sup>b</sup>	
	trt*time < 0.001	LET	9.0 $\pm$ 0.86	25.9 $\pm$ 12.7 <sup>b</sup>	61.7 $\pm$ 19.4 <sup>b</sup>	75.7 $\pm$ 24.7 <sup>b</sup>	76.4 $\pm$ 31.4 <sup>b</sup>	101.7 <sup>c</sup>	

Parameter	P Values	TRT GRP	Predose Mean $\pm$ SEM	Change from Predose Values					
				45 minutes Mean $\pm$ SEM	90 minutes Mean $\pm$ SEM	150 minutes Mean $\pm$ SEM	210 minutes Mean $\pm$ SEM	300 minutes Mean $\pm$ SEM	
Potassium** (mmol/L)	trt = 0.002	VEH	3.93 $\pm$ 0.118*	4.26 $\pm$ 0.139*	4.53 $\pm$ 0.115*	4.43 $\pm$ 0.139*	4.40 $\pm$ 0.241*	4.09 $\pm$ 0.040*	
	time = 0.004	TOX	3.98 $\pm$ 0.157*	4.03 $\pm$ 0.104*	3.94 $\pm$ 0.145*	3.70 $\pm$ 0.159*	3.82 $\pm$ 0.117*	3.94 $\pm$ 0.099*	
	trt*time = 0.002	LET	4.10 $\pm$ 0.065*	5.67 $\pm$ 1.05 <sup>b</sup>	5.52 $\pm$ 0.801 <sup>b</sup>	5.85 $\pm$ 1.11 <sup>b</sup>	6.97 $\pm$ 2.44 <sup>b</sup>	5.94 <sup>b</sup>	
Inorganic Phosphorus** (mg/dl)	trt = 0.031	VEH	9.6 $\pm$ 0.33*	9.6 $\pm$ 0.41*	9.1 $\pm$ 0.51*	9.3 $\pm$ 0.33*	9.2 $\pm$ 0.38*	9.3 $\pm$ 0.38*	
	time < 0.001	TOX	9.4 $\pm$ 0.48*	9.8 $\pm$ 0.63*	10.4 $\pm$ 0.60*	9.8 $\pm$ 0.68*	9.8 $\pm$ 0.62*	10.0 $\pm$ 0.73*	
	trt*time < 0.001	LET	9.3 $\pm$ 0.66*	10.0 $\pm$ 0.99*	11.6 $\pm$ 0.66 <sup>b</sup>	12.9 $\pm$ 0.78 <sup>b</sup>	15.1 $\pm$ 3.45 <sup>b</sup>	13.0 <sup>b</sup>	
Creatinine (mg/dl)	trt < 0.001	VEH	0.85 $\pm$ 0.96	0.05 $\pm$ 0.029*	0.03 $\pm$ 0.111*	-0.05 $\pm$ 0.065*	0.13 $\pm$ 0.048*	0.10 $\pm$ 0.000*	
	time < 0.001	TOX	0.97 $\pm$ 0.105	-0.02 $\pm$ 0.017*	0.08 $\pm$ 0.065*	0.07 $\pm$ 0.120*	0.12 $\pm$ 0.140*	0.28 $\pm$ 0.122*	
	trt*time < 0.001	LET	0.97 $\pm$ 0.099	0.13 $\pm$ 0.088*	0.37 $\pm$ 0.088 <sup>b</sup>	0.67 $\pm$ 0.033 <sup>b</sup>	0.95 $\pm$ 0.050 <sup>b</sup>	1.60 <sup>b</sup>	
Blood Urea Nitrogen (mg/dl)	trt = 0.067	VEH	9.1 $\pm$ 1.31	0.7 $\pm$ 0.31*	1.4 $\pm$ 0.36*	0.3 $\pm$ 1.10*	2.6 $\pm$ 0.55*	2.6 $\pm$ 1.43*	
	time < 0.001	TOX	11.9 $\pm$ 2.43	0.2 $\pm$ 1.37*	2.7 $\pm$ 1.25 <sup>ab</sup>	1.8 $\pm$ 1.63*	2.5 $\pm$ 1.51*	5.9 $\pm$ 2.07 <sup>ab</sup>	
	trt*time < 0.001	LET	12.0 $\pm$ 1.25	1.1 $\pm$ 0.68*	3.8 $\pm$ 0.26 <sup>b</sup>	7.0 $\pm$ 0.75 <sup>b</sup>	10.2 $\pm$ 0.20 <sup>b</sup>	13.5 <sup>b</sup>	
Platelet Count (X 1000)	trt = 0.005	VEH	496 $\pm$ 103.4	-8 $\pm$ 10.3*	-12 $\pm$ 15.5*	-15 $\pm$ 34.2*	-36 $\pm$ 41.7*	-25 $\pm$ 21.5*	
	time = 0.114	TOX	663 $\pm$ 99.9	-50 $\pm$ 22.6*	-84 $\pm$ 50.3*	-143 $\pm$ 47.5 <sup>b</sup>	-151 $\pm$ 53.7 <sup>b</sup>	-101 $\pm$ 53.6 <sup>ab</sup>	
	trt*time = 0.919	LET	581 $\pm$ 25.8	-248 $\pm$ 63.4 <sup>b</sup>	-317 $\pm$ 33.8 <sup>b</sup>	-242 $\pm$ 82.8 <sup>c</sup>	-310 $\pm$ 70.0 <sup>c</sup>	-260 <sup>b</sup>	
Bicarbonate (mmol/L)	trt < 0.001	VEH	24.9 $\pm$ 0.33	-2.0 $\pm$ 0.73*	-1.6 $\pm$ 0.59*	-1.9 $\pm$ 0.64*	-2.6 $\pm$ 0.92*	-3.0 $\pm$ 0.17*	
	time < 0.001	TOX	23.1 $\pm$ 0.62	-0.7 $\pm$ 1.04*	-2.3 $\pm$ 0.89*	-3.2 $\pm$ 0.95*	-3.7 $\pm$ 1.54*	-4.9 $\pm$ 1.35*	
	trt*time < 0.001	LET	26.8 $\pm$ 0.62	-7.5 $\pm$ 2.14 <sup>b</sup>	-10.5 $\pm$ 2.8 <sup>b</sup>	-12.5 $\pm$ 1.9 <sup>b</sup>	-14.8 $\pm$ 4.6 <sup>b</sup>	-16.5 <sup>b</sup>	

Parameter	P Values	TRT GRP	Predose Mean $\pm$ SEM	Change from Predose Values				
				45 minutes Mean $\pm$ SEM	90 minutes Mean $\pm$ SEM	150 minutes Mean $\pm$ SEM	210 minutes Mean $\pm$ SEM	300 minutes Mean $\pm$ SEM
Arterial pH	trt = 0.268	VEH	7.40 $\pm$ 0.012	0.01 $\pm$ 0.016 <sup>ab</sup>	0.02 $\pm$ 0.015 <sup>a</sup>	0.03 $\pm$ 0.021 <sup>a</sup>	0.04 $\pm$ 0.016 <sup>a</sup>	0.07 $\pm$ 0.021 <sup>a</sup>
	time = 0.420	TOX	7.41 $\pm$ 0.014	-0.01 $\pm$ 0.009 <sup>a</sup>	0.02 $\pm$ 0.015 <sup>a</sup>	0.02 $\pm$ 0.014 <sup>a</sup>	0.02 $\pm$ 0.017 <sup>ab</sup>	0.02 $\pm$ 0.017 <sup>b</sup>
	trt*time = 0.001	LET	7.42 $\pm$ 0.006	0.05 $\pm$ 0.032 <sup>b</sup>	-0.06 $\pm$ 0.051 <sup>a</sup>	-0.09 $\pm$ 0.055 <sup>b</sup>	-0.04 $\pm$ 0.025 <sup>b</sup>	-0.08 <sup>c</sup>
Corrected pCO <sub>2</sub> Carbon Dioxide (mmHg)	trt = 0.002	VEH	39.8 $\pm$ 1.74	-3.7 $\pm$ 1.15 <sup>a</sup>	-3.6 $\pm$ 1.69 <sup>a</sup>	-4.7 $\pm$ 1.42 <sup>a</sup>	-6.7 $\pm$ 1.79 <sup>a</sup>	-9.4 $\pm$ 2.04 <sup>a</sup>
	time < 0.001	TOX	36.7 $\pm$ 1.56	-0.5 $\pm$ 1.92 <sup>a</sup>	-4.7 $\pm$ 1.43 <sup>a</sup>	-6.1 $\pm$ 1.18 <sup>a</sup>	-7.5 $\pm$ 2.25 <sup>a</sup>	-8.9 $\pm$ 1.67 <sup>a</sup>
	trt*time = 0.002	LET	41.6 $\pm$ 1.05	-13.5 $\pm$ 4.5 <sup>b</sup>	-12.9 $\pm$ 3.6 <sup>b</sup>	-15.2 $\pm$ 4.2 <sup>b</sup>	-21.9 $\pm$ 7.6 <sup>b</sup>	-22.1 <sup>b</sup>
Base Excess Blood (mmol/L)	trt < 0.001	VEH	1.1 $\pm$ 0.22	-1.2 $\pm$ 0.80 <sup>a</sup>	-0.5 $\pm$ 0.50 <sup>a</sup>	-0.6 $\pm$ 0.76 <sup>a</sup>	-0.7 $\pm$ 0.79 <sup>a</sup>	-0.6 $\pm$ 0.32 <sup>a</sup>
	time < 0.001	TOX	0.1 $\pm$ 0.60	-0.5 $\pm$ 0.91 <sup>a</sup>	-1.3 $\pm$ 0.92 <sup>a</sup>	-1.9 $\pm$ 0.88 <sup>a</sup>	-2.5 $\pm$ 1.31 <sup>a</sup>	-3.7 $\pm$ 1.19 <sup>b</sup>
	trt*time < 0.001	LET	3.3 $\pm$ 0.62	-5.6 $\pm$ 1.56 <sup>b</sup>	-9.9 $\pm$ 3.12 <sup>b</sup>	-12.2 $\pm$ 2.6 <sup>b</sup>	-13.1 $\pm$ 4.7 <sup>b</sup>	-15.0 <sup>c</sup>
Corrected pO <sub>2</sub> Oxygen (mmHg)	trt = 0.016	VEH	71.4 $\pm$ 9.67	-2.0 $\pm$ 1.80 <sup>a</sup>	-0.3 $\pm$ 5.03 <sup>a</sup>	-2.4 $\pm$ 5.86 <sup>a</sup>	6.5 $\pm$ 2.67 <sup>a</sup>	8.5 $\pm$ 5.62 <sup>a</sup>
	time < 0.001	TOX	75.1 $\pm$ 3.47	0.7 $\pm$ 3.07 <sup>a</sup>	-1.4 $\pm$ 3.34 <sup>a</sup>	1.5 $\pm$ 3.41 <sup>a</sup>	9.7 $\pm$ 4.54 <sup>ab</sup>	13.2 $\pm$ 5.56 <sup>a</sup>
	trt*time = 0.042	LET	75.3 $\pm$ 1.60	16.6 $\pm$ 9.42 <sup>b</sup>	16.3 $\pm$ 7.22 <sup>b</sup>	24.8 $\pm$ 12.5 <sup>b</sup>	13.1 $\pm$ 4.75 <sup>b</sup>	37.1 <sup>b</sup>
Hemato-crit (%)	trt = 0.011	VEH	30.0 $\pm$ 0.82	2.5 $\pm$ 1.44 <sup>a</sup>	3.8 $\pm$ 1.65 <sup>a</sup>	4.0 $\pm$ 1.08 <sup>a</sup>	2.0 $\pm$ 1.47 <sup>a</sup>	1.5 $\pm$ 1.19 <sup>a</sup>
	time = 0.917	TOX	28.5 $\pm$ 1.43	1.7 $\pm$ 0.92 <sup>a</sup>	1.7 $\pm$ 1.38 <sup>a</sup>	1.5 $\pm$ 0.42 <sup>a</sup>	2.3 $\pm$ 1.05 <sup>a</sup>	2.7 $\pm$ 0.99 <sup>a</sup>
	trt*time = 0.487	LET	32.0 $\pm$ 0.37	-4.3 $\pm$ 1.56 <sup>b</sup>	-3.3 $\pm$ 1.89 <sup>b</sup>	-2.3 $\pm$ 1.76 <sup>b</sup>	-2.0 $\pm$ 4.00 <sup>b</sup>	2.0 <sup>a</sup>

VEH = vehicle control group; 0  $\mu$ g/kg MCLR.

TOX = toxic-sublethal group; 25  $\mu$ g/kg MCLR.

LET = lethal group; 72  $\mu$ g/kg MCLR.

\*\* = statistical analysis of untransformed data.  
Means with different letters are significantly different ( $p < 0.05$ ).

Table 2. Liver and kidney weights (% live body weight) and liver hemoglobin and iron concentrations in swine intravenously administered a normal saline vehicle (n = 4), or a toxic-sublethal (25 µg/kg; n = 5 or 6), or lethal (72 µg/kg; n = 6) dose of microcystin-LR. Means with different letters are significantly different (p < 0.05).

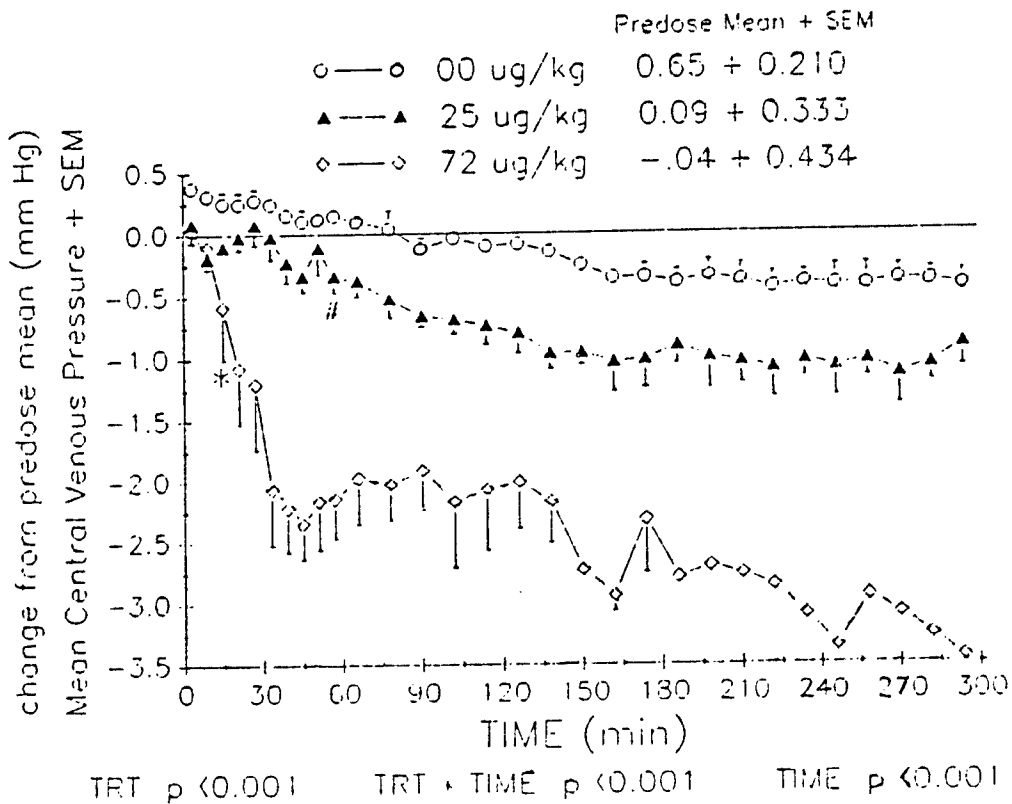
	Treatment Groups		
	Control	Toxic-Sublethal	Lethal
Liver Weight (% BW) (mean ± SD) (range)	2.43 ± 0.221 <sup>a</sup> 2.15 to 2.68	3.00 ± 0.149 <sup>b</sup> 2.87 to 3.26	4.40 ± 0.298 <sup>c</sup> 4.02 to 4.77
Kidney Weight (mean ± SD) (range)	0.247 ± 0.0148 <sup>ab</sup> 0.233 to 0.273	0.271 ± 0.0344 <sup>b</sup> 0.203 to 0.314	0.231 ± 0.0151 <sup>a</sup> 0.209 to 0.256
Liver Hb (g/dl) (mean ± SEM) (range)	2.5 ± 0.33 <sup>a</sup> 1.9 to 3.4	3.3 ± 0.73 <sup>a</sup> 1.9 to 5.7	9.2 ± 1.30 <sup>b</sup> 5.4 to 13.2
Liver Iron (ppm) (mean ± SEM) (range)	74 ± 33.5 <sup>a</sup> 28 to 106	112 ± 68.8 <sup>a</sup> 46 to 226	331 ± 125.8 <sup>b</sup> 200 to 492

SD = standard deviation.

SEM = standard error of the mean.

Means with different letters are significantly different (p < 0.05).

Figure 1. Six- and 12-minute means ( $\pm$  SE) of the change from the predose mean of central venous pressures in gilts intravenously administered a lethal (72  $\mu\text{g/kg}$ ;  $n = 6$  and decreases with time) or toxic-sublethal (25  $\mu\text{g/kg}$ ;  $n = 6$ ) dose of microcystin-LR or the normal saline vehicle ( $n = 3$ ).

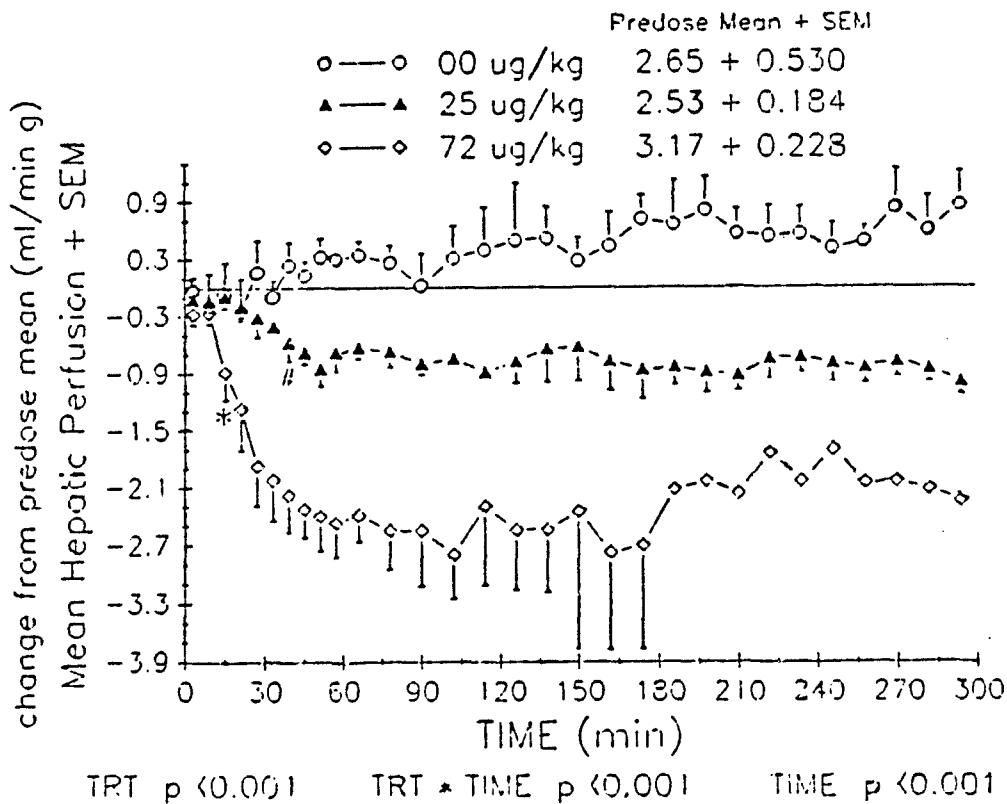


\* indicates time points where the lethal group is significantly different from both the control and toxic-sublethal groups ( $p < 0.05$ ).

# indicates time points where the toxic-sublethal group is significantly different from controls ( $p < 0.05$ ).



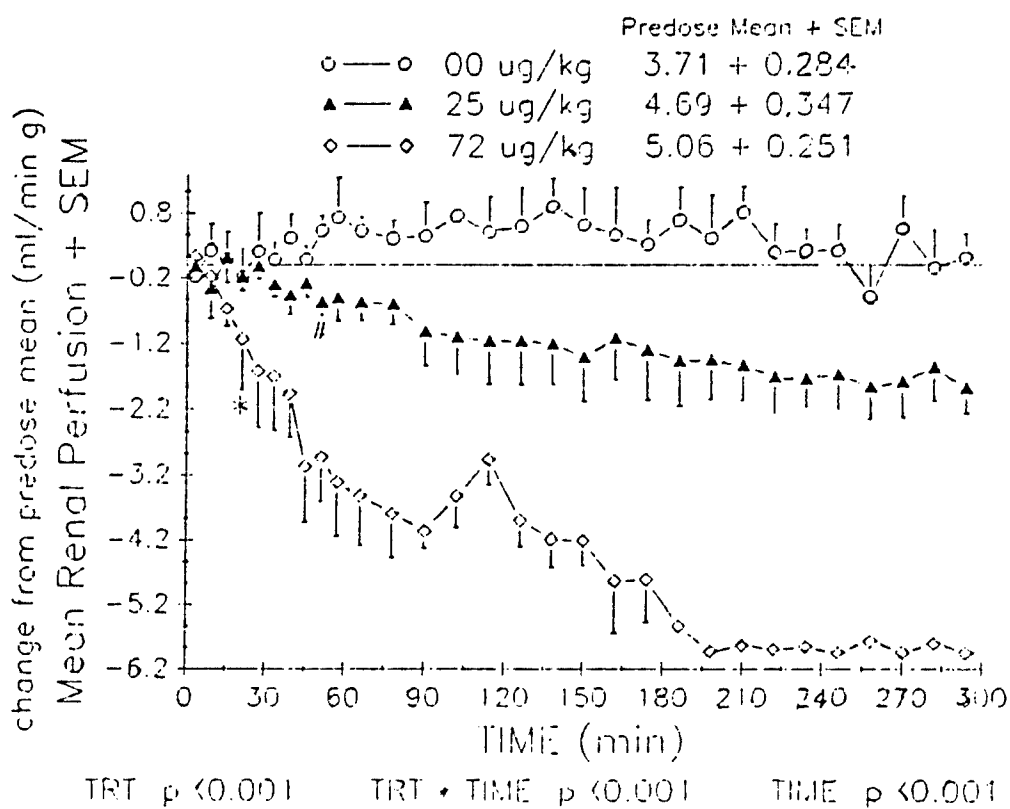
Figure 2. Six- and 12-minute means ( $\pm$  SE) of the change from the predose mean in mean liver perfusions of gilts intravenously administered a lethal (72  $\mu\text{g}/\text{kg}$ ;  $n = 6$  and decreases with time) or toxic-sublethal (25  $\mu\text{g}/\text{kg}$ ;  $n = 6$ ) dose of microcystin-LR or the normal saline vehicle ( $n = 4$ ).



\* indicates time points where the lethal group is significantly different from both the control and toxic-sublethal groups ( $p < 0.05$ ).

# indicates time points where the toxic-sublethal group is significantly different from controls ( $p < 0.05$ ).

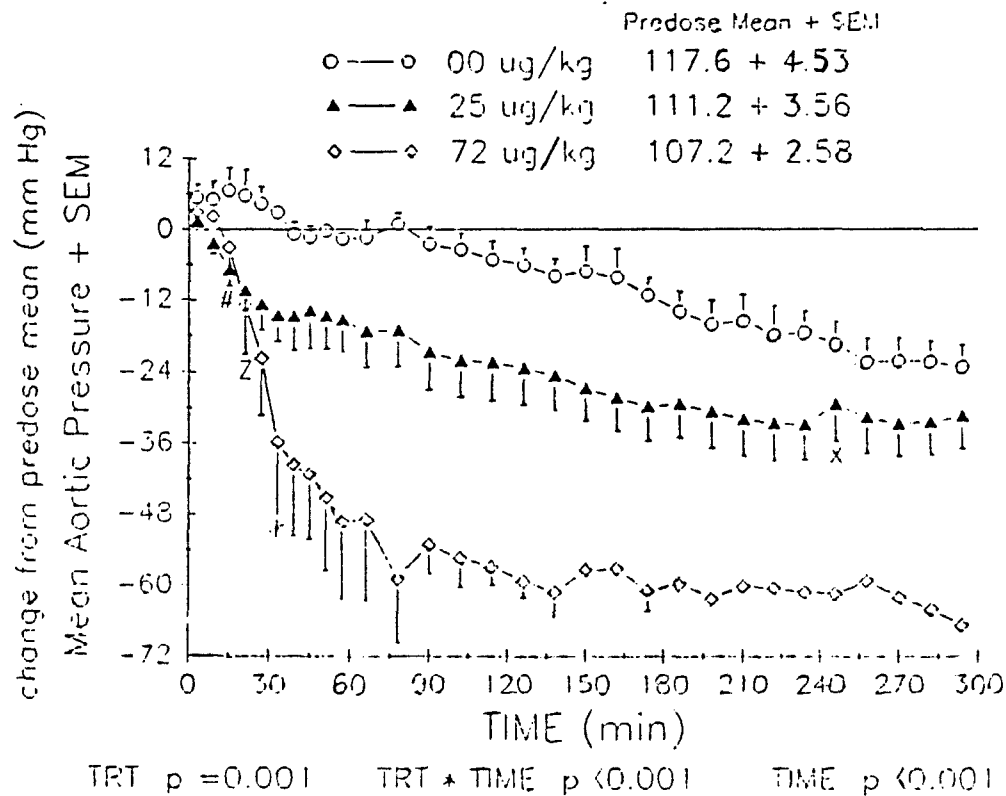
Figure 3. Six- and 12-minute means ( $\pm$  SE) of the change from the predose mean in mean kidney perfusions of gilts intravenously administered a lethal (72  $\mu\text{g/kg}$ ;  $n = 6$  and decreases with time) or toxic-sublethal (25  $\mu\text{g/kg}$ ;  $n = 6$ ) dose of microcystin-LR or the normal saline vehicle ( $n = 4$ ).



\* indicates time points where the lethal group is significantly different from both the control and toxic-sublethal groups ( $p < 0.05$ ).

# indicates time points where the toxic-sublethal group is significantly different from controls ( $p < 0.05$ ).

Figure 4. Six- and 12-minute means ( $\pm$  SE) of the change from the predose mean in mean aortic pressures of gilts intravenously administered a lethal (72  $\mu\text{g}/\text{kg}$ ;  $n = 6$  and decreases with time) or toxic-sublethal (25  $\mu\text{g}/\text{kg}$ ;  $n = 6$ ) dose of microcystin-LR or the normal saline vehicle ( $n = 4$ ).



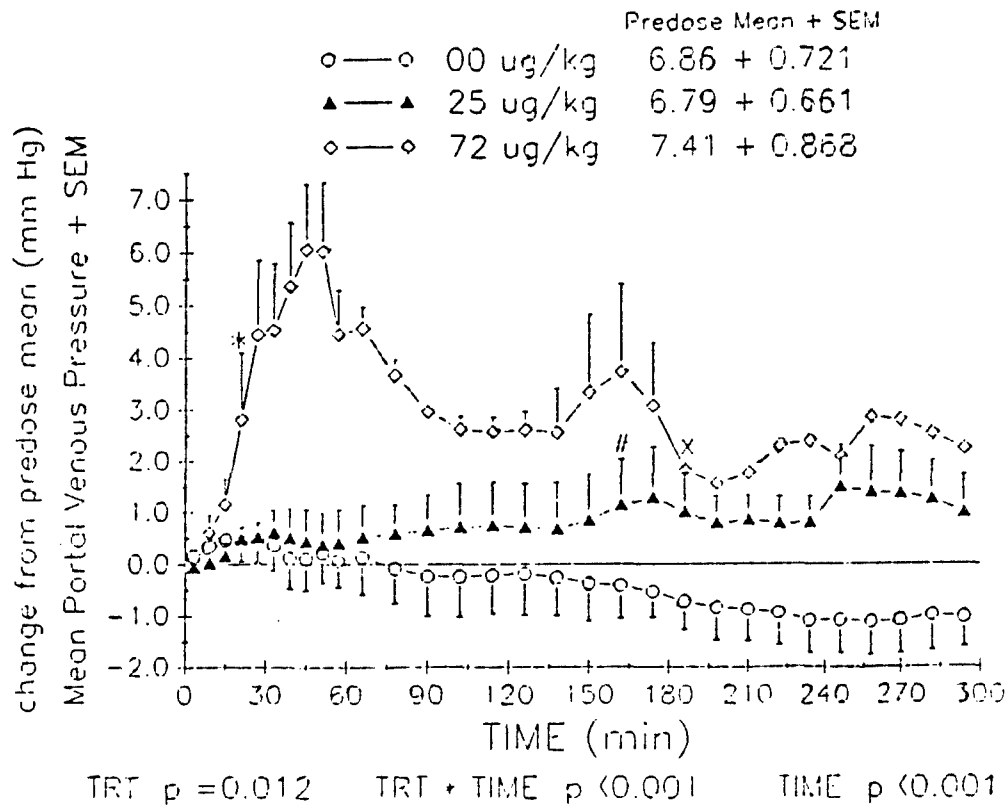
# indicates time points where the toxic-sublethal group is significantly different from controls ( $p < 0.05$ ).

Z indicates time points where the toxic-sublethal group is significantly different from controls ( $p < 0.05$ ).

\* indicates time points where the lethal group is significantly different from both the control and toxic-sublethal groups ( $p < 0.05$ ).

X indicates time points where the toxic-sublethal group is no longer significantly different from the control group ( $p > 0.05$ ).

Figure 5. Six- and 12-minute means ( $\pm$  SE) of the change from the predose mean in mean portal venous pressures of gilts intravenously administered a lethal (72  $\mu\text{g}/\text{kg}$ ;  $n = 6$  and decreases with time) or toxic-sublethal (25  $\mu\text{g}/\text{kg}$ ;  $n = 5$ ) dose of microcystin-LR or the normal saline vehicle ( $n = 4$ ).

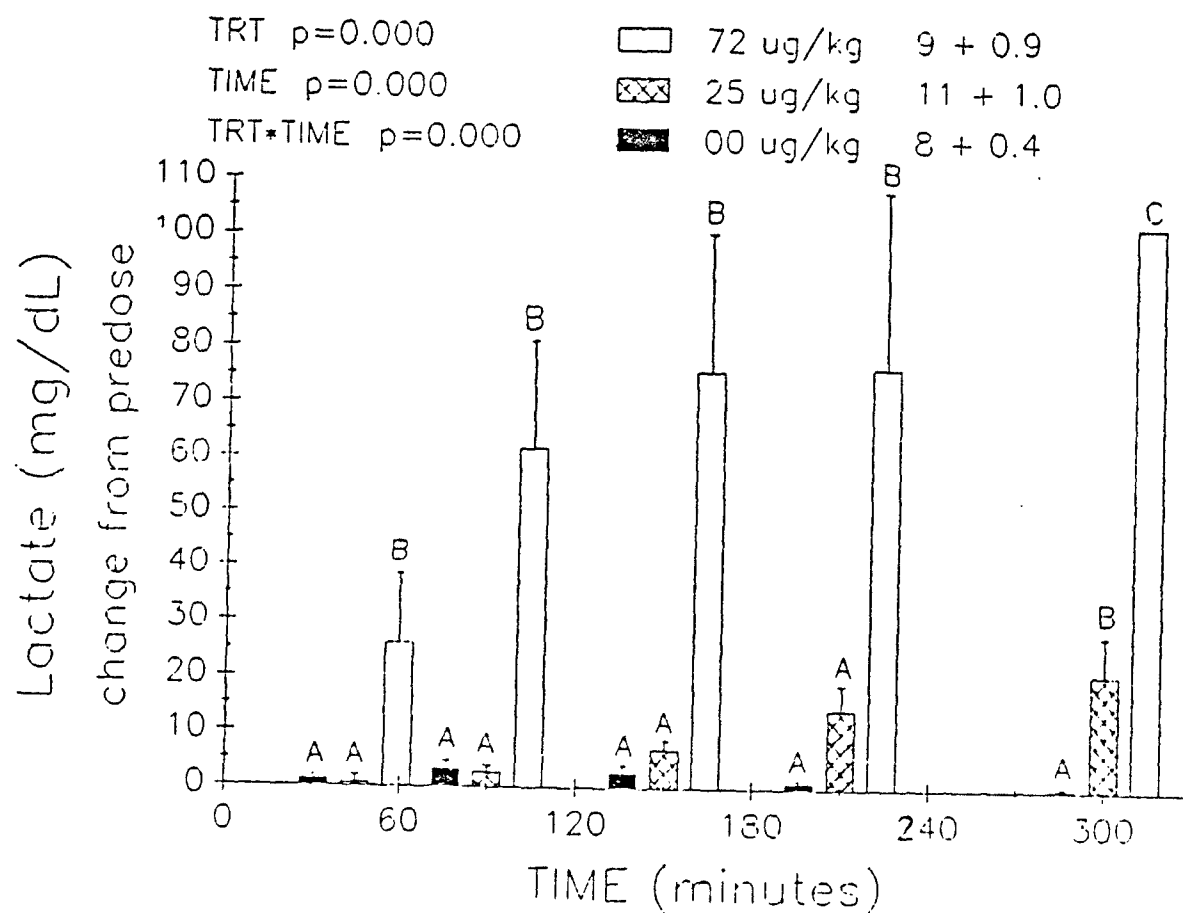


\* indicates time points where the lethal group is significantly different from both the control and toxic-sublethal groups ( $p > 0.05$ ).

# indicates time points where the toxic-sublethal group is significantly different from controls ( $p < 0.05$ ).

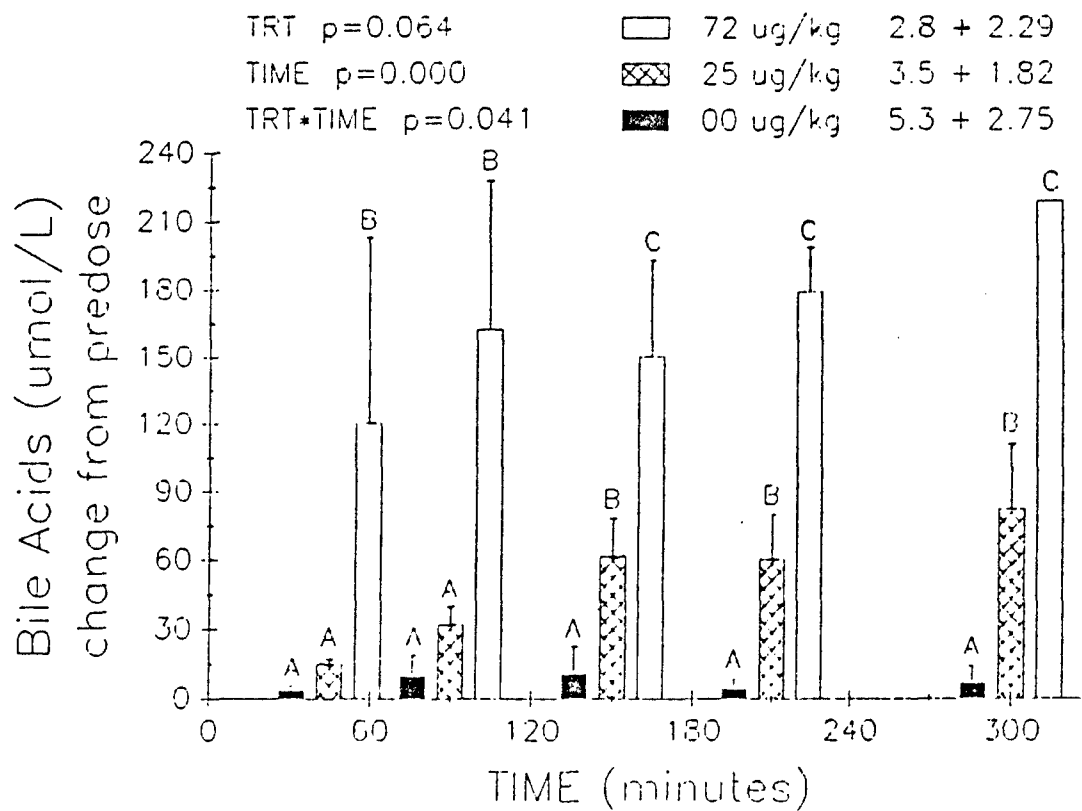
X indicates time points where the toxic-sublethal group is no longer significantly different from the lethal group ( $p > 0.05$ ).

Figure 6. Means ( $\pm$  SE) of the change from the predose mean in serum lactate concentrations of gilts intravenously administered a lethal (72  $\mu$ g/kg;  $n = 6$  and decreases with time) or toxic-sublethal (25  $\mu$ g/kg;  $n = 6$ ) dose of microcystin-LR or the normal saline vehicle ( $n = 4$ ; 00  $\mu$ g/kg). Groups that share the same letter are not significantly different ( $p < 0.05$ ).



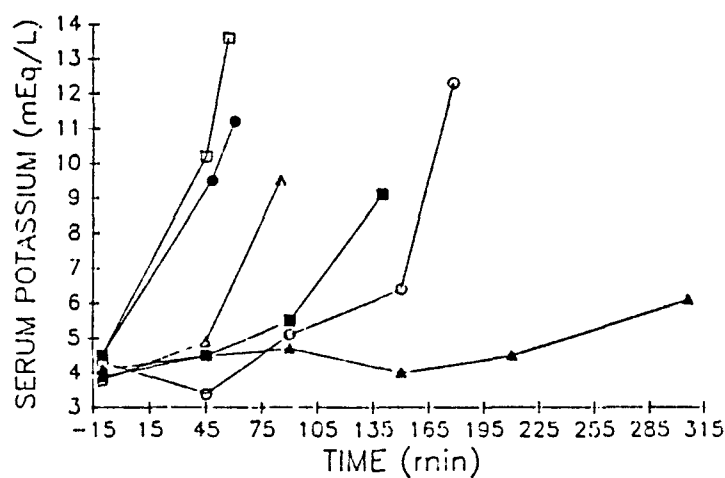
Note: The numbers to the right of the treatment group symbols represent the predose mean  $\pm$  SD.

Figure 7. Means ( $\pm$  SE) of the change from the predose mean in serum bile acid concentrations of gilts intravenously administered a lethal (72  $\mu\text{g/kg}$ ;  $n = 6$  and decreases with time) or toxic-sublethal (25  $\mu\text{g/kg}$ ;  $n = 6$ ) dose of microcystin-LR, or the normal saline vehicle ( $n = 4$ ; 00  $\mu\text{g/kg}$ ). Groups that share the same letter are not significantly different ( $p < 0.05$ ).



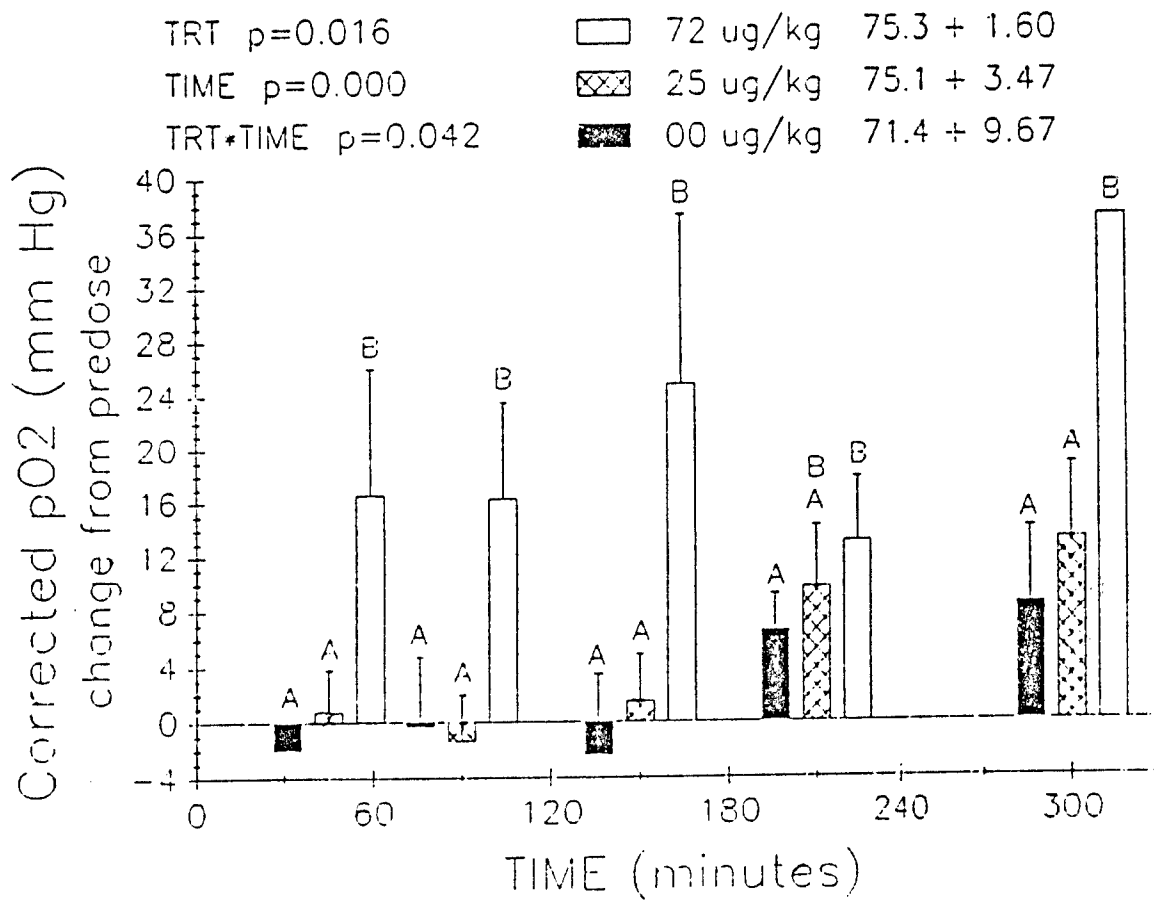
Note: The numbers to the right of the treatment group symbols represent the predose mean  $\pm$  SD.

Figure 8. Changes in serum potassium concentrations in the six gilts intravenously administered a lethal dose (72  $\mu\text{g/kg}$ ) of microcystin-LR.



Note: No serum potassium concentrations in gilts intravenously administered a toxic-sublethal (25  $\mu\text{g/kg}$ ;  $n = 6$ ) dose of microcystin-LR or the normal saline vehicle ( $n = 4$ ) exceeded 5.5 mEq/L as measured by the Hitachi 705.

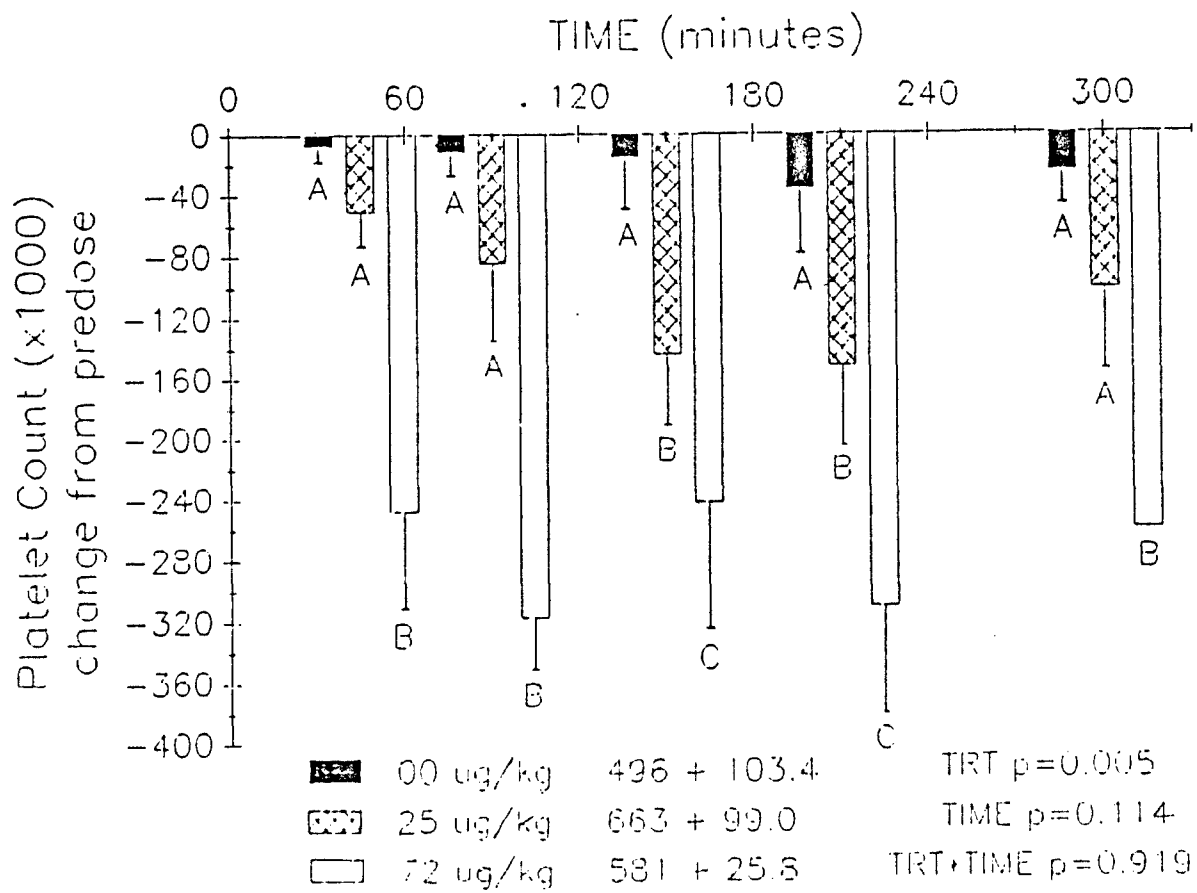
Figure 9. Means ( $\pm$  SE) of the change from the predose mean in arterial oxygen ( $pO_2$ ) of gilts intravenously administered a lethal (72  $\mu\text{g}/\text{kg}$ ;  $n = 6$  and decreases with time) or toxic-sublethal (25  $\mu\text{g}/\text{kg}$ ;  $n = 6$ ) dose of microcystin-LR or the normal saline vehicle ( $n = 4$ ; 00  $\mu\text{g}/\text{kg}$ ). Groups that share the same letter were not significantly different ( $p < 0.05$ ).



Note: The numbers to the right of the treatment group symbols represent the predose mean  $\pm$  SD.

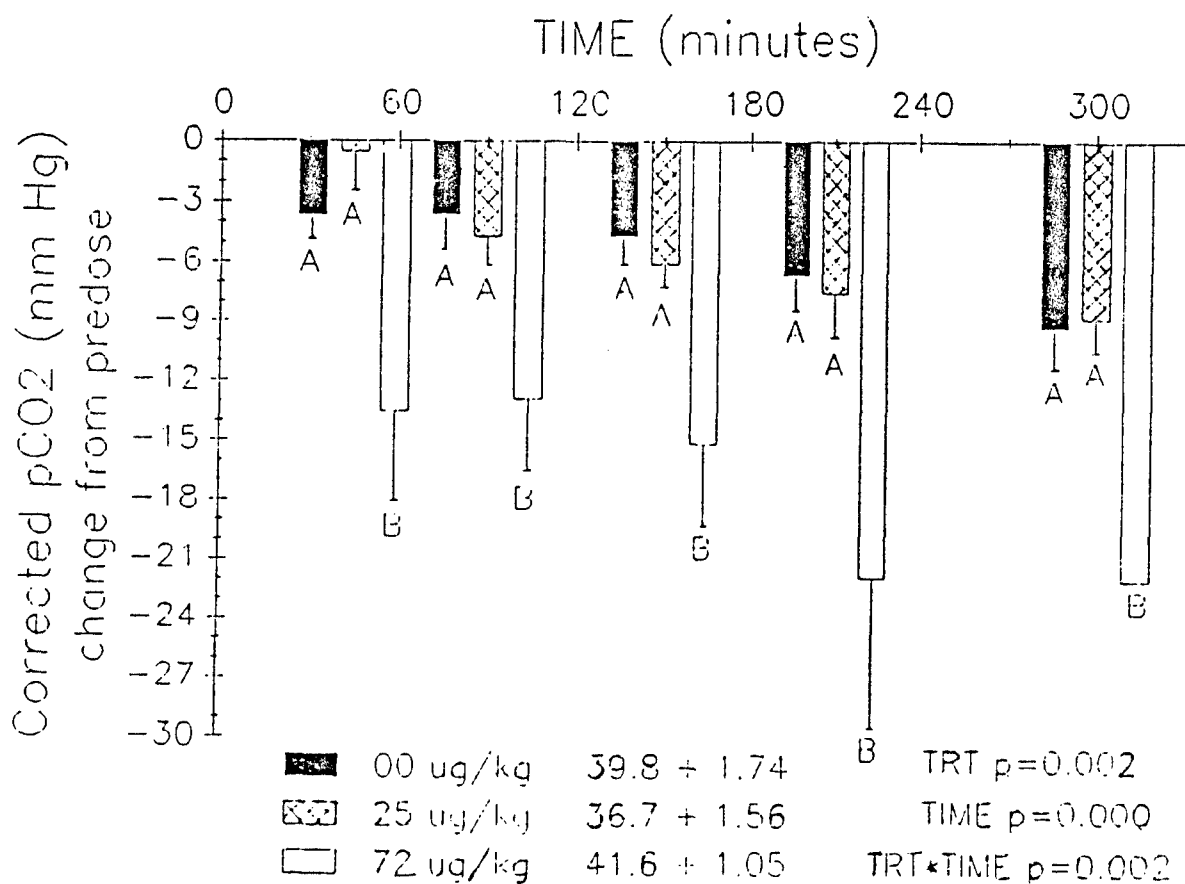


Figure 10. Means ( $\pm$  SE) of the change from the predose mean in platelet counts of gilts intravenously administered a lethal (72  $\mu\text{g/kg}$ ;  $n = 6$  and decreases with time) or toxic-sublethal (25  $\mu\text{g/kg}$ ;  $n = 6$ ) dose of microcystin-LR or the normal saline vehicle ( $n = 4$ ; 00  $\mu\text{g/kg}$ ). Groups that share the same letter were not significantly different ( $p < 0.05$ ).



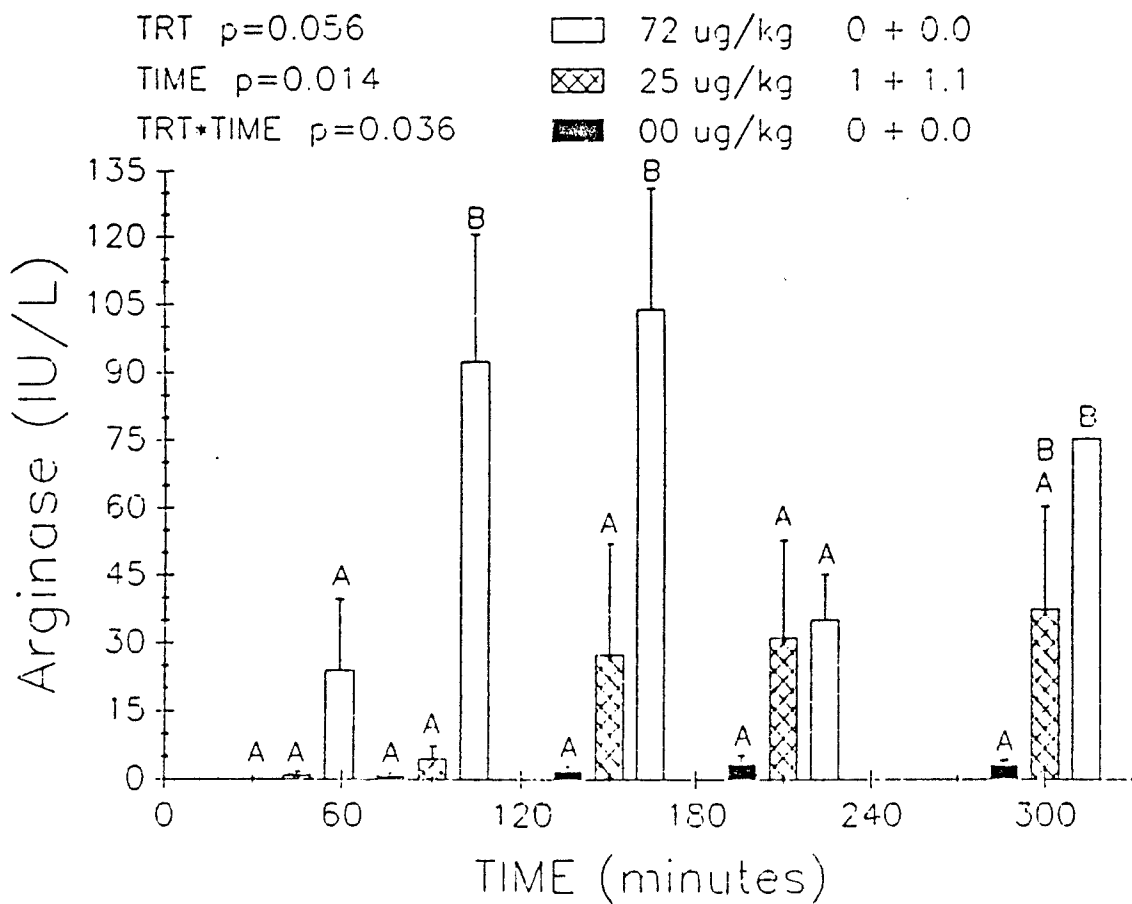
Note: The numbers to the right of the treatment group symbols represent the predose mean  $\pm$  SD.

Figure 11. Means ( $\pm$  SE) of the change from the predose mean in arterial carbon dioxide ( $pCO_2$ ) of gilts intravenously administered a lethal ( $72 \mu g/kg$ ;  $n = 6$  and decreases with time) or toxic-sublethal ( $25 \mu g/kg$ ;  $n = 6$ ) dose of microcystin-LR or the normal saline vehicle ( $n = 4$ ;  $00 \mu g/kg$ ). Groups that share the same letter are not significantly different ( $p < 0.05$ ).



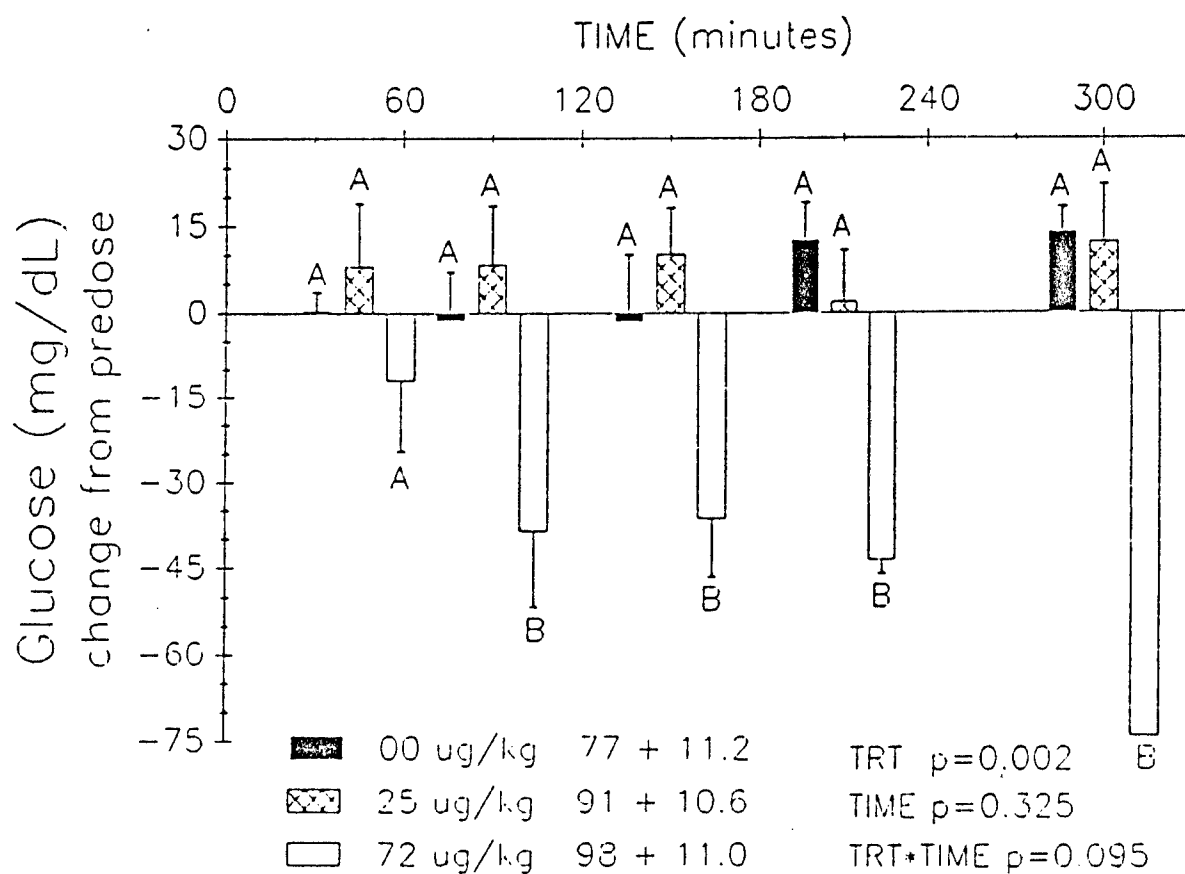
Note: The numbers to the right of the treatment group symbols represent the predose mean  $\pm$  SD.

Figure 12. Means ( $\pm$  SE) of the change from the predose mean in serum arginase activities of gilts intravenously administered a lethal (72  $\mu\text{g}/\text{kg}$ ;  $n = 6$  and decreases with time) or toxic-sublethal (25  $\mu\text{g}/\text{kg}$ ;  $n = 6$ ) dose of microcystin-LR or the normal saline vehicle ( $n = 4$ ; 00  $\mu\text{g}/\text{kg}$ ). Groups that share the same letter are not significantly different ( $p < 0.05$ ).



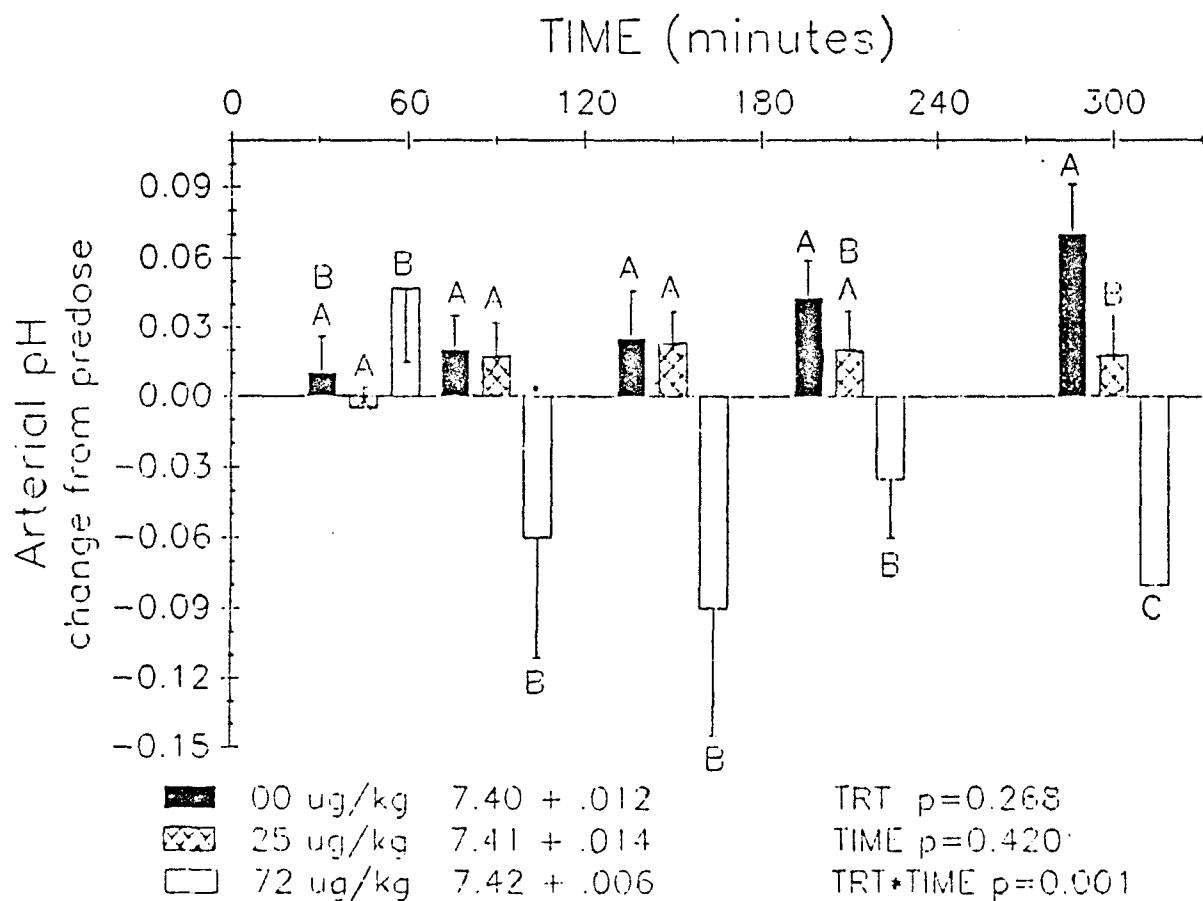
Note: The numbers to the right of the treatment group symbols represent the predose mean  $\pm$  SD.

Figure 13. Means ( $\pm$  SE) of the change from the predose mean in serum glucose concentrations of gilts intravenously administered a lethal (72  $\mu$ g/kg;  $n = 6$  and decreases with time) or toxic-sublethal (25  $\mu$ g/kg;  $n = 6$ ) dose of microcystin-LR or the normal saline vehicle ( $n = 4$ ; 00  $\mu$ g/kg). Groups that share the same letter are not significantly different ( $p < 0.05$ ).



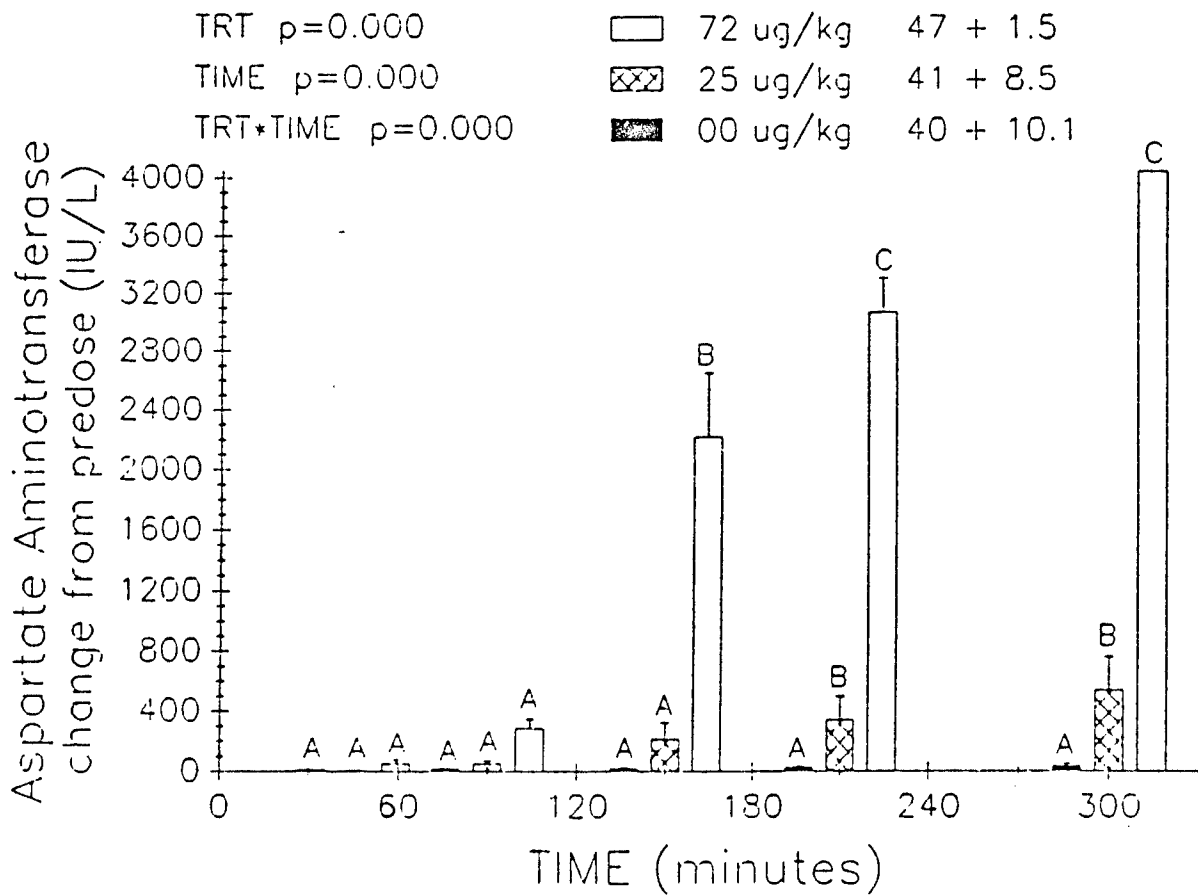
Note: The numbers to the right of the treatment group symbols represent the predose mean  $\pm$  SD.

Figure 14. Means ( $\pm$  SE) of the change from the predose mean in arterial pH of gilts intravenously administered a lethal (72  $\mu\text{g}/\text{kg}$ ;  $n = 6$  and decreases with time) or toxic-sublethal (25  $\mu\text{g}/\text{kg}$ ;  $n = 6$ ) dose of microcystin-LR or the normal saline vehicle ( $n = 4$ ; 00  $\mu\text{g}/\text{kg}$ ). Groups that share the same letter are not significantly different ( $p < 0.05$ ).



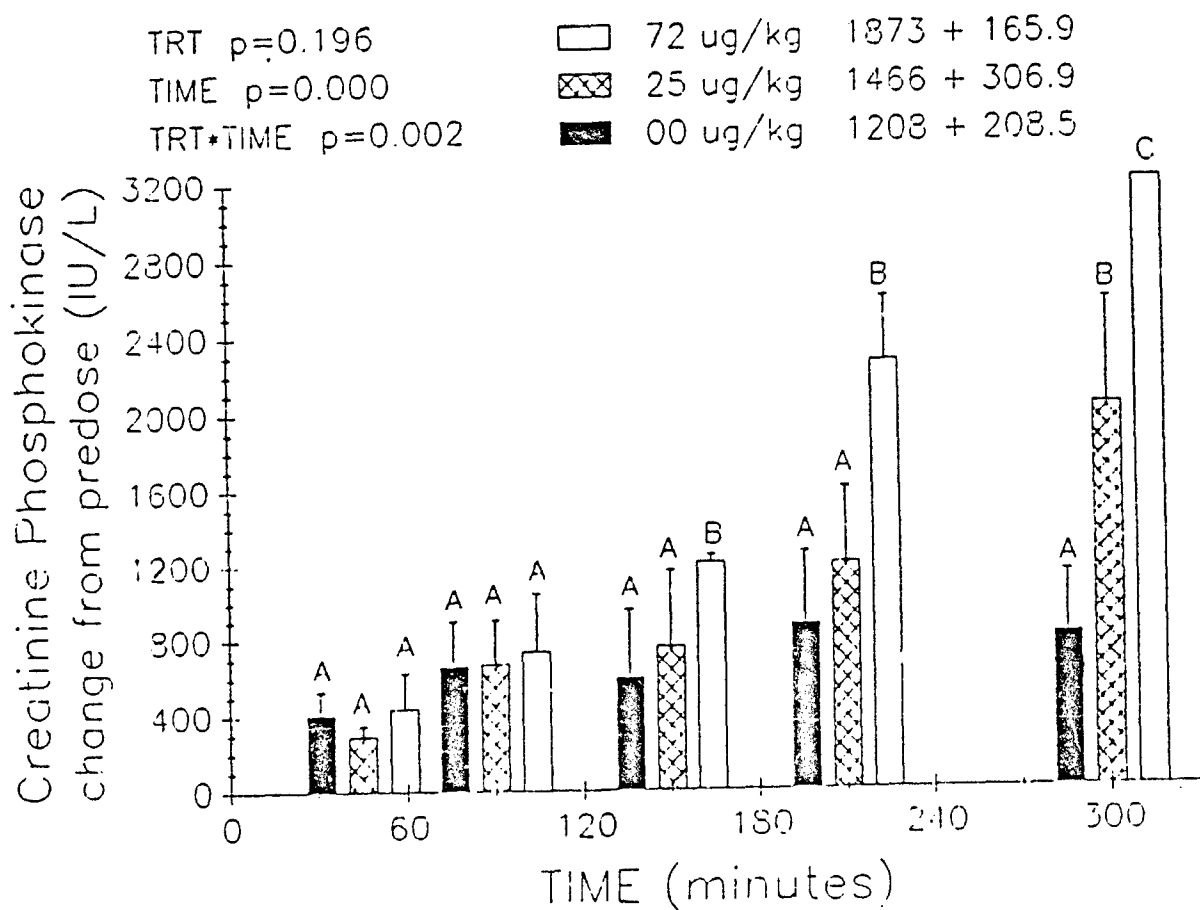
Note: The numbers to the right of the treatment group symbols represent the predose mean  $\pm$  SD.

Figure 15. Means ( $\pm$  SE) of the change from the predose mean in serum aspartate aminotransferase activities of gilts intravenously administered a lethal (72  $\mu\text{g/kg}$ ;  $n = 6$  and decreases with time) or toxic-sublethal (25  $\mu\text{g/kg}$ ;  $n = 6$ ) dose of microcystin-LR or the normal saline vehicle ( $n = 4$ ; 00  $\mu\text{g/kg}$ ). Groups that share the same letter are not significantly different ( $p < 0.05$ ).



Note: The numbers to the right of the treatment group symbols represent the predose mean  $\pm$  SD.

Figure 16. Means ( $\pm$  SE) of the change from the predose mean in serum creatinine phosphokinase activities of gilts intravenously administered a lethal (72  $\mu\text{g}/\text{kg}$ ;  $n = 6$  and decreases with time) or toxic-sublethal (25  $\mu\text{g}/\text{kg}$ ;  $n = 6$ ) dose of microcystin-LR or the normal saline vehicle ( $n = 4$ ; 00  $\mu\text{g}/\text{kg}$ ). Groups that share the same letter are not significantly different ( $p < 0.05$ ).



Note: The numbers to the right of the treatment group symbols represent the predose mean  $\pm$  SD.

VIII. BIOAVAILABILITY OF MICROCYSTIN-LR FROM RAT INTESTINE:  
THE INFLUENCE OF CHOLESTYRAMINE AND SUPERACTIVATED CHARCOAL  
*IN VITRO AND IN VIVO*

A. An Indirect Assessment of the Bioavailability of Intestinally Administered Microcystin-LR in Rats: Influence of Cholestyramine

1. Statement of the Problem, Background, and Rationale

Spontaneous outbreaks of *Microcystis aeruginosa* toxicosis consistently involve oral ingestion of concentrated algal bloom material. In preliminary studies, we attempted to produce the hepatotoxic effects in rats dosed orally using purified toxin or lyophilized algal cell suspensions. However, even at oral doses providing microcystin-LR (MCLR) at greater than 30 times the intraperitoneal or intravenous rat LD<sub>100</sub> (300 µg/kg), we were unable to produce any toxic effects in rats. The goal of the present study, therefore, was to bypass the stomach and assess the bioavailability of microcystin-LR (MCLR) from various segments of the small intestine based on increases in liver weight as a fraction of body weight. Since MCLR is an anion, we tested the hypothesis that an anion exchange resin, cholestyramine resin (CTR), would bind the toxin, thereby reducing its hepatotoxic potential.

2. Experimental Methods

Studies *In Vitro*

CTR (Bristol-Meyers, Evansville, IN) was combined with deionized water at a concentration of 50 mg/ml and mixed on a rocker mixer for 2 hours prior to the



addition of toxin. Varying amounts of MCLR of greater than 95% purity (produced and characterized as previously described in this report) were added in triplicate to tubes containing 1 ml of the CTR suspension. Samples were then mixed on a rocker mixer for 15 minutes and filtered through a 0.2  $\mu$  Acro LC13 disposable filter membrane (Gelman, Ann Arbor, MI). The filtrate was then injected into a Spectra Physics 8800 HPLC system equipped with a Whatman Partisphere C-18 column (4.6 x 120 mm). The mobile phase was 0.01 M ammonium acetate (pH 6) and acetonitrile in a ratio of 75:25 and the flow rate 1.0 ml/minute. Detection was by UV absorption at 240 nm, and the detection limit was 0.02  $\mu$ g/ml.

#### Animals

Sprague-Dawley rats of either sex (93 and 144 g) (Harlan Industries, Indianapolis, IN) were provided food *ad libitum* during an acclimation period lasting at least 1 week. Prior to the study, the animals were subjected to an overnight fast (16 hours) in cages with wire mesh floors to avoid any contact with bedding material. Water was available at all times.

#### Anesthesia and Surgical Preparation

Rats were anesthetized and anesthesia was maintained as needed with ether. Animals were weighed to the nearest 0.1 g, and placed in dorsal recumbency on a heating pad at 38°. A midline incision was made in the abdominal cavity.

To isolate an *in situ* ileal loop (Figure 1), a ligature was placed around the ileum approximately 5 cm orad to the ileocecal junction (ligature A). Ten to 15 cm orad to ligature A, a second ligature was placed around the ileum (ligature B). A small

incision was then made on the antimesenteric side of the isolated ileal segment immediately orad to ligature A, and 2 ml of normal saline was instilled gently near ligature B to flush the intestinal contents out of the antimesenteric incision. The saline solution was removed using a second flush with 1 ml of room air. A third ligature (ligature C) was then used to tie off the area of intestine containing the antimesenteric incision, and a fourth ligature (ligature D) was tied around a 30-gauge needle which had been introduced into the lumen of the ileum and through which the test solution was administered into the loop at a dose of 2.5 or 5.0 mg/kg BW. Following the injection of the MCLR solution, the needle was removed, ligature D was tightened, and the segment examined visually for leakage and then returned to the body cavity. The abdominal incision was closed using 9 mm Autoclip wound clips (Clay Adams, Parsippany, NJ).

To isolate an *in situ* jejunal loop, ligature A was tied 5 cm caudad to the ligament of Treitz and ligature B was placed approximately 10 to 15 cm caudad to ligature A. The loop was flushed, the toxin solution administered, and the abdomen closed as described above.

In trials involving treatment with CTR, the experiment was identical to that described for the toxin administration into the ileal loop, except that ligature D was tied around an 18-gauge needle and test solutions were administered through a three-way stopcock. Thirty seconds following administration of MCLR, 50 mg of CTR in 0.5 ml of H<sub>2</sub>O or an equivalent volume of saline was administered.

In all cases, care was taken to avoid ligating the blood supply to the intestinal segment of interest. Following surgery, the animals were allowed to recover from the anesthesia. All animals were killed by ether anesthesia at 6 hours after treatment. The incision was then reopened and the isolated intestinal loop was carefully removed from the body cavity and blotted dry. A 30-gauge needle was inserted into the isolated segment and a solution of 10% neutral-buffered formalin was injected. The intestinal segment was again observed to insure that no leakage had occurred either through the intestinal wall or around the ligatures. The livers were immediately removed, weighed, and then fixed by immersion in 10% neutral-buffered formalin. The tissues were then routinely processed, embedded in paraffin, cut at 4 to 6  $\mu$ m, stained with hematoxylin and eosin and examined by light microscopy. The liver weight was expressed as a percent of total body weight, and differences between the groups were compared using the Student's one-tailed t-test for unpaired means. A level of  $\alpha = 0.05$  was chosen to detect significant differences.

### 3. Results

Animals given MCLR at either 2.5 or 5.0 mg/kg displayed varying degrees of depression and lethargy beginning approximately 30 minutes after toxin administration and became progressively more severe until the time of death. Within 6 hours after infusion of a single 5 mg/kg dose of MCLR into the ileum, rats experienced labored breathing and appeared to be in a state of circulatory shock. Animals which did not receive MCLR and animals given CTR following toxin administration appeared clinically normal throughout the 6-hour observation period.

All animals which showed clinical signs had similar histologic lesions of varying severity and animals showed a dose dependency in formation of hepatic lesions with lower doses causing less severe lesions. Livers from toxin-treated animals not given CTR appeared dark red and enlarged at the time of death. No other gross lesions were noted in toxin-treated animals. Microscopic lesions observed in toxin-treated animals included rounding of hepatocytes, centrilobular hepatocyte disassociation, and hemorrhage involving centrilobular regions of the liver. Severely affected animals given the 5.0 mg/kg doses of MCLR had severe hepatocyte disassociation, degeneration, necrosis, and hemorrhage throughout the entire liver lobe except for small areas of cells surrounding portal regions. The increases in liver weight associated with toxin administration were determined to be the direct result of hemorrhage into the liver, and lesions formed were similar to hepatic lesions observed in our other studies.

Lesions in animals given CTR following toxin administration included a mild degree of hepatocyte rounding and disassociation of hepatocytes, but lesions were less severe than in any of the rats given toxin alone. Animals not given toxin lacked gross and histologic lesions associated with MCLR administration.

There was a significant increase in liver weights of the rats given MCLR at 5.0 mg/kg when compared to vehicle-treated controls. There was no significant difference in liver weights between male and female rats given the same dose of toxin (5 mg/kg) into the ileal loop (females,  $72 \pm 0.2$  [N = 4], versus males,  $7.0 \pm 0.2$  [N = 5]; mean  $\pm$  SEM).

When MCLR was infused into the ileal loop at 2.5 mg/kg body weight, liver weights were significantly greater than controls but less than that in animals dosed at 5.0 mg/kg. As shown in Figure 2, a linear relationship between toxin dose and liver weight was identified.

When toxin was instilled into the jejunal loop at 5 mg/kg body weight, liver weight was significantly lower than that obtained when an equivalent dose was infused into the ileal loop (ileum,  $7.0 \pm 0.2$  [N = 5], versus jejunum,  $6.0 \pm 0.1$  [N = 3]; mean  $\pm$  SEM). Livers of rats dosed via the ileal loop at 2.5 mg/kg was virtually identical to that found in animals dosed at 5.0 mg/kg via the jejunal loop (Figure 3).

Cholestyramine resin was found to bind MCLR over the range of CTR to toxin ratios tested *in vitro* (Table 1). Furthermore, rats treated via the ileal loop with toxin at 5 mg/kg followed by CTR had liver weights which were similar to vehicle-treated controls and significantly less than animals dosed with MCLR at 5 mg/kg followed by saline (Figure 4).

#### 4. Discussion and Conclusion

In preliminary studies, laboratory animals treated by gavage with MCLR at 5 mg/kg did not appear to be adversely affected, and no liver damage was apparent grossly even at 24 hours after dosing. Even when lyophilized cell suspensions were administered orally (in volumes approaching the maximum that could be given; equivalent to MCLR at 12 mg toxin/kg body weight), no detectable acute toxicity was evident.

Because of the high cost of MCLR, testing with higher oral doses of purified material tends to become prohibitive. Limitations of the capacity of the rat stomach tends to prevent administration of higher oral doses of the cell suspension. Therefore, a model was sought to characterize bioavailability of MCLR administered via the intestinal route as estimated by the increase in liver size attributable to the toxin. The isolated *in situ* ileal loop preparations provided a reproducible system to study the intestinal absorption (bioavailability) of the toxin, as monitored by its hepatotoxic effects. Our results indicate that, while the rat appears to be a less-than-satisfactory model animal for oral toxicity studies using this toxin, it serves as a convenient model for intestinal absorption studies utilizing the *in situ* isolated intestinal loop. The reason that rats survive a high oral dose of the purified compound remains unknown.

CTR is widely available and apparently effectively limits intestinal absorption of MCLR. These experiments with CTR binding of MCLR *in vitro* and *in vivo* suggest that CTR may prove therapeutically effective in cases of animal ingestion of toxin waterblooms. Since CTR itself is not absorbed, it would not contribute to the drug or xenobiotic load of affected animals.

The fact that susceptibility to MCLR was dependent on whether the toxin was infused into the jejunum or ileum is notable since it suggests that the ileum may be a preferential site for absorption. There is evidence from studies *in vitro* that MCLR is transported into hepatocytes by carriers of bile acids (Runnegar et al., 1981). Specific carriers for bile acids are also located in the ileum (Hofmann, 1983). If bile acid carriers in the ileum enhance absorption of MCLR, then it is understandable why

equivalent doses of the toxin produce greater effects when introduced into the ileum as compared to the jejunum. In contrast to the ileum, bile acids are absorbed at a slower rate in the jejunum primarily via passive diffusion (Hofmann, 1983). By analogy, absorption of MCLR from the jejunum may also occur by passive diffusion. Thus, for a given dose of MCLR, a greater degree of toxicity would be expected when infused into the ileum than when infused into the jejunum as observed in the present study.

In summary, this study has: 1) established a reproducible model for studying the intestinal absorption of MCLR, 2) demonstrated that CTR may be a useful therapeutic agent in cases involving known ingestion of MCLR containing cyanobacteria, and 3) provided evidence suggesting site specificity in the intestinal absorption of MCLR.

Table 1. Binding of microcystin-LR to cholestyramine resin *in vitro*. All analyses were run in triplicate.

Cholestyramine (mg)/ml	Microcystin-LR ( $\mu$ g)/ml	% Toxin Removed*
50	25	> 99
50	50	> 99
50	100	> 99
50	200	> 99
25	200	> 99
25	400	> 99
0	50	10.9 $\pm$ 3.1
0	100	4.9 $\pm$ 4.6
50	0	0.0

\*Mean  $\pm$  SE.



Figure 1. Isolated rat ileal loop segment for microcystin-LR infusion.

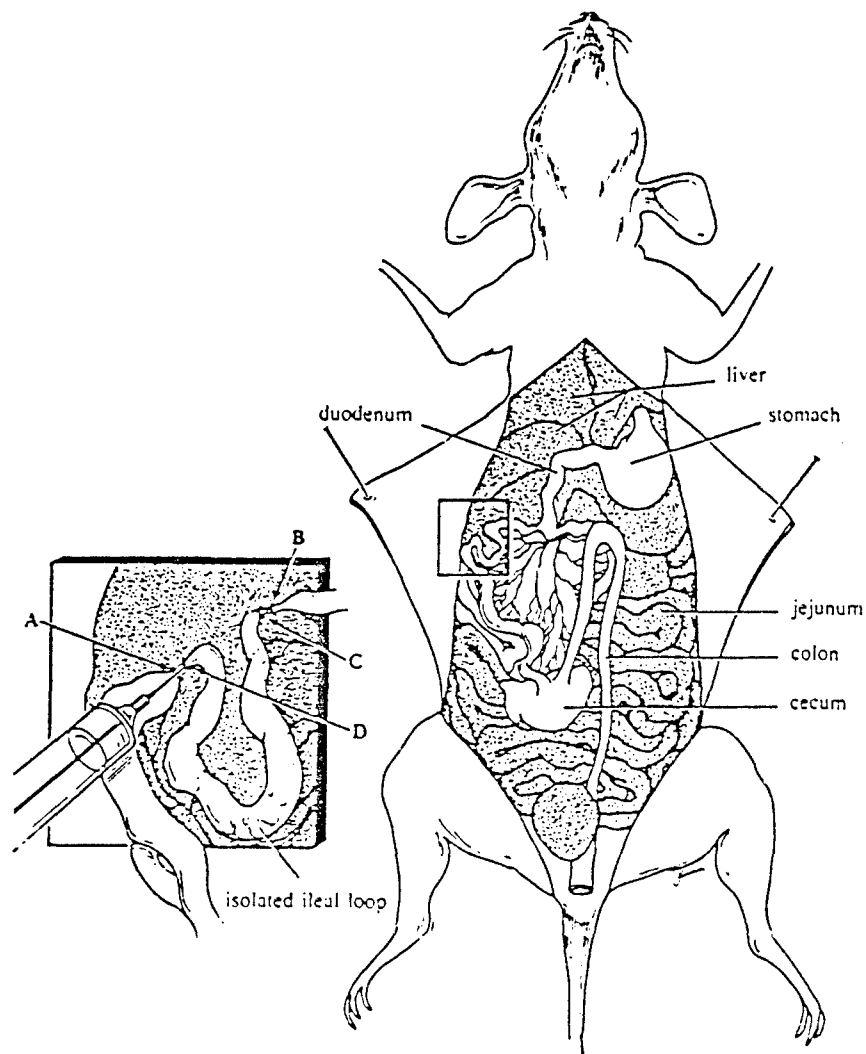


Figure 2. Linear regression analysis of liver weights from animals given microcystin-LR at either 2.5 mg/kg body weight or 5 mg/kg body weight or the trial vehicle via an ileal loop. The straight line is the line of "best fit" according to the method of least squares. Each point represents the value from one animal.

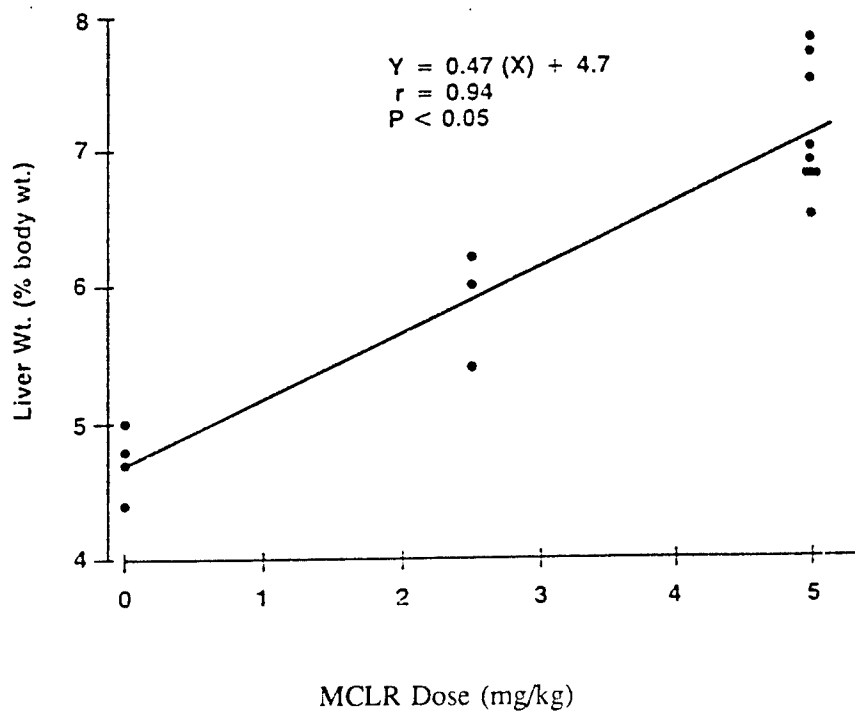


Figure 3. Liver weights (mean  $\pm$  SEM) following ileal or jejunal infusion of microcystin-LR.

Toxin was infused into the ileal (2.5 mg/kg body weight, N = 3) or jejunal loop (5 mg/kg body weight, N = 3). Six hours following treatment, the animals were killed, and livers were removed and weighed.

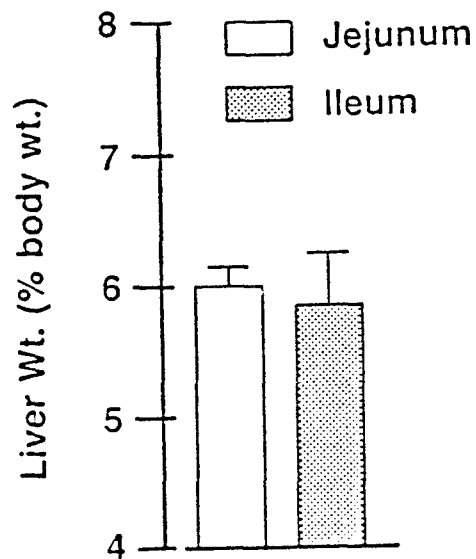
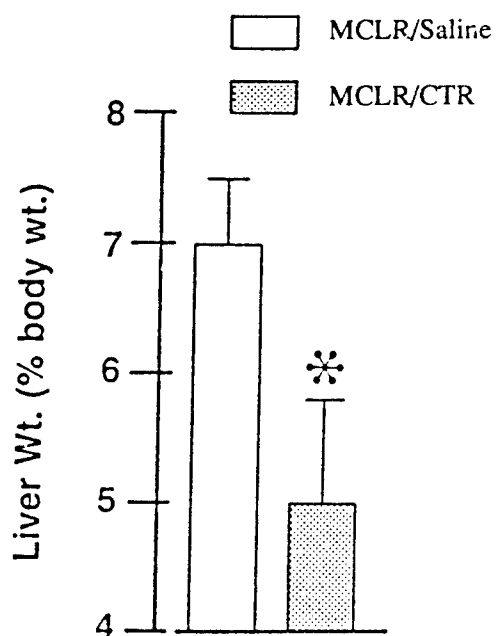


Figure 4. Comparison of liver weights (mean  $\pm$  SEM) from animals given microcystin-LR plus saline (N = 5) or microcystin-LR plus cholestyramine resin (N = 4). \*Denotes values significantly ( $p < 0.05$ ) less than those of the toxin/saline-treated group.



**B. Comparison of the Binding Capacities of Superactivated Charcoal to Microcystin-LR*****In Vivo and In Vitro*****1. Statement of the Problem, Background, and Rationale**

Although cholestyramine resin (CTR) was highly effective both at binding microcystin-LR (MCLR) *in vitro* and preventing its absorption *in vivo* (see previous section), activated charcoal tends to be more widely available and is more commonly employed as an agent to limit the gastrointestinal absorption of xenobiotics. In these studies, we evaluated the ability of superactivated charcoal to bind MCLR *in vitro* and to limit the increase in liver weight of rats exposed via an isolated ileal loop.

**2. Experimental Methods****a. Studies *in vitro***

Superactivated charcoal (superchar) (Gulf Bio-Systems, Inc., Dallas, TX) was used in this experiment. Fifty milligrams of superchar was weighed into individual tubes to which 5.0 ml of normal saline was added. The tubes were capped and then placed on a rocker mixer for 2 hours prior to analysis. Repeated aliquots of superchar in aqueous suspension were removed and the amount of superchar present was calculated on a weight per volume basis.

MCLR was dissolved in deionized water and the appropriate volumes of toxin were added to the superchar suspension so that the concentration of toxin was 50 µg/ml (Table 1). The final volumes of each tube were adjusted to 1.0 ml with deionized water. The experimental samples were then placed on a rocker mixer for 15 minutes followed by centrifugation at 5,000 g for 5 minutes.

The supernatant was removed from each tube and passed through individual 0.2  $\mu$  filters (Gelman Scientific, Ann Arbor, MI) to remove the remaining charcoal. Samples were analyzed by HPLC by the methods of Harada et al. (1988), with UV detection at 238 nm and quantification was accomplished with linear regression against a toxin standard curve.

b. Studies *in vivo*

*In situ* isolated rat ileal segments were prepared according to the method of Dahlem et al. (1989b). Male Sprague-Dawley rats (approximately 100 g body weight) were randomly assigned to one of two groups and given, via the intestinal loop, either water (0.5 ml) followed 30 seconds later by superchar (50 mg) in a saline vehicle (0.5 ml) or MCLR at 5 mg/kg in water (0.5 ml) followed 30 seconds later with superchar (50 mg) in a saline vehicle (0.5 ml). The animals were allowed to recover from surgery, then were killed 6 hours after treatment by an overdose of ether anesthesia. The toxic effects were assessed by changes in liver weight as a percentage of animal whole body weight and the groups compared by Student's t-test. A level of  $\alpha = 0.05$  was chosen to detect significant differences.

3. Results

When mixed with superchar at a ratio of 1:100 (toxin:charcoal), the free toxin concentration in solution was found to be below the limit of detection (20 ppb) in all trials. In the experiments *in vivo*, an approximate ratio of toxin:charcoal 1:100 was again used. Despite the administration of superactivated charcoal, there was a

statistically significant ( $p < 0.01$ ) increase in liver weights as a percent of whole body weights on animals given MCLR as shown in Table 2, indicating that this dose of superchar *in vivo* did not obliterate toxin absorption.

#### 4. Discussion and Conclusion

These results are in contrast to our earlier results obtained with CTR. In that study, a ratio of 1:100 of toxin to CTR infused into similar *in situ* rat gut loop preparations has been more effective in limiting the toxicosis. Liver weights as a percentage of animal whole body weights in rats given MCLR followed by CTR were indistinguishable from those of control animals not given MCLR at all.

One probable reason for the apparent differences in binding of toxin *in vivo* as compared to *in vitro* is that the superactivated charcoal apparently does not stay in suspension and quickly settles out within the gut loop. At necropsy we found the superchar clumped together on the dependent aspect of the mucosa of the isolated gut loop. With constant mixing as occurs on the rocker mixer, the charcoal is not able to settle out so that it presumably can better adsorb the algal toxin. CTR seems more prone to stay in suspension and settles out much slower. Perhaps in an unaltered intestine *in vivo*, the peristaltic movement of ingesta would facilitate mixing of MCLR with either the activated charcoal or the ion-exchange resin. Another factor may be the weight of water present in the superchar which offsets the amount of adsorbent available for binding of the toxin.

In conclusion, it appears (at the concentrations of toxin and absorbents used in these experiments) that superactivated charcoal holds some promise as an adsorbent

for animals orally exposed to MCLR, but CTR may be more efficacious than superchar in reducing the bioavailability and associated toxic effects of microcystin-LR.



Table 1. Binding of microcystin-LR to superactivated charcoal *in vitro*.

Charcoal Concentration ( $\mu\text{g/ml}$ )	Microcystin-LR $\mu\text{g/ml}$	% Absorbed
25	50	<0.01
50	50	< 0.01
100	50	4.0
200	50	7.2
500	50	20.0
1,000	50	45.2
2,500	50	98.4
5,000	50	> 99.0
10,000	50	> 99.0

Table 2. Comparison of relative liver weights (% body weight) of rats dosed via an ileal segment *in situ* with 50 mg of superactivated charcoal and either microcystin-LR at 5 mg/kg (Tox) or the saline (Sal) vehicle.

Tox/Charcoal	Sal/Charcoal
7.35%	4.61%
6.11%	3.97%
6.08%	4.12%
6.90%	3.71%
6.70%	4.13%
	4.06%
Mean = 6.63	Mean = 4.10
SEM = 0.24	SEM = 0.12

**IX. INTERPRETATION OF THE CURRENTLY REPORTED STUDIES ON  
CYTOSKELETAL EFFECTS AND FATE OF ALGAL PEPTIDES IN  
LIGHT OF OTHER RECENT RESEARCH**

Recent work is beginning to shed light on questions regarding the subcellular distribution of the hepatotoxic cyanobacterial toxins, as well as mechanisms by which they may act to cause disruption of cytoskeletal architecture. Studies *in vivo* and *in vitro* with tritiated MCLR have shown that the parent toxin and at least one of its polar biotransformation products appear to bind to the cytosolic protein fraction of rat hepatocytes (Matson et al., 1990; Robinson et al., 1991). Relatively little activity is associated with the insoluble protein fraction which includes cytoskeletal elements (Hooser, 1989). The protein to which the algal toxin seems to bind has an apparent molecular weight of approximately 40,000 and is present in brain, kidney, heart, lung, intestine, testes, skeletal muscle, and fat, in addition to hepatic tissue (Robinson et al., 1991).

Binding of MCLR to hepatic cytosol is inhibited by okadaic acid in a concentration dependent manner (MacKintosh et al., 1990; Robinson et al., 1991). Okadaic acid (Figure 1), a complex polyether fatty acid produced by marine dinoflagellates (*Dinophysis* spp.), is a potent, specific inhibitor of protein phosphatases type 1 and 2A (PP1 and PP2A). It is believed to cause inhibition by binding to the catalytic subunit of these protein phosphatases which are normally present in the cytosol (Yoshizawa et al., 1990). The ability of okadaic acid to inhibit the binding of MCLR coupled with the molecular weight and wide organ distribution of the MCLR binding protein suggests that the cytosolic receptor for microcystin may be a protein phosphatase. This hypothesis is strengthened by recent findings that the microcystins LR, YR, and RR and

nodularin are themselves very potent and specific inhibitors of PP1 and PP2A (Eriksson et al., 1990; Honkanen et al., 1990; MacKintosh et al., 1990; Yoshizawa et al., 1990).

These cyanobacterial toxins also resemble another protein phosphatase inhibitor, calyculin A (Figure 1) (isolated from the marine sponge *Diskodermia calyx* [Fujiki et al., 1989]) in that they inhibit the activity of PP2A with potency similar to okadaic acid but are 10 to 100 times more potent in their inhibition of PP1 (Ishihara et al., 1989; Eriksson et al., 1990). Calyculin A induces morphological changes in fibroblasts in a manner related to reorganization of the cytoskeleton which is remarkably similar to the effects observed in hepatocytes exposed to cyanobacterial peptide toxins (Chartier et al., 1990). This has led to additional speculation that the cytoskeletal changes induced by these toxins may be triggered by inhibition of cytosolic protein phosphatases.

Protein phosphatases type 1 and 2A have broad substrate specificity and appear to be important in the dephosphorylation of rate-limiting enzymes which control many key cellular metabolic functions (Olsson et al., 1987; Cohen, 1989; Haavik et al., 1989; Haystead et al., 1989, 1990). The inhibition of PP1 and PP2A by MCLR, MCRR, and nodularin increases the phosphorylation state of both cytoskeletal and cytosolic proteins of rat hepatocytes by greater than two-fold within 20 minutes of exposure (Eriksson et al., 1990). The general patterns of phosphorylation of proteins observed in hepatocytes treated with okadaic acid (Haystead et al., 1989) and the cyanobacterial toxins are similar (Eriksson et al., 1990). One of the metabolic consequences of protein phosphorylation in hepatocytes treated with either toxin is increased glycogenolysis and glucose production due to activation of phosphorylase a (Cohen et al., 1990;

Eriksson et al., 1990; Pace et al., 1991; Miura et al., 1991). The role of glycogen depletion in the pathogenesis of cyanobacterial toxicosis, if any, remains to be determined.

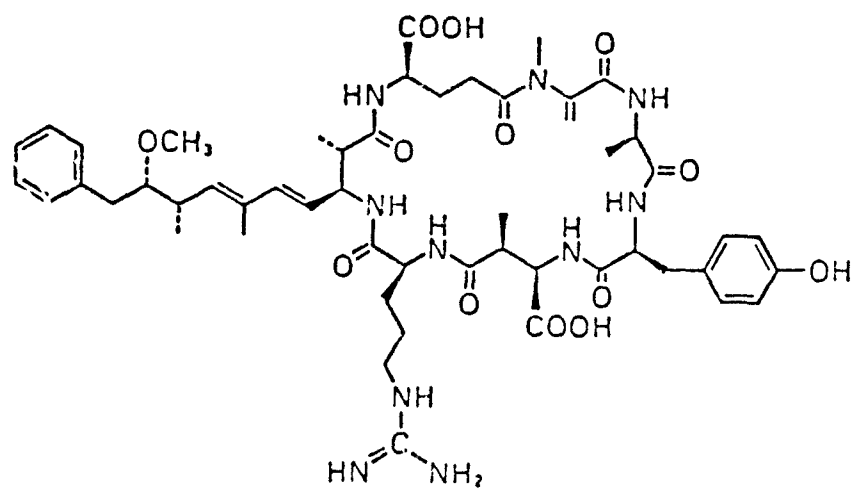
The link between cytosolic protein phosphatases and the marked reorganization of the cytoskeletal network (most notably microfilaments) believed to be responsible for lethality in cases of acute toxicosis (Hooser, 1989; Eriksson et al., 1989) is the subject of current investigation. Eriksson et al. (1990) have shown that treatment of rat hepatocytes with MCLR, MCRR, and nodularin (Figure 1) causes increased phosphorylation of cytoskeletal protein fractions which corresponds to myosin light chain proteins and the cytokeratins which comprise hepatocyte intermediate filaments. These results are analogous to the increased phosphorylation of vimentin and myosin light chain observed in calyculin A-treated fibroblasts (Chartier et al., 1990). Doses required to cause a marked increase in protein phosphorylation correspond well with doses causing complete reorganization of the microfilament network and subsequent hepatocyte deformation (Eriksson et al., 1990).

Assembly and disassembly of cytoskeletal elements is known to be influenced by their phosphorylation state. Several kinases affect microfilament organization and distribution (Herman and Pledger, 1985; Hirst et al., 1986; Lamb et al., 1988) and the assembly and disassembly of intermediate filaments (Inagaki et al., 1987; Geisler and Weber, 1988; Chou et al., 1989, 1990). Cortical microfilaments and intermediate filaments are known to interact in a complex fashion (Heuser and Kirshner, 1980; Bridgman and Reese, 1984; Green et al., 1987) such that alterations of the distribution of one element may perturb the entire cytoskeletal network. One of the consequences of increased phosphorylation of cytoskeletal proteins may be the disruption of liver desmosomes, facilitating hepatocyte detachment and consequent intrahepatic hemorrhage. Recent

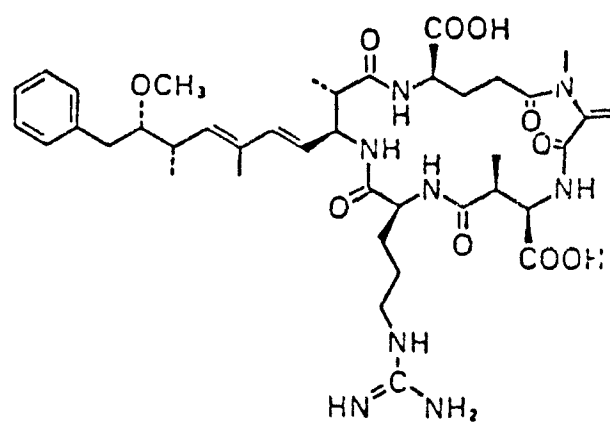
work has shown a decrease in the cytokeratin fraction of liver plasma membrane proteins in MCLR-treated rats (Miura et al., 1989,1991). The cytokeratins are intermediate filament proteins, and as such are associated with liver desmosomes.

The apparently inhibitory effects on protein phosphatases and the resultant increase in phosphorylation state of enzymes and cytoskeletal elements such as intermediate filaments may be responsible for the tendency of the algal peptide hepatotoxins to adhere to precipitable cytoskeletal proteins and to bring about the disruption in actin filaments which seems to result in rounding of hepatocytes, detachment, and lethal intrahepatic hemorrhage. Nevertheless, before this theory can be totally accepted, the cause and effect relationship must be demonstrated between biochemical changes and structural alterations.

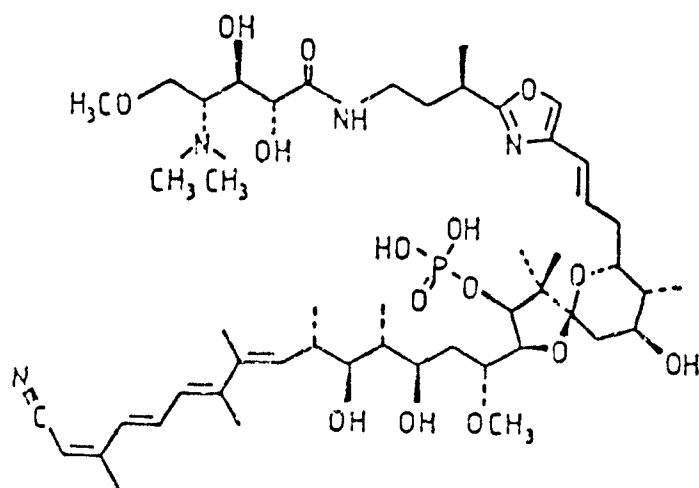
Figure 1. Structures of microcystin, nodularin, calyculin A, and okadaic acid.



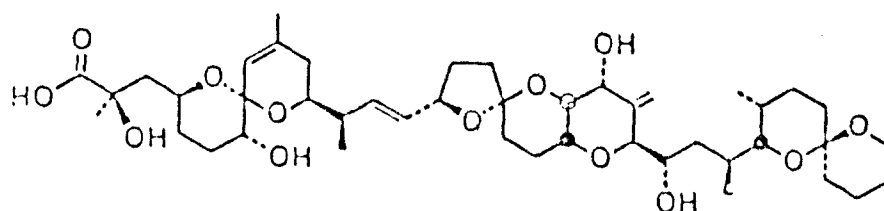
Microcystin YR



Nodularin



Calyculin-A



## X. REFERENCES

- Adams, W. H., Stoner, R. D., Adams, D. G., Slatkin, D. N., and Siegelman, H. W. (1985) Pathophysiologic effects of a toxic peptide from *Microcystis aeruginosa*. *Toxicon* 23(2):441-447.
- Adams, W. H., Stone, J. P., Sylvester, B., Stoner, R. D., Slatkin, D. N., Tempel, N. R., and Siegelman, H. W. (1988) Pathophysiology of cyanoginosin-LR: *In vivo* and *in vitro* studies. *Tox. Appl. Pharmacol.* 96:248-257.
- Arkin, H., Holmes, K. R., Chen, M. M., and Bottje, W. G. (1986) Thermal pulse decay method for simultaneous measurement of local thermal conductivity and blood perfusion: A theoretical analysis. *J. Biomech. Eng.* 108:208-214.
- Arkin, H., Holmes, K. R., and Chen, M. M. (1987) Computer-based system for continuous on-line measurements of tissue blood perfusion. *J. Biomed. Eng.* 9:38-45.
- Asaoka, K., and Takahashi, K. (1981) An enzymatic assay of reduced glutathione using glutathione S-aryltransferase with O-dinitrobenzene as a substrate. *J. Biochem.* 90:1237-1242.
- Ashworth, C. T., and Mason, M. F. (1946) Observations on the pathological changes produced by a toxic substance present in blue-green algae (*Microcystis aeruginosa*). *Am. J. Pathol.* 22(2):369-383.
- Aune, T., and Berg, K. J. (1986) Use of freshly prepared rat hepatocytes to study toxicity of blooms of the blue-green alga *Microcystis aeruginosa* and *Oscillatoria agardhii*. *J. Toxicol. Environ. Health* 19:325-336.



- Beasley, V. R., Coppock, R. W., Simon, J., Ely, R., Buck, W. B., Corley, R. A., Carlson, D. M., and Gorham, P. R. (1983) Apparent blue-green algae poisoning in swine subsequent to ingestion of a bloom dominated by *Anabaena spiroides*. *J. Am. Vet. Med. Assoc.* 182:413-414.
- Beasley, V. R., Cook, W. O., Dahlem, A. M., Hooser, S. B., Lovell, R. A., and Valentine, W. M. (1989) Algae intoxication in livestock and waterfowl. In: G. E. Burrows (ed.), *The Veterinary Clinics of North America Food Animal Practice*. W. B. Saunders Company, Philadelphia, pp. 345-362.
- Berg, K., and Soli, N. E. (1985) Effects of *Oscillatoria agardhii*-toxins on blood pressure and isolated organ preparations. *Acta Vet. Scand.*, 26:374-384.
- Berg, K., Wyman, J., Carmichael, W. and Dabholkar, A. (1988) Isolated rat liver perfusion studies with cyclic hepta peptide toxins of *Microcystis* and *Oscillatoria* (freshwater cyanobacteria). *Toxicon* 26:827-837.
- Bonagura, J. D., and Hamlin, R. L. (1986) Treatment of heart disease: An overview. In: Kirk, R. W. (ed.), *Current Veterinary Therapy IX: Small Animal Practice*, Vol. 9. W. B. Saunders, Philadelphia, pp. 319-323.
- Bossone, C. A., and Hannon, J. P. (1985) A multi-isotope procedure for simultaneously estimating the volume of body fluid compartments of swine. In: M. E. Tumbleson (ed.), *Proceedings of a Conference on Swine in Biomedical Research*. Plenum Press, New York, pp. 49-59.

- Botes, D. P., Viljoen, C. C., Kruger, H., Wessels, P. L., and Williams, D. H. (1982a) Configuration assignments of the amino acid residues and the presence of N-methyldehydroalanine in the toxins from the blue-green alga, *Microcystis aeruginosa*. *Toxicon* 20:1037-1042.
- Botes, D. P., Kruger, H., and Viljoen, C. C. (1982b) Isolation and characterization of four toxins from the blue-green alga, *Microcystis aeruginosa*. *Toxicon* 20(6):945-954.
- Botes, D. P., Tuinman, A. A., Wessels, P. L., Viljoen, C. C., Kruger, H., Williams, D. H., Santikarn, S., Smith, R. J., and Hammond, S. J. (1984) The structure of cyanoginosin-LA, a cyclic heptapeptide toxin from the cyanobacterium *Microcystis aeruginosa*. *J. Chem. Soc. Perkin Trans. 1*:2311-2318.
- Botes, D. P., Wessels, P. L., Kruger, H., Runnegar, M. T. C., Santikarn, S., Smith, R. J., Barna, J. C. J., and Williams, D. H. (1985) Structural studies on cyanoginosins -LR, -YR, -YA, and -YM, peptide toxins from *Microcystis aeruginosa*. *J. Chem. Soc. Perkin Trans. 1*:2747-2748.
- Bourke, A. T. C., and Hawes, R. B. (1983) Freshwater cyanobacteria (blue-green algae) and human health. *Med. J. Aust.* 1:491-492.
- Boyd, J. W. (1981) The mechanisms relating to increases in plasma enzymes and isoenzymes in diseases of animals. *Vet. Clin. Pathol.* 2:9-24.
- Bridgeman, P. C., and Reese, T. S. (1984) *J. Cell Biol.* 99:1655-1688.
- Brobst, D. (1983) Pathophysiologic and adaptive changes in acid-base disorders. *J. Am. Vet. Med. Assoc.* 183:773-780.

- Brooks, W. P., and Codd, G. A. (1986) Extraction and purification of toxic peptides from natural blooms and laboratory isolates of the cyanobacterium *Microcystis aeruginosa*. *Let. Appl. Micro.* 2:1-3.
- Brooks, W. P., and Codd, G. A. (1987) Distribution of *Microcystis aeruginosa* peptide toxin and interactions with hepatic microsomes. *Pharmacol. Toxicol.* 60:187-191.
- Cacciatore, L., and Antonello, S. (1971) Arginase activity of mouse serum and liver tissue in some conditions of experimental liver damage. *Enzymologia* 41:112-120.
- Cargill, C. F., and Shields, R. P. (1971) Plasma arginase as a liver function test. *J. Comp. Pathol.* 81:447-454.
- Carmichael, W. W. (1981) Freshwater blue-green algae (cyanobacteria) toxins—a review. In: W. W. Carmichael (ed.), *The Water Environment: Algal Toxins and Health*. Plenum Press, New York, p. 1.
- Carmichael, W. W. (1988) Toxins of freshwater algae. In: A. T. Tu (ed.), *Handbook of Natural Toxins. 3. Marine Toxins and Venoms*. Marcel Dekkar, New York, pp. 121-147.
- Carmichael, W. W., Eschedor, J. T., Patterson, G. M. L., and Moore, R. E. (1988a) Toxicity and partial structure of a hepatotoxic peptide produced by the cyanobacterium *Nodularia spumigena* Mertens emend. L575 from New Zealand. *Appl. Environ. Microbiol.* 54:2257-2263.
- Carmichael, W. W., Beasley, V. R., Bunner, D. L., Eloff, J. N., Falconer, I., Gorham, P., Harada, K.-I., Min-Juan, Y., Krishnamurthy, T., Moore, R. E., Rinehart, K. L., Runnegar, M. T., Skulburg, O., and Watanabe, M. (1988b) Naming of cyclic peptide toxins from cyanobacteria (blue-green algae). *Toxicon* 26:971-973.

- Carmichael, W. W., Beasley, V., Bunner, D. L., Eloff, J. N., Falconer, I., Gorham, P., Harada, K., Kirshnamurthy, T., Moore, R. E., Rinehart, K. L., Runnegar, M., Skulberg, O. M., Watanabe, M., and Yu, M.-J. Toxicon, in press.
- Chartier, L., Rankin, L., Allen, R., Kato, Y., Fusetani, N., Karaki, H., Watabe, S., and Hartshorne, D. (1990) *Cell Motil. Cytoskeleton* 18:26-40.
- Chou, Y.-H., Rosevear, E., and Goldman, R. D. (1989) *Natl. Acad. Sci. USA* 86:1885-1889.
- Chou, Y.-H., Bischoff, J. R., Beach, D., and Goldman, R. D. (1990) *Cell* 62:1063-1071.
- Codd, G. A., and Carmichael, W. W. (1982) Toxicity of a clinical isolate of the cyanobacterium *Microcystis aeruginosa* from Great Britain. *FEMS Microbiol. Let.* 13:409-411.
- Codd, G. A., and Poon, G. K. (1988) Cyanobacteria toxins. In: L. J. Rogers and J. G. Gallon (eds.), *Cyanobacteria toxins*. Oxford Science Publications, Clarendon Press, Oxford, England.
- Cohen, P. (1989) *Annu. Rev. Biochem.* 58:453-508.
- Cohen, P., Holmes, C. F. B., and Tsukitani, Y. (1990) *Trends Biochem. Sci.* 15:98-102.
- Cornelius, C. E., Douglas, G. M., Gronwall, R. R., and Freedland, R. A. (1963) Comparative studies on plasma arginase and transaminases in hepatic necrosis. *Cornell Vet.* 53:181-191.
- Cornelius, C. E. (1970) Liver function. In: Kaneko, J. J. (ed.), *Clinical Biochemistry of Domestic Animals*. Academic Press, New York, pp. 230-236.
- Côté, L.-M., Lovell, R. A., Jeffery, E. H., Carmichael, W. W., and Beasley, V. R. (1986) Failure of blue-green algae (*Microcystis aeruginosa*) hepatotoxin to alter *in vitro* mouse liver enzymatic activity. Proc. 8th Rocky Mountain Regional Meeting of Am. Chem. Soc., July 25-28, Denver, CO.

- Dabholkar, A. S., and Carmichael, W. W. (1987) Ultrastructural changes in the mouse liver induced by hepatotoxin from the freshwater cyanobacterium *Microcystin aeruginosa* strain 7820. *Toxicon* 25:285-292.
- Dahlem, A. M. (1989) Structure/toxicity relationships and fate of low molecular weight peptide toxins from cyanobacteria. PhD Thesis, University of Illinois.
- Dahlem, A. M., Harada, K. I., Harvis, C. A., Rinehart, K. L., Munro, M. H. G., Blunt, J. W., Mulligan, P. E., and Beasley, V. R. (1987) Structure/toxicity relationship of the dehydroamino acid from a cyclic peptide hepatotoxin produced by blue-green algae. The Toxicologist, Abstr. of 26th Ann. Meeting of Soc. Toxicol., Washington, DC.
- Dahlem, A. M., Beasley, V. R., Harada, K.-I., Matsuura, K., Suzuki, M., Harvis, C. A., Rinehart, K. L., and Carmichael, W. W. (1989a) The role of  $\alpha,\beta$ -unsaturated amino acids in the toxicity of microcystin-LR and nodularin, two hepatotoxins from cyanobacteria. *Toxicologist* 8:168 (#670), Abstr.
- Dahlem, A. M., Hassan, A. S., Swanson, S. P., Carmichael, W. W., and Beasley, V. R. (1989b) A model system for studying the bioavailability of intestinally administered microcystin-LR, a hepatotoxic peptide from the cyanobacterium *Microcystis aeruginosa*. *Pharmacol. Toxicol.* 64:177.
- Dahlem, A. M., Beasley, V. R., Hooser, S. B., Harada, K., Matsuura, K., Suzuki, M., Rinehart, K. L., Harvis, C. A., and Carmichael, W. W. (1990) The structure/toxicity relationship of alpha, beta-unsaturated amino acids in microcystin-LR and nodularin, two monocyclic peptide hepatotoxins from cyanobacteria. *Chem. Res. Toxicol.*, in press.

- Doust, R. (1958) The cell population of liver tissue and the cytological reference base. In: R. W. Brauer (ed.), *Liver Function, A Symposium on Approaches to the Quantitative Description of Liver Function*. Publication No. 4, American Institute of Biological Sciences, Washington, DC, pp. 3-10
- Drew, R., and Miners, J. O. (1984) The effects of buthionine sulfoximine (BSO) on glutathione depletion and xenobiotic biotransformation. *Biochem. Pharmacol.* 33:2989-2994.
- Duncan, J. R., and Prasse, K. W. (1977) *Veterinary Laboratory Medicine Clinical Pathology*. Iowa State University Press, Ames, Iowa.
- Eaton, D. L. and Klaassen, C. D. (1978) Carrier-mediated transport of ouabain in isolated hepatocytes. *J. Pharmac. Exp. Ther.* 205:480-488.
- Edler, L., Ferno, S., Lind, M. G., Lundberg, R., and Nilsson, P. O. (1985) Mortality of dogs associated with a bloom of the cyanobacterium *Nodularia spumigena* in the Baltic Sea. *Ophelia* 24:103-109.
- Elleman, T. C., Falconer, I. R., Jackson, A. R. B., and Runnegar, M. T. (1978) Isolation, characterization and pathology of the toxin from a *Microcystis aeruginosa* (= *Anacystis cynea* bloom). *Aust. J. Biol. Sci.* 31:209-218.
- Eriksson, J. E., Meriluoto, A. O., Kujari, H. P., Osterlund, K., Fagerlund, K., and Hallbom, L. (1988) Preliminary characterization of a toxin isolated from the cyanobacterium *Nodularia spumigena*. *Toxicon* 26:161-166.

- Eriksson, J. E., Paatero, G. I., Meriluoto, J. A., Codd, G., Kass, G. E., Nicotera, P. and Orrenius, S. (1989) Rapid microfilament reorganization induced in isolated rat hepatocytes by microcystin-LR, a cyclic peptide toxin. *Exp. Cell. Res.* 185:86-100.
- Eriksson, J. E., Tooivola, D., Meriluoto, J. A. O., Karaki, H., Han, Y.-G., and Hartshorne, D. (1990) *Biochem. Biophys. Res. Comm.* 173:1347-1353.
- Estrela, J. M., Saez, G. T., Such, L., and Vina, J. (1983) The effect of cysteine and N-acetylcysteine on rat liver glutathione (GSH). *Biochem. Pharmacol.* 32:3483.
- Falconer, I. R., Jackson, A. R. B., Langley, J., and Runnegar, M. T. (1981) Liver pathology in mice by the blue-green alga *Microcystis aeruginosa*. *Aust. J. Biol. Sci.* 34:179-187.
- Falconer, I. R., Beresford, A. M., and Runnegar, M. T. C. (1983) Evidence of liver damage by a toxin from a bloom of the blue-green alga *Microcystis aeruginosa*. *Med. J. Aust.* 1:511-514.
- Falconer, I. R., Buckley, T., and Runnegar, M. T. C. (1986) Biological half-life, organ distribution and excretion of  $^{125}\text{I}$ -labeled toxic peptide from the blue-green alga *Microcystis aeruginosa*. *Aust. J. Biol. Sci.* 39:17-21.
- Faulstich, H., and Münter, K. (1986) New aspects of phalloidin poisoning. *Klin. Wochenschr.* 64(Suppl. VII):66-70.
- Fleiss, J. L. (1981) *Statistical Methods for Rates and Proportions*, 2nd edition. John Wiley, New York, pp. 100-109.
- Fox, P. R. (1986) Cor pulmonale. In: Kirk, R. W. (ed.), *Current Veterinary Therapy IX: Small Animal Practice*, Vol. 9. W. B. Saunders, Philadelphia, pp. 313-317.

- Fox, J. E., Boyles, J. K., Reynolds, C. C. and Phillips, D. R. (1984) Actin filament content and organization in unstimulated platelets. *J. Cell. Biol.* 98:1985-1991.
- Francis, G. (1878) Poisonous Australian lake. *Nature (London)* 18:11-12.
- Frimmer, M. (1982) Organotropism by carrier mediated transport. *Trends Pharmacol. Sci.* 3:395-397.
- Fujiki, H., Suganoma, M., Yoshizawa, S., Kanazawa, H., Sugimura, T., Manam, S., Kahn, S. M., Jiang, W., Hoshina, S., and Weinstein, I. B. (1989) *Molecular Carcinogenesis*. 2:184-187.
- Galey, F. D., Beasley, V. R., Carmichael, W. W., Kleppe, G., Hooser, S. B., and Haschek, W. M. (1987) Blue-green algae (*Microcystis aeruginosa*) hepatotoxicosis in dairy cows. *Am. J. Vet. Res.* 48:1415-1420.
- Gatherole, P. S., and Thiel, P. G. (1987) Liquid chromatographic determination of the cyanoginosins, toxins produced by the cyanobacterium *Microcystis aeruginosa*. *J. Chromatog.* 408:435-440.
- Geisler, N., and Weber, K. (1988) *EMBO J.* 7:15-20.
- Glende, E. A. Jr. (1972) Carbon tetrachloride-induced protection against carbon tetrachloride toxicity. *Biochem. Pharmacol.* 21:1697-1702.
- Gorham, P. R. (1960) Toxic water blooms of blue-green algae. *Can. Vet. J.* 1:235-245.
- Green, T., and Lock, E. A. (1984) The metabolism of xenobiotic conjugates and renal injury. In: P. H. Bach and E. A. Lock (eds.), *Renal Heterogeneity and Target Cell Toxicity*. Proc. Second Internat. Symp. Nephrotox., John Wiley and Sons, p. 135.
- Green, K. G., Geiger, B., Jones, J. C. R., Talian, J. C., and Goldman, R. D. (1987) *J. Cell Biol.* 104:1389-1402.



- Greenberg, D. M. (1960) Arginase. In: Boyer, P. D., Lardy, H., and Myrback, K. (eds.), *The Enzymes*. Academic Press, New York, pp. 259-267.
- Gross, E. (1975) Subtilin and nisin: The chemistry and biology of peptides with  $\alpha,\beta$ -unsaturated amino acids. In: R. Walter and J. Meienhofer (eds.), *Peptides: Chemistry, Structure and Biology*. Ann Arbor Scientific, Ann Arbor, MI, pp. 31-42.
- Haavik, J., Schelling, D. L., Campbell, D. G., Anderson, K. K., Flatmark, T., and Cohen, P. (1989) FEBS Lett. 251:36-42.
- Harada, K.-I., Matsuura, K., Suzuki, M., Oka, H., Watanabe, M. F., Oishi, S., Dahlem, A. M., Beasley, V. R., and Carmichael, W. W. (1988a) Analysis and purification of toxic peptides from cyanobacteria by reversed-phase high-performance liquid chromatography. *J. Chrom.* 448:275-283.
- Harada, K. I., Suzuki, M., Dahlem, A. M., Beasley, V. R., Carmichael, W. W., and Rinehart, K. L. (1988b) Improved method for purification of toxic peptides produced by cyanobacteria. *Toxicon* 26:433-439.
- Hawkins, P. R., Ronnegar, M. T., and Jackson, A. R. B. (1985) Severe hepatotoxicity caused by the tropical cyanobacterium (blue-green alga) *Cylindrospermopsis raciborskii* (Woloszynska) Seenya and Subba Raju isolated from a domestic water supply reservoir. *Appl. Environ. Micro.* 50:1292.
- Haystead, T. J., Sim, A. T. R., Carling, D., Honnor, R. C., Tsukitani, Y., Cohen, P., and Hardie, D. G. (1989) *Nature* 337:78-81.
- Haystead, T. A. J., Moore, E., Cohen, P., and Hardie, D. G. (1990) *Eur. J. Biochem.* 187:199-205.

- Herman, B., and Pledger, W. J. (1985) J. Cell Biol. 100:1031-1040.
- Heuser, J., and Kirshner, M. W. (1980) J. Cell Biol. 86:212-234.
- Hirst, R., Horwitz, A., Buck, C., and Rohrschneider, L. (1986) Proc. Natl. Acad. Sci. USA 83:6470-6474.
- Hofmann, A. F. (1983) The enterohepatic circulation of bile acids in health and disease. In: M. H. Sleisenger and J. S. Fordtran (eds.), *Gastrointestinal Disease*. W. B. Saunders Co. Publishing, Philadelphia, PA, pp. 115-134.
- Honkanen, R. E., Zwiller, J., Moore, R. E., Daily, S. L., Khattri, B. S., Dukelow, M., and Boynton, A. L. (1990) J. Biol. Chem. 265:19401-19404.
- Hooser, S. B. (1989) Toxicopathology of microcystin-LR *in vivo* and *in vitro*. PhD Thesis, Univ. of Illinois, Urbana, Illinois, 214 pp.
- Hooser, S. B., Basgall, E. J., Beasley, V. R., and Haschek, W. M. (1988) Sequential ultrastructural hepatic, pulmonary and renal changes due to *Microcystis aeruginosa*. Toxicologist 8(1):219, Abstr. 871.
- Hooser, S. B., Beasley, V. R., Carmichael, W. W., Lovell, R. A., and Haschek, W. M. (1989a) Toxicity of microcystin-LR, a cyclic heptapeptide toxin from *Microcystis aeruginosa* in rats and mice. Vet. Pathol. 26:246-252.
- Hooser, S. B., Beasley, V. R., Kuhlenschmidt, M. S., and Haschek, W. M. (1989b) Microcystin-LR induces morphologic and cytoskeletal hepatocyte changes *in vitro* and *in vivo*. Toxicologist 9(11):127.

- Hooser, S. B., Waite, L. L., Beasley, W. V., Carmichael, W. W., Kuhlenschmidt, M. S., and Haschek, W. M. (1989c) Microcystin-A induces morphologic and cytoskeletal hepatocyte changes *in vitro*. *Toxicon* 27:50-51.
- Hooser, S. B., Beasley, V. R., Basgall, E. J., Carmichael, W. W. and Haschek, W. M. (1990a) Ultrastructural changes induced by microcystin-LR in rats. *Vet. Pathol.* 27:9-15.
- Hooser, S. B., Beasley, V. R., Waite, L. L., Kuhlenschmidt, M. S., Carmichael, W. W. and Haschek, W. M. (1990b) Actin filament alterations in rat hepatocytes induced *in vivo* and *in vitro* by microcystin-LR, a hepatotoxin from the blue-green alga, *Microcystis aeruginosa*. *Vet. Pathol.*, in press.
- Hooser, S. B., Beasley, V. R., Waite, L. L., Kuhlenschmidt, M. S., Carmichael, W. W., and Haschek, W. M. Cytoskeletal alterations in rat hepatocytes induced by microcystin-LR, a hepatotoxin from the blue-green alga *Microcystis aeruginosa*. *Toxicol. Appl. Pharm.*, submitted.
- Igwe, O. J. (1986) Biologically active intermediates generated by the reduced glutathione conjugation pathway---Toxicological implications. *Biochem. Pharmacol.* 35:2987.
- Inagaki, M., Nishi, Y., Nishizawa, K., Matsuyama, M., and Sato, C. (1987) *Nature*. 328:649-652.
- Ishihara, H., Martin, B. L., Brautigan, D. L., Karaki, H., Ozaki, H., Kato, Y., Fusetani, N., Watabe, S., Hashimoto, K., Uemura, D., and Hartshorne, D. J. (1989) *Biochem. Biophys. Res. Comm.* 159:871-877.
- Jackson, A. R. B., McInnes, A., Falconer, I. R., and Runnegar, M. T. C. (1983) Toxicity for sheep of the blue-green alga, *Microcystis aeruginosa*. *Toxicon* 3(Suppl):191-194.

- Jackson, A. R. B., McInnes, A., Falconer, I. R., and Runnegar, M. T. C. (1984) Clinical and pathological changes in sheep experimentally poisoned by the blue-green alga, *Microcystis aeruginosa*. Vet. Pathol. 21:102-113.
- Kfir, R., Johannson, E., and Botes, D. P. (1986) Monoclonal antibody specific for cyanoginosin-LA: Preparation and characterization. Toxicon 24:543-552.
- Konst, H., McKercher, P. D., Gorham, P. R., Robertson, A., and Howell, J. (1965) Symptoms and pathology produced by toxic *Microcystis aeruginosa* NRC-1 in laboratory and comestic animals. Can. J. Comp. Med. Vet. Sci. 29:221-228.
- Krishnamurthy, T., Carmichael, W. W., and Sarver, E. W. (1986a) Toxic peptides from freshwater cyanobacteria (blue-green algae). I. Isolation, purification, and characterization of peptides from *Microcystis aeruginosa* and *Anabaena flos-aquae*. Toxicon 24:865-873.
- Krishnamurthy, T., Szafraniec, L., Sarver, E. W., Hunt, D. F., Shabanowitz, J., Carmichael, W. W., Missler, S., Skulberg, O., and Codd, G. (1986b) Amino acid sequences of fresh water blue-green algal toxic peptides by fast atom bombardment tandem mass spectrometric technique. Abstracts of papers. 34th Ann. Conf. Mass Spectrometry Allied Topics, Cincinnati, OH, pp. 93-94.
- Kuhlenschmidt, M. S., Schmell, E., Slife, C. W., Kuhlenschmidt, T. B., Sieber, F., Lee, Y. C. and Roseman, S. (1982) Studies on the intercellular adhesion of rat and chicken hepatocytes. Conditions affecting cell-cell specificity. J. Biol. Chem. 257:3157-3164.
- Kuhlenschmidt, T. B., Kuhlenschmidt, M. S., Roseman, S. and Lee, Y. C. (1984) Binding and endocytosis of glycoproteins by isolated chicken hepatocytes. Biochemistry 23:6437-6444.

- Kungsuwan, A., Noguchi, T., Watanabe, M. F., Matsunaga, S., Watabe, S., and Hashimoto, K. (1987) Isolation of two toxins from the blue-green alga *Microcystis aeruginosa*. Nippon Suisan Gakkaishi 53:2051-2054.
- Kusumi, T., Ooi, T., Watanabe, M., Takahash, H., and Kakisawa, H. (1987) Cyanoviridin-RR, a toxin from the cyanobacterium (blue-green alga) *Microcystis viridis*. Tetrahedron Lett. 28:4695-4698.
- Lafranconi, W. M., Glatt, H., and Oesch, F. (1986) Xenobiotic metabolizing enzymes of rat liver nonparenchymal cells. Toxicol. Appl. Pharmacol. 84:500-511.
- Lamb, N. J. C., Fernandez, A., Conti, M. A., Adelstein, R., Glass, D. B., Welch, W. J., and Feramisco, J. R. (1988) J. Cell Biol. 106:1955-1970.
- Louw, P. G. J., and Smit, J. D. (1950) The active constituent of the poisonous algae, *Microcystis toxica* stephens; with a note on experimental coses of algae poisoning in small animals. S. Afr. Ind. Chem. 4:62-66.
- Lovell, R. A., Beasley, V. R., Dahlem, A. M., and Carmichael, W. W. (1985) The effects of prior administration(s) of phenobarbital or piperonyl butoxide on the toxicity of microcystin-LR in Balb/c mice. Unpublished data.
- Lovell, R. A., Schaeffer, D. J., Hooser, S. B., Dahlem, A. M., Haschek, W. M., Carmichael, W. W., and Beasley, V. R. (1989) Toxicity of one or two intraperitoneal doses of microcystin-LR in two strains of male mice. J. Environ. Pathol. Toxicol. Oncol. 9:221-238.
- MacKintosh, C., Beattie, K. A., Klumpp, S., Cohen, P., and Codd, G. A. (1990) FEBS Lett. 264:187-192.

- Mahmood, N. A., Carmichael, W. W., and Pfahler, D. (1988) Anticholinesterase poisonings in dogs from a cyanobacteria (blue-green algae) bloom dominated by *Anabaena flos-aquae*. *Am. J. Vet. Res.* 49:500-503.
- Massarrat, S. (1965) Enzyme kinetics, half-life and immunological properties of I-131-labeled transaminases in pig blood. *Nature* 206:508-509.
- Matson, C. F., Robinson, N. A., and Pace, J. S. (1990) *FASEB J.* 4:141A.
- Matsuo, H., and Norita, L. (1975) Improved tritium-labeling for quantitative C-terminal analysis. In: S. B. Needleman (ed.), *Protein Sequence Determination: A Sourcebook of Methods and Techniques*. Springer-Verlag, New York, pp. 104-113.
- Meriluoto, J. A. O., and Eriksson, J. E. (1988) Rapid analysis of cyanobacterial peptide toxins. *J. Chromatog.* 438:93-99.
- Mia, K. S., and Koger, H. D. (1978) Direct colorimetric determination of serum arginase in various domestic animals. *Am. J. Vet. Res.* 39:1381-1383.
- Miller, L. C., and Tainter, M. L. (1944) Estimation of the ED50 and its error by means of logarithmic-probit graph paper. *Proc. Soc. Exp. Biol. (New York)* 57:261-264.
- Miura, G. A., Robinson, N. A., Geisbert, T. W., Bostrain K. A., White, J. D., and Pace, J. G. (1989) *Toxicon* 27:1229-1240.
- Miura, G. A., Robinson, N. A., Lawrence, W. B., and Pace, J. G. (1991) *Toxicon* 29:337-346.
- Noda, K., Shimohigashi, Y., and Izumiya, N. (1983)  $\alpha,\beta$ -dehydroamino acids and peptides. In: N. L. Benolton (ed.), *The Peptides*. Academic Press, Inc., New York, pp. 285-339.
- Oishi, S., and Watanabe, M. F. (1986) Acute toxicity of *Microcystis aeruginosa* and its cardiovascular effects. *Environ. Res.* 40:518-524.

- Olsson, H., and Belfrage, P. (1987) *Eur. J. Biochem.* 168:399-405.
- Osheim, D. L., and Ross, R. P. (1985) Atomic absorption spectrophotometric determination of liver copper: Collaborative study. *J. Assoc. Off. Anal. Chem.* 68:44-45.
- Ostensvik, O., Skulberg, O. M., and Soli, N. E. (1981) Toxicity studies with blue-green algae from Norwegian inland waters. In: Carmichael, W. W. (ed.), *The Water Environment: Algal Toxins and Health*. Plenum Press, New York, pp. 315-324.
- Pace, J. G., Robinson, N. A., Miura, G. A., Matson, C. F., Geisbert, T. W., and White, C. F. (1991) *Toxicol. Appl. Pharmacol.* 107:391-401.
- Painuly, P., Perez, R., Fukai, T., and Shimizu, Y. (1988) The structure of a cyclic peptide toxin, cyanogenosin-RR from *Microcystis aeruginosa*. *Tetrahedron Let.* 29:11-14.
- Phyllis, J. W. (1976) *Veterinary Physiology*. W. B. Saunders Company, Philadelphia, p. 278.
- Porembska, Z., Baranczyk, A., and Jachimowicz, J. (1971) Arginase isoenzymes in liver and kidney of some mammals. *Acta Biochem.* 18:79-85.
- Prentki, M., Chaponnier, C., Jeanrenand, B., and Gabbiani, G. (1979) Actin microfilaments, cell shape, and secretory processes in isolated rat hepatocytes. *J. Cell Biol.* 81:592-607.
- Reid, E., and Williamson, R. (1974) Centrifugation. In: S. Fleischer and L. Packer (eds.), *Methods in Enzymology*, Vol. XXXI. pp. 713-734.
- Rinehart, K. L., Harada, K.-I., Namikoshi, M., Chen, C., Harvis, C. A., Munro, M. H. G., Blunt, J. W., Mulligan, P. E., Beasley, V. R., Dahlem, A. M., and Carmichael, W. W. (1988) Nodularin, microcystin, and the configuration of Adda. *J. Am. Chem. Soc.* 110:8557-8558.

- Robinson, N. A., Mirua, G. A., Geisbert, T., Bostian, K., White, J., and Pace, J. G. (1988) Structural effects and subcellular distribution of [<sup>3</sup>H]cyanoginosin-LR in perfused rat liver. 9th World Cong. Anim., Plant, and Microbial Toxins fo the Int. Soc. Toxicol., Stillwater, OK, p. 74, July 31-August 5, Abstr.
- Pobinson, N. A., Miura, G. A., Matson, C. F., Dinterman, R. E., and Pace, J. G. (1989) Characterization of chemically tritiated microcystin-LR and its distribution in mice. *Toxicon* 27:1035-1042.
- Robinson, N. A., Matson, C. F., and Pace, J. G. (1991) *Toxicologist* 11(1):622.
- Runnegar, M. T., and Falconer, I. R. (1981) Isolation, characterization, and pathology of the toxin from the blue-green alga *Microcystis aeruginosa*. In: W. W. Carmichael (ed.), *The Water Environment: Algal Toxins and Health*. Plenum Press, New York, pp. 325-342.
- Runnegar, M. T. C., and Falconer, I. R. (1982) The *in vivo* and *in vitro* biological effects of the peptide hepatotoxin from the blue-green alga, *Microcystis aeruginosa*. *S. Afr. J. Sci.* 78:363-366.
- Runnegar, M. T., and Falconer, I. R. (1986) Effect of toxin from the cyanobacterium *Microcystis aeruginosa* on ultrastructural morphology and actin polymerization in isolated hepatocytes. *Toxicon* 24:109-115.
- Runnegar, M. T., Falconer, I. R., and Silver, J. (1981) Deformation of isolated rat hepatocytes by a peptide hepatotoxin from the blue-green alga *Microcystis aeruginosa*. *Arch. Pharmacol.* 317:268-272.
- Runnegar, M. T. C., Falconer, I. R., Buckley, T., and Jackson, A. R. B. (1986) Lethal potency and tissue distribution of <sup>125</sup>I-labelled toxic peptides. *Toxicon* 24:506-509.



- Runnegar, M. T. C., Andrews, J., Gerdes, R. G., and Falconer, I. R. (1987) Injury to hepatocytes induced by a peptide toxin from the cyanobacterium *Microcystis aeruginosa*. *Toxicon* 25:1235.
- Runnegar, M. T. C., Jackson, A. R. B., and Falconer, I. R. (1988) Toxicity of the cyanobacterium *Nodularia spumigena* Mertens. *Toxicon* 26:143-151.
- Sager, P. R., Syversen, T. L., Clarkson, T. W., Cavanagh, J. B., Elgsaeter, A., Guldberg, H. C., Lee, S. D., Lichtman, M. A., Mottet, N. K., and Olmsted, J. B. (1986) Structure and function of the cytoskeleton. In: T. Clarkson, P. Sager, and T. Syversen (eds.), *The Cytoskeleton: A Target for Toxic Agents*. Plenum Press, New York, NY, pp. 3-21.
- Sasner, J. J. Jr., Ikawa, M., and Foxail, T. L. (1984) Studies on *Aphanizomenon* and *Microcystis* toxins. In: E. P. Ragelis (ed.), *Seafood Toxins*. Am. Chem. Soc. Symp. Series 262, Washington, DC, pp. 391-406.
- Schwimmer, M., and Schwimmer, D. (1968) Medical aspects of phycology. In: D. F. Jackson (ed.), *Algae, Man and the Environment*. Syracuse University Press, Syracuse, New York, pp. 279-358.
- Shimohigashi, Y., Lee, S., Kato, T., and Izumiya, N. (1978) Cyclic peptides. IV. Synthesis of diastereomeric dihydro-AM-toxin I and its analogs. *Bull. Chem. Soc. Jpn.* 51:584-588.
- Siegelman, A. W., Adams, N. H., Stoner, R. D., and Slatkin, D. W. (1984) Toxins of *Microcystis aeruginosa* and their hematologic and histopathological effects. In: E. Ragelis (ed.), *Seafood Toxins*. Am. Chem. Soc. Symp. Series 262, Washington, DC, p. 407.
- Skrzypek-Osieceka, I., Rahden-Staron, I., and Porembaska, Z. (1980) Subcellular localization of arginase in rat liver. *Acta Biochem. Pol.* 27:203-208.

- Slatkin, D. N., Stoner, R. D., Adams, W. H., Kycia, J. H., and Siegelman, H. W. (1983) Atypical pulmonary thrombosis caused by a toxic cyanobacterial peptide. *Science* 220:1383-1385.
- Snedecor, G. W., and Cochran, W. G. (1967) *Statistical Methods*, Vol. 6. Iowa State University Press, Ames, pp. 152-156.
- Steyn, D. G. (1945) Poisoning of algae and human beings by algae. *S. Afr. J. Sci.* 41:243.
- Stowe, C. M., Monson, E., Abdullah, A. S., and Barnes, D. (1981) Blue-green algae poisoning (*Microcystis aeruginosa*) in a dairy herd. *Bov. Clin.* 1:6-8.
- Sumitani, A. (1977) Immunological studies of liver arginase in man and various kinds of vertebrates. *Hiroshima J. Med. Sci.* 26:59-80.
- Sun, J. D., Ragsdale, S. S., Benson, J. M., and Henderson, R. F. (1985) Effects of the long-term depletion of reduced glutathione in mice administered L-buthionine-S,R-sulfoximine. *Fund. Appl. Toxicol.* 5:913-919.
- Theiss, W. C., and Carmichael, W. W. (1986) Physiological effects of a peptide toxin produced by the freshwater cyanobacteria (blue-green algae) *Microcystis aeruginosa* strain 7820. In: P. S. Steyn and R. Vleggar (eds.), *Mycotoxins and Phycotoxins, Bioactive Molecules*, Vol. I. Elsevier, Amsterdam, pp. 353-364.
- Tukey, J. W. (1977) *Exploratory Data Analysis*. Reading, A, Addison-Wesley.
- Tustin, R. C., van Rensburg, S. J., and Eloff, J. N. (1973) Hepatic damage in the primate following ingestion of toxic algae. In: S. J. Saunders and J. Terblanche (eds.), *Liver: Proceedings International Liver Congress*. Pitman Medical, London, pp. 383-385.

- Velleman, P. F., and Hoaglin, D. C. (1981) *Applications, Basic and Computing of Exploratory Data Analysis*. Duxbury Press, Boston, MA.
- Vina, J., Romero, T. J., Estrela, J. M., and Vina, J. R. (1980) Effect of acetaminophen (paracetamol) and its antagonist, on glutathione (GSH) content in rat liver. *Biochem. Pharmacol.* 29:1968-1970.
- Wanson, J. C., and Mosselmans, R. (1980) Coculture of adult rat hepatocytes and sinusoidal cells: A new experimental model for the study of ultrastructural and functional properties of liver cells. In: H. Popper, F. Gudat, L. Bianchi, and W. Reutter (eds.), *Communications of Liver Cells*. MTP Press, Ltd., Lancaster, England, pp. 239-251.
- Weiland, T. (1977) Modification of actins by phallotoxins. *Naturwissen.* 64:303-309.
- Weiland, T. (1986) Molecular mechanisms of toxicity. In: A. Rich (ed.), *Peptides of Poisonous Amanita Mushrooms*. Springer-Verlag, New York, NY, p. 161.
- Weiland, T., Nassal, M., Kramer, W., Fricker, G., Bickel, U. and Kurz, G. (1984) Identity of hepatic membrane transport systems for bile salts, phalloidin, and antamanide by photoaffinity labeling. *Proc. Natn. Acad. Sci.* 81:5232-5236.
- Wilkinson, L. (1988) SYSTAT: The system for statistics. Systat, Inc., Evanston, IL.
- Winer, B. J. (1971) *Statistical Principles in Experimental Design*, 2nd edition. McGraw-Hill Book Company, New York.
- Yoshizawa, S., Matsushima, M., Watanabe, M. F., Harada, K., Ichihara, A., Carmichael, W. W., and Fujiki, H. (1990) *J. Cancer Res. Clin. Oncol.* 116:609-614.

- Zachary, J. M., Cleveland, G., Kwock, L., Laurence, T., Weissman, R. M., Nabell, L., Fried, F. A., Staab, E. V., Risinger, M. A., and Lin, S. (1986) Actin filament organization of the Dunning R3327 rat prostatic adenocarcinoma system: Correlation with metastatic potential. *Cancer Res.* 46:926-932.
- Zand, M. S., and Albrecht-Beuhler, G. (1989) What structures, besides adhesions, prevent cells from rounding up? *Cell. Motil.* 13:195-211, 1989.
- Ziegler, K., and Frimmer, M. (1986) Molecular aspects of cytoprotection by modified somatostatins. *Klin. Wschr.* 64(Suppl VII):87-89.
- Zin, L. L., and Edwards, W. C. (1979) Toxicity of blue-green algae in livestock. *Bov. Pract.* 14:151-153.

## ANATOXINS

### I. CHARACTERIZATION OF THE NEUROMUSCULAR BLOCKADE PRODUCED *IN VIVO* BY ANATOXIN-A IN THE RAT; AND THE INFLUENCE OF STRUCTURAL CONFIGURATION

#### A. Statement of the Problem, Background, and Rationale

Most studies of the toxic effects of (+)anatoxin-a (antx-a) on skeletal muscle and motor neurons have utilized systems *in vitro*, often relying upon single cell preparations. Although experiments *in vitro* can yield detailed information regarding specific sites and mechanisms of action, caution must be exercised in extrapolation of results to intact animals. The isolation of tissues from biochemical processes and the use of high concentrations and/or prolonged periods of exposure may alter the action of the agent under investigation and precludes the influences of pharmacokinetics *in vivo*.

It was surmised that a detailed assessment of the neuromuscular blockade produced by (+)antx-a in the IV dosed rat could yield information that would very likely be relevant to physiologic effects produced under circumstances of natural exposure. Specifically, the indirectly evoked compound action potentials (ECAP) of the plantar muscles of the rat were used to determine the dose response and duration of action of the neuromuscular blockade produced by (+)antx-a *in vivo*. The effect of (+)antx-a on the latency and duration of the ECAP and maximum motor nerve conduction velocity were investigated. In addition, LD<sub>50</sub>

values for IP doses of (+)antx-a and racemic antx-a in mice, and the lethal potency of (-)antx-a were evaluated.

## **B. Experimental Methods**

### Anatoxin-a

Hydrochloride salts of synthetic (+)antx-a, (-)antx-a, and racemic antx-a were assessed to be > 95% pure based on: a) thin-layer chromatography using silica gel plates and a mobile phase of n-butanol-acetic acid-water (2:1:1) and visualization by iodine vapor and ultraviolet absorption, b) chemical and electron ionization mass spectroscopy, and c) high-performance liquid chromatography using a mobile phase of 0.01 M aqueous ammonium chloride-methanol (9:1) and detection by UV absorbance at 227 nm. All doses of antx-a in this report refer to its hydrochloride salt.

### LD<sub>50</sub> Determinations

Five treatment groups each consisting of six male Balb/c mice (Harlan Sprague-Dawley, Indianapolis, IN) (20 to 28 g) were dosed IP with 0.4 to 0.7 ml of normal saline containing (+)antx-a hydrochloride or racemic antx-a hydrochloride. All animals were observed for a 30-minute period following toxin administration and the number of deaths in each treatment group recorded. LD<sub>50</sub>s were determined using the trimmed logit method (Sanathanan et al., 1987).

### Toxicity Assessment of (-)Anatoxin-a

Male Balb/c mice (24 to 28 g) were dosed IP with (-)antx-a at 1, 5, 9, 20, 40, or 73 mg/kg in 0.2 to 1.0 ml of 0.9% saline. One animal was used at each dose. The mice were

observed for 30 minutes following administration of toxin at which time they were subjected to euthanasia with an IP injection of sodium pentobarbital.

#### Dose Response and Duration of Action

Male Sprague-Dawley rats (Harlan Sprague-Dawley, Indianapolis, IN) (320 to 420 g) were used in this investigation. Anesthesia was induced by inhalation of methoxyflurane and IP injection of sodium pentobarbital at 50 mg/kg, then maintained by IV injection of sodium pentobarbital. Respiration was supported with a Harvard rodent respirator using a 16-gauge catheter as an endotracheal tube.

To assess neuromuscular transmission, the posterior tibial nerve was stimulated at the medial side of the tarsus with supramaximal electrical stimulation by pulses of 100 msec duration applied at 0.2 Hz for single pulses and at 10 Hz for repetitive stimulation using subdermal needle electrodes. The ECAP of the lumbrical or interosseous muscles on the plantar surface of the hind foot were recorded with subdermal electrodes and a Tracor Northern EMG 3601. Nominal parameters for data acquisition were 500 data points, acquisition time 10 ms, low filter 0.5 Hz, and high filter 3,000 Hz. Temperature was maintained using radiant heat and monitored with a thermistor applied to the ventral surface of the thigh. The amplitude of the ECAP was determined from the maximum negative deflection relative to the isoelectric line. Amplitudes for repetitive stimulation were determined in the same manner and decrements calculated from the ratio of the fourth ECAP to the first ECAP.

Three treatment groups, each consisting of four rats, were dosed IV with of 0.1 to 0.5 ml of normal saline containing 50, 100, 200, or 800 mg of (+)antx-a hydrochloride/kg body weight. A control group of four rats was administered 0.2 ml of normal saline.

The ECAP was measured until at least 75% of the pret toxin ECAP amplitude had been recovered. The following values relating to the time profile of blockade were measured: a) onset time, the time from injection to maximum reduction of the ECAP; b) duration of action, the time from injection of antx-a to 75% recovery of the predose ECAP; and c) the maximum depression of the ECAP observed. For repetitive stimulation, the maximum decrement and the duration of a decrement  $> 15\%$  were determined.

Following arcsin transformation (Winer, 1971), values of the groups for percent depression and percent decrement were compared using multivariate analysis of variance followed by linear contrasts. After square root transformation to achieve homogeneous variances (Winer, 1971), the durations of action for (+)antx-a hydrochloride induced depression and decrement of the ECAP were compared using one-way analysis of variance and Tukey's HSD test. To compensate for small sample size while conserving statistical power, a significance level of  $\alpha < 0.1$  was chosen for these comparisons. With one exception (Table 1), P values for significantly different groups were actually  $\leq 0.05$ . The  $ED_{50}$  for depression of the ECAP was estimated using the trimmed logit method (Sanathanan et al., 1987).

#### Nerve Conduction Velocity, ECAP Latency, and Duration Measurements

Methods for anesthesia and data acquisition were the same as those described above in the dose response and duration of action studies. To measure motor nerve conduction



velocity, a proximal stimulating cathode electrode was placed near the sciatic nerve and a distal stimulating cathode electrode was used on the posterior tibial nerve at the medial side of the ankle. Maximum motor nerve conduction velocity was calculated by taking the distance between the two stimulating sites and dividing by the difference in the latency times.

Two treatment groups, each consisting of four rats, were dosed IV with either 0.2 ml of normal saline or approximately 0.2 ml of normal saline containing a dose of (+)antx-a hydrochloride at 100 µg/kg body weight. The latency, duration, and depression of the ECAP, as well as nerve conduction velocity were monitored for a period of 15 minutes following injection of saline or saline with toxin. Each data point consisted of the average of 3 measurements for each animal taken at 1-minute intervals. The 15-minute time period permitted maximal changes in these parameters to occur. Maximum motor nerve conduction velocities (m/sec) were compared using univariate repeated measures analysis. For repeated measures analysis of percent change in latency, the RTI rank transformation (Conover and Iman, 1981) was used to remove heterogeneity due to values at two time points for one treated animal being more than an order of magnitude larger than any other value in either group. To compensate for small sample sizes while conserving statistical power, a significance level of  $\alpha = 0.1$  was chosen for these comparisons.

### C. Results

#### LD<sub>50</sub> Determinations

Percent lethality for the (+)antx-a hydrochloride and racemic antx-a hydrochloride dosed groups plotted against dose are shown in Figure 1. The LD<sub>50</sub>s (95% confidence

limits) for (+)antx-a hydrochloride and racemic antx-a hydrochloride were 386  $\mu\text{g/kg}$  (365, 408  $\mu\text{g/kg}$ ) and 913  $\mu\text{g/kg}$  (846, 985  $\mu\text{g/kg}$ ), respectively. No deaths or clinical signs were observed in mice given (-)antx-a hydrochloride at up to 73 mg/kg.

#### Dose Response and Duration of Effect

The amplitude of the ECAP decreased rapidly and the negative component of the action potential increased in duration in response to (+)antx-a. A typical response of the ECAP following administration of (+)antx-a at 100  $\mu\text{g/kg}$  is shown in Figure 2. There was a gradual return toward a normal amplitude and shape of the action potential. The mean responses for depression of the ECAP following single stimulations from doses of (+)antx-a hydrochloride at 0, 50, 100, and 200  $\mu\text{g/kg}$  are shown in Figure 3. The individual responses of the ECAP in four rats given (+)antx-a hydrochloride at 800  $\mu\text{g/kg}$  are presented in Figure 4. The time corresponding to the final measurement represents the survival time in this group of animals. Survival times, defined as time between dosing and cessation of heart beat despite continuous ventilation, were 135, 150, 150, and 225 minutes.

Significant differences for maximum depression were observed at each dose of (+)antx-a hydrochloride. The maximum depression, onset time for maximum depression, and duration of effect for each dose of (+)antx-a hydrochloride are presented in Table 1. The  $\text{ED}_{50}$  for depression of the ECAP was 47  $\mu\text{g/kg}$  (95% confidence limits of 39 and 57  $\mu\text{g/kg}$ ). A significant difference for duration of effect existed among the 50  $\mu\text{g/kg}$ , 100  $\mu\text{g/kg}$ , and control groups but not between the 100  $\mu\text{g/kg}$  and 200  $\mu\text{g/kg}$  treatment groups. Rats given (+)antx-a at 800  $\mu\text{g/kg}$  did not recover 75% of the predose ECAP amplitude.

The decrease in amplitude of the ECAP following repetitive stimulation in a rat dosed with (+)antx-a at 100  $\mu\text{g/kg}$  is shown in Figure 5. The mean decrements of the fourth ECAP as a function of time following repetitive stimulation for groups of four animals given (+)antx-a hydrochloride at 0, 50, 100, or 200  $\mu\text{g/kg}$  are depicted in Figure 6. The maximum decrements and durations of a decrement of  $> 15\%$  at each dose are listed in Table 2.

#### Latency and Duration of the ECAP and Nerve Conduction Velocity

The ranges of the mean percent changes in latency of the ECAP were 0.1 to 3.1 for the control group and 1.7 to 11.8 for the (+)antx-a (100  $\mu\text{g/kg}$ ) treatment group. No significant changes in latency of the ECAP were observed.

Mean percent changes for amplitude and duration of the ECAP with respect to time are shown in Figure 7. No change was detected in either parameter following administration of normal saline. Following (+)antx-a administration, the mean ( $\pm$  SD) values for maximum depression in the amplitude of the ECAP and time to maximum depression were 85 ( $\pm$  7) percent and 8.5 ( $\pm$  1.4) minutes. The mean ( $\pm$  SD) maximum percent increase in the duration of the negative component of the action potential was 87 ( $\pm$  39).

Mean nerve conduction velocity values with respect to time for the two treatment groups are presented in Figure 8. Mean predose values of nerve conduction velocities ( $\pm$  SD) for the control and (+)antx-a groups were 43 ( $\pm$  0.2) and 40 ( $\pm$  3.5) m/s, respectively. No significant differences in nerve conduction velocities were observed between the treatment and control groups either before or after treatment.

#### D. Discussion

Previous studies on the agonist potency of (+)antx-a using contracture of frog rectus abdominis *in vitro* have indicated that the toxin was 2.5 and 150 times more potent than racemic antx-a and (-)antx-a, respectively (Swanson et al., 1985; Spivak et al., 1983). If the lethal action of antx-a in mammals is mediated via neuromuscular blockade in skeletal muscles, similar ratios of the LD<sub>50</sub>s for the various forms of antx-a should be expected. Our LD<sub>50</sub> values indicate that, in mice, (+)antx-a was 2.4 times (95% confidence limits of 2.1 and 2.7) and at least 180 times as potent as racemic and (-)antx-a, respectively. The approximately two-fold difference between (+)antx-a and racemic antx-a and the inability to produce death with (-)antx-a suggest that (-)antx-a has minimal effect, either as an agonist or antagonist, at the lethal site(s) of action.

In the assessment of neuromuscular blockade, electromyographic responses have been shown to be correlated with tension measurements of muscle contraction (Calvey, 1984), and electromyography offers technical advantages over tension measurements. For example, electromyography does not depend upon perfect alignment or constant tension for accurate measurements. Additionally, electromyography can provide insight into the electrical events occurring in muscle not available from force measurements. The precision obtained with these electromyographic methods were sufficient to establish dose response relationships for antx-a that can be used for future comparisons of responses following various therapeutic agents or protocols.

The percentage of postsynaptic acetylcholine receptors that must be blocked before there is a decrease in function of a muscle is referred to as the "margin of safety for

neuromuscular transmission" (Paton and Waud, 1967). The margin of safety will vary with the muscle and species involved but is typically greater than 70% (Paton and Waud, 1967; Waud and Waud, 1972). The diaphragm has been shown to have a greater margin of safety than other skeletal muscles both *in vivo* and *in vitro* (Paton and Waud, 1967; Waud and Waud, 1972; Taylor et al., 1964; Lu, 1970). This decreased tendency of the diaphragm to become paralyzed has been termed the "respiratory sparing effect." The greater resistance of the diaphragm to neuromuscular blockade dictates that a greater concentration of neuromuscular blocking agent must be present at this site to experience a given degree of paralysis when compared to other skeletal muscles. Ratios of the  $ED_{50}$  for paralysis of a peripheral muscle, to the  $LD_{50}$  of neuromuscular blocking agents have been used as indices of their respiratory sparing effect. These ratios depend on the agent, species, and muscles involved but are typically less than three for neuromuscular blocking drugs that are used clinically (Taylor et al., 1964; Lu, 1970). Comparing the  $ED_{50}$  of 47  $\mu\text{g/kg}$  obtained for neuromuscular blockade of the plantar muscles of the rat to the  $LD_{50}$  of 386  $\mu\text{g/kg}$  in mice yields a ratio of eight for the respiratory sparing effect of (+)antx-a. The higher respiratory sparing effect may be a property of antx-a or a result of comparing values from two species. Neuromuscular blocking agents, especially depolarizing agents, demonstrate considerable species dependency regarding potency. Indeed, with regard to both the  $LD_{90}$  and the ability of antx-a to produce neuromuscular blockade *in vitro*, there is a two- to three-fold difference between mallard ducks and ring-necked pheasants (Carmichael et al., 1978). Therefore,  $LD_{50}$  determination of (+)antx-a in the rat would be desirable to assess more accurately the respiratory sparing effect in this species.

The dose dependency for (+)antx-a induced maximum depression of the ECAP is readily apparent in Figure 1 and Table 1. The time to onset of maximum depression appeared to be shorter with larger doses as evidenced by the values of 8.5 minutes (Figure 7) and between 1 to 5 minutes (Table 1) observed for doses of 100  $\mu\text{g/kg}$  and 800  $\mu\text{g/kg}$ , respectively. A more critical comparison of onset times was not possible due to the 4-minute interval between measurements in the 800  $\mu\text{g/kg}$  trial.

There is little published information on dose response and pharmacodynamic aspects of the effects of neuromuscular blocking agents in the rat, making comparisons with antx-a difficult. It has been shown for pancuronium, one of the most potent neuromuscular blocking agents used medically, that doses required to produce a 90% neuromuscular blockade in peripheral muscle are: 30  $\mu\text{g/kg}$  in the cat; 17  $\mu\text{g/kg}$  in the dog; 36  $\mu\text{g/kg}$  in man; and 73  $\mu\text{g/kg}$  in the pig (MacLagan, 1976). The IV dose of (+)antx-a producing a similar degree of blockade in the rat is between 100 to 200  $\mu\text{g/kg}$ . Tubocurarine possesses one of the longest durations of action for commonly used neuromuscular blocking agents. The intervals from injection of doses of tubocurarine producing a 90% neuromuscular blockade to 50% recovery in several species were: 20 minutes in the cat; 20 to 40 minutes in the dog; and 35 minutes in man (MacLagan, 1976). Intravenous doses of (+)antx-a producing a similar blockade required approximately 80 to 90 minutes for 75% recovery in the rat. The return of neuromuscular function following iv doses of antx-a at 200  $\mu\text{g/kg}$  or less in the rat is in sharp contrast to the response observed following PO administration in a 6-week-old calf in which spontaneous respiration did not occur, despite the fact that

the animal was provided ventilatory support for 30 hours (Carmichael et al., 1975; Carmichael et al., 1977).

If only one mechanism accounted for both the depression of the ECAP from single stimulation and the decrement of the ECAP following repetitive stimulation, a correlation between the degree of depression and decrement would be expected. Such a correlation was not observed, however, for antx-a. Depression of the ECAP followed a well-defined dose dependency, whereas the decrement demonstrated an all or none response. Also, the amplitude of the ECAP after a single stimulus was reduced by 50% at doses of antx-a which were insufficient to produce a decrement after repetitive stimulation.

The amplitude of the ECAP after a single stimulus and the decrement of the ECAP following repetitive stimulation are modified electrophysiologic counterparts of peak tetanic tension and tetanic fade, respectively. The sensitivity of peak tetanic tension relative to tetanic fade differs for d-tubocurarine, pancuronium, and hexamethonium (Galvinovic, 1979). These results in conjunction with measurements of miniature endplate potentials and endplate potentials (Gibbs and Marshall, 1984; Galindo, 1971), posttetanic repetitive activity (Standaert, 1964; Riker et al., 1957; Baker et al., 1986), and quantification of evoked release of acetylcholine (Vizi et al., 1987) support the existence of presynaptic sites of action for nicotinic antagonists. Decrease of peak tetanic tension is considered to result from occupancy of postjunctional acetylcholine receptors by an antagonist (Paton and Waud, 1967; Bowman, 1980). Tetanic fade is believed to occur from either a presynaptic action on the nerve, which decreases the amount of transmitter released (Gibbs and Marshall, 1984; Galindo, 1971; Standaert, 1964; Vizi et al., 1987; Bowman, 1980), or an additional

frequency-dependent postsynaptic event. Proposed mechanisms for a presynaptic action that decreases the release of transmitter include: 1) membrane stabilization, 2) interference with metabolic turnover or mobilization of acetylcholine, and 3) prevention of positive feedback on the motor nerve terminal by acetylcholine. Molecules acting as ion channel conductance modulators through direct interaction with open ion channels present a possible postsynaptic mechanism for a frequency dependent failure of neuromuscular transmission (Gibbs and Marshall, 1984; Bowman, 1980; Colquhoun et al., 1979; Dreyer, 1982). Because the interaction is dependent on the channels being in the open state, this type of action is modulated by processes affecting the population of open channels such as repetitive stimulation. Such an interaction with open ion channels has not been observed for antx-a (Aronson and Witkop, 1981; Spivak et al., 1980). Therefore, the results obtained here support the presence of a presynaptic site of action in addition to the nicotinic agonist activity of antx-a on postjunctional receptors. This conclusion was also corroborated by the observation that (+)antx-a produced a concentration dependent decrease in the quantal content of endplate potentials of frog sartorius muscle evoked from nerve stimulation at 5, 10, and 20 Hz *in vitro* (Biggs and Dryden, 1977). The mechanism producing the decrement is important when considering a natural toxicosis due to the fact that units in normal muscle can fire at rates of 20 to 50 Hz (Zaimis, 1976).

None of the four animals administered antx-a at 800 µg/kg displayed a 75% return of the amplitude and all animals died within 4 hours of toxin administration despite continuous mechanical support of respiration. All four animals given the toxin at 800 µg/kg seemed to show a trend of partial return of the ECAP until deterioration occurred just prior to



death. Although in three animals, return of the ECAP was never greater than 5%, it is notable that one animal temporarily experienced a return of approximately 60%, an amount typically sufficient for voluntary respiration. Mice dosed IP with (+)antx-a at 350 to 450  $\mu\text{g/kg}$  and not provided respiratory support (during the  $\text{LD}_{50}$  determination) experienced an acute onset of clinical signs and death occurred within 15 minutes of toxin administration. Mice surviving the first 15 minutes recovered. Overall, the results obtained here suggest that sufficiently high doses of (+)antx-a can be lethal through at least two apparently different mechanisms. The first and more sensitive could result from a rapidly developed neuromuscular blockade, i.e., respiratory paralysis, and a second, unrelated to respiration, developing over several hours. Therefore, with sufficient exposure to antx-a, therapeutic measures in addition to respiratory support and detoxification are likely to be required in order to sustain life.

Administration of antx-a results in a decrease in the rate of rise, amplitude, and overshoot and a prolongation of the decay time of the ECAP. The decrease in amplitude of the ECAP, at least in part, results from failure of individual muscle fibers to generate an action potential. The increased duration of the ECAP may result from a direct action on individual fibers before complete neuromuscular blockade and/or a desynchronization in latency of the single cell action potentials producing a temporal expansion of the ECAP.

Antx-a induced differential slowing of conduction velocities in the motor neurons of a nerve could expand the range of latencies observed in this study. This appears unlikely, however, considering the absence of either a decrease in the maximal motor nerve conduction velocity or an increase in the latency of muscle fibers innervated by the fastest

conducting neurons. Similarly, if the variation in time interval between action potentials of fibers within the same motor unit (termed "jitter") increased due to variations in synaptic delay as observed for d-tubocurarine (Ekstedt and Stalberg, 1969), a desynchronization of the individual action potentials would result. An increase in jitter is suggested by the larger variation in values of latency and maximal nerve conduction velocity observed for the (+)antx-a treated rats compared to controls. Because of the composite nature of the ECAP, either of the above processes could contribute to the observed increase in duration noted with antx-a.

A third explanation could involve processes on the cellular level which might alter the shape of the individual action potentials. This would represent an effect of antx-a on the muscle cell other than complete blockade of neuromuscular transmission. Evidence to suggest that such changes at least contribute to the effects of antx-a on the ECAP was derived from results obtained using single-cell preparations *in vitro*. Qualitatively the changes observed for single-cell preparations produced by carbachol *in vitro* (Nastuk, 1971) and (+)antx-a *in vitro* (Spivak et al., 1980) were identical to those reported here for the ECAP after antx-a administration *in vivo*. Therefore, mechanisms producing a change in the individual action potentials of muscle cells may independently account for the antx-a induced alterations of the ECAP.

In summary, electromyography can be used to quantify the degree of neuromuscular blockade produced by antx-a *in vivo* with adequate precision to enable evaluation of therapeutic agents and protocols. Results obtained from our repetitive stimulation investigations support earlier reports from studies *in vitro* which suggested a physiologically

significant presynaptic site of action for antx-a. Exposures to antx-a producing a blockade of up to 95% of neuromuscular transmission were reversible with mechanical support of respiration. However, sufficiently high exposures to antx-a appear to be lethal through at least two apparently different, but dose-dependent, mechanisms so that, at sufficiently high doses, presently unidentified therapeutic measures in addition to respiratory support are likely to be required to enable animals to survive.

Table 1. Maximum depression, onset time for maximum depression, and duration of action for depression of the ECAP from (+)antx-a.<sup>a</sup>

(+)Anatoxin-a ( $\mu\text{g/kg}$ )	Maximum Depression (%)	Onset Time (minutes)	Duration of Effect (minutes)
0	$3 \pm 4$ (A) <sup>b</sup>	-	-
50	$53 \pm 15$ (B)	10	$31 \pm 11$ (A)
100	$82 \pm 7$ (C)	10	$80 \pm 24$ (B) <sup>c</sup>
200	$95 \pm 2$ (D)	10	$93 \pm 48$ (B)
800	$100 \pm 1$ (E)	< 5	-

<sup>a</sup>Values are means  $\pm$  SD.

<sup>b</sup>Values with different letters are significantly different ( $P_{\text{actual}} < 0.05$ ).

<sup>c</sup> $P_{\text{actual}} = 0.065$ .

Table 2. Maximum decrement and duration of > 15% decrement of the fourth ECAP from (+)anatoxin-a following repetitive stimulation.<sup>a</sup>

(+)Anatoxin-a ( $\mu\text{g/kg}$ )	Maximum Decrement of the ECAP (%)	Duration of > 15% Decrement (minutes)
0	$6 \pm 5$ (A) <sup>b</sup>	-
50	$13 \pm 22$ (A)	$4 \pm 7$ (A)
100	$46 \pm 18$ (B)	$24 \pm 14$ (B)
200	$59 \pm 8$ (B)	$69 \pm 27$ (C)

<sup>a</sup>Values were mean  $\pm$  SD.

<sup>b</sup>Values with different letters are significantly different ( $P_{\text{actual}} < 0.05$ ).

Figure 1. Percent deaths observed following IP administration of either (+)anatoxin-a (●; given at 350, 365, 385, 400, or 450  $\mu\text{g/kg}$  BW) or racemic anatoxin-a ( $\Delta$ ; given at 800, 850, 950, 1,000, or 1,050  $\mu\text{g/kg}$  BW). Each dose was given to a group of six male Balb/c mice. The fraction of dosed animals that died (percent dead) is plotted against dose (log scale).

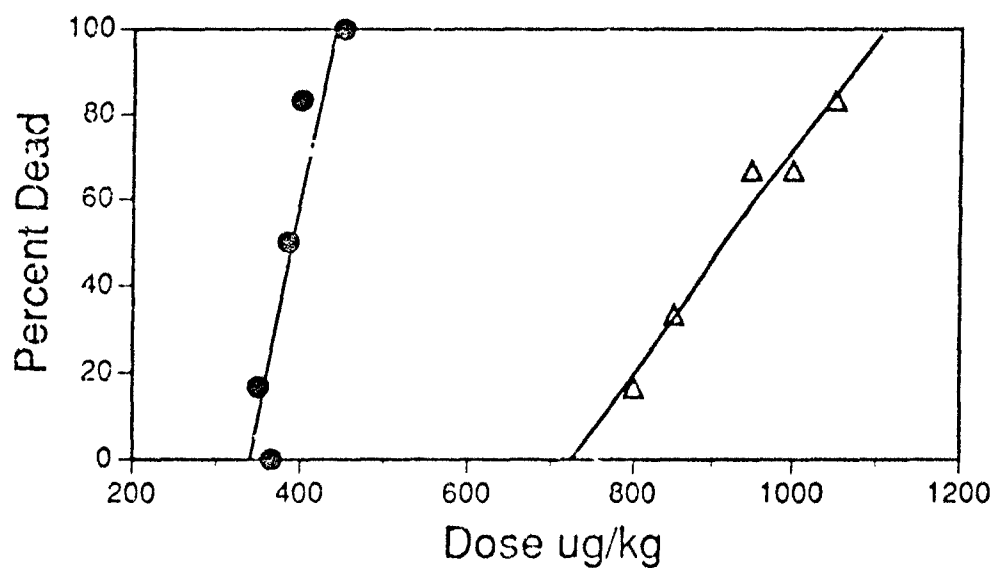


Figure 2. Evoked compound action potentials in a rat predose (a), and at 1 minute (b), 10 minutes (c), 60 minutes (d), and 120 minutes (e) after IV administration of (+)anatoxin-a hydrochloride at 100  $\mu\text{g/kg}$ .

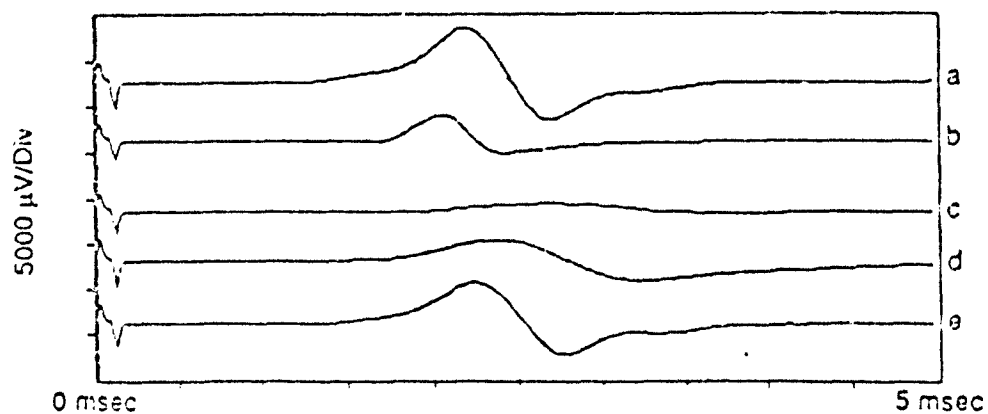


Figure 3. Mean responses for the depression in amplitude of the evoked compound muscle action potential as a function of time following IV administration of (+)anatoxin-a hydrochloride (N = 4).

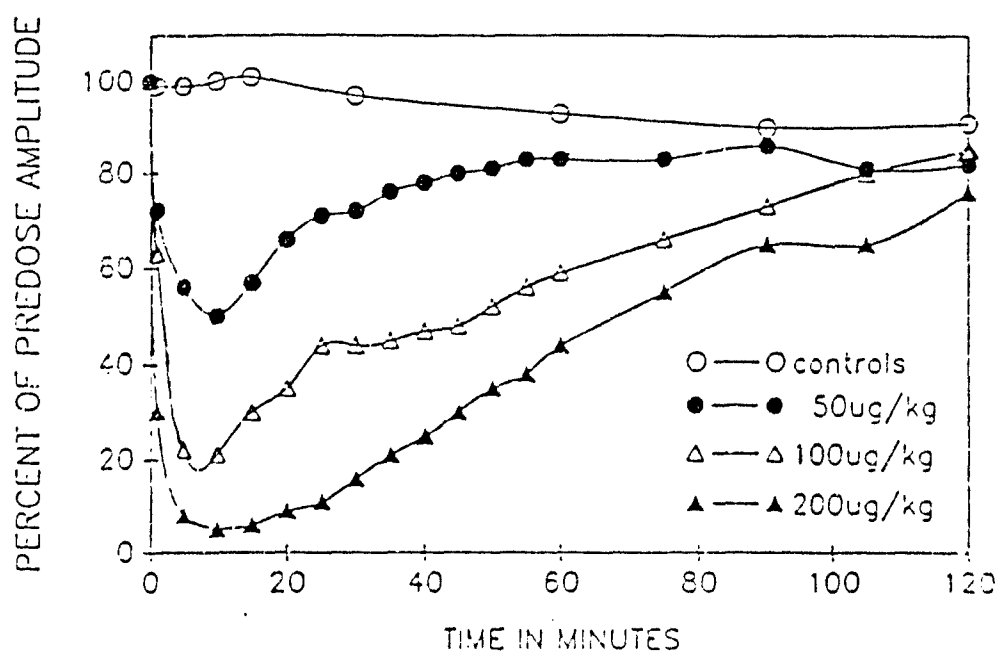




Figure 4. Percent depression of the evoked compound muscle action potentials in four animals as a function of time following IV administration of (+)anatoxin-a hydrochloride at 800  $\mu\text{g/kg}$  body weight. Survival times are indicated by the time of the final measurement (before death).

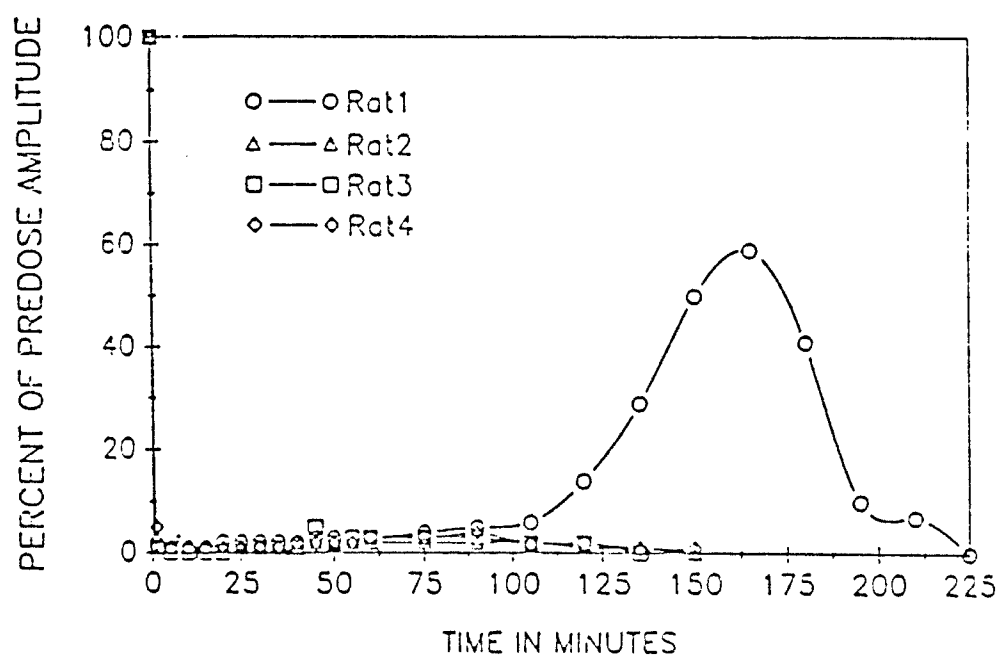


Figure 5. Evoked compound muscle action potentials in a rat resulting from four repetitive stimulations applied at 10 Hz (A) before and (B) 10 minutes after IV administration of (+)anatoxin-a hydrochloride at 100  $\mu\text{g/kg}$ .

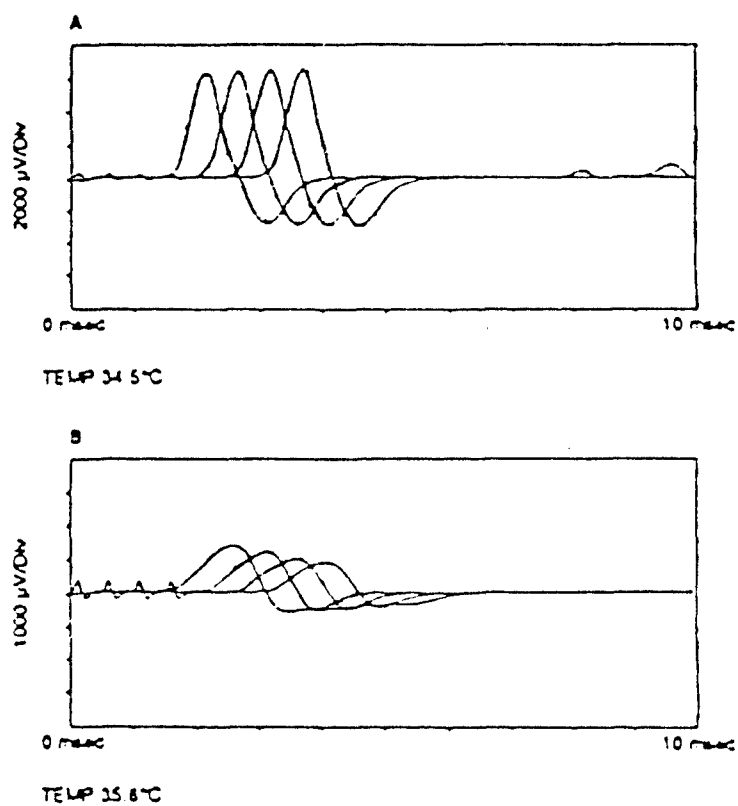


Figure 6. Mean responses for the decrement of the fourth evoked compound muscle action potential relative to the first action potential in a train of four repetitive stimulations at 10 Hz as a function of time following iv administration of (+)anatoxin-a hydrochloride (N = 4).

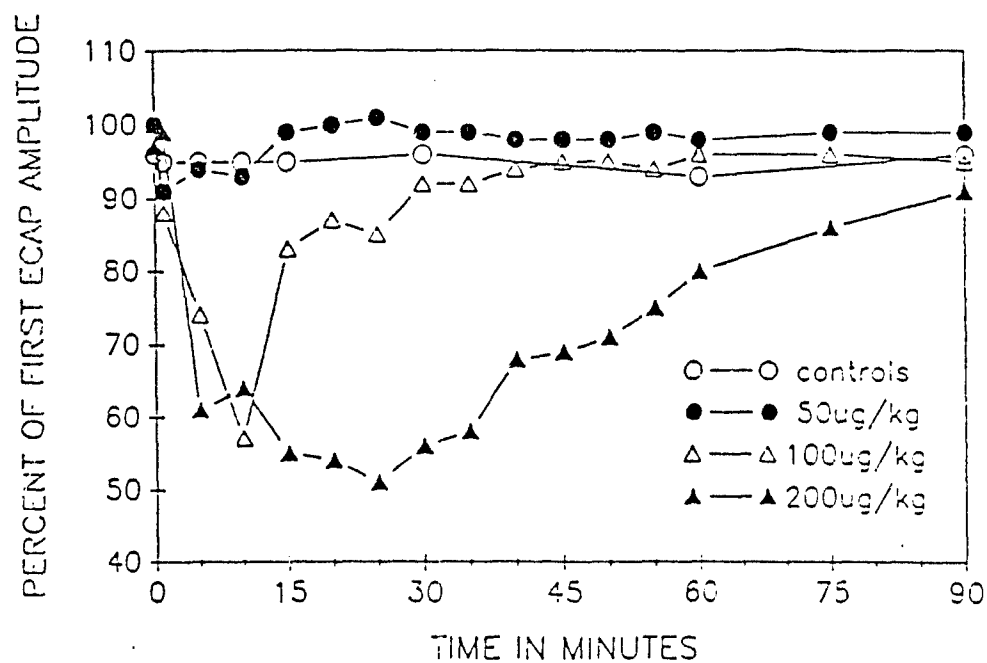


Figure 7. Mean percent changes (and their SD: which are shown when larger than the symbol size) in amplitude and duration of the evoked compound action potential following IV administration of normal saline or (+)anatoxin-a at 100  $\mu\text{g/kg}$  ( $N = 4$ ).

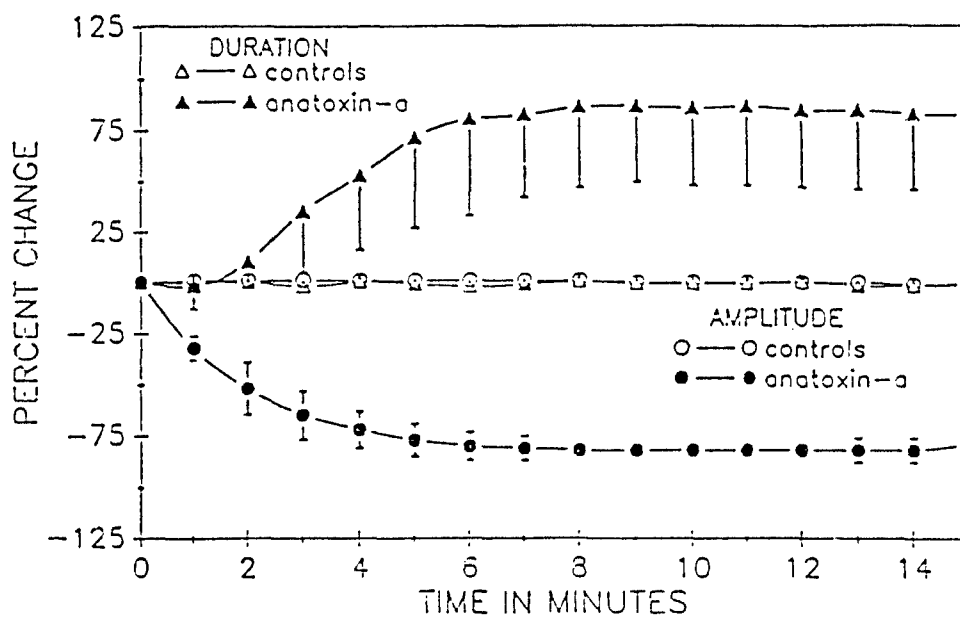
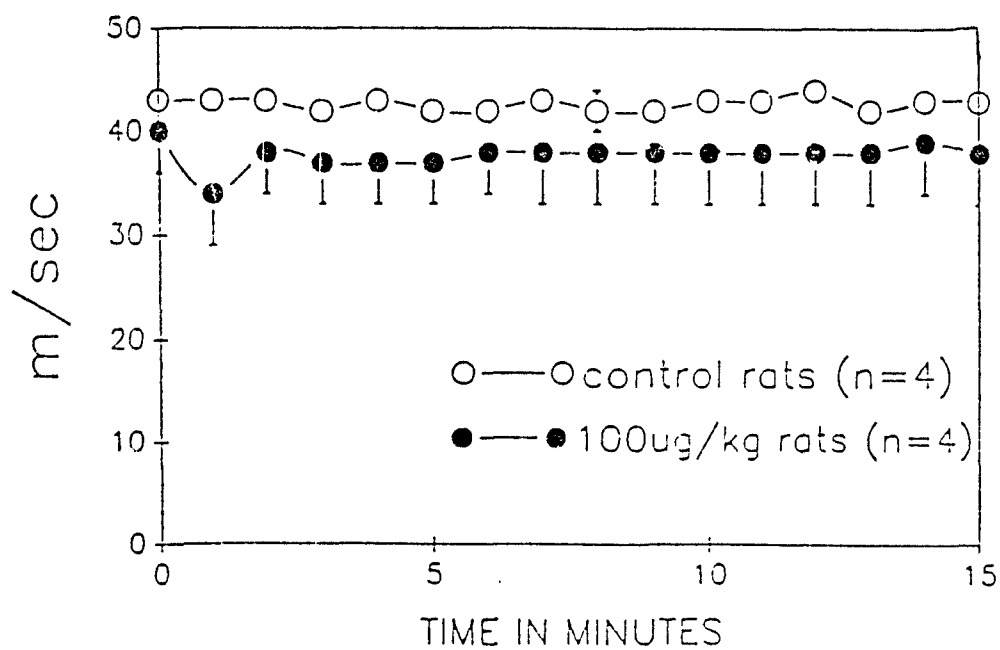


Figure 8. Mean motor nerve conduction velocities (and their SD: which are shown when larger than symbol size) in rats administered IV normal saline or (+)anatoxin-a at 100  $\mu\text{g}/\text{kg}$ .



## II. ANATOXIN-A(S)

### Background on Algal Neurotoxins; Anatoxin-a and Anatoxin-a(s)

Blue-green algal neurotoxins include the anatoxins (antx) and the aphantoxins. Neurotoxic cyanobacteria have been isolated from North America, England, and Finland (Carmichael, 1982; Carmichael and Mahmood, 1984; Sivonen et al., 1989), and there is also a report of neurotoxic effects caused by *Anabaena* in Australia (Carmichael, 1988).

Aphantoxins I and II produced by *Aphanizomenon flos-aquae* NH-1 and NH-5 are identical to the purine alkaloids neosaxitoxin and saxitoxin, respective, and act by inhibiting nerve conduction via blockade of sodium channels (Aldeman, 1982; Mahmood and Carmichael, 1986a). Aphantoxins studied to date have come from algal blooms or laboratory strains of *Aphanizomenon flos-aquae* collected from lakes and ponds in New Hampshire (Carmichael, 1988).

Antxs are neurotoxins that have been isolated from Canadian strains of the freshwater cyanobacterium *Anabaena flos-aquae* and include antx-a, -b, -a(s), and -b(s) (Carmichael and Gorham, 1978). Antxs were distinguished from one another based on minimum lethal dose, survival time, and clinical signs produced after administration of lyophilized culture material in various animals. Some of the most severe cases of algal poisoning involving deaths of cattle, dogs, ducks, swine, waterfowl, and other wildlife were in association with blooms of *Anabaena flos-aquae* (Deem and Thorp, 1939; Dillenberg and Dehnelt, 1960; Fitch et al., 1934; Hammer, 1968; Gorham, 1964; Stewart et al., 1950). Gorham et al. (1964) described the first successful

laboratory culture of toxic isolates of *A. flos-aquae*. These toxic isolates were collected from Burton Lake, Saskatchewan, Canada.

Of the antxs, only antx-a produced by *A. flos-aquae* had been structurally identified prior to 1989. It is the secondary amine, 2-acetyl-9-azabicyclo (4-2-1) non-2-ene (Hubner, 1972; Devlin et al., 1977) and is a highly toxic postsynaptic depolarizing neuromuscular blocking agent that affects both nicotinic and muscarinic acetylcholine (ACh) receptors (Carmichael et al., 1975, 1979; Spivak et al., 1980, 1983; Aronson and Witkop, 1981). In addition, antx-a has presynaptic actions which result in a reduction of the frequency and quantal content of miniature end plate potentials (Biggs and Dryden, 1977). Before it was structurally identified, antx-a was sometimes referred to as the "very fast death factor." A mouse IP LD<sub>50</sub> of antx-a was reported by Carmichael (1982) to be 0.25 mg/kg. Antx-a has been produced in the laboratory using *A. flos-aquae* NRC-44-1, which was originally isolated from Burton Lake in Canada.

Anatoxin-a(s) [antx-a(s)] is a recently characterized low-molecular-weight alkaloid cholinesterase (ChE)-inhibiting neurotoxin that has been produced in the laboratory from *Anabaena flos-aquae* NRC-525-17. Based on nuclear magnetic resonance and mass spectroscopy, antx-a(s) has a molecular weight of 252 daltons. The toxin has a highly acidic phosphodiester group placed between two basic nitrogens giving the compound highly ionic properties (Matsunaga and Moore, personal communication, 1989). The toxin has a five-membered ring structure composed in part by a N-C-N guanidium group. The so-called "inactive form" of the toxin appears to be a mixture of two known degradation products of molecular weights, 111 (monomethylphosphate) and 141. Antx-a(s) is the first recognized, naturally occurring organophosphorus inhibitor of ChE.

*A. flos-aquae* NRC-525-17 was originally isolated in 1965 from an algal bloom in Buffalo Pound Lake, Saskatchewan, Canada (Carmichael and Gorham, 1978; Mahmood and Carmichael, 1986b). Composition of that bloom at that time was 90% *A. flos-aquae* and 10% *Aphanizomenon flos-aquae*. Over 20 dogs (from 1960 to 1970) and a few calves (during 1965) were believed to have been poisoned by cyanobacteria in this lake. Antx-a(s) reportedly had the same minimum lethal dose and survival time as antx-a but also produced hypersalivation (and excessive lacrimation) prior to respiratory arrest in mice, rats, and chicks and was therefore designated with the "(s)" (Carmichael and Gorham, 1978).

At the onset of the studies described in this section, considerable knowledge gaps existed with regard to both anatoxin-a and anatoxin-a(s). In the case of the former compound, the relative toxicity of isomeric forms had not been explored, and of greater importance, questions with regard to the cause of death and the reversibility of the toxicosis in animals provided artificial respiration were unresolved.

In the case of anatoxin-a(s), questions of toxin purity, stability, and structure initially presented a considerable challenge. Although the toxin was known to be an inhibitor of cholinesterase, whether and how this would account for toxic effects in animals had not been explored. No studies involving localization of cholinesterase inhibition in tissues or detailed physiologic measurements of exposed animals had been done. The susceptibility of various animal species likely to be exposed in the field was open to question. Finally, the influence of therapies had been examined only in a very preliminary way. The currently reported studies have provided information to address each of these areas.



## A. Absence of Effects of Anatoxin-A(s) on Mouse Brain Cholinesterase Activity

### 1. Statement of the Problem, Background, and Rationale

Physiologically distinct neurotoxins, isolated from strains of the freshwater cyanobacterium, *Anabaena flos-aquae*, have been termed anatoxins (antx)-a, -b, -d, -a(s), and -b(s) (Carmichael and Gorham, 1978). Mahmood and Carmichael (1987) postulated that the mechanism of antx-a(s) toxicity was cholinesterase (ChE) inhibition after demonstrating that antx-a(s) irreversibly inhibited electric eel acetylcholinesterase (EC 3.1.1.7) *in vitro* and inhibited rat whole blood ChE activity *in vivo*. Because of its polar character, as evidenced by solubility only in polar solvents such as water, methanol, and ethanol, we postulated that antx-a(s) may have limited ability to cross the blood brain barrier (BBB). In developing prognoses and therapeutic protocols for a cholinesterase inhibitor, it is critical to know whether the central nervous system is affected and to be able to predict how long therapy will be needed. The goals of this study were to quantify any effect of antx-a(s) on brain ChE while comparing its activity with those of well-characterized inhibitors of ChE in mice dosed IP and to determine the persistence of clinical signs of toxicosis.

### 2. Experimental Methods

Five groups of male Balb/c 4-7 mice (25 to 35 g) (Harlan Sprague-Dawley, Indianapolis, IN) were dosed IP with an extract containing antx-a(s) at doses of 225, 228.75, 232.50, 240, or 690 µg/kg, physostigmine salicylate (Antilirium, O'Neal, Jones and Feldman, Inc., St. Louis, MO) at doses of 650, 700, 725, 750, or 950 µg/kg, pyridostigmine bromide (Regonol, Organon, Inc., West Orange, NJ), at 1,150, 1,450,

2,100, 2,150, or 2,250  $\mu\text{g/kg}$ , paraoxon (Sigma Chemical Co., St. Louis, MO) at doses of 1,000, 1,250, 1,275, 1,312, or 1,375  $\mu\text{g/kg}$ , or a control solution of distilled water containing 1% ethanol. Antx-a(s), produced by the method of Mahmood and Carmichael (1986b), was brought into solution with ethanol such that the dosing solution contained less than 1% ethanol. At the time of this study, the structure of antx-a(s) was unknown and purification methods were still in a state of development. Although the toxin was semipurified, a major portion of the remaining material used in this study was low-molecular-weight salts from the culture media (with which toxicity has not been associated upon repeated testing).

Five groups of four to seven mice each were dosed with each toxicant: 32 mice with antx-a(s); 35 each with pyridostigmine, physostigmine, and paraoxon; and 20 with 1% ethanol in water. Different doses of each toxicant were used for each group of mice to determine an  $\text{LD}_{50}$  for each compound. Mice were observed at 0 to 5, 10, 20, 30, 40, 50, and 60 minutes and every 30 minutes thereafter up to 18 hours and at 24 hours postdosing for clinical signs including diarrhea, salivation, lacrimation, tremors, increased/decreased movement, and dyspnea each of which were scored. Time to death was recorded in minutes. Mice surviving for 24 hours were killed by cervical dislocation. Brains of mice were removed, frozen in liquid nitrogen, stored at  $-80^{\circ}\text{C}$ , and assayed within 24 hours for ChE activity using a modification of the Ellman Method (Ellman et al., 1961) using 1% octyl phenoxy polyethoxyethanol in the phosphate buffer.

### Statistical Analyses

Data were analyzed using a SAS (SAS Institute, Cary, NC) General Linear Model. Covariate analysis accounted for dose and dose-drug interactions. Tukey's analysis was used to make comparisons among the ChE activities of mice of the control group, those of the toxicant groups that died and those killed at 24 hours. Clinical sign data, at each time point, were transformed to + (at least one abnormality present) or - (no abnormalities) before analysis. For survival data and duration of clinical signs, comparisons among toxicants were performed with the SAS Lifetest in conjunction with the Wilcoxon Test. LD<sub>50</sub> values were calculated by SAS probit analysis.

### 3. Results

LD<sub>50</sub>s for the extract containing antx-a(s), paraoxon, physostigmine, and pyridostigmine were determined to be 0.228, 1.25, 0.73, and 2.15 mg/kg body weight, respectively.

In mice given antx-a(s), clinical signs included hypersalivation, mucoid lacrimation, urination, diarrhea, tremors, fasciculations, rales, dyspnea, cyanotic oral mucous membranes, and clonic rolling seizures at death. Clinical signs persisted longer ( $p < 0.0001$ ) in mice given antx-a(s) than in mice given the carbamates but were similar in duration to those of the paraoxon group. The survival time of mice injected with antx-a(s) was significantly longer ( $p = 0.049$ ) than in mice given paraoxon but not the carbamates. Examination of Figure 1, however, reveals that

survival times of mice given antx-a(s) were longer than in mice given the carbamates, except for mice given the highest doses of antx-a(s).

No inhibition of whole brain ChE was observed in mice that died or were killed at 24 hours after antx-a(s) administration, despite the fact that some animals were still displaying clinical signs at that time (Table 1). As expected, paraoxon causes persistent clinical signs and inhibited brain ChE, and the carbamates exerted effects of a more reversible nature. Physostigmine gained access to the CNS and inhibited brain ChE, whereas the charged carbamate, pyridostigmine, did not. Inability to inhibit brain ChE on the part of antx-a(s) could result from an inability of the toxin to cross the blood brain barrier. In this regard, antx-a(s) behaved similarly to the charged carbamate, pyridostigmine. Metabolism of antx-a(s) might also have reduced exposure of the brain, but sufficient toxin reached other sites of action to produce marked clinical signs of toxicosis leading to death in some of the animals. The persistence of clinical signs of antx-a(s) toxicosis was consistent with slowly reversible or irreversible inhibition of ChE *in vivo*, and in this way, the toxin resembled the irreversible inhibitor paraoxon, but the duration of effect could also have been accounted for by a relatively longer tissue half-life of antx-a(s) compared to the other toxicants. Because the algal extract used in this experiment contained impurities in addition to antx-a(s), it is possible that some of the clinical signs observed may not have been due solely to the toxin. However, in recent studies in which animals have been dosed IP with a range of preparations from lysed whole cells

to the highly purified toxin, the clinical syndrome, time course, and pattern of ChE inhibition have been identical.

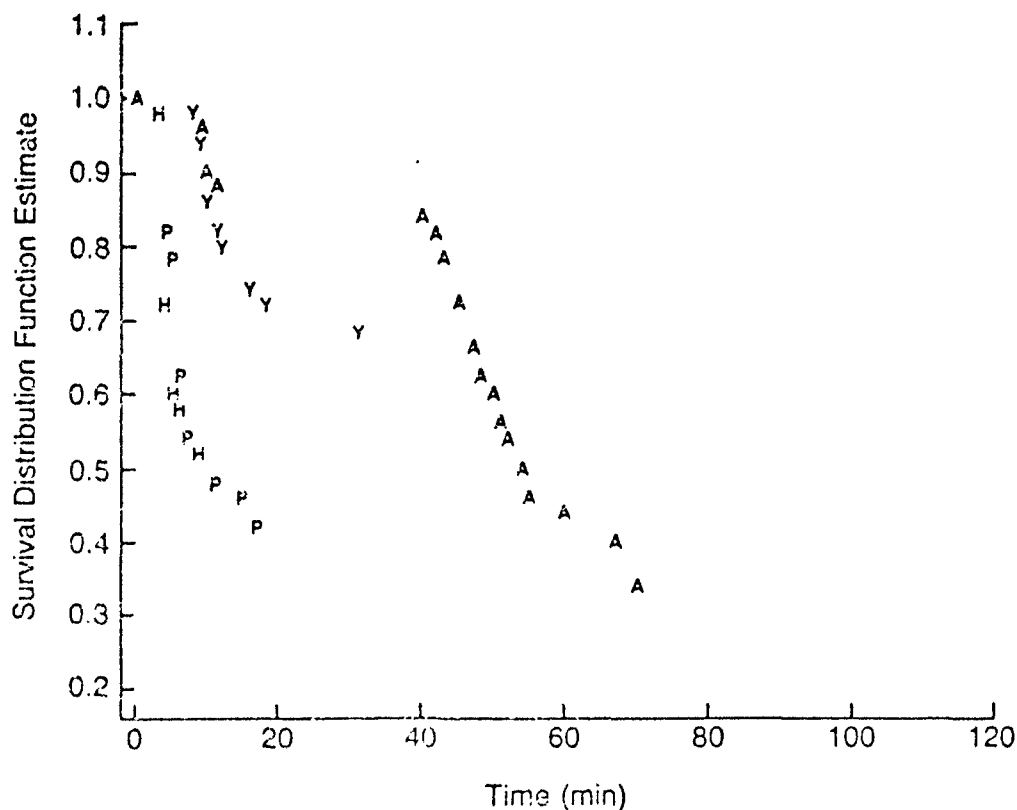
The delayed lethality of death in mice from the extract containing antx-a(s), as compared to that induced by the much more lipophilic toxicant paraoxon, may have been a result of comparatively slower absorption and distribution of the polar algal toxin such that it could not reach critical sites of action as readily. However, it probably did not reflect time required for bioactivation of antx-a(s).

Table 1. Effect of antx-a(s), paraoxon, physostigmine, and pyridostigmine on brain ChE activity of mice dosed IP that died prior to 24 hours or were killed at 24 hours.

Toxicant	N	Brain ChE ( $\mu$ mole/g/minute) Mean $\pm$ SD	
		Died < 24 hours	Killed at 24 hours
Antx-a(s)	32	10.6 $\pm$ 0.7 <sup>a</sup>	10.4 $\pm$ 0.7 <sup>a</sup>
Control	20		10.5 $\pm$ 0.5 <sup>a</sup>
Pyridostigmine	35	10.1 $\pm$ 1.1 <sup>a</sup>	10.3 $\pm$ 0.8 <sup>a</sup>
Physostigmine	35	1.9 $\pm$ 0.5 <sup>b</sup>	10.5 $\pm$ 0.8 <sup>a</sup>
Paraoxon	35	0.11 $\pm$ 0.07 <sup>c</sup>	3.8 $\pm$ 0.4 <sup>b</sup>

Lettered superscripts are the results of Tukey's analyses; treatment groups with different superscript letters were significantly different ( $p < 0.05$ ).

Figure 1. Survival distribution function versus time in mice given doses to bracket the  $LD_{50}$  of the extract containing antx-a(s) (A), paraoxon (P), physostigmine salicylate (H), and pyridostigmine bromide (Y). For the extract containing anatoxin-a(s), at 225, 228.75, 232.50, 240, 240, and 690  $\mu\text{g/kg}$  survival rates were 5/7, 4/7, 0/7, 2/7, and 0/4, respectively. For paraoxon, survival rates at 1,000, 1,250, 1,275, 1,312, and 1,375, were 7/7, 4/7, 3/7, 0/7, and 1/7, respectively. For physostigmine, at 650, 700, 725, 750, and 950  $\mu\text{g/kg}$ , survival rates were 6/7, 7/7, 3/7, 2/7, and 0/7, respectively. Finally, for pyridostigmine, at 1,150, 1,450, 2,100, 2,150, and 2,250  $\mu\text{g/kg}$ , survival rates were 7/7, 4/7, 3/7, 0/7, and 1/7, respectively. The survival distribution function is calculated based on survival times of mice and utilizes the right censored observations from mice killed at 24 hours in this study. Time is in minutes.



**B. Reversal of Peripheral Cholinesterase Inhibition; Clinical Signs and Postmortem Findings in Mice Dosed Intraperitoneally with Anatoxin-a(s)**

1. Statement of the Problem, Background, and Rationale

Properties of cholinesterase (ChE)-inhibiting agents that play an important role in toxicosis include the ability to cross the blood brain barrier (BBB) and their duration (reversibility) of ChE inhibition in exposed animals (Taylor, 1985). The purpose of the present study was to characterize the reversibility of anatoxin-a(s) [antx-a(s)]-induced inhibition of ChE in the plasma, red blood cells (RBC), and diaphragms of mice exposed intraperitoneally. To aid in interpretation, antx-a(s) was compared with two well-known ChE inhibitors, the organophosphorus compound paraoxon and the carbamate pyridostigmine bromide. Paraoxon and pyridostigmine represent irreversible and reversible inhibitors of ChE *in vitro*, respectively. Moreover, they also present ChE inhibitors that are widely distributed (paraoxon) and excluded from the central nervous system (pyridostigmine). Additional response parameters included clinical signs and histologic changes in selected tissues. Toxicants were administered at predetermined LD<sub>40</sub> doses in order that marked ChE inhibition, clinical signs, and lethality would occur, yet enough mice would survive to make the desired comparisons.

2. Experimental Methods

Toxicant Preparation

Antx-a(s), produced by the method of Mahmood and Carmichael (1986b), was stored at -20°C prior to use and brought into solution with ethanol such that the final



dosing solution contained less than 1% ethanol. Paraoxon (Sigma Chemical Co., St. Louis, MO), stored at a concentration of less than 10 mM at -20°C in dry acetone, contained less than 1% acetone in the final dosing solution. Distilled water was used in diluting toxicants for dosing. The control solution (distilled water with 1% ethanol) was administered at a volume/body weight equal to that used with antx-a(s), which was the maximum volume given.

#### Experimental Design

Male Balb/c (Harlan Sprague-Dawley Inc., Indianapolis, IN) mice (25 to 35 g) were provided food (Lab Blox, Wayne Research Animal Diet, Bemis Co., Peoria, IL) and water *ad libitum* and housed in air-conditioned quarters on a 10/14-hour dark/light cycle. The mice were dosed IP with a control solution or one of the following toxicants at predetermined LD<sub>50</sub> doses: an extract containing antx-a(s) (0.29 mg/kg), paraoxon (1.23 mg/kg), or pyridostigmine bromide (Regonol, Organon Inc., West Orange, NJ; 2.11 mg/kg).

On dosing days, groups of six mice were randomly assigned to each LD<sub>50</sub> treatment or control group. Mice from each toxicant group were killed by decapitation at the following randomly assigned time points: prior to dosing, 5, 15, 30, 60, or 240 minutes or 1, 2, or 8 days postdosing. Replicate groups of mice were dosed until at least four mice given each toxicant or the control solution had survived long enough to be killed at each time point. Four additional mice were dosed with the control solution and killed by cervical dislocation at 5, 15, 30, and 60 minutes postdosing in order to compare diaphragm ChE activities with those of mice in the

toxicant-dosed groups that died. After decapitation, blood and diaphragm from each of the mice were collected for ChE assays.

#### ChE Assays

Plasma and RBCs were separated from whole blood by centrifugation (548 g, 5 minutes), and plasma ChE activities were assayed by the Ellman method (Ellman et al., 1961), using a Lambda 3 UV/VIS spectrophotometer (Perkin Elmer, Norwalk, CT). For RBC ChE determinations, 50  $\mu$ l of RBC was lysed with 0.95 ml of 5% octyl phenoxy polytheoxyethanol (Triton X-100, Sigma Chemical Co., St. Louis, MO), 100  $\mu$ l of the lysate diluted to 10 ml with pH 8 phosphate buffer, and 3 ml analyzed as above. Diaphragms of mice were excised, blotted, weighed, and stored at -80°C for less than 1 day prior to analysis. The diaphragms were then homogenized with 0.05 ml of pH 8 phosphate buffer/mg of tissue in a Boreck Tissue Grinder (Fisher Co., Itasca, IL), the homogenate centrifuged (67 g, 10 minutes), and 100  $\mu$ l of supernatant added to 2.5 ml of pH 8 phosphate buffer for analysis as above.

#### Evaluation and Scoring of Clinical Sign Data

Monitoring for clinical signs including hypersalivation, diarrhea, lacrimation, respiratory difficulty, tremors, and fasciculations was conducted routinely at 0, 5, 10, 15, 30, 120, 180, and 240 minutes and 1 day and daily thereafter for 7 days. Hypersalivation, diarrhea, and lacrimation were scored on a scale of 1 to 4 (1 = normal, 4 = severely increased). Respiratory difficulty, tremors, and fasciculations were recorded as present or absent. The duration of a clinical sign of toxicosis was recorded as the mean of the time of the final observation of the

abnormality and the subsequent observation time. Survival time was recorded to the nearest minute.

#### Histologic Studies

Brain, sciatic nerve, diaphragm, lung, heart, spleen, gastrointestinal tract, pancreas, liver, and kidney from mice that died or were killed 24 hours or more postdosing and lung from all mice that died or were killed prior to 24 hours were fixed in 10% neutral-buffered formalin, sectioned at 6  $\mu$ , and stained with hematoxylin and eosin.

#### Statistical Analysis

LD<sub>50</sub> doses were calculated using the SAS probit analysis program (SAS Institute, 1985). Comparisons with regard to plasma, RBC, and diaphragm ChE activities were performed using the SAS General Linear Model with Tukey's test. Comparison of survival data and duration of clinical signs among toxicant-dosed groups of mice were analyzed by the SAS Lifetest in conjunction with the Wilcoxon Test. A level of  $\alpha = 0.05$  was chosen to identify significant differences.

### 3. Results

Significant inhibition of plasma and diaphragm ChE by antx-a(s) lasted for more than 1 but less than 2 days, whereas inhibition of RBC ChE lasted for 8 days. The time required for recovery from antx-a(s)-induced ChE inhibition in diaphragm, RBC, and plasma was generally similar to or longer than that with paraoxon and longer than with pyridostigmine (Figure 1a, 1b, and 1c). In mice that died as a result of antx-a(s) administration, diaphragm ChE activity was significantly inhibited as compared to

controls, but the extent of inhibition was still significantly less severe than in mice that died following administration of paraoxon or pyridostigmine (Table 1). Mean survival times (first 24 hours) for antx-a(s), paraoxon, and pyridostigmine were 93, 11, and 15 minutes, respectively; and thus, survival times of mice given antx-a(s) were significantly longer than with pyridostigmine or paraoxon ( $p = 0.0001$  and  $0.0004$ , respectively).

Muscarinic effects (lacrimation, diarrhea, and salivation) of antx-a(s) were at least as severe as with paraoxon and pyridostigmine, whereas nicotinic effects (fasciculations and tremors) of antx-a(s) appeared less severe (Figure 2).

Small and large intestinal lumens were dilated in mice that died following administration of any of the three toxicants. No lesions were detected on histologic examination of tissues from control or toxicant-dosed mice.

#### 4. Discussion and Conclusion

The persistence of inhibition of ChE caused by paraoxon and pyridostigmine in plasma was comparable to the effects of slowly reversible or irreversible ChE inhibitors, such as many organophosphorus compounds and long-acting (long half-life) carbamates, respectively (Taylor, 1985; Murphy, 1986; Frawley et al., 1952). Thus, the prolonged effect of antx-a(s) on plasma ChE was similar to the irreversible or slowly reversible inhibition of plasma ChE in which the return of ChE activity is principally a result of regeneration of the plasma enzyme by the liver. This is consistent with the fact that antx-a(s) is an organophosphorus toxin.

ChE of RBCs appeared to be most susceptible to persistent inhibition by antx-a(s) *in vivo*, and inhibition of RBC ChE by antx-a(s) lasted longer than with the irreversible ChE inhibitor paraoxon, although the differences were not statistically significant. Similarly, antx-a(s) has been observed to bind to RBC ChE more tightly than another organophosphorus agent, diisopropylfluorophosphate (Mahmood et al., 1987). The incomplete recovery of RBC ChE activity by 8 days after dosing with antx-a(s) is also highly suggestive of irreversible inhibition of this enzyme. ChE activity in such a case would tend to recover in response to synthesis of new RBCs (RBC turnover in the mouse is 20 to 45 days) (Taylor, 1985; Murphy, 1986; Frawley et al., 1952; Jain, 1986).

Clinical signs of toxicosis caused by organophosphorus-based irreversible inhibitors of ChE generally persist much longer than with carbamates, as was evident in the present comparison of paraoxon and pyridostigmine (Taylor, 1985; Murphy, 1986). The persistence of clinical signs induced by antx-a(s) was longer than with pyridostigmine and similar to that induced by paraoxon. Thus the present findings *in vivo* were compatible with the suggestion, based on studies *in vitro*, that antx-a(s) is an irreversible inhibitor of ChE. Persistent inhibition of ChE could also have been due to a longer tissue half-life of antx-a(s) compared to the other toxicants, but antx-a(s) is not a very stable compound in solution unless stored in acidic conditions at low temperatures, and therefore the likelihood of rapid hydrolysis resulting in inactive products seems highly likely.

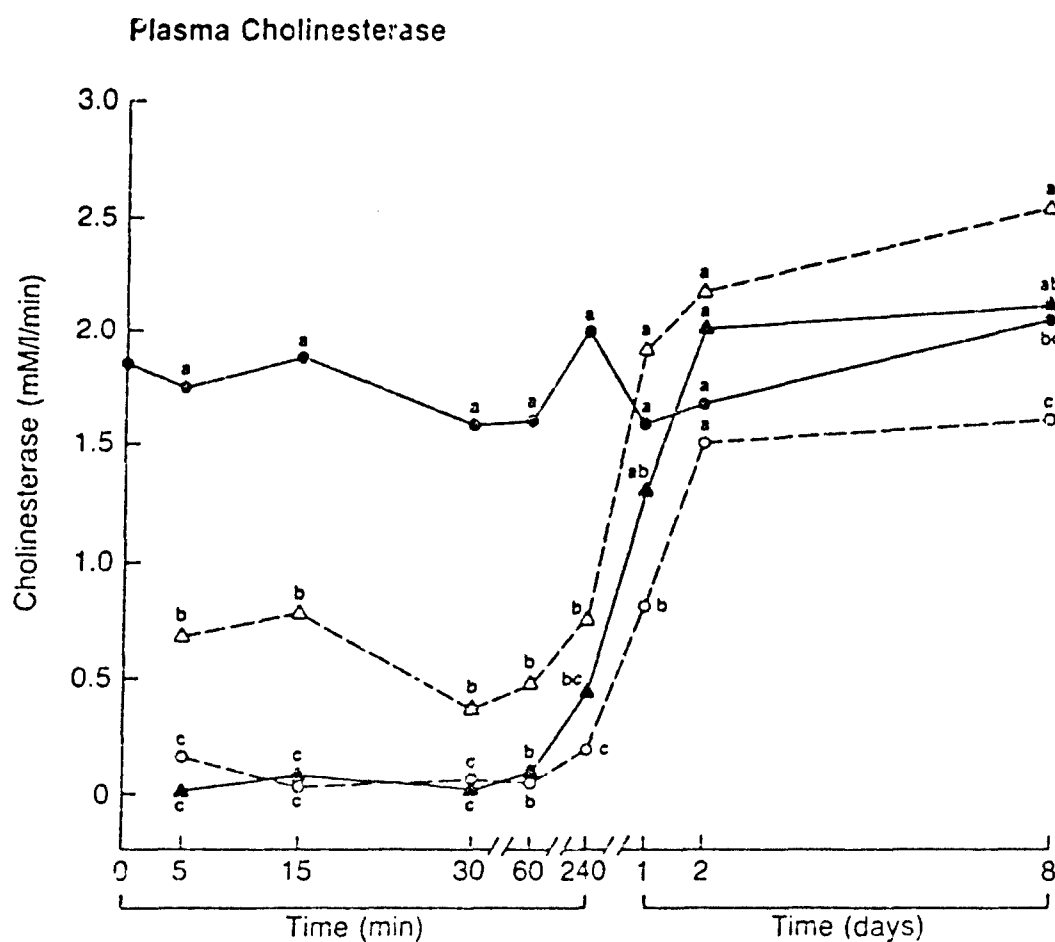
Prolonged survival followed by death in antx-a(s)-dosed mice also given atropine seems to suggest that nicotinic effects may have become important in the lethal syndrome after muscarinic receptors are blocked (Mahmood and Carmichael, 1986b). Muscarinic signs were more severe in antx-a(s)-dosed mice than in those given the other toxicants, while inhibition of diaphragm ChE and nicotinic signs appeared less severe. Since diaphragm ChE activities were similar in mice that survived antx-a(s) administration (up to 1 day postdosing) and those that died after being given the toxin, and since the degree of inhibition of ChE in diaphragm was less with antx-a(s) than with the other compounds, the peripheral nicotinic effects associated with antx-a(s) toxicosis could be of less importance and the muscarinic effects of greater toxicological significance than in lethal poisoning caused by either pyridostigmine or paraoxon.

Table 1. Comparison of diaphragm ChE activities of control mice and mice that died within 24 hours after IP injection of antx-a(s), paraoxon, and pyridostigmine.

Toxicant	Dose μg/kg	Diaphragm ChE Activity (μmole/g/minute)		
		N	Mean ± SD	Tukey's Grouping*
Control		4	1.1 ± 0.3	A
Antx-a(s)	0.29	8	0.73 ± 0.14	B
Pyridostigmine	2.11	27	0.29 ± 0.26	C
Paraoxon	1.23	19	0.03 ± 0.08	C

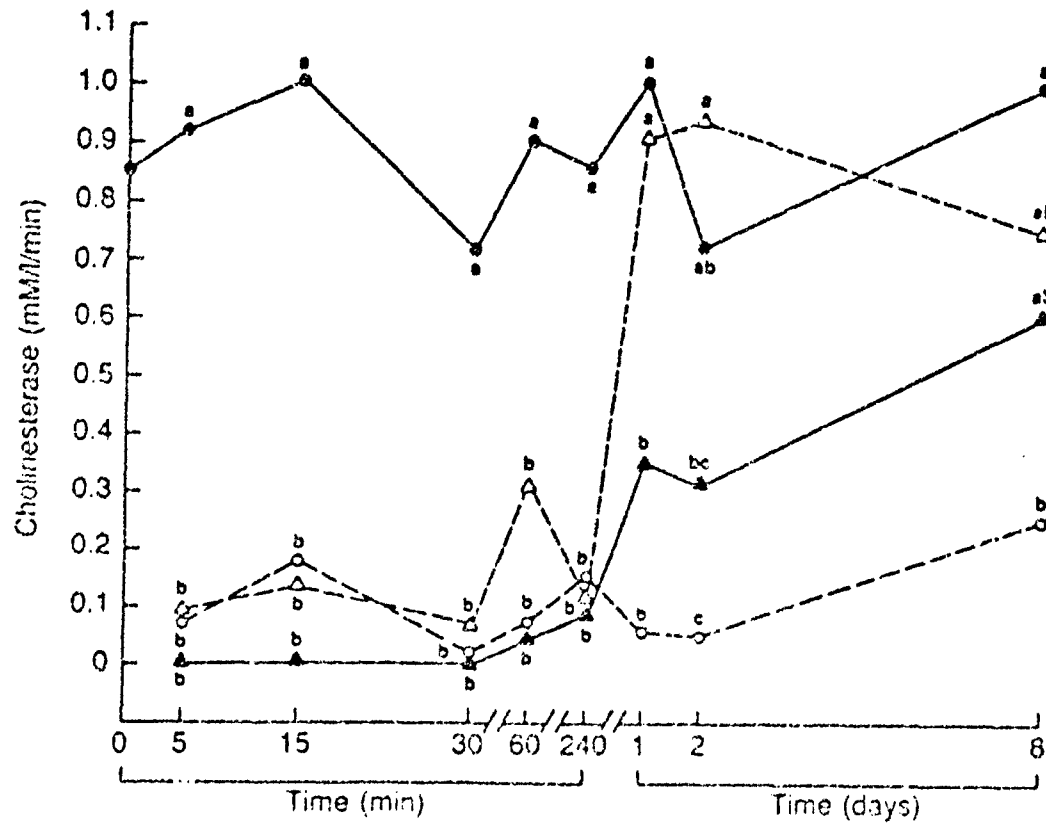
\*Treatment groups with different letters were significantly different ( $p < 0.05$ ).

Figure 1. Plasma ChE, RBC ChE, and diaphragm ChE activities of control mice (•) and mice given antx-a(s) at 0.29 mg/kg (○), paraoxon at 1.23 mg/kg (▲), or pyridostigmine bromide at 2.11 mg/kg (Δ) by IP injection. At each time point, treatment groups with different small letters next to the plotted mean observations are significantly different ( $p < 0.05$ ).





## Red Blood Cell Cholinesterase



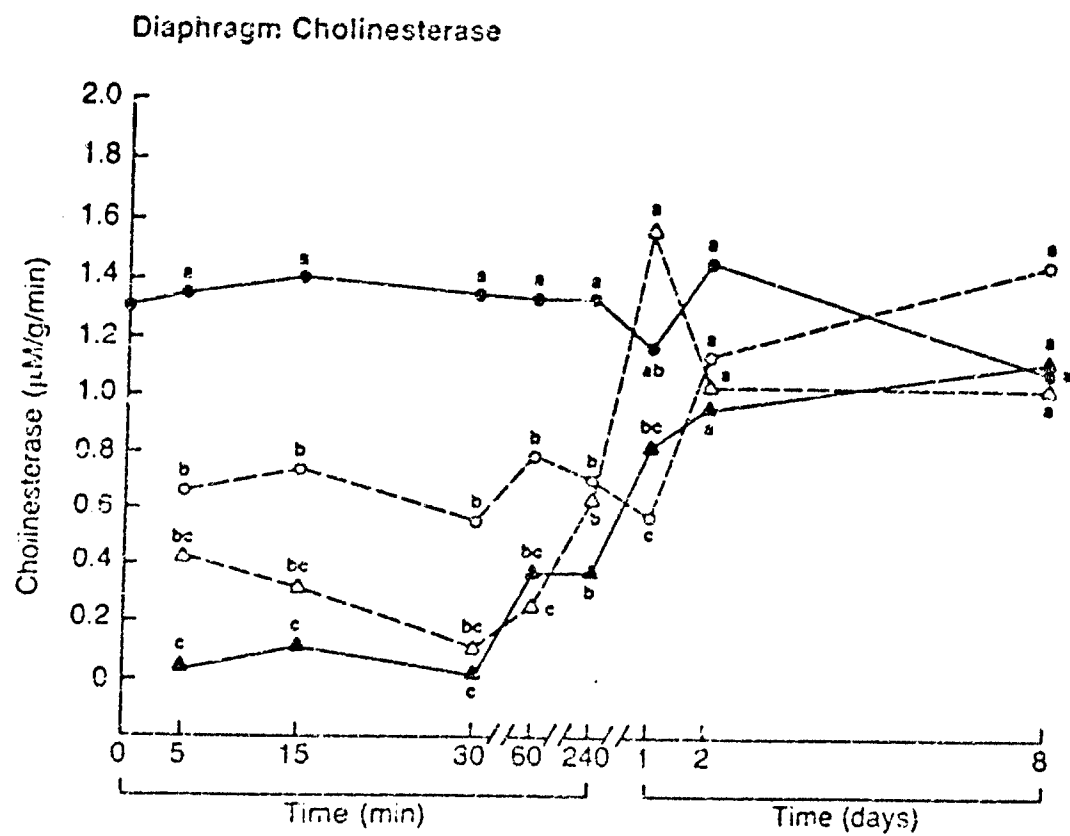
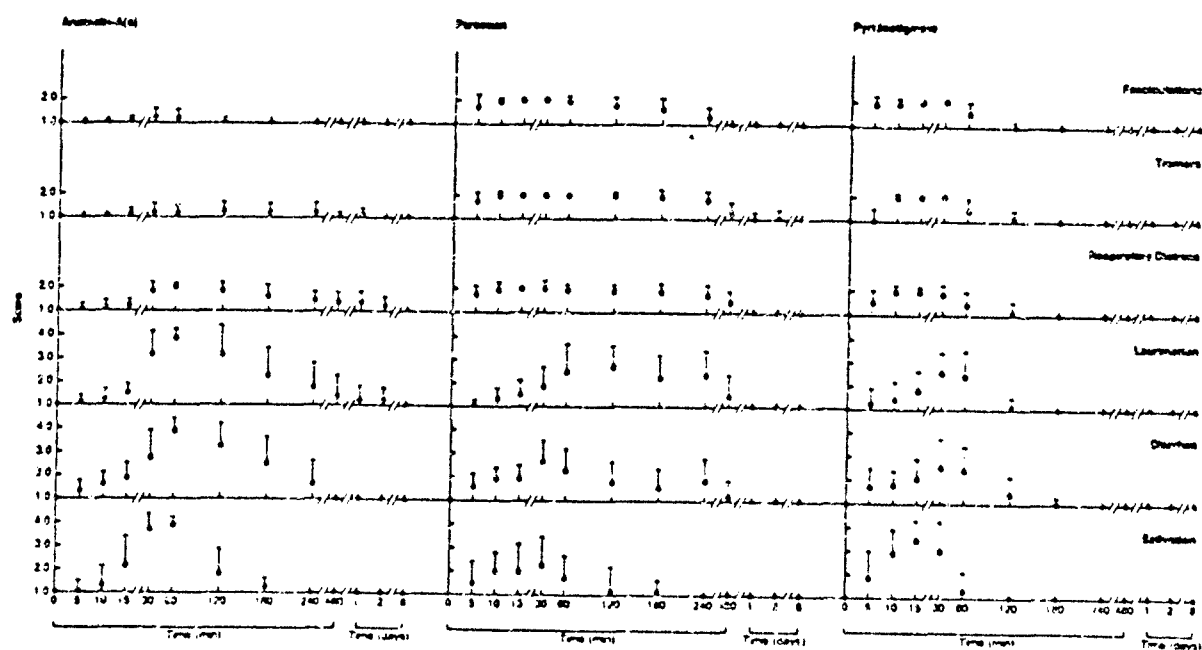


Figure 2. Mean values ( $\pm$  SD) for clinical signs: salivation, diarrhea, and lacrimation graded 1 to 4; and means for clinical signs: tremors and fasciculations graded 1 to 2 (absent or present) of mice given anatoxin-a(s) at 0.29 mg/kg, paraoxon at 1.23 mg/kg, or pyridostigmine bromide at 2.11 mg/kg by IP injection.



C. **Inhibition of Strictly Peripheral Cholinesterase by Neurotoxins from *Anabaena flos-aquae* in Ducks, Swine, Mice, and a Steer**

1. Statement of the Problem, Background, and Rationale

The previous study with semipurified antx-a(s) in mice dosed IP indicated that cholinesterase (ChE) inhibition induced by the toxin was limited to the periphery. This was surmised to be a result of an inability of the polar toxin to cross the blood brain barrier. Whether other cholinesterase inhibitors might also be present in whole algal bloom material or whether the blood brain barriers of other species might be less able to exclude algal inhibitors of ChE remained open to speculation. Moreover, the pathophysiologic events leading to the death of exposed animals was unclear. The purpose of the present study was to examine two algal blooms associated with spontaneous cases of sudden death (one involving ducks and the other involving swine) for ChE-inhibiting toxins by means of: (a) analysis for antx-a(s) and insecticides (in case of agricultural contamination), (b) ChE assays both *in vitro* and with tissues from field cases, and (c) ChE assays and pathophysiology studies in experimentally dosed animals.

2. Experimental Methods

Source of Algal Bloom Material and Case Histories

Algal material was collected following two spontaneous outbreaks of toxicosis in Illinois. In the first case, the algae was collected from a 0.015-ha surface, 7.3-m deep pond near Tolono, Illinois, during July of 1986. Five muscovy ducks had suddenly died, and clinical signs were noted in two other ducks including ataxia,

sternal and lateral recumbency, and apparent paralysis of the wings. Fifteen muscovies and four mallards had recently used the pond, 12 and one of which, respectively, had hatched 5 months previously; but only young muscovy ducks were affected. One clinically affected duck had returned to normal within 60 hours. One affected and five dead ducks were submitted for diagnostic examination. Bloom material was obtained from the pond, strained through gauze, and refrigerated at 4°C for future dosing studies.

In the second case, algal bloom material was collected from a 0.14-ha surface, 2.4-m deep pond near Griggsville, Illinois, in September of 1986. This pond served as the source of water for 17 sows, six boars, and 85 pigs weighing 18 to 23 kg. The sudden death of four sows, one boar, and eight pigs, as well as hypersalivation, dyspnea, ataxia, and recumbency in two pigs had been associated with ingestion of the algae. Frozen and formalin-fixed brain, diaphragm, eyes, kidney, liver, and lung were obtained from a sow subjected to necropsy on the farm. Bloom material was collected and refrigerated at 4°C for future dosing studies.

#### Algae Identification, Extraction and Purification, LD<sub>50</sub>s, and ChE Assay *In Vitro*

Algae was identified by light microscopy. The Tolono algae was extracted, redissolved, and analyzed with a Beckman Model 344 high-performance liquid chromatograph using methods identical to those for isolation of antx-a(s) from laboratory cultures (Mahmood and Carmichael, 1986b). LD<sub>50</sub>s for purified extracts were determined using five groups of five male ICR Swiss mice (18 to 22 g) given 25, 50, 100, or 200 µg of purified extract/kg. Animals were monitored for 2 hours

postdosing. The purified extract was also evaluated in electric eel AChE assays *in vitro* (Mahmood and Carmichael, 1987). In addition, lyophilized Tolono cells were subjected to toxin purification using  $C_{18}$  HPLC with comparisons to antx-a(s) from *A. flos-aquae* NRC-525-17 by Dr. Ken-Ichi Harada at Meijo University, Nagoya, Japan.

#### Insecticide Analysis

Both algal blooms were assayed for insecticide contamination. For carbamate analysis, 100-ml samples of dense algal bloom material were concentrated on a Waters Sep-pak  $C_{18}$  cartridge, eluted with 4 to 5 ml acetonitrile, and analyzed on a Series 3B Perkin-Elmer HPLC pump with an LC75 UV detector and a 650 10LC fluorescence detector in tandem. For organophosphorus or organochlorine insecticides, 100-ml samples were extracted with isooctane and analyzed on a Shimadzu GC-Mini-12 high-performance liquid chromatograph with OV-17 and OV-210 packed columns and a nitrogen-phosphorus detector and on a Hewlett-Packard gas chromatograph with an ECD detector.

#### IP Dosing Studies with Mice

Supernatant from Tolono algae was produced by freezing, thawing, and centrifugation (10,300 g for 10 minutes). Four male Swis-Webster mice (23 to 37 g) were injected IP, one each with 1.0, 0.5, or 0.25 ml of supernatant or 1.0 ml of distilled water (DW). Brain, diaphragm, and lung were collected at postmortem for ChE assays. The control mouse was killed by cervical dislocation after the other mice had died. Four additional mice were similarly dosed IP, one each with 0.20, 0.125, or 0.05 ml of supernatant or 0.2 ml of DW. Mice which displayed severe clinical

signs (10 to 20 minutes postdosing) including dyspnea, hypersalivation, or marked tremors were killed by decapitation and blood was collected with heparin for ChE assays.

Supernatant from Griggsville algae was similarly prepared and given IP to four mice. Two each were dosed with 0.3 ml of the supernatant or 1.0 ml of DW. Mice were killed and blood and tissues were collected as above for ChE assays.

#### Repeated Oral Dosing Studies with Mice

Male Swiss-Webster mice (25 to 42 g) were treated by gavage with the Tolono algae. Five mice were dosed daily, three with strained algae at 22 ml/kg for 5 days and two with DW. At 3 hours postdosing on day 5, mice were killed by decapitation and blood and tissues were collected as above for ChE assays. In addition, three mice were treated by gavage with Griggsville algae supernatant at 22 ml/kg for five days, and two were similarly dosed with DW.

#### Oral Dosing of Ducks

A 5-month-old muscovy duck (1.8 kg) from the affected farm was dosed by intracrop intubation with a no. 10 French polypropylene catheter with strained Tolono algae at 22 ml/kg daily for 4 days. Subsequently, six 6-month-old muscovy ducks (2 to 3 kg) were fed a complete ration (Growena L Duck Chow, Ralston Purina, St. Louis, MO) twice daily, provided water *ad libitum*, and given 5 days to become acclimated to the laboratory. Four of these ducks were similarly dosed with 22 ml of strained Tolono algae/kg at 0, 24, 48, 72, and 75 hours. Two ducks were given DW. Ducks surviving 78 hours were killed by decapitation. Blood for plasma ChE assays

was collected from the wing vein with a heparinized syringe prior to dosing and before decapitation or death. Brain, eyes, lung, and pectoral muscle of ducks were collected for ChE assays.

#### Intragastric Dosing Studies with Swine

Three pigs (14 to 17.5 kg) were obtained from the Veterinary Medicine Research Farm, fed a 16% protein, corn-soybean-based diet twice daily, and provided water *ad libitum*. The animals were given a preanesthetic dose of atropine and anesthetized with halothane. Carotid and jugular catheters (16-gauge Tygon Microbore tubing, A. Daigger and Sons, Chicago, IL) were surgically placed, capped, filled with heparin, and buried subcutaneously. After 2 days for recovery, each pig was held off feed for 12 hours prior to dosing and catheters were exteriorized under lidocaine-induced local anesthesia. Two pigs (no. 1 and 2) were treated by gavage with strained Tolono algae at 22 ml/kg. Pig no. 3 was similarly given DW at 22 ml/kg.

When hypersalivation was observed, pig no. 2 was given atropine sulfate at 0.5 mg/kg (one-fourth IV, three-fourths IM) and superactivated charcoal (SuperChar-Vet, Gulf Biosystems, Dallas, TX) at 2.2 g/kg mixed in five times as much water by stomach tube. Paired blood samples were collected at least every 30 minutes from pig no. 1 and 3 (until the death of pig no. 1) for ChE assays, blood gas determinations, and assessments of hematologic and serum biochemical parameters. Blood gases were measured on an IL-813 Instrumentation Laboratories (Lexington, MA) blood gas machine. Heart rate, respiratory rate, and rectal temperature were recorded at the same times. Pig no. 3 (control) was killed by electrocution at 8 minutes after pig



no. 1 died. With pig no. 2, blood gases were measured every 30 to 60 minutes for the first 7 hours. Blood from pig no. 2 for ChE assays was collected at the same times as for blood gases and daily thereafter until 72 hours postdosing, when the pig was killed by electrocution. At postmortem, brain, diaphragm, eyes, and lung were collected from all pigs for ChE assays.

#### Intraruminal and Parenteral Administration to a Steer

A 4-month-old, ruminating, cross-bred steer (145 kg) was fed alfalfa hay and provided water *ad libitum*. Anesthesia was induced with glyceryl guaiacolate-xylazine-ketamine (Thurmon and Benson, 1986), and carotid and jugular catheters were implanted, filled with heparin, and buried SC. Forty-eight hours later (the first day of dosing), catheters were exteriorized under lidocaine-induced local anesthesia. The steer was held off feed from 12 hours. An initial intraruminal dose of the strained Tolono algae at 22 ml/kg was followed 24 hours later by a second dose at 35 ml/kg. Feeding was resumed at 1 day after the second dosing. Blood in EDTA was collected for ChE assays predosing and at 1, 2, 24, 36, 48, and 72 hours after the initial dosing.

At 48 hours after the second intraruminal dose, the steer was dosed parenterally (intended to be IP) with 300 ml of supernatant produced by freezing, thawing, and centrifuging (23,200 g for 10 minutes) the Tolono algae. A second IP dose of 250 ml was given 35 minutes later. Each injection was made via the left paralumbar fossa under lidocaine-induced local anesthesia. Blood was collected for hematologic and serum biochemical assays before the IP dosing and 5 minutes before death. Arterial

blood gases, mean aortic and central venous blood pressure, heart rate, respiratory rate, and rectal temperature were determined and blood was collected in EDTA for ChE assays at least every 10 minutes after IP dosing. Blood pressures were measured using Model P23 Gould Statham (Hato Ray, Puerto Rico) pressure transducers and a Gilson physiograph. Brain, diaphragm, eyes, and lung were collected at postmortem for ChE assays.

#### Histologic Studies

Adrenal gland, brain, diaphragm, sections of the digestive tract, heart, kidney, liver, pancreas, pectoral muscle, and spleen of the pigs, steer, and/or ducks from dosing experiments and of the ducks and the sow from the field cases were collected postmortem and fixed in 10% buffered formalin, sectioned at 6  $\mu$ m, and stained with hematoxylin and eosin for histologic examination.

#### ChE Determinations

ChE assays on whole blood, plasma, diaphragm, lung, and pectoral muscle were performed using the method of Ellman et al. (1961). Red blood cells (RBC) were separated from plasma by centrifugation at 547.4 g for 5 minutes and RBC ChE activity was determined using a modification of the Ellman method, such that RBCs were lysed with octyl phenoxy polyethoxyethanol (1:19, v/v). Brain and retina tissues were analyzed by a different modification of the Ellman method (Harlin and Ness, 1986; Harlin, 1987).

### 3. Results

#### Algae Identification, Insecticide Analyses, Assays *In Vitro*, Purification, and Bioassay

In both cases, algae were identified as *A. flos-aquae*. Insecticides were not detected in the bloom material. The Tolono and Griggsville algae contained 93.1 and 97.6% water, respectively.

In the electric eel AChE assay performed *in vitro*, incubation of a control solution or 0.2, 0.4, 1.0, 4.0, and 10.0 ng HPLC-purified extract/ $\mu$ l of assay fluid caused 0, 46, 58, 64, and 100% ChE inhibition, respectively. The degree of inhibition per nanogram of extract was comparable with that induced by the standards of antx-a(s) used. Analysis of Tolono extract by  $C_{18}$  HPLC revealed a toxin-causing cholinergic effect in a mouse bioassay but with a retention time different from that of the antx-a(s) standard, suggesting the presence of a different ChE-inhibiting toxin(s).

#### LD<sub>50</sub>, Clinical Signs, and Cholinesterase Inhibition in Mice

The LD<sub>50</sub> of the extract purified (Mahmood and Carmichael, 1986b) from Tolono algae was 37.5  $\mu$ g/kg in mice. Clinical signs in these mice included hypersalivation, lacrimation, urination, muscle fasciculations, respiratory distress, cyanosis, and terminal clonic convulsions.

Similar clinical signs were noted in mice dosed IP with supernatant from the bloom materials or with purified extracts. Inhibition of ChE consistently occurred in tissues of mice dosed IP except for the brain (Table 1). Following intragastric administration of bloom material or similar administration of purified extracts for 5 days, the mice did not develop clinical signs. Also, ChE inhibition was not observed

in tissues of mice given the Tolono algae. Gross lesions in affected mice included hepatic and renal congestion and diarrhea.

#### Effects on Ducks Dosed by Gavage

Clinical signs were not observed until ducks had been dosed at least twice. Three ducks died after repeated dosing with Tolono algae (Table 2). Clinical signs, in usual order of onset, included: severe hypersalivation, regurgitation of algae, diarrhea/urination, polydipsia, muscle tremors, depression, paresis of wings and legs, ataxia, recumbency, dilatation of cutaneous blood vessels in webbed feet, dyspnea with open-mouth breathing, opisthotonus, intermittent tonic seizures, and death. Ducks often appeared relatively normal until stressed. Attempts to pick them up frequently resulted in ataxia, recumbency, paresis of legs and wings, or tonic seizures.

ChE was inhibited in plasma, lung, and pectoral muscle but not in brain or retina of the algae-dosed ducks (Table 2). Gross lesions in affected ducks included evidence of diarrhea and excessive saliva in the esophagus. Histological examinations were unremarkable.

#### Effects on Pigs

Within 30 minutes of dosing with algae, the first pig developed profuse salivation and mucoid nasal discharge, followed by dilation of the rectal sphincter, bruxism, muscle fasciculations, tremors, vomiting, defecation, urination, coughing, prolonged capillary refill time, cold ears, dyspnea, cyanosis, struggling, and death at 1.4 hours after dosing. Hematologic examination revealed mild hemoconcentration, and  $pO_2$  decreased to 51.6 mmHg. Whole blood, plasma, and RBC ChE became

progressively inhibited (Table 3). ChE of diaphragm and lung appeared to be inhibited, unlike the response of brain and retina ChE activity (Table 4). At postmortem, 150 ml of clear viscous fluid (presumably saliva) was noted in the stomach. No histologic lesions were detected.

Marked hypersalivation was noted at 19 minutes postdosing in the second algae-dosed pig, at which time atropine and activated charcoal were administered. Excessive salivation ceased in response to atropine, but prominent muscle fasciculations developed and persisted for 18 hours. Atropine was administered two more times over the next 12 hours when hypersalivation returned. Blood arterial  $pO_2$  and blood pH never decreased below 70 mmHg and 7.4, respectively, and the pig never became clinical dyspneic. ChE activity of blood, plasma, and RBCs decreased progressively after dosing and within 1 hour had reached less than 10% of predose values. When the pig was killed at 72 hours postdosing, whole blood, plasma, and RBC ChE activities were still only 16, 22, and 5% of predose values, respectively. ChE assays suggested inhibition of the enzyme in diaphragm and lung but not brain (Table 4). Postmortem examination revealed mild gastric erosions. No histologic lesions were noted apart from those associated with the gastric erosions.

In the control pig, no remarkable changes occurred in ChE values or in hematologic, serum biochemistry, blood gas, or pH values. Also no gross or histologic lesions were detected.

Assays of tissues from the sow from Griggsville suggested enzyme inhibition in the diaphragm and lung but not in brain or retina (Table 4). No histologic lesions were observed in the submitted tissues.

#### Effects on the Steer

No clinical signs or inhibition of whole blood, plasma, or RBC ChE were observed after intraruminal administrations of Tolono algae. After parenteral dosing, however, arterial blood  $pO_2$  decreased,  $pCO_2$  increased, pH decreased, and inhibition of whole blood, plasma, and RBC ChE occurred (Table 5). Clinical signs included hypersalivation, paresis, tremors, dyspnea, recumbency, and cyanosis followed by death at 75 minutes after the initial injection. Changes in mean aortic and central venous blood pressure, heart, and respiratory rate were unremarkable until the steer was recumbent and moribund. Hematologic and serum biochemistry parameters were never altered beyond normal ranges. ChE activity of brain, diaphragm, lung, and retina were 4.5, 0.07, below the detection limit (0.03), and 23.5  $\mu\text{mol/g/minute}$ , respectively, as compared to historical controls for brain and retina of  $4.2 \pm 0.84$  and  $21.1 \pm 1.8$   $\mu\text{mol/g/minute}$  (mean  $\pm$  SD), respectively. Postmortem examination revealed that a portion of the first IP injection had been deposited retroperitoneally. Histologic examination of other tissues revealed no lesions.

#### 4. Discussion

As indicated by effects on ChE in whole blood, plasma, RBC, diaphragm, lung, and pectoral muscle of experimentally dosed animals and in tissues from the naturally exposed ducks and swine, as well as electric eel AChE *in vitro*, ChE-inhibiting

neurotoxins were indeed present in the algal material from both field cases. The consistent inhibition of ChE across a range of species in tissues other than brain or retina indicates that these toxin(s) inhibit the enzyme in peripheral locations but apparently not in the central nervous system. Toxin was absorbed and distributed in amounts sufficient to inhibit peripheral tissues and to cause clinical signs and lethality. Thus, it is assumed that these toxin(s) are unable to cross the blood brain barrier. In fact, all algal ChE inhibitors examined in our laboratory, including antx-a(s) and ChE-inhibiting toxin(s) in extracts of algae from another field case involving sudden death of a dog (Cook, unpublished data), have appeared to act only on peripheral ChE. When animals are found dead in the field, such as in the present cases, brain and retina are the tissues most often used to indicate exposure to ChE-inhibiting toxicants (Harlin and Ness, 1986; Harlin, 1987; Osweiler et al., 1984). In cases similar to those reported here, a diagnosis of death due to a cholinesterase inhibitor would be missed if only brain and retinal ChE assays and insecticide analyses are performed. Diagnoses may be hampered further by problems that may occur in confirming any algal toxicosis, such as rapidly changing populations of algal species in blooms and rapid breakdown of algae and toxins, especially the labile ChE-inhibiting toxins.

Toxin(s) in Tolono algae specifically inhibited AChE both in the purified eel preparation *in vitro* and RBCs *in vivo*. Inhibition *in vitro* indicates that the toxin(s) in Tolono algae does not require activation *in vivo*, which is similar to the case of antx-a(s). Although the pattern of ChE inhibition and clinical signs in animals

exposed to the Tolono algae were indistinguishable from those observed with antx-a(s), the chemical analysis indicated that a different toxin(s) was present.

Based on blood gases and respiratory difficulty and cyanosis in all affected animals prior to death, death was an apparent result of hypoxia and acidosis. Respiratory failure may have resulted from peripheral ChE inhibition since the decline in enzyme activity in blood paralleled the severity of clinical signs in animals and the degree of ChE inhibition in peripheral tissues at the time of clinical signs and death was consistent with the effects of other ChE inhibitors (Oswiler et al., 1984; Frawley et al., 1952; Holmstedt, 1959). The combination of activated charcoal and atropine may have been lifesaving in one pig administered a potentially toxic dose of algae.

Large death losses in chickens, ducks, turkeys, and waterfowl with histories similar to the present cases have been reported in the literature in association with *A. flos-aquae* blooms, but definitive diagnoses in these early reports were frequently lacking (Gorham, 1964; Deem and Thorp, 1939; Fitch et al., 1934). The present study seems to confirm the natural occurrence of toxicoses in waterfowl due to ChE-inhibiting toxins of *A. flos-aquae* and suggests that toxicity can be cumulative over a period of days. Polydypsia in the ducks of this study was probably a result of dehydration from profuse salivation and urination/defecation. In nature, a combination of the resultant further ingestion of algae and the irreversible nature of ChE inhibition induced by these toxins would be likely to bring about progressively more severe toxicosis.



Major death losses in swine and cattle have also been reported in the literature in association with *A. flos-aquae* blooms (Gorham, 1964; Fitch et al., 1934; Hammer, 1968). We have confirmed that toxicosis due to algal ChE-inhibiting toxins can occur naturally in swine, and in fact, swine seemed to be the species most susceptible to intragastric administration of the Tolono algae. Sudden deaths in dogs in suspected field cases suggest that dogs may also be extremely susceptible (Carmichael and Gorham, 1978; Mahmood et al., 1988; Cook, unpublished data). The absence of clinical signs or inhibition of blood ChE after two intraruminal doses of strained Tolono algae in the steer of this study may indicate that cattle are not very susceptible to these toxins; and previous reports of suspected poisoning in cattle by neurotoxic cyanobacteria may have been due to other toxins such as aphantoxins (saxitoxin and neosaxitoxin) or the nicotinic agonist, antx-a, which is known to be toxic to orally exposed cattle (Carmichael et al., 1977). Antx-a(s) is more stable in highly acidic than in neutral aqueous solutions (Mahmood and Carmichael, 1987). Differences between species, including gastric versus ruminal pH, volume, and emptying time may be involved so that species with smaller, highly acidic stomachs may be more at risk.

Table 1. ChE activities in mice dosed IP with supernatant from freeze-lysed algae from Tolono and Griggsville, Illinois.

Mouse Number and Dose	ChE				
	Whole Blood	Plasma	Brain	Diaphragm	Lung
	(mmol/L/minute)		(μmol/g/minute)		
Tolono					
1. Control	ND	ND	12.7	1.9	2.1
2. 1.0 ml supernatant*	ND	ND	15.2	0.18	0.14
3. 0.50 ml supernatant*	ND	ND	15.0	0.55	0.25
4. 0.25 ml supernatant*	ND	ND	11.6	0.28	0.36
5. Control	1.8	2.5	ND	ND	ND
6. 0.20 ml supernatant	BDL	0.06	ND	ND	ND
7. 0.125 ml supernatant	BDL	0.04	ND	ND	ND
8. 0.05 ml supernatant	BDL	0.11	ND	ND	ND
Griggsville					
1. Control	1.8	2.6	10.2	1.5	2.7
2. Control	2.0	3.1	12.9	1.2	2.8
3. 0.30 ml supernatant	BDL	BDL	12.9	BDL	0.33
4. 0.30 ml supernatant	BDL	BDL	12.2	0.56	0.33

ND, not determined; BDL, below detection limits of 0.03 mmol/L/minute for whole blood or plasma and of 0.03 μmol/g/minute for brain, diaphragm, and lung.

\*Mice died 5 to 15 minutes postdosing.

Table 2. ChE activities in muscovy ducks following successive administration via crop intubation of Tolono algae at 22 ml/kg, and brain ChE activity in clinically or lethally poisoned ducks from the Tolono field case.

Procedure/Response of Duck	ChE					
	Plasma (nmol/L/minute)		Tissue (µmol/g/minute)			
	Predose	Prideath	Brain	Lung	Pectoral Muscle	Retina
Died after 2 doses	0.27	BDL	12.8	0.20	0.09	8.9
Died after 4 doses <sup>a</sup>	0.23	BDL	13.0	0.14	0.08	9.1
Decapitated after 5 doses <sup>b</sup>	0.29	0.05	13.0	0.37	0.20	10.4
Decapitated after 5 doses <sup>c</sup>	0.22	0.03	12.7	0.48	0.10	10.9
Died after 5 doses	0.26	BDL	12.1	0.25	0.09	7.0
Control	0.27	0.26	12.7	0.78	0.27	8.5
Control	0.29	0.27	12.9	0.78	0.36	8.9
Field death	ND	ND	12.7	ND	ND	ND
Field case <sup>c</sup>	ND	ND	12.6	ND	ND	ND

BDL, below detection limit; ND, not determined.

<sup>a</sup>Duck from affected farm.

<sup>b</sup>Mild clinical signs when killed.

<sup>c</sup>Moderate clinical signs when killed.

Table 3. Whole blood, plasma, and red blood cell (RBC) ChE in pig no. 1 given a lethal intragastric dose of Tolono algae at 22 ml/kg.

Time (minutes)	ChE (mmol/L/minute)		
	Whole Blood	Plasma	RBC
Predose	1.4	0.27	2.2
30	0.07	0.06	0.07
60	BDL	0.05	0.06
82	BDL	0.04	BDL

BDL, below detection limit of 0.03 mmol/L/minute.

Table 4. Tissue ChE activity in pigs dosed with Tolono algae at 22 ml/kg and in a sow that died in the field at Griggsville, Illinois.

Pig Number	ChE ( $\mu\text{mol/g/minute}$ )			
	Brain	Diaphragm	Lung	Retina
1. Lethal dose <sup>a</sup>	5.6	0.09	0.09	16.9
2. Lethal dose and treated <sup>b</sup>	6.0	0.13	0.30	ND
3. Control	6.0	0.27	0.45	13.2
4. Sow <sup>c</sup>	4.4	BDL	0.13	13.1

ND, not determined; BDL, below detection limit of 0.03  $\mu\text{mol/g/minute}$ .

<sup>a</sup>Dosed, not treated, and died 1.4 hours after dosing.

<sup>b</sup>Dosed, treated with activated charcoal and atropine, and survived until killed by electrocution at 3 days postdosing.

<sup>c</sup>Field death, found dead beside pond in Griggsville in association with the algal bloom.

Table 5. Whole blood, plasma, and red blood cell (RBC) ChE activity, and blood gases and pH in a steer dosed parenterally with a supernatant of centrifuged freeze-lysed algae from Tolono, Illinois.

Time (minutes)	ChE (mmol/L/minute)			Blood Gases (mmHg)		Blood pH
	Whole Blood	Plasma	RBC	pO <sub>2</sub>	pCO <sub>2</sub>	
Pre-dose	1.7	0.12	2.8	87.8	40.9	7.40
0 (dosed: 300 ml IP/retroperitoneal)						
5	0.93	0.07	2.8	ND	ND	ND
10	0.63	0.03	0.95	87.6	36.2	7.40
20	0.17	BDL	0.16	99.3	39.6	7.39
30	0.13	BDL	0.04	94.6	36.8	7.39
35 (redosed: 250 ml supernatant IP)						
40	ND	ND	ND	81.9	36.8	7.40
50	BDL	BDL	0.04	ND	ND	ND
60	BDL	BDL	BDL	44.3	32.3	7.22
70	BDL	BDL	BDL	41.0	46.5	7.32
75	ND	ND	ND	41.0	52.6	7.26

ND, not determined; BDL, below detection limit of 0.03 mmol/L/minute for whole blood, plasma, and RBC.

**D. Regional Brain Cholinesterase Activity in Rats Given Anatoxin-a(s) or Paraoxon Intraperitoneally**

1. Statement of the Problem, Background, and Rationale

The mechanism of action of anatoxin-a(s) [antx-a(s)] has been postulated to be cholinesterase (ChE) inhibition (Mahmood and Carmichael, 1986b, 1987) based on toxin-induced irreversible inhibition of electric eel acetylcholinesterase (EC 3.1.1.7) *in vitro* and inhibition of blood ChE and clinical signs in exposed animals. The ability of ChE-inhibiting agents to cross the blood brain barrier and inhibit brain ChE influences the resultant toxicosis (Taylor, 1985). Moreover, different regions of the brain may exclude xenobiotics more effectively than others.

The goal of the present study was to determine whether antx-a(s) given intraperitoneally would inhibit ChE in specific areas of the central nervous system, including the medulla which contains the respiratory center nuclei and the hypothalamus which has regions containing vessels that are more permeable to macromolecules (Guyton, 1976; Jacobs, 1982; Norton, 1986). To aid in interpretation, antx-a(s) was compared with the well-known peripheral and central ChE inhibitor, the organophosphorus compound paraoxon. Whole-blood ChE activity was monitored to quantify inhibition of peripheral ChE activity and to confirm systemic absorption of the test compounds.

## 2. Experimental Methods

### Animals

Forty male Long-Evans rats (300 to 380 g) were provided food (Rodent Laboratory Chow 5001, Purina Mills, Richmond, IN) and water *ad libitum* and housed on a 12/12-hour light/dark cycle.

### Toxicants

Antx-a(s) was isolated and characterized by the method of Harada et al. (1988) from cultures of *A. flos-aquae* strain NRC-525-17 (Mahmood and Carmichael, 1987). Thin-layer chromatography had indicated purity of 80 to 90%, and a major portion of the remaining material used in this study was low-molecular-weight salts from the culture media and purification process (with which no toxicity was associated upon repeated testing). The approximate LD<sub>50</sub> of a similarly purified specimen was determined to be 31 µg/kg in mice dosed intraperitoneally (Carmichael, W., unpublished data). Antx-a(s) was stored under nitrogen gas at -20°C prior to use, brought into solution with 1 mM acetic acid, and diluted with physiological saline. Paraoxon (Sigma Chemical, St. Louis, MO) stored at a concentration of < 10 mM at -20°C in dry acetone was diluted with physiological saline so that the final dosing solution contained < 1% acetone. The control solution was comprised of saline containing acetic acid at the highest concentration used with antx-a(s) and was administered at a volume/body weight equal to that used with antx-a(s).



### Experimental Design

In order to establish the toxicity of the test material, an intraperitoneal 24-hour  $LD_{50}$  for antx-a(s) was determined with eight rats using the up-and-down procedure of Bruce (1985). Groups of rats were subsequently dosed intraperitoneally with antx-a(s), paraoxon, or a control solution. Eight rats per treatment group were used for brain ChE determination. Doses of antx-a(s) included: (a) 1.5  $\mu\text{g/kg}$  which was a threshold dose and produced barely detectable clinical signs, primarily diarrhea and decreased movement; (b) 3.0  $\mu\text{g/kg}$  which produced clinical signs of hypersalivation, lacrimation, diarrhea, decreased movement, mild tremors and fasciculations, dyspnea, and ataxia; and (c) 9.0  $\mu\text{g/kg}$  which was consistently lethal within 1 hour of dosing. Paraoxon was given at 800  $\mu\text{g/kg}$  which produced clinical signs similar to the intermediate dose of antx-a(s).

### Specimens and ChE Assays

Rats lethally dosed with antx-a(s) were bled at the time of death via the caudal abdominal vena cava for whole-blood ChE assays. At 2 hours postdosing, surviving rats were anesthetized with carbon dioxide gas, bled similarly for whole-blood ChE assays, and killed by exsanguination. Brains of the rats were dissected as previously described (Glowinski and Iversen, 1966) into eight regions: cerebellum, cortex, medulla, midbrain, hippocampus, hypothalamus, olfactory lobes, and striatum, and the spinal cord within the first three cervical vertebrae was removed. Brain and spinal cord tissues were weighed, immediately frozen, and stored at  $-20^{\circ}\text{C}$  until assayed within 48 hours for ChE activity.

ChE assays on blood were performed by the method of Ellman et al. (1961). Nervous tissue ChE activity was assayed by the Ellman method with modifications by Harlin and Ness (1986).

#### Statistical Analysis

The 24-hour LD<sub>50</sub> was calculated by the method of Salsburg (1984). Comparisons among treatment groups for brain, spinal cord, and whole-blood ChE activities were performed using the SAS General Linear Model with Tukey's test (SAS Institute, 1985). A level of  $\alpha = 0.05$  was chosen to identify statistically significant differences.

### 3. Results

The LD<sub>50</sub> of antx-a(s) in rats dosed IP was 5.3 µg/kg. Blood, brain, and spinal cord ChE results are shown in Tables 1 and 2. Inhibition of whole-blood ChE activity was observed in all rats given either antx-a(s) or paraoxon. Significant inhibition of ChE activity was present (but not in all regions) in the brain and spinal cord of rats given paraoxon but not in any region of the brain or spinal cord of rats given antx-a(s).

### 4. Discussion

Given intraperitoneally, antx-a(s) does not appear to be able to inhibit ChE in any of the regions evaluated in the central nervous system, including the highly cholinceptive olfactory lobes of the brain (Shipley and Nickel, 1987). Also, no inhibition of ChE was evident in the medulla oblongata which contains the respiratory center nuclei, suggesting that respiratory failure was not a result of a build up of

excessive acetylcholine at synapses of the medulla. Also, no inhibition of ChE was noted in the hypothalamus which contains the median eminence, a small area with increased vascular permeability to macromolecules (Guyton, 1976; Jacobs, 1982; Norton, 1986).

Antx-a(s) is likely to be strongly ionized at physiological pH, and strongly ionized compounds, such as quaternary amines, are commonly unable to penetrate the central nervous system from the circulation (Mayer et al., 1980). Thus, the lack of ChE inhibition in the central nervous system seems likely to be due to inability of the toxin to cross the blood brain barrier. Although metabolism of antx-a(s) might also have reduced exposure of the brain, toxin was absorbed from the peritoneal cavity and presented to other sites in amounts sufficient to inhibit whole-blood ChE and induce clinical signs of toxicosis including death.

The findings of the present study suggest that antx-a(s) is strictly a peripheral ChE inhibitor.

Table 1. Cholinesterase activity in areas of the brain and spinal cord of rats dosed intraperitoneally with antx-a(s) compared to paraoxon.

Treatment <sup>a</sup>	Cholinesterase ( $\mu\text{mol} \cdot \text{g}^{-1} \cdot \text{min}^{-1}$ ) (mean $\pm$ SD)								
	Cerebellum	Cortex	Hippocampus	Hypothalamus	Medulla	Midbrain	Olfactory Lobes	Striatum	Spinal Cord
Control	4.3 $\pm$ 0.24	11.5 $\pm$ 1.1	8.1 $\pm$ 0.73	11.4 $\pm$ 1.6	12.8 $\pm$ 0.59	13.7 $\pm$ 1.2	5.7 $\pm$ 0.59	53.4 $\pm$ 5.0	9.1 $\pm$ 0.6?
Anatoxin-a(s)									
1.5 $\mu\text{g}/\text{kg}$	4.5 $\pm$ 0.23	11.2 $\pm$ 1.3	8.8 $\pm$ 1.5	11.2 $\pm$ 1.8	12.4 $\pm$ 0.75	12.3 $\pm$ 0.75	5.8 $\pm$ 0.61	54.9 $\pm$ 7.1	9.1 $\pm$ 0.45
3.0 $\mu\text{g}/\text{kg}$	5.1 $\pm$ 1.82	11.4 $\pm$ 0.9	8.3 $\pm$ 0.53	11.3 $\pm$ 1.6	12.5 $\pm$ 0.91	13.7 $\pm$ 0.45	5.9 $\pm$ 0.86	53.8 $\pm$ 5.2	9.2 $\pm$ 0.69
9.0 $\mu\text{g}/\text{kg}$	4.1 $\pm$ 0.35	11.5 $\pm$ 1.2	8.0 $\pm$ 0.46	11.8 $\pm$ 1.1	11.8 $\pm$ 1.1	14.3 $\pm$ 1.1	5.7 $\pm$ 0.45	50.5 $\pm$ 13.0	8.5 $\pm$ 0.71
Paraoxon (800 $\mu\text{g}/\text{kg}$ ) <sup>b</sup>	1.3 $\pm$ 0.25	2.3 $\pm$ 0.79	2.0 $\pm$ 0.41	3.1 $\pm$ 0.54	2.7 $\pm$ 0.56	3.1 $\pm$ 0.69	1.4 $\pm$ 0.35	9.9 $\pm$ 3.6	1.9 $\pm$ 0.62

<sup>a</sup>N = 7 or 8 for each treatment group.

<sup>b</sup>For all tissues analyzed, the cholinesterase activities of the paraoxon treatment group were significantly lower ( $p < 0.05$ ) by Tukey's test than those of the other treatments. Control group values were not statistically different from any of the groups given antx-a(s).

Table 2. Whole-blood cholinesterase activity in rats dosed intraperitoneally with antx-a(s), paraoxon, and a control solution.

Treatment <sup>a</sup>	Cholinesterase (mmol • l <sup>-1</sup> • min <sup>-1</sup> ) <sup>b</sup> (mean ± SD)
Control	1.1 ± 0.11 <sup>A</sup>
Anatoxin-a(s)	
1.5 µg/kg	0.48 ± 0.38 <sup>B</sup>
3.0 µg/kg	0.15 ± 0.04 <sup>C</sup>
9.0 µg/kg	0.05 ± 0.04 <sup>C</sup>
Paraoxon (800 µg/kg)	0.13 ± 0.08 <sup>C</sup>

<sup>a</sup>N = 7 or 8 for each treatment group.

<sup>b</sup>Treatment groups with different uppercase superscript letters were significantly different (p < 0.05) by Tukey's test.

## E. Effect of Anatoxin-a(s) on Cardiac and Pulmonary Function and Phrenic Nerve Activity in Rats

### 1. Statement of the Problem, Background, and Rationale

Death as a result of poisoning by low-molecular-weight anticholinesterase agents has commonly been attributed primarily to respiratory failure arising from effects on the central nervous system (de Candole et al., 1953; Rickett et al., 1986; Beers et al., 1987). Measurement of phrenic nerve activity is effective for differentiating peripherally from centrally mediated respiratory failure (de Candole et al., 1953; Wright, 1954; Rickett et al., 1986). Clinical signs in mice and rats given anatoxin-a(s) [antx-a(s)] include dyspnea, seizures, and death from apparent respiratory failure (Mahmood and Carmichael, 1986b; Cook et al., 1988). Studies *in vitro* have demonstrated antx-a(s)-induced direct muscarinic stimulation and indirect nicotinic and muscarinic stimulation via inhibition of ChE and buildup of acetylcholine (Hyde and Carmichael, 1988,1989). Mice given antx-a(s) at 0.5 or 1.0 mg/kg body weight intraperitoneally (IP) after pretreatment with atropine sulfate (50 mg/kg) IP had no parasympathetic signs of toxicosis and had longer survival times than mice given toxin alone but still died (Mahmood and Carmichael, 1986b). After IP injection of antx-a(s), no inhibition of whole brain ChE activity of mice was observed, suggesting that this toxin is unable to cross the blood brain barrier (Cook et al., 1988). The goals of the present study were to: (1) determine whether there is a direct effect of antx-a(s) on central mediation of respiration by monitoring phrenic nerve potentials, (2) characterize any effects of the toxin on respiratory rate and tidal volume, and

(3) determine the nature and severity of antx-a(s)-induced effects on heart rate and mean blood pressure.

## 2. Experimental Methods

### Rats

Four male Sprague-Dawley rats (Harlan Sprague-Dawley, Inc., Indianapolis, IN) ( $478 \pm 35$  g; mean  $\pm$  SD) were provided food and water *ad libitum* and housed in air-conditioned quarters on a 12-hour light/12-hour dark cycle.

### Anesthesia

Anesthesia was induced by halothane and subsequently maintained by an IP injection of  $\alpha$ -chloralose (60 mg/kg; Aldrich Chemical, Milwaukee, WI) and urethane (800 mg/kg; Aldrich Chemical, Milwaukee, WI) prior to surgical procedures. This regimen provided a stable level of anesthesia throughout the study.

### Surgical Procedures, Instrumentation, and Physiological Measurements

The cervical portion of the trachea was dissected free, incised, and intubated with a 14-gauge, 6.4-cm Teflon catheter (Longwell, Becton Dickson, Rutherford, NJ). Sutures around the trachea secured the catheter and provided an air-tight seal. The right carotid artery was isolated, separated from the vagus, ligated, and catheterized with PE 50 polyethylene tubing (Clay Adams, Parsippany, NJ) for measurement of arterial blood pressure. The left jugular vein was isolated and catheterized with PE 50 tubing in such a way that the tip of the catheter was placed in the anterior vena cava. Jugular and arterial catheters were kept patent by flushing with heparinized Ringer's solution.

The right phrenic nerve was exposed from the point at which it diverged from the fifth cervical nerve, transected, and the cranial end laid across bipolar silver hook electrodes for recording nerve potentials. The phrenic nerve preparation was stabilized by tightly suturing the surrounding skin to a solid ring support. This construction also formed a pocket that permitted the phrenic nerve and electrodes to be continually maintained in a pool of mineral oil. The phrenic nerve signal was amplified with a Grass P511 AC preamplifier using a band pass of 100 Hz to 10 KHz. The signal was full-wave rectified and integrated (Gould integrator), using a reset time of 0.033 second (integrate sample/hold). The temperature of rats during surgical procedures was maintained with heating pads.

Tidal volumes were determined from flow measurements made with a Fleisch 0000 pneumotachograph (OEM Medical, Richmond, VA) attached to the tracheal catheter and a Validyne 45/16 transducer (Northridge, CA), which were integrated to provide tidal volume measurements. Medical grade air was blown (0.2 L/minute) into the tracheal catheter through a three-way connector to provide a bias flow of air in order to reduce the dead space and ensure sufficient oxygenation of the animal. Heart rate, blood pressure, phrenic nerve activity, and tidal volume signals were recorded on a Gould 2400 chart recorder. Changes in phrenic nerve activity were determined by the percentage change in the amplitude of the integrated signal during toxin administration compared to the predosing period.



### Toxicant Preparation

Antx-a(s) was purified by the method of Harada et al. (1988) from batch cultures of *A. flos-aquae* strain NRC-525-17. Thin-layer chromatography indicated purity of 90 to 95%. In addition to antx-a(s), the majority of the remaining material used in this study was low-molecular-weight salts from the culture media and purification process (with which toxicity has not been associated upon repeated testing). The 2-hour mouse IP LD<sub>50</sub> of the toxin used in this study was 21 µg/kg. Antx-a(s) was stored under nitrogen gas at -20°C prior to use and brought into solution for dosing with physiologic saline (0.9% sodium chloride injection, USP, Abbott Laboratories, North Chicago, IL) so that the dosing solution contained 50 µg of antx-a(s)/ml. Physiologic saline was also used as the control solution in this study. The saline control solution and toxin solution were administered IV by a Harvard (South Natick, MA) Model 907 infusion pump at a constant rate of 0.033 ml/minute.

### Dosing Protocol

Rats were monitored while being infused with saline for 3 minutes before initial toxin administration so that they could serve as their own controls. Rats were subsequently infused with antx-a(s) until they died, as indicated by cessation of phrenic nerve activity. In preliminary studies, rats instrumented as above and continuously infused with saline IV for 20 minutes did not exhibit appreciable changes in heart rate, mean arterial blood pressure, tidal volume, minute volume, respiratory rate, or amplitude of integrated phrenic nerve signals.

### Statistical Methods

Multivariate repeated measures analysis was performed to detect significant changes over time in the following parameters: blood pressure, heart rate, tidal volume, respiratory rate, minute volume, and phrenic nerve amplitude. When overall trends were deemed significant by the repeated measures analysis, linear contrasts were used to determine significant differences at 1-minute intervals postdosing compared to the control period. In all analyses, a level of  $\alpha = 0.05$  was chosen to detect significant differences.

### 3. Results

In response to antx-a(s) administration, rats first developed hypersalivation and chromodacryorrhea and, later, muscle tremors and fasciculations. Visual inspection of the animals indicated that respiratory effort initially increased over time in response to the infusion of antx-a(s) and then decreased just prior to death. Mean survival time (from initial toxin exposure to death) was  $8.7 \pm 0.2$  minutes (mean  $\pm$  SE).

Blood pressure, heart rate, tidal volume, respiratory rate, respiratory minute volume, and phrenic nerve activity are presented in Figure 1a-f. Significant ( $p < 0.01$ ) decreases occurred over time in blood pressure, heart rate, tidal volume, respiratory rate, and minute volume. A mild decrease in heart rate and mean arterial pressure were the first observed effects of the toxin. Subsequently, as measured over 30 seconds, heart rate declined markedly to an average reduction of  $165 \pm 14$  beats/minute (mean  $\pm$  SE) or 47% of the value for the predose period. There was a concurrent decline in arterial blood pressure of  $24.1 \pm 8$  mmHg (mean  $\pm$  SE) or 22%

of the mean value for the predose period. Most of the decrease in the mean arterial blood pressure resulted from a reduction in diastolic pressure. These reductions in heart rate and blood pressure occurred by  $3.47 \pm 0.3$  minutes (mean  $\pm$  SE) after the start of toxin infusion at a time when minute volume had declined by only  $15.4 \pm 3\%$  (mean  $\pm$  SE) of the predose mean value.

Reductions also occurred in tidal volume, respiratory rate, and minute volume, although only with respiratory rate were values at none of the time points after dosing significantly lower as compared to the control period. Phrenic nerve amplitude significantly increased at the same time that the respiratory function parameters decreased.

#### 4. Discussion and Conclusion

The marked and consistent increase in phrenic nerve activity of rats given antx-a(s) indicates that the toxin has no centrally mediated inhibitory effect on respiration. These results are compatible with the previous observation that the toxin does not inhibit whole brain ChE activity in mice dosed IP and probably has only peripheral activity owing to an apparent inability to cross the blood brain barrier (Cook et al., 1988).

The marked reductions in the heart rate and blood pressure suggest that antx-a(s) exerts important effects on the cardiovascular system, probably as a result of acetylcholine accumulation due to inhibition of ChE. Alternatively, direct muscarinic effects of this toxin have been observed with isolated denervated guinea pig ileum *in vitro* (Hyde and Carmichael, 1988,1989). Mice and rats given antx-a(s) display

muscarinic signs including defecation, lacrimation, hypersalivation, and urination after toxin exposure (Mahmood and Carmichael, 1986b; Cook et al., 1988). In addition, mice survived significantly longer when given atropine prior to antx-a(s) administration and did not display the severe muscarinic signs seen with mice given toxin alone (Mahmood and Carmichael, 1986b). Thus, whether by virtue of inhibition of ChE, by direct agonist activity, or by a combination of the two, antx-a(s) apparently causes muscarinic stimulation, and atropine apparently is able to block most, if not all, such effects of the toxin at least temporarily.

Administration of antx-a(s) did not induce hypertension in the rat, in contrast with other ChE-inhibiting agents such as isopropyl methyl phosphonofluoridate (sarin), diisopropylfluorophosphate (DFP), and diethylnitrophenylphosphate (paraoxon) (Holmstedt, 1959). Hypertension in rats caused by these compounds, however, has been postulated to be a result of an action in the central nervous system. A similar effect by antx-a(s) may not be possible if the toxin cannot penetrate the blood brain barrier. Instead, in the present study, there was a decrease in diastolic blood pressure that accounted for most of the decrease in mean arterial blood pressure, suggesting a possible loss of vascular tone.

Antx-a(s)-induced inhibition of ChE resulting in nicotinic effects of excessive acetylcholine was suspected to have been at least partially responsible for the observed gradual decrease in tidal and minute volumes because these changes occurred despite a marked increase in phrenic nerve activity. Much of the observed decrease in minute volume appeared to be a result of a decrease in tidal volume and not in respiratory

rate. Indirect nicotinic effects of antx-a(s) by inhibition of ChE have also been observed *in vitro* in frog rectus abdominis muscle and on electrically stimulated rat phrenic nerve-diaphragm preparations. However, evidence from studies *in vitro* with chick biveuter cervicis and frog rectus abdominis muscles suggest that antx-a(s) is not a direct neuromuscular blocking agent: instead, the toxin enhanced the response of acetylcholine and antagonized the blockade induced by d-tubocurarine. Also, antx-a(s) did not change the dose response curve of the neuromuscular blocking agent antx-a (Hyde and Carmichael, 1988). Thus, in the present study, observations *in vivo* were consistent with previous evidence indicating an absence of direct neuromuscular blockade *in vitro*. The present study indicates that this indirect neuromuscular blockade effect of antx-a(s) would ultimately very likely contribute to the toxin-associated lethality.

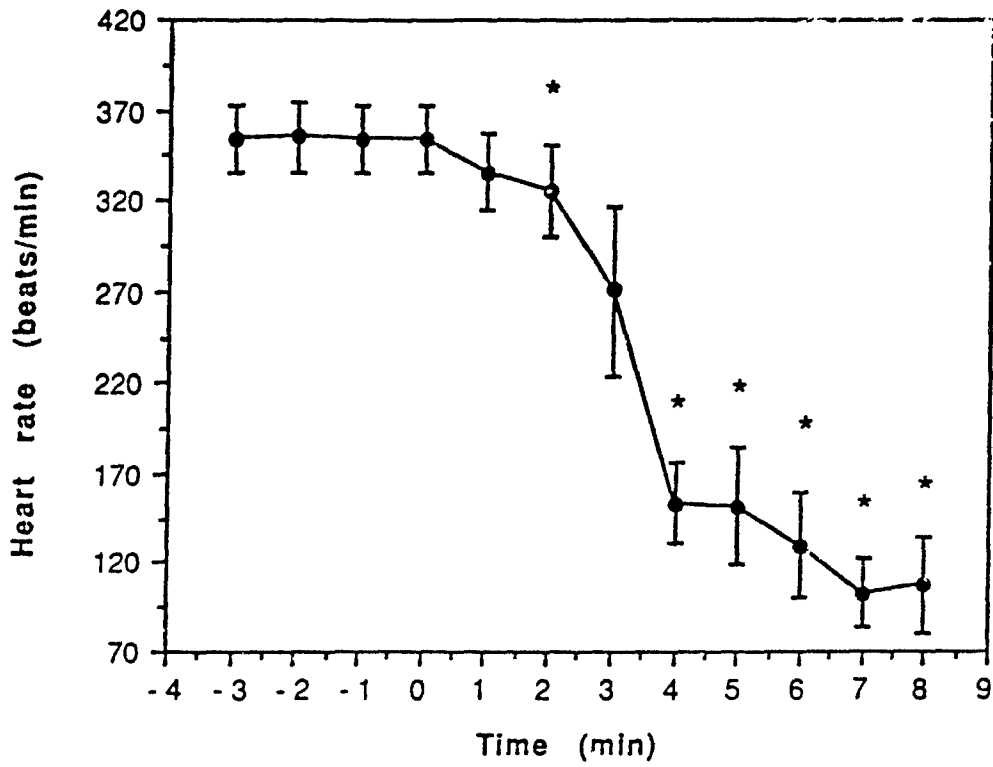
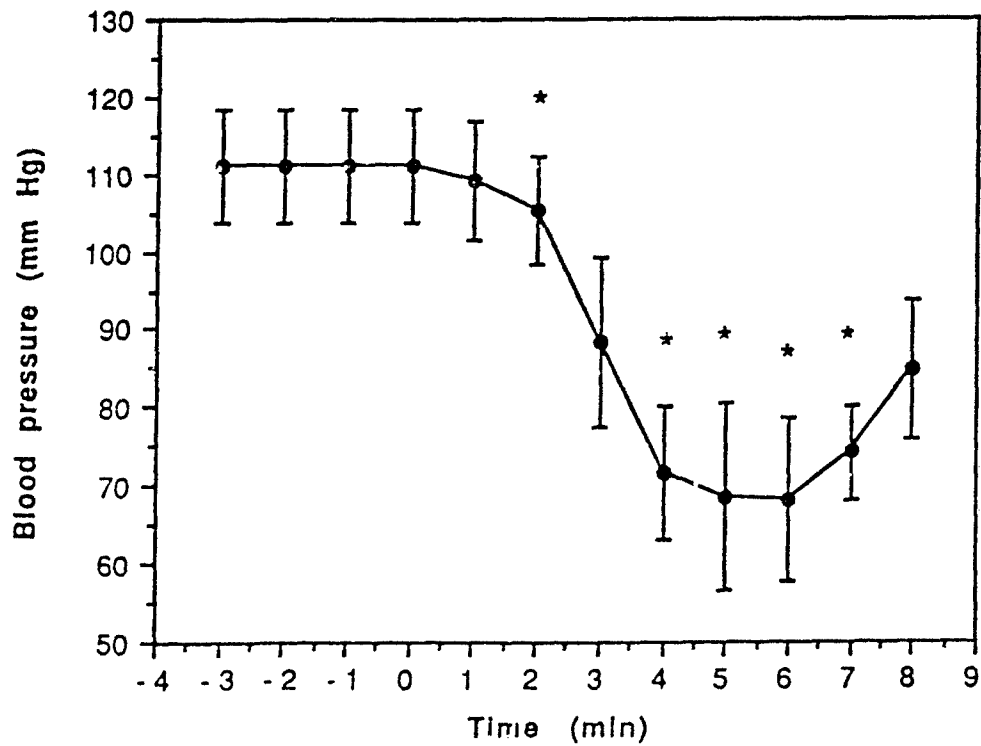
In previous studies, unanesthetized rats given antx-a(s) IP developed clonic seizures and died (Cook et al., 1989b). In the present study, anesthetized rats did not develop seizures—but still died—indicating that seizures are not the sole cause of death in animals exposed to antx-a(s).

In conclusion, antx-a(s), unlike most known low-molecular-weight organophosphorus ChE-inhibiting agents, did not have a profound inhibitory action on centrally mediated respiration but apparently did have an important effect on the peripheral responses of the cardiovascular and respiratory systems. If the cardiovascular effects of antx-a(s) are not sufficiently severe to cause lethality (see next section), progressive neuromuscular blockade of the muscles of respiration still

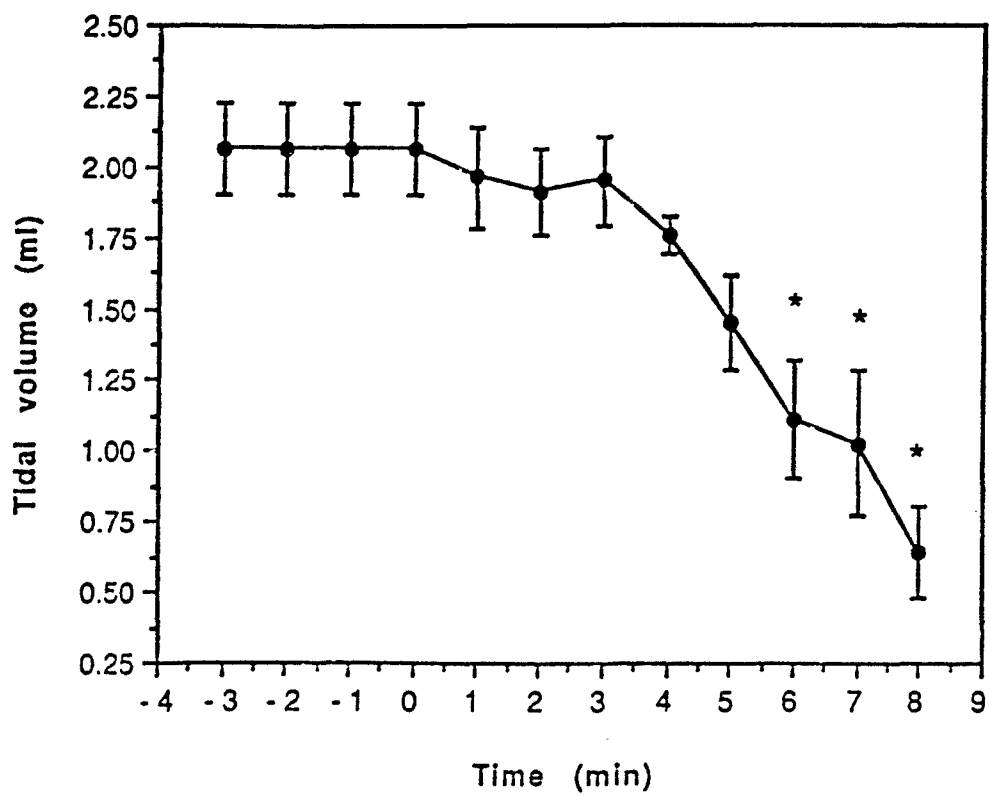
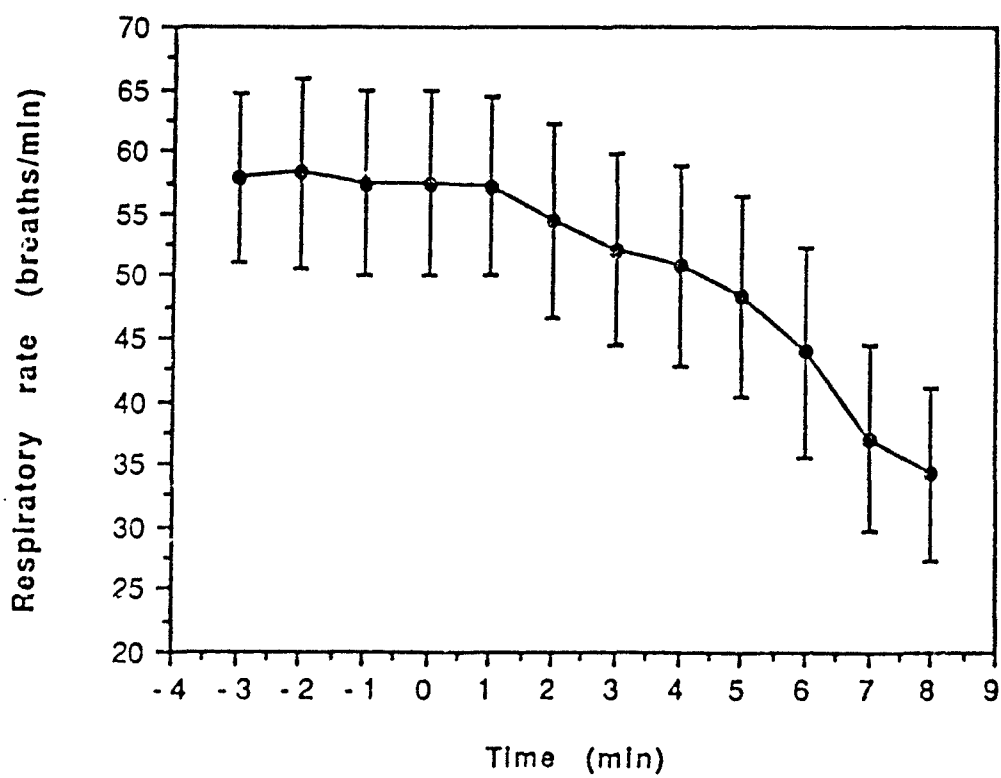
may, alone or in combination with the cardiovascular alterations, ultimately lead to death.

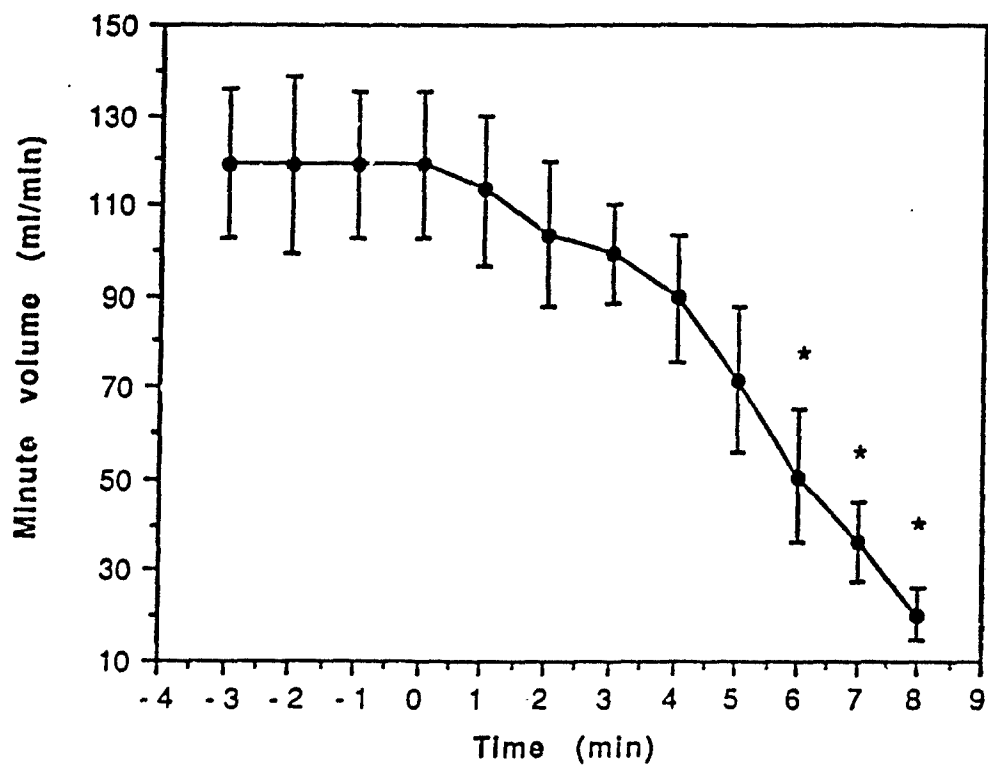
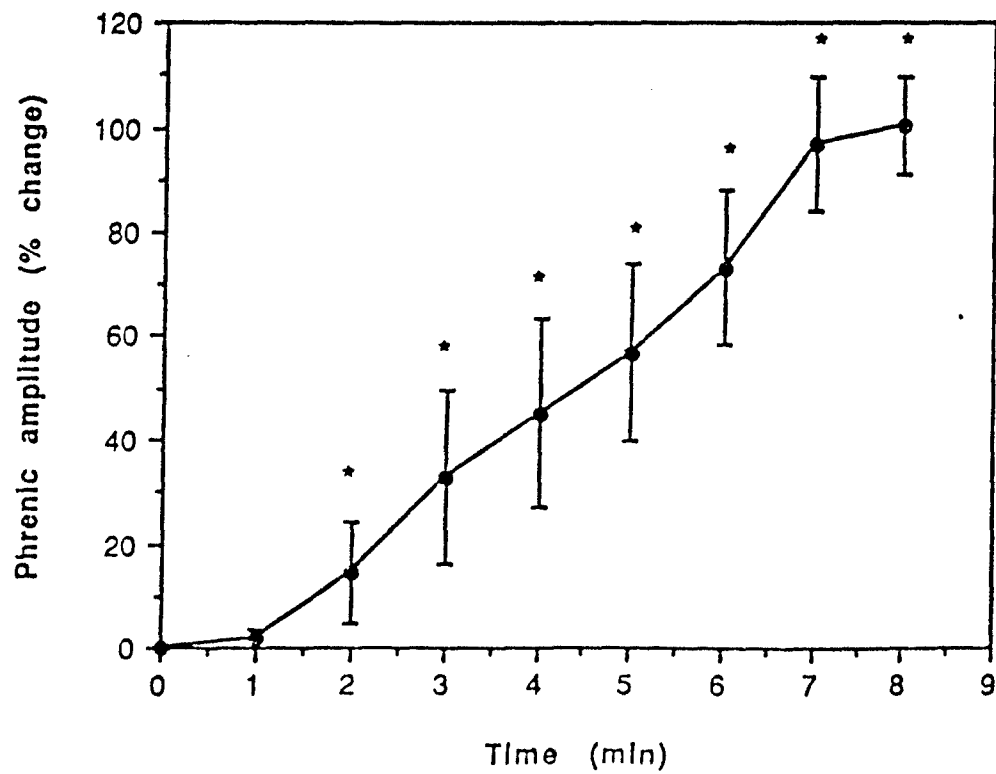
Figure 1. Effects of antx-a(s) on: A) heart rate, B) mean arterial blood pressure, C) tidal volume, D) respiratory rate, E) minute volume, and F) phrenic nerve activity in anesthetized rats. Data are presented as the mean  $\pm$  SE (N = 4). Phrenic nerve amplitudes are expressed as the percentage change from the predose period (average of 12 observations, four animals at three time points [-3, -2, and -1 minutes]).

\*Represents time points significantly different ( $p < 0.05$ ) from: a) the predose period (average of 16 predose observations; four animals at four times spaced 1 minute apart [-3, -2, -1, and 0 minutes]) in heart rate, blood pressure, respiratory rate, and tidal and minute volume data; and b) from time 0 in phrenic nerve data. Asterisks are shown only on curves in which the overall repeated measures analysis revealed a significant trend over time.

**A****B**



**C****D**

**E****F**

**F. Pathophysiologic Effects of Anatoxin-a(s) in Anesthetized Rats: The Influence of Atropine and Artificial Respiration**

**1. Statement of the Problem, Background, and Rationale**

Anatoxin-a(s) [antx-a(s)] is a polar low-molecular-weight cholinesterase (ChE) inhibitor produced by *Anabaena flos-aquae* strain NRC-525-17 (Mahmood and Carmichael, 1987; Matsunaga et al., 1989). *A. flos-aquae* is a species of blue-green algae that has been repeatedly associated with poisoning of domestic and wild animals (Gorham, 1964). Deaths of dogs, pigs, and ducks in the field have been diagnosed as having occurred as a result of consumption of ChE-inhibiting neurotoxins from *A. flos-aquae* (Mahmood et al., 1988; Cook et al., 1989a). Clinical signs in mice and rats given antx-a(s) include dyspnea, seizures, and death. Although respiratory failure has been suggested (Mahmood and Carmichael, 1986b; Cook et al., 1988), proof of this assertion in animals given antx-a(s) was lacking. After intraperitoneal dosing, antx-a(s) did not inhibit whole brain ChE activity of mice, suggesting that the toxin is unable to cross the blood brain barrier (Cook et al., 1988) and, therefore, could not inhibit central respiratory drive.

The goals of the present studies were to evaluate the peripheral mechanisms of antx-a(s) toxicosis by assessing: 1) the effects of the toxin on the cardiovascular and respiratory systems in atropinized and nonatropinized rats, 2) the relative importance of cardiovascular versus respiratory system effects by ventilation during toxin administration, and 3) the influence of antx-a(s) on neuromuscular transmission to the

muscles of respiration by measuring phrenic nerve activity concurrently with diaphragm electromyographic (EMG) activity during toxicosis.

### 3. Experimental Methods

#### Rats

Twenty male Sprague-Dawley rats ( $485 \pm 34$  g; mean  $\pm$  SD) (Harlan Sprague-Dawley, Indianapolis, IN) were provided food and water *ad libitum* and housed in air-conditioned quarters on a 12/12-hour light/dark cycle.

#### Toxicant Preparation

Antx-a(s) was isolated in the laboratory of W. Carmichael at Wright State University, Dayton, OH, from batch cultures of *A. flos-aquae* strain NRC-525-17 (Matsunaga et al., 1989). Thin-layer chromatography indicated a purity of 90 to 95%. The 2-hour mouse intraperitoneal  $LD_{50}$  of the toxin used was 21  $\mu$ g/kg. Antx-a(s) was brought into solution for dosing with physiologic saline (0.9% NaCl injection, USP, Abbott Laboratories, Chicago, IL). Physiologic saline was also used as the control solution in this study.

#### Anesthesia

Anesthesia was induced by halothane and subsequently maintained by a single intraperitoneal dose of  $\alpha$ -chloralose (60 mg/kg) and urethane (800 mg/kg) prior to surgical procedures. This anesthetic regimen provided a stable level of anesthesia for the duration of the experiment.

### Dosing Protocol

The toxin and control solutions were administered intravenously to the rats using a Harvard (Southnatick, MA) Model 907 infusion pump. Rats were dosed at 3.5  $\mu$ g of antx-a(s)/kg/minute. The same volume of saline alone was given to control rats.

### Surgical Procedures, Instrumentation, and Physiologic Measurements

The cervical portion of the trachea was dissected free, incised, and intubated with a 14-gauge, 6.4 cm Teflon catheter (Longdwell, Becton Dickson, Rutherford, NJ). Sutures around the trachea assured an air-tight seal.

For measurement of arterial blood pressure, the right carotid artery was also isolated in the cervical region, separated from the vagus nerve, ligated, and catheterized with PE 50 tubing (Clay Adams, Parsippany, NJ). Heart rate was derived from the blood pressure signal. The left jugular vein was similarly isolated and catheterized for administration of toxin and control solutions.

The right phrenic nerve was exposed where it diverged from the fifth cervical nerve, transected, and the caudal end laid across bipolar silver hook electrodes for recording nerve potentials. The signal was amplified with a Grass P511 AC preamplifier using a band pass of 100 Hz to 10 KHz. The signal was also full wave rectified and integrated (Gould integrator) using a reset time of 0.033 seconds (integrate sample/hold). Body temperatures of rats during the surgical procedure were maintained using a heating pad.

Respiratory tidal volumes were determined from flow measurements obtained using a Fleish 0000 pneumotachograph (OEM Medical, Richmond, VA) attached to

the tracheal catheter and a Validyne 45/16 transducer (Northridge, CA). Using a three-way connector, medical grade air was blown (0.2 l/minute) into the tracheal catheter to provide a bias flow of air in order to reduce the dead space and ensure sufficient oxygen availability for the animal.

Diaphragm EMGs were recorded by two hook-shaped Teflon-coated 25-gauge silver wire electrodes that had been inserted into the left lateral aspect of the diaphragm by way of a 25-gauge needle. The EMG signal was amplified, rectified, and integrated as described above for the phrenic nerve signal.

In rodents that were ventilated, a Harvard (Southnatick, MA) Model 683 ventilator was used with the rate and volume adjusted so that integrated phrenic nerve activity was recordable. Heart rate, blood pressure, and tidal volume signals were also integrated prior to recording. Changes in phrenic nerve and diaphragm EMG activity were calculated based on measurement of the amplitude of the integrated signals in mm and comparing selected times postdosing to the predose period.

#### Experimental Design

In the first study, in order to assess the significance of the muscarinic effects of antx-a(s), rats (N = 6) were pretreated with atropine sulfate (50 mg/kg) 15 minutes prior to toxin administration and compared to rats (N = 6) given only toxin. Measurements included arterial blood pressure, heart rate, and tidal volume. Toxin was infused intravenously until rats died (as indicated by cessation of phrenic nerve activity). Survival time to the nearest second and the amount of toxin administered were recorded. Rats served as their own controls; baseline parameters were recorded

while saline was infused in each rat for 3 minutes immediately prior to toxin administration.

In the second study, the effects of ventilation (as a means of pulmonary support) on antx-a(s) toxicosis were evaluated. Rats ( $N = 3$ ) were ventilated with air and concurrently infused intravenously with toxin. The predicted end point of the experiment was to be either animal death or the delivery of a total of 170  $\mu\text{g}$  of antx-a(s)/kg (over 4.7 times the mean lethal dose determined in the first study). Rats served as their own controls and the same parameters were measured as in the first study except tidal volume and minute volumes were not recorded.

In the third study, toxin was infused continuously until the rats ( $N = 5$ ) died. Respiration was not supported. In addition to diaphragm EMG activity, the same parameters were measured as in the second study. Rats served as their own controls as described above.

#### Statistical Analysis

Comparison of survival time between rats given toxin and those pretreated with atropine prior to toxin administration was performed using Bartlett's test for homogeneity of variances followed by a two-tailed  $t$ -test. For heart rate, blood pressure, respiratory rate, and respiratory tidal and minute volume, comparisons between rats given toxin and those given atropine and toxin were analyzed by multivariate repeated measures analysis, and when overall treatment differences were detected, univariate comparisons (linear contrasts) were used to identify significant differences between the two groups at each time point. In rats that were ventilated,

multivariate repeated measures analyses were used, and for parameters in which significant trends over time were present, linear contrasts were used to detect differences between predosing observations and those at 3-minute intervals postdosing. To adjust for the low number of animals in these studies, a level of  $\alpha = 0.10$  was chosen *a priori* to detect significant differences.

### 3. Results

In the first study, rats given atropine before antx-a(s) lived significantly longer ( $p < 0.05$ ) than rats given toxin alone:  $12.8 \pm 1.0$  minute (mean  $\pm$  SE) versus  $10.1 \pm 0.5$  minute, respectively. Moreover, the rats given atropine received a higher mean lethal dose of toxin  $45.2 \pm 3.5$   $\mu\text{g/kg}$  (mean  $\pm$  SE) and range (34.2 to 55.6  $\mu\text{g/kg}$ ) as compared to the mean lethal dose of  $35.9 \pm 1.7$   $\mu\text{g/kg}$  and range (30.1 to 42.6  $\mu\text{g/kg}$ ) for rats given toxin alone.

Significant reductions in blood pressure ( $p = 0.095$ ), heart rate ( $p = 0.016$ ), and tidal volume ( $p = 0.098$ ) were present in rats given toxin alone as compared to rats given atropine and toxin (Figures 1A-F). Blood pressure and heart rate in atropinized rats decreased markedly only after profound reductions in respiratory tidal and minute volumes were observed. With regard to phrenic nerve amplitude ( $p = 0.058$ ), there were overall trends such that this parameter increased faster in rats given toxin alone as compared to rats given atropine and toxin.

In the second study, ventilated rats survived administration of antx-a(s) at 170  $\mu\text{g/kg}$ , 4.7 times the median average lethal dose and over four times the highest dose needed to cause lethality in the first study. The animals lived (as indicated by



continued phrenic nerve activity) despite sudden and marked reductions in heart rate and blood pressure (Figures 2A-C), similar to those observed in rats given toxin alone in the first study. Blood pressure and heart rate eventually stabilized at low values.

In the third study, diaphragm EMG activity in antx-a(s)-dosed rats increased and then became more nonsynchronous, until EMG activity was not matched in any way to phrenic nerve activity. Despite a progressive increase in the amplitude of the bursts of phrenic nerve activity, the EMG activity was eventually markedly decreased, although it was again somewhat more synchronous prior to death (Figures 3A-B).

#### 4. Discussion

As in previous studies, there was no evidence of inhibition of centrally mediated respiratory drive as indicated by there having been only an increase in phrenic nerve amplitude, even when rats survived significantly longer as a result of atropine pretreatment. The decrease in respiratory rate in nonatropinized rats given antx-a(s) was likely a result of an increase in the respiratory and/or expiratory time of respiration.

The muscarinic effects of the toxin were clearly important in lethality induced by antx-a(s), since atropinized rats survived significantly longer than nonatropinized rats, and since atropine treatment stabilized the heart rate, blood pressure, and respiratory rate of antx-a(s)-dosed rats and diminished the severity of the reductions in tidal and minute volumes. Because the atropinized rats lived longer, they were infused with more toxin before death occurred. Although a similar increase in survival time was observed previously in mice pretreated with atropine (50 mg/kg) 15

minutes before intraperitoneal dosing with 0.5 and 1.0 mg of antx-a(s)/kg, the mechanism of atropine protection was not investigated (Mahmood and Carmichael, 1986b). Since relatively large doses of antx-a(s) were used in the present studies and in the studies of Mahmood and Carmichael (1986b), it cannot be said that atropine sulfate could not be life-saving in spontaneous cases of antx-a(s) toxicosis. Based on significantly increased survival times in rats and mice given antx-a(s), atropine should be a part of a treatment plan for antx-a(s) toxicosis.

Despite the benefits of atropine in the present study, since all the rats pretreated with the drug still died after having survived an average of only about 2 minutes longer than rats given toxin alone (and after having received approximately 25% more antx-a[s] than nonatropinized rats), blockade of muscarinic receptors did not afford more than a minimally protective effect. Assuming that the parenterally dosed rat is an appropriate model, other animals exposed to large quantities of algae and antx-a(s), such as in natural exposure where sudden death is the primary clinical sign, may not survive with atropine treatment alone.

Animals in the second study survived when artificially ventilated during continuous toxin infusion and retained central respiratory drive as indicated by phrenic nerve activity despite being given more than four times the lethal dose. This suggests that the effects of antx-a(s) on the cardiovascular or other nonpulmonary systems alone were not lethal. Also, since animals survived through the use of the ventilator, inhibition of diffusion of oxygen across the pulmonary membranes and into the

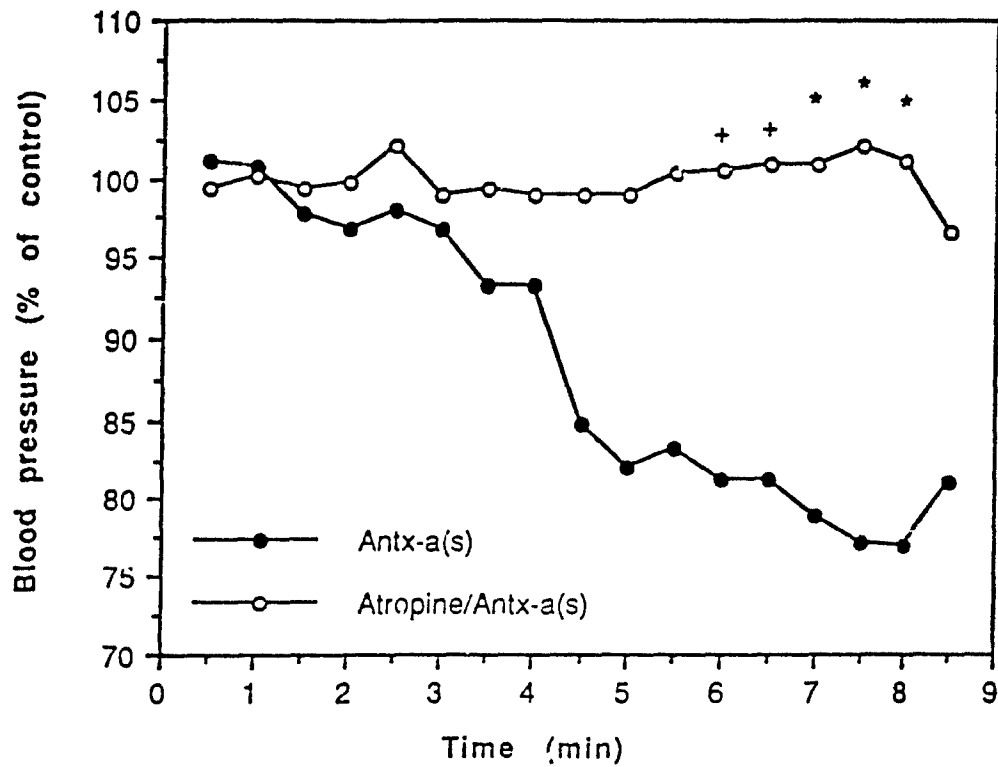
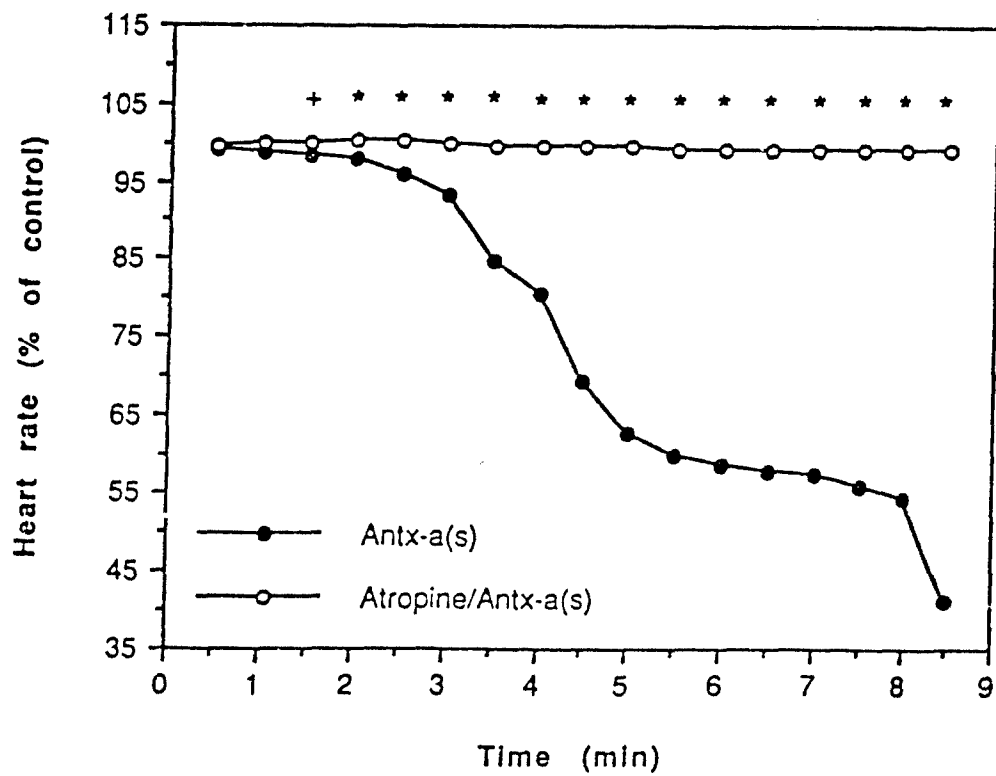
pulmonary capillaries as a result of possible secretions was not an overwhelming mechanism of antx-a(s).

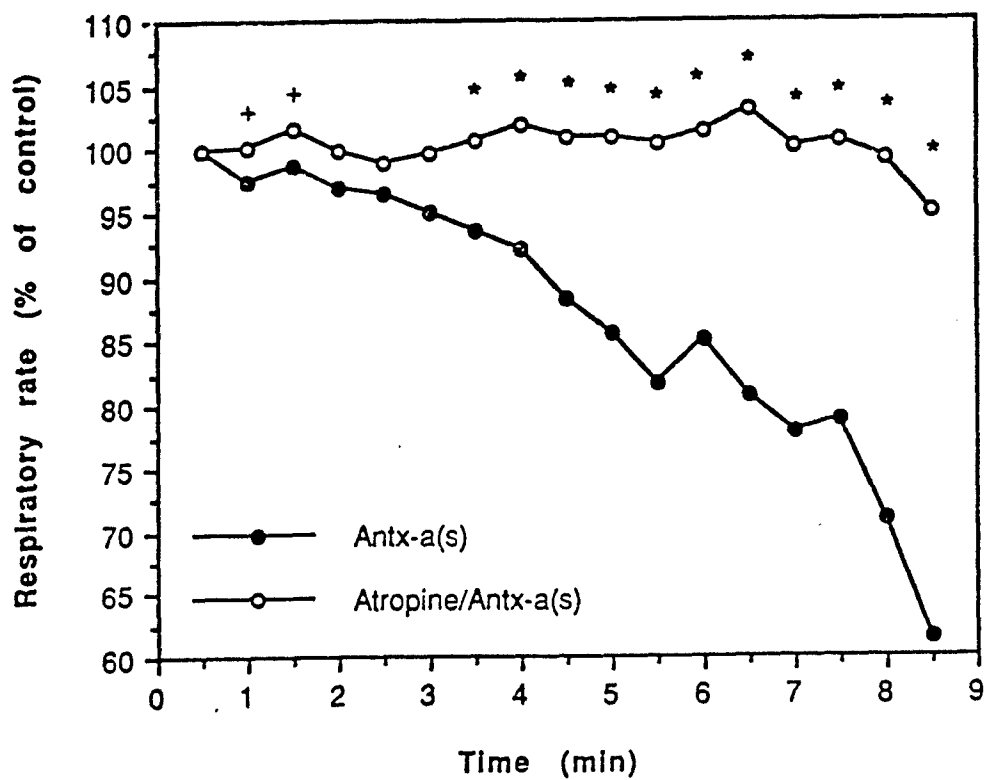
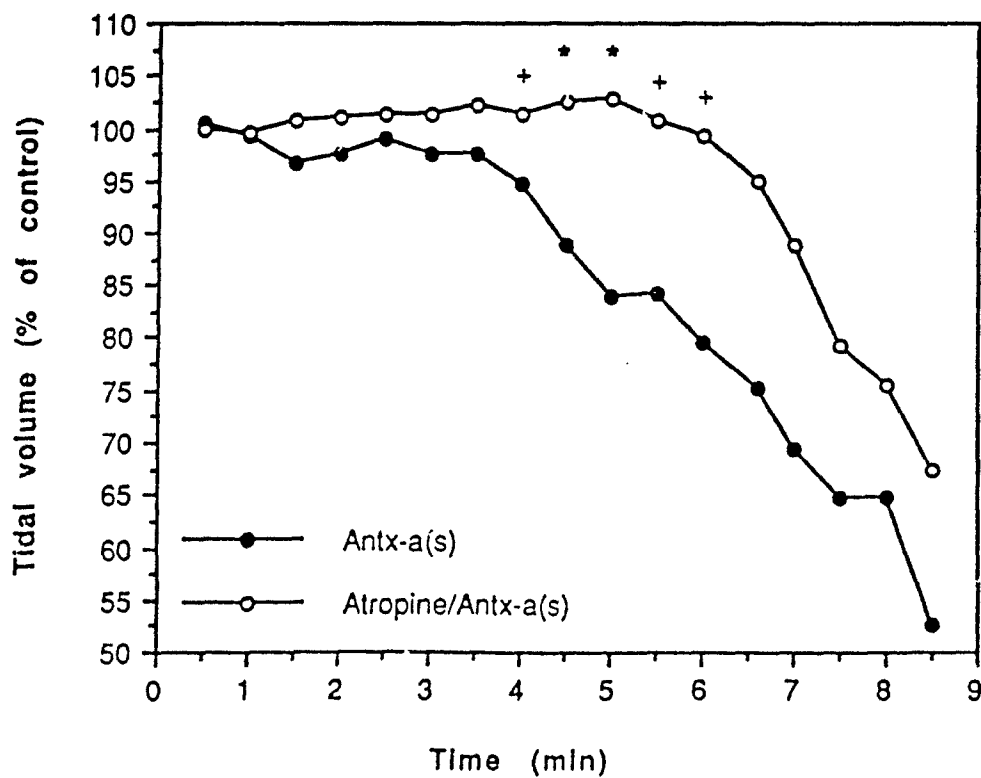
In the third study, paralysis of the diaphragm in the lethal syndrome caused by antx-a(s) *in vivo* was conclusively demonstrated. Phrenic nerve impulses are bilaterally emitted (Wright, 1954); thus, the asynchronous and marked decrease in contralateral EMG activity that occurred despite the progressive increase in phrenic nerve amplitude clearly suggests that these EMG changes were a result of peripheral actions of antx-a(s). Based on these results, it appears that paralysis of the diaphragm and muscles of respiration is the most important lethal mechanism of antx-a(s). Changes in the EMG in response to infusion of antx-a(s) including the increased amplitude of activity, then the more random activity, and finally the decrease in amplitude were comparable to what has been observed in isolated rat phrenic nerve-diaphragm preparations exposed to other ChE inhibitors *in vitro* (Barnes and Duff, 1953; Holmstedt, 1959). *In vitro*, antx-a(s) has been observed to bring about twitch potentials in the rat phrenic nerve-diaphragm preparation and tetanic fade in conjunction with a high rate of electrical stimulation (100 Hz) as a result of the nicotinic effects of antx-a(s) presumably caused by inhibition of ChE (Mahmood and Carmichael, 1986b). The role of nicotinic effect at concentrations of antx-a(s) associated with lethality in intact animals remained open to speculation, however.

In conclusion, antx-a(s)-induced lethality is likely to be a result primarily of the nicotinic effects (due to cholinergic blockade) of the toxin as a result of ChE inhibition in the muscles of respiration, but muscarinic effects of the toxin on the

cardiovascular and respiratory systems seem to play a significant role in lethal toxicoses.

Figure 1. Study 1: A) mean arterial blood pressure, B) heart rate, C) respiratory rate, D) tidal volume, E) minute volume, and F) amplitude of integrated phrenic nerve signals in anesthetized rats (N = 5 to 6) pretreated with atropine sulfate intraperitoneally at 50 mg/kg 15 minutes prior to initiation of a continuous intravenous infusion of antx-a(s) as compared to rats given only the latter. Data are presented as the percent change from the control period (average of observations at seven time points at 30-second intervals). When multivariate repeated measures analysis detected significant treatment effects ( $p < 0.01$ ), (\*) and (+) represent time points at which treatment groups were significantly different from each other by linear contrast analysis at  $p \leq 0.05$  and  $p \leq 0.10$ , respectively. Both curves are truncated at the time at which the first animal given either treatment died.

**A****B**

**C****D**

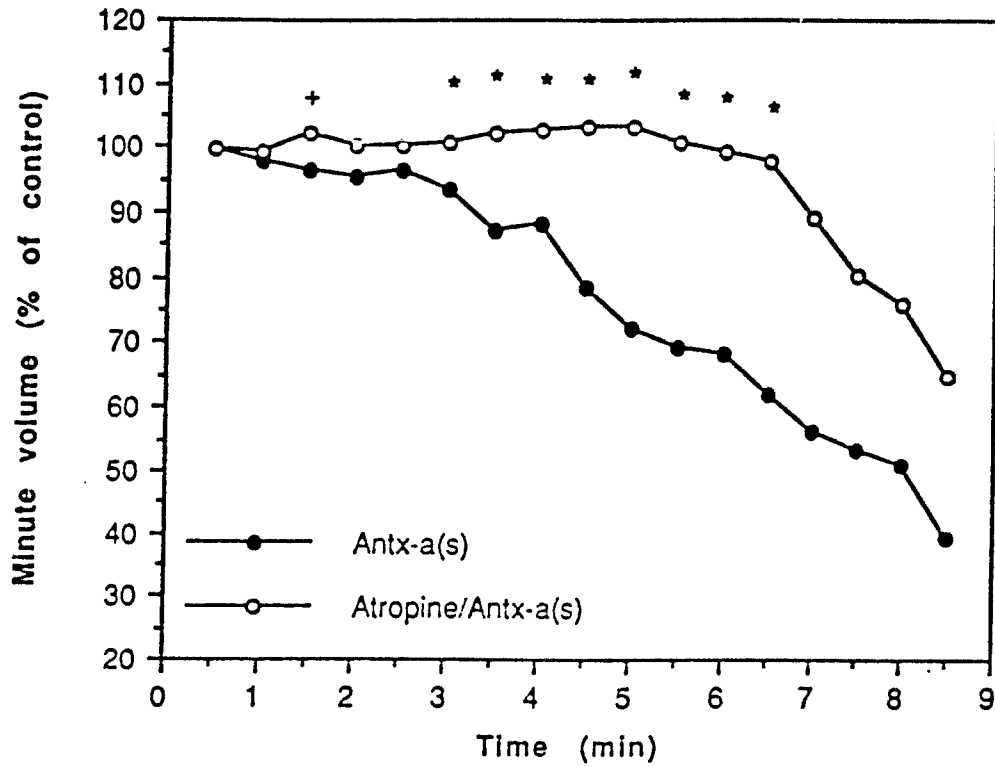
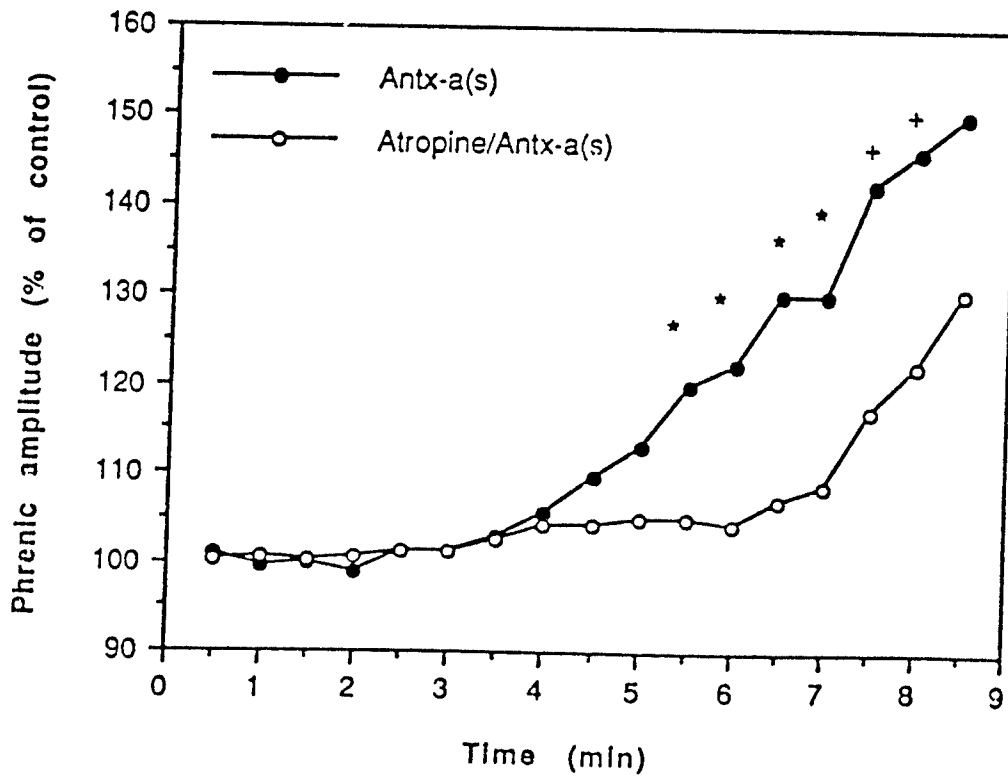
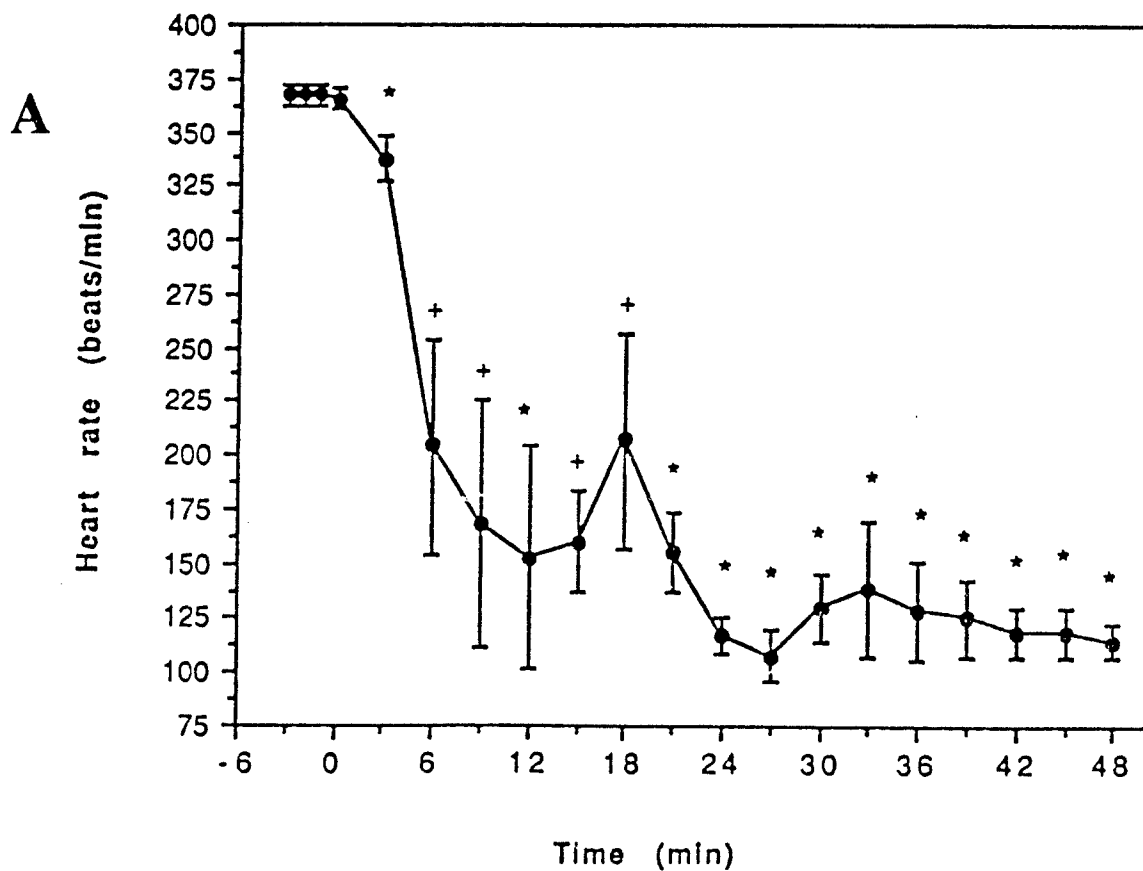
**E****F**



Figure 2. Study 2: A) heart rate, B) mean arterial blood pressure, and C) number of integrated phrenic nerve signals per minute (mean  $\pm$  SE) at 3-minute intervals in anesthetized rats ( $N = 3$ ) ventilated during continuous intravenous infusion of antx-a(s). When multivariate repeated measures analysis detected significant differences over time, (\*) and (+) represent time points at which observations after dosing were significantly different from the control period by linear contrast analysis at  $p \leq 0.05$  and  $p \leq 0.10$ , respectively. Despite the modest decrease in the rate of phrenic nerve impulses, no significant trend was detected by multivariate repeated measures analysis.



410

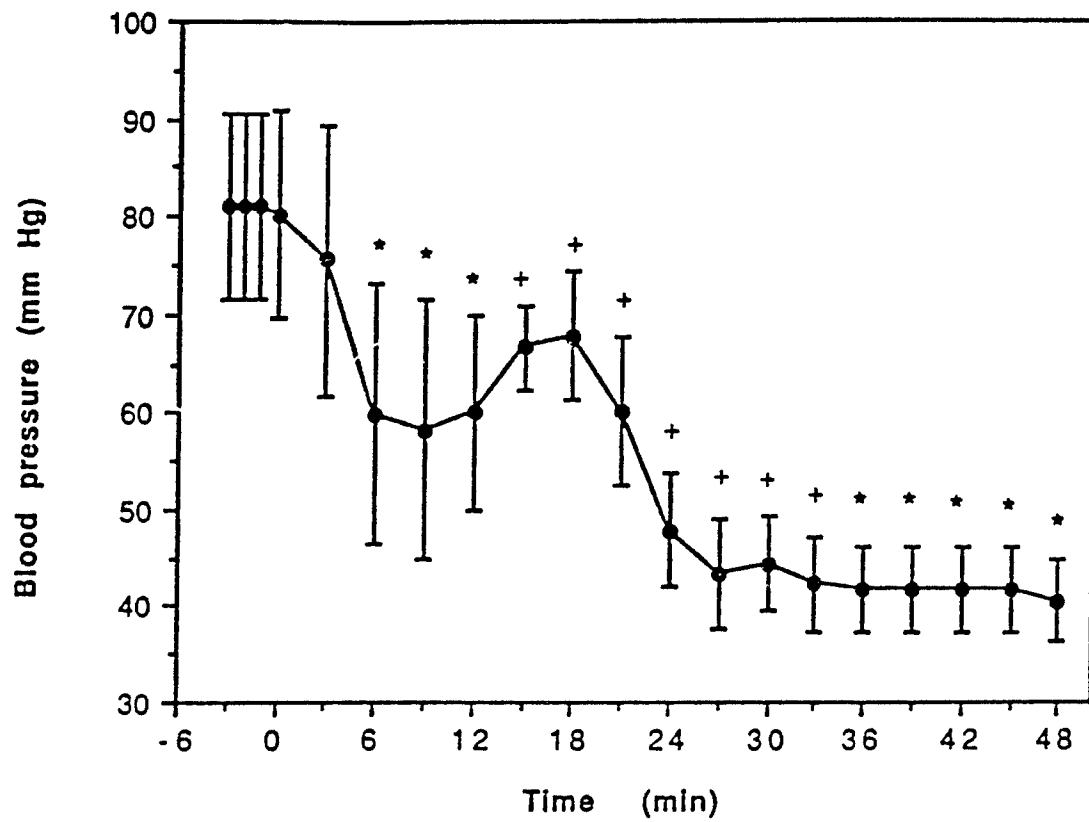
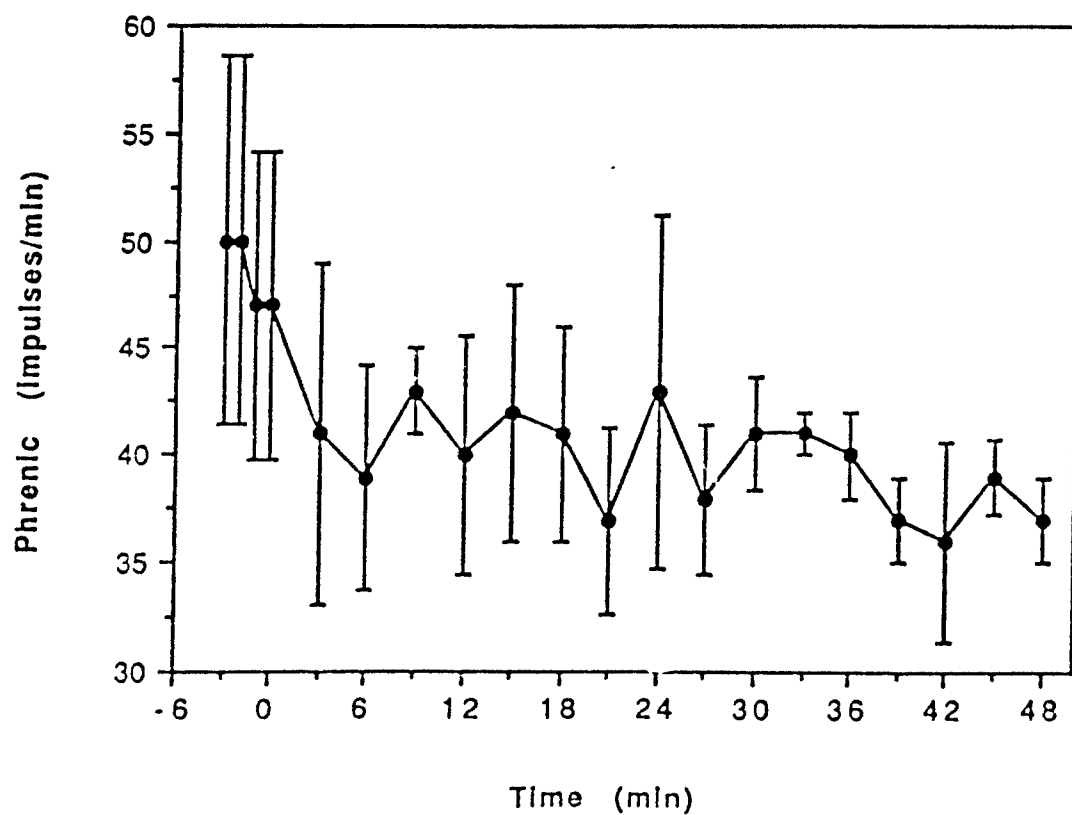
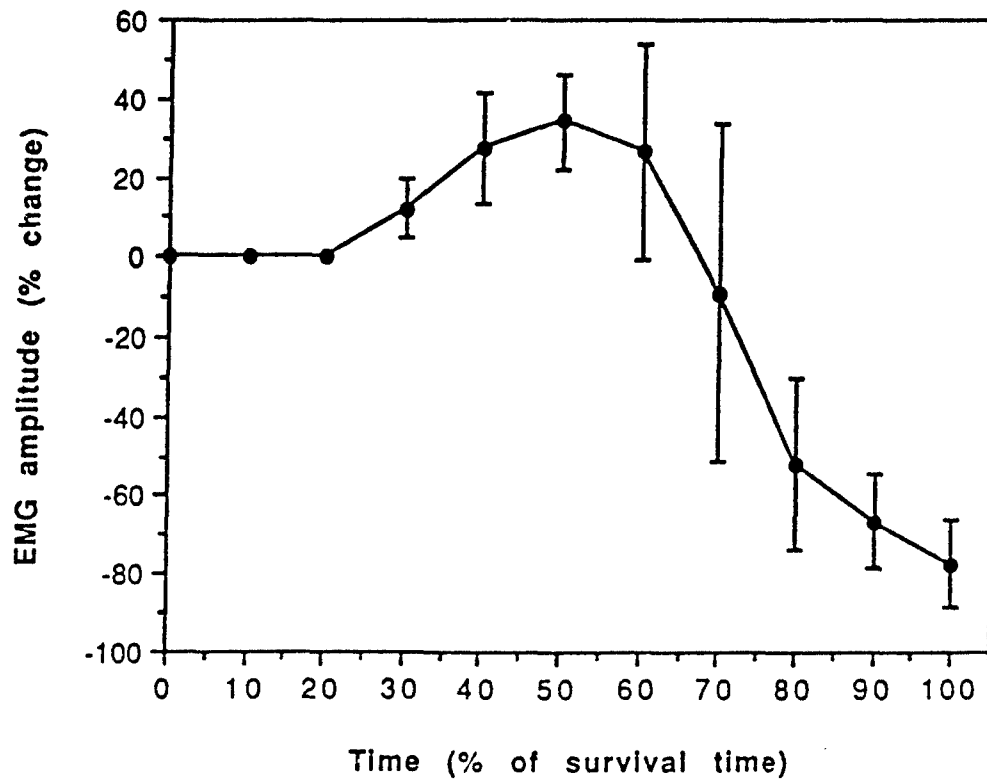
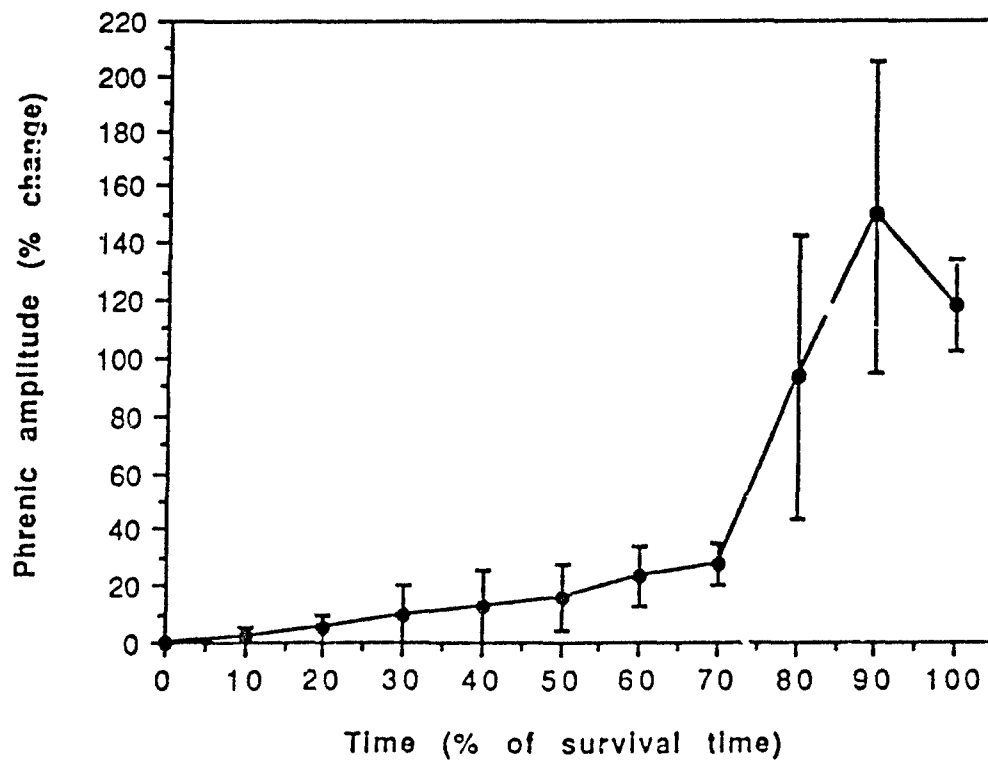
**B****C**

Figure 3. Study 3: amplitude of the integrated A) electromyographic and B) phrenic nerve signals (means  $\pm$  SE) in anesthetized rats ( $N = 5$ ) continuously infused intravenously with antx-a(s) until death. Data are presented as the percent change from the control period versus the percentage of the time between the initiation of dosing and death of the animal (% of survival time).

**A****B**

**G. Stability of Anatoxin-a(s) *In Vitro* as Measured by Inhibition of Human Plasma Cholinesterase Over Time**

1. Statement of the Problem, Background, and Rationale

Since the structure and purity of anatoxin-a(s) [antx-a(s)] was unknown until near the end of these studies, toxin stability could not be determined by conventional analytical techniques. Since the toxin was known to be a ChE inhibitor and ChE inhibition has been proposed as the primary mechanism of action involved in toxicity (Mahmood and Carmichael, 1986b, 1987), an *in vitro* ChE assay system was developed to assess the stability of the toxin.

We hypothesized that antx-a(s) would be stable when stored dry at -20°C in vials filled with gaseous nitrogen.

2. Experimental Methods

Stability studies were completed before the final physiologic studies in anesthetized rats. Antx-a(s) was isolated from batch cultures of *A. flos-aquae* strain NRC-525-17. The algae had been grown by the method of Mahmood and Carmichael (1986b). Toxin purification was conducted in the laboratory of W. Carmichael at Wright State University, OH, by the method of Harada (Harada et al., 1988).

Antx-a(s) in 6 µg quantities was stored as a solid in vials under nitrogen gas at -20°C prior to use. The equivalent of 35 ml of freeze-dried human plasma ChE (Sera Chem, Fischer Co., Itasca, IL) was diluted with 175 ml of pH 8 phosphate buffer and stored in 5 ml quantities at -20°C.

Initially, cuvettes after 5 minutes of incubation at room temperature were incubated for 30 minutes in a 38°C water bath and then for 5 minutes in a 25°C water bath. Different concentrations of antx-a(s) (in a volume of 100 µl) were added to 3 ml of pH 8 phosphate buffer in the cuvettes in order to generate a curve of micrograms of toxin versus ChE activity in this system. From this data, an amount of toxin (0.001 µg) that produced approximately 50% inhibition of the plasma cholinesterases was chosen.

Further work indicated that incubation at 37°C did not appear to speed up ChE inhibition and that neither incubated nor nonincubated samples appeared to plateau over a 1-hour period (Table 2). Based on these findings, incubation of the toxin and enzyme at 38°C was deleted, and 40 minutes after mixing the toxin with enzyme was chosen as a time that would provide approximately 50% inhibition. Subsequent work indicated that 0.01 µg of toxin (0.0003 µg of antx-a(s)/ml of diluted human plasma) caused approximately 52% and 49% inhibition at room temperature and 37°C, respectively, of the human plasma ChE activity at 40 minutes after mixing.

To assess the stability of antx-a(s), 100 µl of the human plasma solution and 100 µl of either a 1 mM acetic acid solution or 0.001 µg of antx-a(s) diluted to 100 µl with 1 mM acetic acid were added to 3 ml of pH 8 phosphate buffer in a cuvette. Six samples were prepared at one time: three samples with vehicle (1 mM acetic acid) and three with toxin in the same volume of acetic acid. Solutions were mixed, incubated at room temperature for 40 minutes, and assayed for ChE activity after

addition of 50  $\mu$ l of 0.01 M dithionitrobenzoic acid and 20  $\mu$ l of 0.075 M acetylthiocholine iodide.

Measurement of absorbance at 412 nm in all six samples was performed simultaneously over 3 minutes with a Shimadzu 160 UV/VIS spectrophotometer (Shimadzu Co., Columbia, MD). The change in absorbance is a measure of the rate at which ChE cleaves acetylthiocholine iodide. Nine replicates of six samples each were performed. Stability of the enzyme and activity of the toxin were determined after 0, 1, 2, 3, 6, and 9 months of storage.

### 3. Results

Results of ChE assays are presented in Tables 1-3.

### 4. Discussion and Conclusion

Relatively high enzyme stability over 6 months of storage was reflected in the results shown in Table 3. There appeared to have been very little breakdown of the toxin; almost all of the change in variability over time in the enzyme plus toxin group can be explained by the minimal variability in ChE activity from month to month. These results are in contrast with those at Wright State University, Dayton, OH, where antx-a(s) was stored as a solid in vials at  $-80^{\circ}\text{C}$  and under which conditions there was an estimated daily loss of 1% of toxin activity. The addition of gaseous nitrogen may slow the breakdown of toxin by removing moisture that condenses in the vials in response to freezing/thawing, thereby decreasing hydrolysis. Storage of antx-a(s) at subzero temperatures and under gaseous nitrogen is recommended to minimize toxin degradation.

Table 1. Inhibition of human plasma cholinesterase activity as a function of the concentration of anatoxin-a(s).

Antx-a(s) Log dose ( $\mu$ g)	N	Plasma Cholinesterase (mmole/L/minute)	SD	CV %	% Inhibition
0.0 preexperiment	6	17.6	0.87	4.9	0
-1.0	6	0.0	-	-	100
-1.5	6	0.0	-	-	100
-2.0	6	0.4	0.24	73.6 8	97.7
-2.5	6	2.2	0.27	12.6 3	87.5
-3.0	6	10.8	0.4	3.7	38.6
-3.3	6	13.0	0.46	3.5	26.1
-3.5	6	14.4	0.97	6.7	18.2
-4.0	6	16.0	1.0	6.5	9.1
-4.3	6	17.3	1.2	6.8	1.7
0.0 postexperiment	6	18.0	1.3	7.1	-



Table 2. Effects of incubation time and temperature on the inhibition of cholinesterase in diluted human plasma by anatoxin-a(s) at 0.0003  $\mu\text{g/ml}$ .

Total Assay Time (minutes)	N	Time (minutes)	Cholinesterase Activity	
			37°C	Room Temperature
10 control	1	-	-	17.8
10	1	-	-	14.0
15	1	5	11.9	-
15 control	1	5	17.6	-
20	1	10	10.8	11.7
30	1	20	9.6	10.5
40	1	30	9.0	8.5
50	1	40	7.5	7.0
60	1	50	6.7	6.3
70	1	60	6.3	5.6
70 control	1	60	18.6	18.6

Cholinesterase results are in mmole/L/minute.

Table 3. Results of assays run at 0, 1, 2, 3, 6, and 9 months to determine the stability of anatoxin-a(s) using human plasma cholinesterase *in vitro*.

Treatment	Month	Cholinesterase Activity				
		Mean (mmole/L/minute)	SD	%CV	Units Inhibited	% Inhibition versus Control
Control	0	18.7	0.64	3.4%		
Toxin		8.48	0.34	3.9%	10.24	54.7%
Control	1	17.65	0.54	3.0%		
Toxin	1	7.71	0.35	4.5%	9.94	56.3%
Control	2	18.33	0.59	3.3%		
Toxin	2	8.04	0.26	3.2%	10.29	56.1%
Control	3	16.83	0.45	2.7%		
Toxin	3	7.38	0.34	4.5%	9.45	56.2%
Control	6	17.37	0.54	3.1%		
Toxin	6	7.81	0.33	3.4%	9.55	55.0%
Control	9	16.44	0.64	3.9%		
Toxin	9	7.81	0.47	6.0%	8.52	52.5%

N = 27 for all assays.

## III. REFERENCES

- Aldeman, W. J., Fohlmeister, J. H., Sasner, J. J., and Ikawa, M. (1982) Sodium channels blocked by aphantoxin obtained from the blue-green alga, *Aphanizomenon flos-aquae*. *Toxicon* 20:513-516.
- Aronston, R. S., and Witkop, W. (1981) Anatoxin-a interactions with cholinergic synaptic molecules. *Proc. Natl. Acad. Sci.* 78:4639.
- Baker, T., Agüero, A., Stanec, A., and Lowndes, H. E. (1986) Prejunctional effects of vecuronium in the cat. *Anesthesiology* 65:480.
- Barnes, J. M., and Duff, J. I. (1953) The role of cholinesterase at the myoneural junction. *Brit. J. Pharmacol.* 8:334-339.
- Beers, E. T., Rockwood, J., Garcia, C. O., Perrone, B. L., and Chang, F. (1987) Effects on selected cardiovascular and pulmonary parameters of maintaining arterial oxygen during and after agent-induced respiratory arrest. *Proc. Sixth Med. Chem. Defense Biosci. Rev., U.S. Army Med. Res. and Development Command, Aberdeen Proving Grounds, MD*, pp. 175-182.
- Biggs, D. F., and Dryden, W. F. (1977) Action of anatoxin I at the neuromuscular junction. *Proc. West. Pharmacol. Soc.* 20:461.
- Bowman, W. C. (1980) Prejunctional and postjunctional cholinergic receptors at the neuromuscular junction. *Anesth. Analg.* 59:935.
- Bruce, R. D. (1985) An up-and-down procedure for acute toxicity testing. *Fund. Appl. Toxicol.* 5:151-157.

- Calvey, T. N. (1984) Assessment of neuromuscular blockade by electromyography: A review. *J. R. Soc. Med.* 77:56.
- Carmichael, W. W. (1982) Chemical and toxicological studies of the toxic freshwater cyanobacteria *Microcystis aeruginosa*, *Anabaena flos-aquae* and *Aphanizomenon flos-aquae*. *S. Afr. J. Sci.* 78:367-372.
- Carmichael, W. W. (1988) Toxins of freshwater algae. In: A. T. Tu (ed.), *Handbook of Natural Toxins: Marine Toxins and Venoms*, Vol. 3. Marcel Dekker, New York, pp. 121-147.
- Carmichael, W. W., and Gorham, P. R. (1978) Anatoxins from the clones of *Anabaena flos-aquae* isolated from lakes of western Canada. *Mitt. Int. Verein. Limnol.* 22:285.
- Carmichael, W. W., and Mahmood, N. A. (1984) Toxins from freshwater cyanobacteria. In: E. P. Ragelis (ed.), *Seafood Toxins American Chemical Society Symposium Series 262*. American Chemistry Society Publications, Washington, DC, pp. 376-389.
- Carmichael, W. W., Biggs, D. F., and Gorham, P. R. (1975) Toxicology and pharmacological action of *Anabaena flos-aquae* toxin. *Science* 187:542.
- Carmichael, W. W., Gorham, P. R., and Biggs, D. F. (1977) Oral toxicity to calves of the freshwater cyanophyte (blue-green alga) *Anabaena flos-aquae* NRC-44-1. *Can. Vet. J.* 18:71-75.
- Carmichael, W. W., Biggs, D. F., and Peterson, M. A. (1979) Pharmacology of anatoxin-a, produced by the freshwater cyanophyte *Anabaena flos-aquae* NRC-44-1. *Toxicon* 17:229-236.

- Colquhoun, D., Dryer, F., and Sheridan, R. E. (1979) The actions of tubocurarine at the frog neuromuscular junction. *J. Physiol.* 293:247.
- Conover, W. I., and Iman, R. L. (1981) Rank transformation as a bridge between parametric and nonparametric statistics. *Am. Stat.* 35:124.
- Cook, W. O., Beasley, V. R., Dahlem, A. M., Dellinger, J. A., Harlin, K. S., and Carmichael, W. W. (1988) Comparison of effects of anatoxin-a(s) and paraoxon, physostigmine, and pyridostigmine on mouse brain cholinesterase activity. *Toxicon* 8:750-753.
- Cook, W. O., Beasley, V. R., Lovell, R. A., Dahlem, A. M., Hooser, S. B., Mahmood, N. A., and Carmichael, W. W. (1989a) Consistent inhibition of peripheral cholinesterases by neurotoxins from the freshwater cyanobacterium *Anabaena flos-aquae*: Studies of ducks, swine, mice and a steer. *Environ. Toxicol. Chem.* 8:915-922.
- Cook, W. O., Dellinger, J. A., Singh, S. S., Dahlem, A. M., Carmichael, W. W., and Beasley, V. R. (1989b) Regional brain cholinesterase in rats injected intraperitoneally with anatoxin-a(s) or paraoxon. *Toxicol. Let.* 49:29-34.
- de Candole, C. A., Douglas, W. W., Lovatt, C., Evans, C. L., Holmes, R., Spencer, K. O., Torrance, R. W., and Wilson, K. M. (1953) The failure of respiration in death by anticholinesterase poisoning. *Br. J. Pharmacol.* 8:466-475.
- Deem, A. W., and Thorp, R. (1939) Toxic algae in Colorado. *J. Am. Vet. Med. Assoc.* 95:542-544.
- Devlin, J. P., Edwards, O. E., Gorham, P. R., Hunter, N. R., Pike, R. K., and Stavric, B. (1977) Anatoxin-a, a toxic alkaloid from *Anabaena flos-aquae* NRC-4h. *Can. J. Chem.* 55:1367-1371.

- Dillenberg, H. O., and Dehnel, M. K. (1960) Toxic waterbloom in Saskatchewan, 1959. *Can. Med. Assoc. J.* 83:1151-1154.
- Dreyer, F. (1982) Acetylcholine receptor. *Br. J. Anaesth.* 54:115.
- Ekstedt, J., and Stalberg, E. (1969) The effect of nonparalytic doses of d-tubocurarine on individual motor end-plates in man, studied with a new electrophysiological method. *Electroencephalogr. Clin. Neurophysiol.* 27:536.
- Ellman, G. E., Courtney, K. D., Andres, V., and Featherstone, R. M. (1961) A new and rapid colorimetric determination of acetylcholinesterase activity. *Biochem. Pharmacol.* 7:88.
- Fitch, C. P., Bishop, L. M., and Boyd, W. L. (1934) "Water bloom" as a cause of poisoning in domestic animals. *Cornell Vet.* 24:30-39.
- Frawley, J. P., Hagan, E. C., and Fitzhugh, O. G. (1952) A comparative pharmacological and toxicological study of organic phosphate-anticholinesterase compounds. *J. Pharmacol. Exp. Therap.* 105:156-165.
- Galindo, A. (1971) Prejunctional effect of curare: Its relative importance. *J. Neurophysiol.* 34:289.
- Galvinovic, M. I. (1979) Presynaptic action of curare. *J. Physiol.* 290:499.
- Gibbs, A. J., and Marshall, I. G. (1984) Pre- and postjunctional effects of tubocurarine and other nicotinic antagonists during repetitive stimulation in the rat. *J. Physiol.* 351:275.
- Glowinski, J., and Iversen, L. L. (1966) Regional studies of catecholamines in the rat brain. I. The disposition of [ $^3\text{H}$ ]norepinephrine, [ $^3\text{H}$ ]dopamine and [ $^3\text{H}$ ]dopa in various regions of the brain. *J. Neurochem.* 13:655-669.

- Gorham, P. R. (1964) Toxic algae. In: D. F. Jackson (ed.), *Algae, Man, and Environment*. Plenum Press, New York, NY, pp. 307-336.
- Gorham, P. R., McLachlan, J., Hammer, U. T., and Kim, W. K. (1964) Isolation and culture of toxic strains of *Anabaena flos-aquae* (Lyngb.) de Breb. *Verhandelingen Internationale Vereinigung Limnologie* 15:796-804.
- Guyton, A. C. (1976) The blood-cerebrospinal fluid and blood-brain barriers. In: *Textbook of Medical Physiology*. W. B. Saunders, Philadelphia, p. 418.
- Hammer, U. T. (1968) Toxic blue-green algae in Saskatchewan. *Can. Vet. J.* 9(10):221-229.
- Harada, K.-I., Kimura, Y., Suzuki, M., Dahlem, A. M., Beasley, V. R., and Carmichael, W. W. (1988) Structural studies on a neurotoxin, anatoxin-a(s) produced by a toxin blue-green algae. I. Development of an isolation method. *Abstr. Ann. Meet. Pharmaceutical Soc. Japan, Hiroshima, Japan, April 4-6.*
- Harlin, K. S. (1987) Bovine retina cholinesterase determinations and possible applications for postmortem diagnosis of organophosphate insecticide poisoning. *Cattle Res. Com. Rpt., Ill. Dept. Ag., Springfield, Il.*
- Harlin, K. S., and Ness, D. (1986) Brain cholinesterase-normal enzyme activity levels in several large and small animal species. *Proc. Am. Assoc. Vet. Lab. Diagnosticians, Louisville, KY, October 19-21, pp. 457-469.*
- Holmstedt, B. (1959) Pharmacology of organophosphorus cholinesterase inhibitors. *Pharmacol. Rev.* 11:567-688.
- Hubner, C. S. (1972) The crystal structure and absolute configuration of 2,9-diacetyl-9-azabicyclo (4,2,1) non-2,3-ene. *Acta Crystallography* B28:2577-2582.

- Hyde, E. G., and Carmichael, W. W. (1988) Anatoxin-a(s) effects on isolated muscle. *Toxicologist* 8:40.
- Hyde, E. G., and Carmichael, W. W. (1989) Studies of the ionic channel properties of anatoxin-a(s). *Toxicon* 27:52-53.
- Jacobs, A. M. (1982) Vascular permeability and neurotoxicity. In: C. L. Mitchell (ed.), *Nervous System Toxicology*. Raven Press, New York, pp. 285-298.
- Jain, N. C. (1986) The erythrocytes: Its morphology, metabolism, and survival. In: *Veterinary Hematology*, 4th ed. Lea and Febiger, Philadelphia, pp. 527-562.
- Lu, T. (1970) Affinity of curare-like compounds and their potency in blocking neuromuscular transmission. *J. Pharmacol. Exp. Ther.* 174:560.
- MacLagan, J. (1976) Competitive neuromuscular blocking drugs. In: E. Zaimis (ed.), *Neuromuscular Junction*. Springer-Verlag, New York, p. 421.
- Mahmood, N. A., and Carmichael, W. W. (1986a) Paralytic shellfish poisons produced by the freshwater cyanobacterium *Aphanizomenon flos-aquae* NH-5. *Toxicon* 24:175-186.
- Mahmood, N. A., and Carmichael, W. W. (1986b) The pharmacology of anatoxin-a(s), a neurotoxin produced by the freshwater cyanobacterium *Anabaena flos-aquae* NRC-525-17. *Toxicon* 24:425.
- Mahmood, N. A., and Carmichael, W. W. (1987) Anatoxin-a(s), an irreversible anticholinesterase from blue-green *Anabaena flos-aquae* NRC-525-17. *Toxicon* 25:1221.
- Mahmood, N. A., et al. (1987) Kinetic analysis of the inhibition of acetylcholinesterase (EC 3.1.1.7) by anatoxin-a(s). Part 1. Conf. Natural Toxins from Aquatic and Marine Environ., Woods Hole, MA, August (abstr.).



- Mahmood, N. A., Carmichael, W. W., and Pfahler, D. (1988) Anticholinesterase poisonings in dogs from a cyanobacteria (blue-green algae) bloom dominated by *Anabaena flos-aquae*. *Am. J. Vet. Res.* 49:500-503.
- Matsunaga, S., Moore, R. E., and Niemeczura, W. P. (1989) Anatoxin-a(s), a potent anticholinesterase from *Anabaena flos-aquae*. *J. Am. Chem. Soc.* 111:8021-8023.
- Mayer, S. E., Melmon, K. L., and Gilman, A. G. (1980) Central nervous system and cerebrospinal fluid. In: A. G. Gilman, L. S. Goodman, T. W. Rall, and F. Murad (eds.), *The Pharmacologic Basis of Therapeutics*. Macmillan Publishing, New York, p. 10.
- Murphy, S. D. (1986) Toxic effects of pesticides. In: C. D. Klaassen, M. O. Amdur, J. D. Doull (eds.), *Toxicology*, 3rd ed. New York: Macmillan Publishing Co., pp. 519-581.
- Nastuk, W. L. (1971) Mechanisms of neuromuscular blockade. *Ann. N.Y. Acad. Sci.* 183:171.
- Norton, S. (1986) Toxic responses of the nervous system. In: C. D. Klaassen, M. O. Amdur, and J. Doull (eds.), *Casarett and Doull's Toxicology*. Macmillan, New York, pp. 359-360.
- Osweiler, G. D., Carson, T. L., Buck, W. B., and Van Gelder, G. A. (1984) Organophosphorus and carbamate insecticides. In: *Clinical and Diagnostic Veterinary Toxicology*, 3rd ed. Kendall/Hunt, Dubuque, IA, pp. 298-317.
- Paton, W. D. M., and Waud, D. R. (1967) The margin of safety of neuromuscular transmission. *J. Physiol.* 191:59.
- Rickett, D. L., Glenn, J. F., and Beers, E. T. (1986) Central respiratory effects versus neuromuscular actions of nerve agents. *Neurotoxicology* 7:225-236.

- Riker, W. F. Jr., Roberts, J., Standaert, F. G., and Fujimori, H. (1957) The motor nerve terminal as a primary focus of drug-induced facilitation of neuromuscular transmission. *J. Pharmacol. Exp. Ther.* 121:286.
- Salsburg, D. S. (1984) *Statistics for Toxicologists*. Marcel Dekker, New York, p. 21.
- Sanathanan, L. P., Gade, E. T., and Shipkowitz, N. L. (1987) Trimmed logit method for estimating the  $ED_{50}$  in quantal bioassay. *Biometrics* 43:825.
- SAS Institute. (1985) *SAS User's Guide: Statistics*, 5th ed. SAS Institute Inc., Cary, NC, pp. 433-646.
- Shipley, M. T., and Nickel, W. T. (1987) Action of soman on brain cholinergic circuits. *Proc. Sixth Med. Chem. Defense Biosci. Rev., U.S. Army Med. Res. Develop. Com., Aberdeen Proving Ground, MD, August 4-6*, pp. 147-155.
- Sivonen, K., Himberg, K., Luukkainen, R., Niemela, S., Poon, G., and Codd, G. A. (1989) Primary characterization of neurotoxic cyanobacterial blooms and strains from Finland. *Toxic. Assess.*, in press.
- Spivak, C. E., Witkop, B., and Albuquerque, E. X. (1980) Anatoxin-a: A novel potent agonist at the nicotinic receptor. *Mol. Pharmacol.* 18:384.
- Spivak, C. E., Waters, J., Witkip, B., and Albuquerque, E. X. (1983) Potencies and channel properties induced by semirigid agonists at frog nicotinic acetylcholine receptors. *Mol. Pharmacol.* 23:337.
- Standaert, F. G. (1964) The action of d-tubocurarine on the motor nerve terminal. *J. Pharmacol. Exper. Ther.* 143:181.

- Stewart, A. G., Barnum, D. A., and Henderson, J. A. (1950) Algal poisoning in Ontario. *Can. J. Comp. Med. Vet. Sci.* 14:197-202.
- Swanson, K. L., Allen, C. N., Dronston, R. S., Rapoport, H., and Albuquerque, E. X. (1985) Molecular mechanisms of the potent and stereospecific nicotinic receptor agonist (+)anatoxin-a. *Mol. Pharmacol.* 29:250.
- Taylor, P. (1985) Anticholinesterase agents. In: A. G. Gilman, L. S. Goodman, T. W. Rall, and F. Murad (eds.), *The Pharmacologic Basis of Therapeutics*. Macmillan Publishing, New York, pp. 110-129.
- Taylor, D. B., Prior, R. D., and Bevan, J. A. (1964) The relative sensitivities of diaphragm and other muscles of the guinea pig to neuromuscular blocking agents. *J. Pharmacol. Exper. Ther.* 143:187.
- Thurmon, J. C., and Benson, G. J. (1986) Anesthesia in ruminants and swine. In: J. L. Howard (ed.), *Current Veterinary Therapy*, Vol. 2—Food Animal Practice. W. B. Saunders, Philadelphia, PA, pp. 51-71.
- Vizi, E. S., Somogyi, G. T., Nagashima, H., Duncalf, D., Chaudhy, I. A., Kobayoshi, O., Goldiner, P. L., and Foldes, F. F. (1987) Tubocurarine and pancuronium inhibit release of acetylcholine from the mouse hemidiaphragm preparation. *Br. J. Anaesth.* 59:226.
- Waud, B. E., and Waud, D. R. (1972) The margin of safety of neuromuscular transmission in the muscle of the diaphragm. *Anesthesiology* 37:417.
- Winer, B. J. (1971) *Statistical Principles in Experimental Design*. McGraw-Hill, New York.
- Wright, P. G. (1954) An analysis of the central and peripheral components of respiratory failure produced by anticholinesterase poisoning in the rabbit. *J. Physiol.* 126:52-70.

Zaimis, E. (1976) Depolarizing neuromuscular blocking drugs. In: E. Zaimis (ed.),  
*Neuromuscular Junction*. Springer-Verlag, New York, pp. 365.

**CHRONOLOGICAL BIBLIOGRAPHY OF ALL PUBLICATIONS  
SUPPORTED BY THE CONTRACT**

**ALGAL PEPTIDE HEPATOTOXINS**

**Experimental (Refereed)**

Galey, F. D., Beasley, V. R., Carmichael, W. W., Kleppe, G., Hooser, S. B., and Haschek, W. M.

(1987) Blue-green algae (*Microcystis aeruginosa*) hepatotoxicosis in dairy cows. *Am. J. Vet. Res.* 48:1415-1420.

Harada, K.-I., Suzuki, M., Dahlem, A. M., Beasley, V. R., Carmichael, W. W., and Rinehart,

K. L. (1988) Improved method for purification of toxic peptides produced by cyanobacteria. *Toxicon* 26:443-439.

Harada, K.-I., Matsuura, K., Suzuki, M., Watanabe, M. F., Oishi, S., Dahlem, A. M., Beasley,

V. R., and Carmichael, W. W. (1988) Analysis and purification of toxic peptides from cyanobacteria by reversed-phase high-performance liquid chromatography. *J. Chrom.* 448:275-283.

Rinehart, K. L., Harada, K.-I., Namikoshi, M., Chen, C., Harvis, C. A., Munro, M. H. G., Blunt,

J. W., Mulligan, P. E., Beasley, V. R., Dahlem, A. M., and Carmichael, W. W. (1988) Nodularin, microcystin, and the configuration of Adda. *J. Am. Chem. Soc.* 110:8557-8558.

Beasley, V. R., Cook, W. O., Dahlem, A. M., Hooser, S. B., Lovell, R. A., and Valentine, W. M.

(1989) Algae intoxication in livestock and waterfowl. *Vet. Clin. N. Am.* 5:345-361.

- Beasley, V. R., Dahlem, A. M., Cook, W. M., Valentine, W., Lovell, R. A., Hooser, S. B., Harada, K. I., Suzuki, M., and Carmichael, W. W. (1989) Diagnostic and clinically important aspects of cyanobacterial (blue-green algal) toxicoses. *J. Vet. Diagn. Invest.* 1:359-365.
- Dahlem, A. M., Hassan, A. S., Swanson, S. P., Carmichael, W. W., and Beasley, V. R. (1989) A model system for studying the bioavailability of intestinally administered microcystin-LR, a hepatotoxic peptide from the cyanobacterium *Microcystis aeruginosa*. *Pharmacol. Toxicol.* 64:177-181.
- Hooser, S. B., Beasley, V. R., Lovell, R. A., Carmichael, W. W., and Haschek, W. M. (1989) Toxicity of microcystin-LR, a cyclic heptapeptide hepatotoxin from *Microcystis aeruginosa*, in rats and mice. *Vet. Pathol.* 26:246-252.
- Lovell, R. A., Schaeffer, D. J., Hooser, S. B., Haschek, W. M., Dahlem, A. M., Carmichael, W. W., and Beasley, V. R. (1989) Toxicity of one or two intraperitoneal doses of microcystin-LR in two strains of male mice. *J. Environ. Pathol. Toxicol. Oncol.* 9:221-238.
- Namikoshi, M., Rinehart, K. L., Dahlem, A. M., Beasley, V. R., and Carmichael, W. W. (1989) Total synthesis of adda, the unique C<sub>20</sub> amino acid of cyanobacterial hepatotoxins. *Tetrahedron Let.* 30:4349-4352.
- Harada, K.-I., Kimura, Y., Ogawa, K., Suzuki, M., Dahlem, A. M., Beasley, V. R., and Carmichael, W. W. (1989) A new procedure for the analysis and purification of naturally occurring anatoxin-a from the blue-green alga, *Anabaena flos-aquae*. *Toxicon.* 27:1289-1296.

- Harada, K.-I., Matsuura, K., Suzuki, M., Watanabe, M. F., Oishi, S., Dahlem, A. M., Beasley, V. R., and Carmichael, W. W. (1990) Isolation and characterization of the minor components associated with microcystins LR and RR in the cyanobacterium (blue-green algae). *Toxicon* 28:55-64.
- Hooser, S. B., Beasley, V. R., Waite, L. L., Kuhlenschmidt, M. S., Carmichael, W. W., and Haschek, W. M. (1990) Microcystin-LR induced ultrastructural changes in rats. *Vet. Pathol.* 27:9-15.
- Hooser, S. B., Kuhlenschmidt, M. S., Beasley, V. R., Carmichael, W. W., and Haschek, W. M. (1991) Uptake and subcellular localization of tritiated dihydromicrocystin-LR in rat hepatocyte suspensions and perfused liver. *Toxicon* 29:589-601.
- Hooser, S. B., Beasley, V. R., Waite, L. L., Kuhlenschmidt, M. S., Carmichael, W. W., and Haschek, W. M. (1991) Actin filament alterations in rat hepatocytes induced *in vivo* and *in vitro* by microcystin-LR, a hepatotoxin from the blue-green alga, *Microcystis aeruginosa*. *Vet. Path.* 28:259-266.
- Hooser, S. B., Kuhlenschmidt, M. S., Dahlem, A. M., Beasley, V. R., Carmichael, W. W., and Haschek, W. M. (1991) Uptake and subcellular localization of tritiated dihydromicrocystin-LR in rat hepatocyte suspensions and perfused liver. *Toxicon* 29:589-602.

#### Theses

- Dahlem, A. M. (1989) Structure/toxicity relationships and fate of low molecular weight peptide toxins from cyanobacteria. PhD Thesis. College of Veterinary Medicine, University of Illinois at Urbana-Champaign.

Hooser, S. B. (1989) Toxicopathology of microcystin-LR *in vivo* and *in vitro*. PhD Thesis.

College of Veterinary Medicine, University of Illinois at Urbana-Champaign.

Lovell, R. A. (1989) The toxicity of microcystin-LR in swine and mice. PhD Thesis. College of Veterinary Medicine, University of Illinois at Urbana-Champaign.

#### **In Press**

Dahlem, A. M., Beasley, V. R., Hooser, S. B., Harada, K.-I., Matsuura, K., Suzuki, M., Rinehart, K. L., Harvis, C. A., and Carmichael, W. W. (1991) The structure/toxicity relationship of dehydro amino acids in microcystin-LR and nodularin, two monocyclic peptide hepatotoxins from cyanobacteria. *Chem. Res. Toxicol.*

Hooser, S. B., Beasley, V. R., Waite, L. L., Kuhlenschmidt, M. S., Carmichael, W. W., and Haschek, W. M. (1991) Cytoskeletal alterations in rat hepatocytes induced *in vivo* and *in vitro* by microcystin-LR, a hepatotoxin from the blue-green alga, *Microcystis aeruginosa*. *Vet. Pathol.*

Lovell, R. A., Beasley, V. R., Hooser, S. B., Haschek, W. M., Dahlem, A. M., and Carmichael, W. W. Comparison of the hepatotoxic effects of intragastrically administered whole *Microcystis aeruginosa* cells and intravenously administered purified microcystin-A in two littermate gilts. *J. Am. Vet. Med. Assoc.*

#### **Submitted for Publication**

Dahlem, A. M., Swanson, S. P., Harada, K.-I., Suzuki, M., Buetow, B. B., Carmichael, W. W., and Beasley, V. R. The distribution and elimination of intraperitoneally administered dihydro-microcystin-LR in mice. *Chem. Res. Toxicol.*



Namikoshi, M., Rinehart, K. L., Sakai, R., Stotts, R. R., Beasley, V. R., Carmichael, W. W., and Evans, W. R. Identification of twelve hepatotoxins from a Homer Lake bloom of the cyanobacteria *Microcystin aeruginosa*, *M. viridis*, and *M. wesenbergii*; nine new microcystins. J. Am. Chem. Soc.

### In Preparation

Dahlem, A. M., Chen, C., Namikoshi, M., Rinehart, K. L., Carmichael, W. W., and Beasley, V. R. Structure-toxicity relationships in monocyclic peptide hepatotoxins from cyanobacteria. Toxicon.

Dahlem, A. M., Hassan, A. S., Waite, L. L., Carmichael, W. W., and Beasley, V. R. Evidence for a role of glutathione in the toxicity of microcystin-LR, a hepatotoxin from the cyanobacterium *Microcystis aeruginosa*. Toxicon.

Lovell, R. A., Holmes, K. R., Beasley, V. R., et al. The toxicity of microcystin-LR in swine: Preliminary findings. J. Environ. Pathol. Toxicol. Oncol.

Lovell, R. A., Holmes, K. R., Beasley, V. R., et al. The effects of microcystin-LR on hemodynamic, organ perfusion, clinical pathology, gross necropsy, and blood gas parameters in swine. Am. J. Vet. Res.

Lovell, R. A., Hoffmann, W. E., Valentine, W. M., Lund, L. A., Dahlem, A. M., Carmichael, W. W., and Beasley, V. R. Arginase activity in twelve tissues and serum, serum arginase half-life and changes in serum arginase activity following administration of microcystin-LR (cyanoginosin-LR) in swine. Enzyme.

## ALGAL NEUROTOXINS

## Experimental (Referced)

- Cook, W. O., Beasley, V. R., Dahlem, A. M., Dellinger, J. A., Harlin, K. S., and Carmichael, W. W. (1988) Comparison of effects of anatoxin-a(s) and paraoxon, physostigmine and pyridostigmine on mouse brain cholinesterase activity. *Toxicon* 26:750-753.
- Cook, W. O., Beasley, V. R., Lovell, R. A., Dahlem, A. M., Hooser, S. B., Mahmood, N. B., and Carmichael, W. W. (1989) Consistent inhibition of peripheral cholinesterases by neurotoxins from the freshwater cyanobacterium *Anabaena flos-aquae*: Studies of ducks, swine, mice and a steer. *Environ. Toxicol. Chem.* 8:915-922.
- Cook, W. O., Dellinger, J. A., Singh S. S., Dahlem, A. M., Carmichael, W. W., and Beasley, V. R. (1989) Regional brain cholinesterase activity in rats injected intraperitoneally with anatoxin-a(s) or paraoxon. *Toxicol. Let.* 49:29-34.
- Cook, W. O., Iwamoto, G. A., Schaeffer, D. J., and Beasley, V. R. (1989) Effect of anatoxin-a(s) from *Anabaena flos-aquae* NRC 525-17 on blood pressure, heart rate, respiratory rate, tidal volume, minute volume, and phrenic nerve activity in rats. *J. Environ. Pathol. Toxicol. Oncol.* 9:393-400.
- Harada, K.-I., Kimura, Y., Ogawa, K., Suzuki, M., Dahlem, A. M., Beasley, V. R., and Carmichael, W. W. (1989) A new procedure for the analysis and purification of naturally occurring anatoxin-a from the blue-green alga *Anabaena flos-aquae*. *Toxicon* 12:1289-1296.

Cook, W. O., Iwamoto, G. A., Schaeffer, D. J., Carmichael, W. W., and Beasley, V. R. (1990) Pathophysiologic effects of anatoxin-a(s) in anaesthetized rats: The influence of atropine and artificial respiration. *Pharmacol. Toxicol.* 67:151-155.

Cook, W. O., Dahlem, A. M., Harlin, K. S., Beasley, V. R., Hooser, S. B., Haschek, W. M., and Carmichael, W. W. (1991) Reversal of cholinesterase inhibition and clinical signs and postmortem findings in mice after intraperitoneal administration of anatoxin-a(s), paraoxon, or pyridostigmine. *Vet. Hum. Toxicol.* 33:1-4.

Valentine, W.M., Schaeffer, D.J., and Beasley, V.R. (1991). Electromyographic assessment of the neuromuscular blockade Produced in vivo by anatoxin-a in the rat. *Toxicon* 29: 347-357.

#### **Theses**

Cook, W. O. (1989) Pathophysiologic effects of anatoxin-a(s), a toxin from the cyanobacterium *Anabaena flos-aquae*. PhD Thesis. College of Veterinary Medicine, University of Illinois at Urbana-Champaign.

#### **In Preparation**

Cook, W. O., Dellinger, J. A., Carmichael, W. W., and Beasley, V. R. Acute behavioral toxicity of the cyanobacterial neurotoxins, anatoxin-a(s), in rats. *Neurobehav. Toxicol. Teratol.*

Cook, W. O., Singh, S. S., Beasley, V. R., and Dellinger, J. A. Cholinesterase inhibition and neurobehavioral effects in paraoxon treated Long-Evans rats. *Neurobehav. Toxicol. Teratol.*

Singh, S. S., Dellinger, J. A., Cook, W. O., and Beasley, V. R. Neurobehavioral effects of nicotine, atropine, and physostigmine in Long-Evans rats. *Pharmacol. Biochem. Behavior.*

**LIST OF PERSONNEL RECEIVING CONTRACT SUPPORT,  
INCLUDING DEGREES RECEIVED**

**PRINCIPAL/CO-INVESTIGATORS**

Val R. Beasley, Principal Investigator	Wanda M. Haschek-Hock, Co-Investigator
Wayne W. Carmichael, Co-Investigator	

**PhD DEGREES RECEIVED**

William O. Cook III	Randall A. Lovell
Andrew M. Dahlem	Nik A. Mahmood
Steven Blair Hooser	

**RESEARCHERS**

James D. Fikes	Billy Moore
Francis D. Galey	David Schaeffer
Richard Lambert	Patti M. Thorn
Gregg Lundeen	William M. Valentine
Nik A. Mahmood	

**TECHNICAL STAFF**

Geneieve Dumonceaux

Jean Miller

Joni Dye

Kimberly Powers

Bernard Buetow

John Scott

Richard Manuel

Leslie Waite

**CLERICAL/SECRETARIAL STAFF**

Sally Campbell

Carol Schaeffer

Patrice Carlson